uOttawa

L'Université canadienne
Canada's university

FACULTÉ DES ÉTUDES SUPÉRIEURES ET POSTOCTORALES

uOttawa

L'Université canadienne
Canada's university

FACULTY OF GRADUATE AND POSDOCTORAL STUDIES

Julie A. D. Grabowy
AUTEUR DE LA THÈSE / AUTHOR OF THESIS

Ph.D. (Chemistry)
GRADE / DEGREE

Department of Chemistry
FACULTÉ, ÉCOLE, DÉPARTEMENT / FACULTY, SCHOOL, DEPARTMENT

Experimental and Theoretical Studies of the Energetics of Gas-phase Organic Cluster Ions

TITRE DE LA THÈSE / TITLE OF THESIS

Paul Mayer
DIRECTEUR (DIRECTRICE) DE LA THÈSE / THESIS SUPERVISOR

CO-DIRECTEUR (CO-DIRECTRICE) DE LA THÈSE / THESIS CO-SUPERVISOR

EXAMINATEURS (EXAMINATRICES) DE LA THÈSE / THESIS EXAMINERS

Diethard Kurt Bohme

Robert Burk

Natalie Goto

Alain St-Amant

Gary W. Slater
LE DOYEN DE LA FACULTÉ DES ÉTUDES SUPÉRIEURES ET POSTDOCTORALES /
DEAN OF THE FACULTY OF GRADUATE AND POSTDOCORAL STUDIES

EXPERIMENTAL AND THEORETICAL STUDIES OF THE ENERGETICS OF GAS-PHASE ORGANIC CLUSTER IONS

by

Julie Ann Douglas Grabowy, M.Sc.

A thesis submitted to the
Faculty of Graduate and Postdoctoral Studies

In partial fulfillment of the requirements of
the degree of Doctor of Philosophy

In the Ottawa-Carleton Chemistry Institute
Department of Chemistry, University of Ottawa
Ottawa, Ontario, Canada

July 2005

Candidate	Supervisor
Julie A. D. Grabowy	Dr. Paul M. Mayer

Your file Votre référence
ISBN: 0-494-10969-6
Our file Notre référence
ISBN: 0-494-10969-6

This thesis is dedicated with love to

my maternal grandparents, Alex and Beulah Lamb,

whose love has always been a source of inspiration to me.

Abstract

Mass spectrometry was used in combination with theoretical calculations and statistical rate theories to probe both the unimolecular dissociation and isomerization characteristics of proton-bound molecular pairs. These proton-bound pairs have been found to dissociate by simple hydrogen bond cleavage or rearrange via a unimolecular S_N2 mechanism to form an isomeric complex that loses water. The proton-bound pair rearranges to an intermediate ion complex (IC) via TS_a followed by the formation of the thermodynamically stable isomer that loses water via TS_b. Empirical relationships based on the number of stabilizing alkyl groups on the central S_N2 carbon and differences in proton affinities have been developed for estimating the energies of the two transition states (TS_a and TS_b) and IC in the isomerization reaction.

The entropy of activation, $\Delta S^{\ddagger}$, for the dissociation of the proton-bound pairs to CH_3CNH^+ and ROH was found to change systematically with molecular functionality, with the entropy decreasing from 70 J K^{-1} mol^{-1} in $(CH_3CN)(CH_3OH)H^+$ to 6 J K^{-1} mol^{-1} in $(CH_3CN)((CH_3)_2CHOH)H^+$. This systematic change was not observed in the dissociation to CH_3CN and ROH_2^+ or in the thermodynamic entropy change for the dissociation. The entropies of activation for the competing dissociation channels for $(CH_3CN)(CH_3OH)H^+$ and $(CH_3CN)(CH_3CH_2OH)H^+$ were the same within error and thus $\Delta(\Delta S^{\ddagger}) \approx 0$ while this value ranged from 40- 45 J K^{-1} mol^{-1} for the propanol-containing pairs,. The $\Delta(\Delta S)$ for all four proton-bound pairs was zero.

The unimolecular dissociation of the series of $(NO)(A)^+$ cluster ions (where A = benzene, pyridine, furan, thiophene and benzonitrile) was examined using tandem mass spectrometry and evidence was found for the participation of excited states in their dissociation. The unimolecular dissociation of metastable ionic complexes generated by NO chemical ionization of benzonitrile changes as a function of ion source pressure. As the NO concentration in the source increases, the metastable ion (MI) mass spectrum goes from being dominated by NO^+ to one dominated by ionized benzonitrile and its fragmentation products. A similar result is observed when A = pyridine. When A = benzene, the MI mass spectrum is dominated by the ionized aromatic, a result that is consistent with the adiabatic dissociation of the ground singlet-state of the complex. The MI mass spectra of the complexes involving furan and thiophene are consistent with the dissociation of the lowest energy singlet-state.

Acknowledgements

I would first like to thank my supervisor, Dr. Paul Mayer, for his patient guidance of this thesis work. His door was always open to my many questions and his approachable nature made me feel as though there was nothing I couldn't ask! He truly has a gift for knowing how to make the most difficult concepts seem so simple! During my M.Sc. and Ph.D. degrees, he has taught me how to critically evaluate my own work and to believe in myself; for that I owe my thanks.

Special thanks go out the following people -- To Dr. John Holmes for his helpful comments and listening ear; to Sander (Dr. A.A. Mommers) for imparting to me his wealth of knowledge of mass spectrometers, music and life itself; and to Clem (Dr. C. Kazakoff) for his early morning discussions. Big thanks also go out to my colleagues (past and present in no particular order) for making this journey more than just an exercise in higher knowledge — Dr. Emma Rennie, Dr. Richard Ochran, Dr. Jie Cao, Xian Wang, Annick St-Amand, Abdul Alhazmi, Anne-Marie Boulanger, Mohammad Qadura, Clement Poon, Danielle Dubien, Marie-Soleil Giguère, and Janeen (Auld) Casey.

Last, but by no means least, I would like to thank my family for their never-ending love and support. Special thanks goes to my loving husband, Mark, for being my rock of support throughout this journey and for his ability to always make me laugh and to my sister, Jessica, for always knowing how to brighten my day. I would also like to thank my mother for instilling in me the ambition to further my studies (and even get a Ph.D.!) and lastly, to the Grabowy family (Henry, Joseph and Anna) for their love and support.

Contents

List of Tables

List of Figures

Abbreviations

BE	Binding Energy
BIRD	Blackbody Infrared Dissociation
CID	Collision-Induced Dissociation
DFT	Density Functional Theory
FFR	Field-Free Region
HF	Hartree-Fock Theory
KERD	Kinetic Energy Release Distribution
MIKES	Mass-Analyzed Ion Kinetic Energy Spectroscopy
m/z	mass-to-charge ratio
MO	Molecular Orbital
MP2	Second-Order Moller-Plesset Perturbation Theory
$N^{\ddagger}$	Sum of States of Transition State
PES	Potential Energy Surface
RRKM	Rice-Ramsperger-Kassel-Marcus Theory
S_N2	Bimolecular Nucleophilic Substitution
TPEPICO	Threshold Photoelectron Photoion Coincidence
TS	Transition State
VTST	Variational Transition State Theory
ZPE	Zero-point Energy
$\Delta S^{\ddagger}$	Entropy of Activation
ΔS	Thermodynamic Entropy
$\rho(E)$	Density of States

CHAPTER 1

INTRODUCTION

1.1 A Synopsis of The Thesis

The work presented in this thesis comprises an experimental and theoretical study of the unimolecular reactions of gas-phase ions. Chapter 1 provides the reader with a brief description of the thesis material while chapter 2 serves to introduce some of the techniques and concepts that are frequently used in the study of gaseous ions. Chapter 3 involves a discussion of empirical relationships that have been derived for predicting the energetics of isomerization of proton-bound pairs, while chapter 4 describes a study of the entropic effects associated with the dissociation of such proton-bound pairs. Chapters 5 and 6 concern an experimental and theoretical investigation of $(NO)(aromatic)^+$ cluster ions involving benzene, pyridine, thiophene, furan and benzonitrile. The final chapter, chapter 7, provides a summary of the experimental and theoretical methods employed in this thesis, to which the reader may refer for additional information.

1.2 Detailed Summary of Thesis Work

Today, the technique of mass spectrometry is not only used for fundamental chemical studies of reaction kinetics and thermodynamics but finds itself among the chosen analytical methods for pharmaceutical, environmental and forensic analyses. With the

advent of modern electronics and ultrahigh vacuum techniques, commercial instruments of extreme capability and versatility have come of age. Mass spectrometers are now employed in virtually every industry and are used in research laboratories, industrial plants, hospitals and even in interstellar space.

The technique of mass spectrometry involves gas-phase ions and a central feature to the chemistry of gas-phase species is their propensity for rearrangement. In the gas-phase, many thermodynamically stable isomers have been identified; some isomers are of a conventional form while others exhibit a non-conventional form— let us now consider the following example, ionized n-propanol (Figure 1.1). Most of us will undoubtedly be familiar with the conventional form of this ion, whose connectivity is $CH_3CH_2CH_2OH^{+\bullet}$; this structure of the ion, however, is not the most thermodynamically stable form. The distonic form of this ion, $\bullet CH_2CH_2CH_2OH_2^+$, which involves a separation between the charge and radical sites, lies 17 kJ mol^{-1} lower in energy than the conventional form.[1] Two other isomers of ionized n-propanol have been identified in the gas-phase: an ion-dipole complex between the cyclopropane ion and a neutral water molecule and the distonic form of the covalently bonded association between ionized propene and water. These two ions were theoretically probed (at MP2/6-31+G* level of theory) by Bouchoux *et al*;[2] the covalently bonded association was found to sit 48 kJ mol^{-1} lower in energy than the conventional form while that of the ion-dipole complex resides 7 kJ mol^{-1} higher in energy. As in the cases of the distonic and ion-dipole forms of ionized n-propanol, many of these non-conventional ions have been found to be more stable (i.e., lower in energy) than their conventional forms and play an important role in the mechanisms for ion isomerization and dissociation.

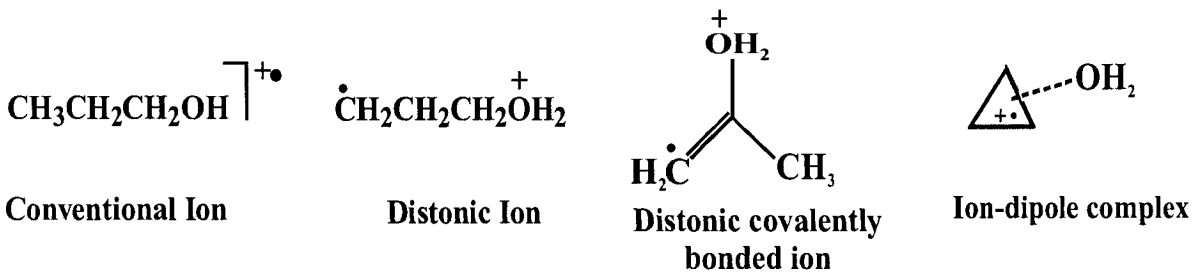

Figure 1.1 Isomers of ionized n-propanol, $C_3H_8O^{+\bullet}$.

Another type of gas-phase ion is the bridged ion; one example is a proton-bound pair such as the acetonitrile-methanol proton-bound pair, $(CH_3CN)(CH_3OH)H^+$. These ions consist of two molecules that are electrostatically bound to one another by a central ion; protons are often the connecting ion (as in a proton-bound pair) although metal ions also assume this role. Both covalently and electrostatically bound ions have been found to isomerize in the gas phase. One example of a covalently bound species that undergoes gas-phase rearrangement is ionized methylacetate.[3] The methylacetate ion, $CH_3CO_2CH_3^{+\bullet}$, rearranges in the gas-phase to form the $CH_3CO^{\bullet}$ ••• H^+••• OCH_2 ion, which may then dissociate to produce $^{\bullet}CH_2OH$ radicals and the acetyl cation, CH_3CO^+ (Figure 1.2).

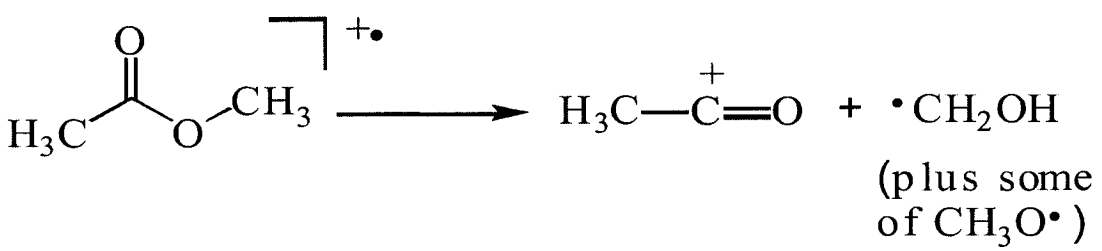

Figure 1.2 The dissociation of ionized methylacetate.

Ionized methylacetate, rather than isomerising to lose $^{\bullet}CH_2OH$ radicals, may also dissociate to yield a small amount of $CH_3O^{\bullet}$ radicals as shown in the potential energy surface in Figure 1.3.[4] The rearrangement of gas-phase ions is not limited to covalently bound species since even electrostatically bound species such as proton-bound pairs can undergo extensive rearrangement reactions. Throughout this thesis, we will encounter examples of electrostatically bound species that isomerize in the gas-phase.

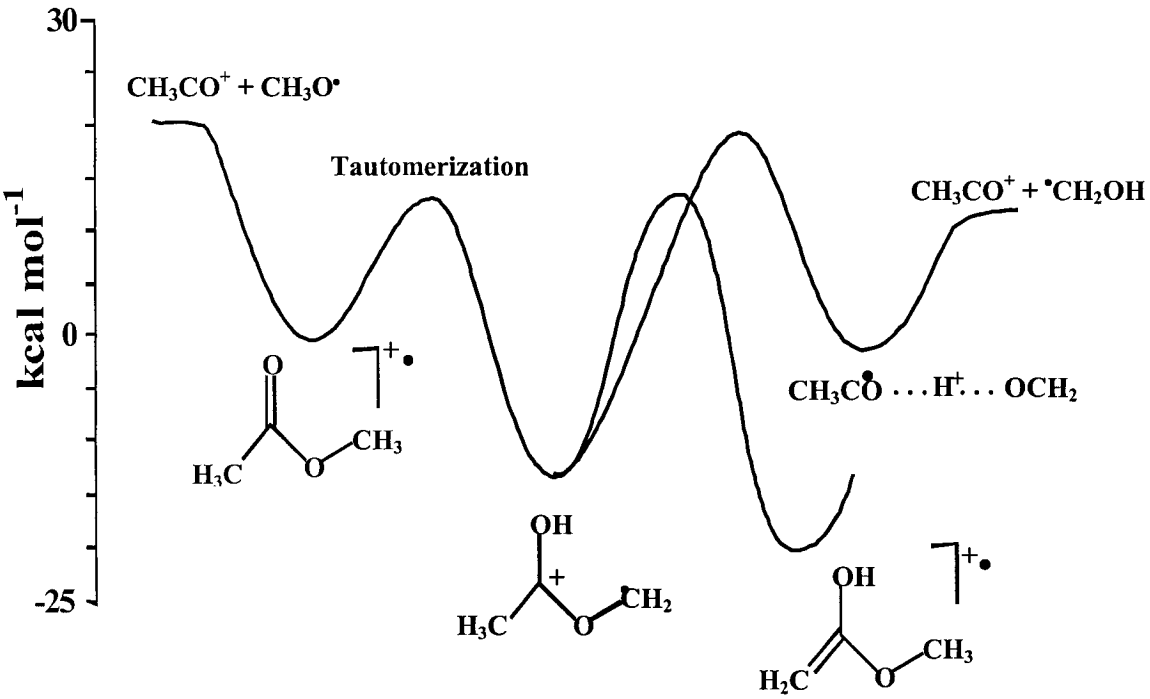

Figure 1.3 Potential Energy Surface for the rearrangement of ionized methylacetate.

The search for meaningful trends in chemical reactivity and their correlation with molecular parameters is one of the fundamental goals of chemistry. One well-established mechanism for the reaction of gas-phase and solution ions is the bimolecular nucleophilic substitution or S_N2 reaction.[5] This type of reaction has been used to study the role of steric

and solvent effects[6] and structure-reactivity correlations[7] in chemical reactivity. While the S_N2 reaction has been studied extensively in solution, interpretation of the results is often complicated by the effects of solvation. It is these solvent effects that result in the large difference between the rates and mechanisms of gas-phase and solution-phase S_N2 reactions. Both experimental and theoretical studies have shown that a gas-phase S_N2 reaction can be characterized by a double-well potential energy surface (PES) with a central barrier separating two ion-molecule complexes;[8-17] this discovery is in sharp contrast with the PES derived for an S_N2 reaction occurring in solution, which consists of a transition state that directly connects reactants and products (Figure 1.4). These differences can be attributed to the effects of solvation. In aqueous solution, the ion-dipole attraction (responsible for the two minima shown below in the gas-phase PES) is nullified by the energy required to partially desolvate the ion, resulting in a unimodal energy profile with a large central barrier.

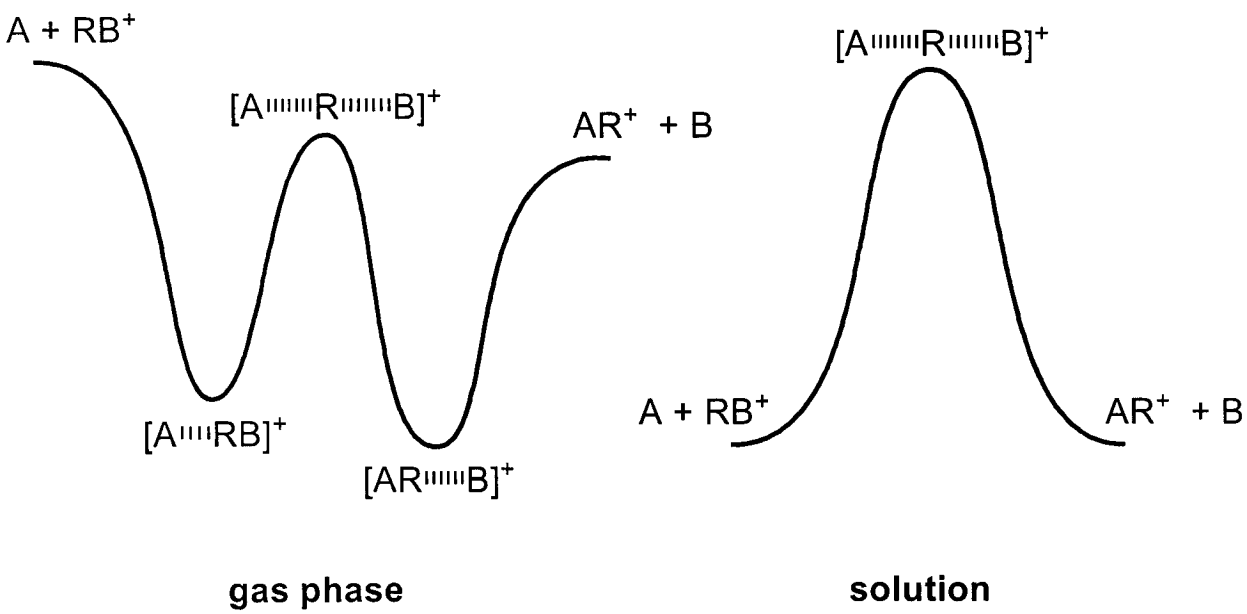

Figure 1.4 Schematic energy profiles highlighting the differences between gas-phase and solution-phase S_N2 reactions.

In the gas-phase, the reactants ($A + RB^+$) initially come together to form an ion-molecule complex ($A\bullet\bullet\bullet RB^+$) followed by the net S_N2 reaction to form a second ion-molecule complex ($AR^+\bullet\bullet\bullet B$) before dissociating into products ($AR^+ + B$). This type of gas-phase reaction was first investigated experimentally by Bohme[16, 17] using the flowing afterglow technique and by Brauman,[14, 18] using the trapped ion, pulsed ion cyclotron resonance (ICR) technique. Based on these observations, Brauman concluded that these reactions are best described by a double well potential with a secondary central barrier and that the variation observed in the reaction rates or reaction efficiencies was primarily due to the variation of the central barrier height. McMahon and co-workers later contributed to the knowledge of these reactions by using a combination of mass spectrometry[8] and theory[19] to probe the characteristics (e.g., transition state barrier heights and ion-dipole well depths) of the gas-phase S_N2 potential energy surface. The rate constants for these ion-molecule reactions were found to vary from collision controlled (10^{-9} cm^3 $molecule^{-1}$ s^{-1})[14, 16] to very slow ($10^{-12} - 10^{-13}$ cm^3 $molecule^{-1}$ s^{-1})[14, 16]. Some ion-molecule reactions will undoubtedly be slower than others and this is due to entropic or steric constraints which are difficult to overcome. The S_N2 reaction in solution is orders of magnitude slower than that occurring in the gas phase; this is due to the preferential solvation of the reactants (principally the ion) over the transition state. Another qualitative feature worth mentioning is that the gas-phase S_N2 reaction barrier frequently has a lower potential energy than the reactants while in the condensed phase, the barrier is higher than the reactants.

Much of mechanistic chemistry has been devoted to understanding the effects of structure and energetics on reactivity and models have been developed to explain these

effects in S_N2 reactions. By studying the S_N2 reaction in the absence of solvent (i.e., the gas phase), intrinsic relations between structure and energetics can be revealed.

The reader may well be familiar with the bimolecular S_N2 reaction that occurs both in the gas-phase[20,21] and in solution. This thesis will however serve to introduce the reader to a unimolecular internal S_N2-type reaction that occurs in the gas-phase. The families of acetonitrile-alcohol and alcohol-alcohol proton-bound pairs have been found to isomerize in the gas-phase to lose water through an internal S_N2-type mechanism. This mechanism was deduced from a combination of mass spectrometry (the dissociation of metastable and collisionally activated cluster ions together with isotopic labelling) and *ab initio* molecular orbital calculations.[22, 23] The potential energy surface (PES) for the $(CH_3CN)(CH_3OH)H^+$ proton-bound pair is shown in Figure 1.5(b); its PES differs slightly from the two-well PES originally proposed by Brauman in that it has an intermediate complex that connects two transition states. The isomerization mechanism of a nitrile-alcohol proton-bound pair proceeds as follows: the reactants come together to form a proton-bound pair $(ACN)(ROH)H^+$ [A,R = alkyl group] in the ion source of the mass spectrometer that subsequently isomerizes to an intermediate ion $(ACN{\bullet\bullet\bullet}R{\bullet\bullet\bullet}OH_2)^+$ via a transition state (which will be referred to as TS_a); the C–O bond in this intermediate ion is then stretched (through a high energy transition state, TS_b) to form a thermodynamically stable isomer $(ACNR)(H_2O)^+$, which then dissociates to lose water. This mechanism (as observed for the acetonitrile-methanol proton-bound pair) may be schematically represented as shown below in Figure 1.5(a) although the energetics of these reactions is typically represented in the form of a potential energy surface (Figure 1.5(b)).

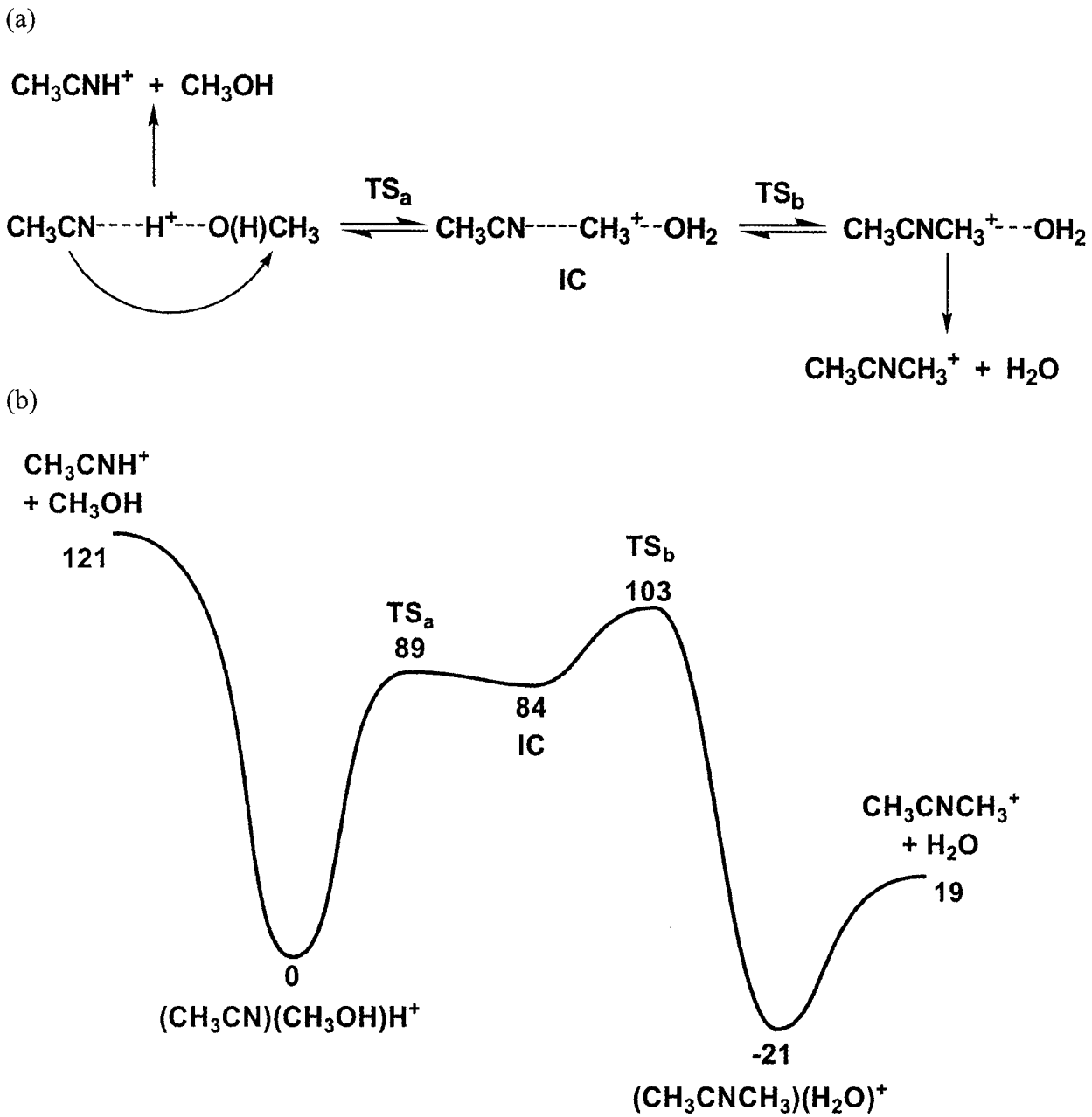

Figure 1.5 (a) Reaction scheme and (b) Potential energy surface for the acetonitrile-methanol proton-bound pair. Relative energies at the MP2/6-31+G(d) level of theory.[24]

1.2.1 Energetics of Dissociation

Over the past few decades, the techniques of mass spectrometry and computational chemistry have become complimentary in the elucidation of the structures of gas-phase ions. Mass spectrometry has been used to identify key features of potential energy surfaces while theoretical calculations have allowed the transition states governing the rearrangement processes of ions to be determined. Theoretical calculations, depending upon the size of the ion and level of theory studied, can be costly in terms of the resources required to successfully complete a geometry optimization. As such, establishing trends based upon the chemical reactivity of an ion and correlating these trends with fundamental molecular parameters such as proton affinity is greatly desired. The successful derivation of an empirical relationship would then allow ion energetics to be determined in the absence of expensive theoretical calculations.

Proton-bound pairs, such as the families of nitrile-alcohol and alcohol-alcohol proton-bound pairs, can undergo simple bond cleavage reactions or isomerize into thermodynamically more stable isomers which then lose water. The energetics of these two pathways is often discussed through the use of a potential energy surface. The dissociation of nitrile and alcohol-containing proton-bound pairs has been discussed empirically in two previous publications. Larson and McMahon[25] derived an expression for the hydrogen bond strength in alcohol-alcohol proton-bound pairs that relates the strength of the hydrogen bond in the pair to the proton affinity of the two molecules involved. Similarly, an empirical expression for the dissociation of nitrile-containing proton-bound pairs was derived by

Mayer;[26] this relationship correlates the binding energy (BE) of nitrile-containing proton-bound pairs with the difference in their proton affinities (ΔPA). These two works have enabled scientists to directly calculate the binding energies of proton-bound pairs from empirical formulae with the knowledge of relative proton affinities, which in itself may eliminate lengthy experimental work. Less work, however, has been done regarding the isomerization pathway. Chapter 3 of this thesis addresses this problem by deriving empirical formulae which may be used for predicting the energetics of the intermediates and transition states of the internal S_N2 reaction occurring in gas-phase proton-bound pairs. By using the combination of tandem mass spectrometry and *ab initio* theory, a relationship that exists between the relative ion peak intensities observed in the tandem mass spectra of proton-bound pairs and their calculated barrier heights was illustrated. This relationship was subsequently refined to three empirical formulae, one for each significant feature on the potential energy surface involved in the isomerization channel. The empirical formulae were developed for the intermediate complex (IC), the first transition state, TS_a, (which connects the proton-bound pair to IC) and the high energy transition state, TS_b, (which joins IC to the thermodynamically stable isomer of the proton-bound pair) and are based upon differences in proton affinities and the number of substituents on the central S_N2 carbon. These relationships (similarly to those discussed above for the dissociation energies) can be useful for quickly predicting an ion's tendency for gas-phase rearrangement.

1.2.2 Entropy of Dissociation

Figure 1.5(b) illustrated the rearrangement of the acetonitrile-methanol proton-bound pair into its thermodynamically more stable isomer. This proton-bound pair may, however, also dissociate via its lowest energy dissociation channel to produce protonated acetonitrile and neutral methanol. Chapter 4 of this work addresses the entropy of activation ($\Delta S^{\ddagger}$) for a single dissociation channel and examines how it changes with molecular functionality and how it relates to ΔS for the reaction. Transition state theory (TST) can be used to determine the tightness or looseness of the transition state molecular configuration as compared to that of the reactants and hence the entropy of activation, $\Delta S^{\ddagger}$. From the thermodynamic version of transition state theory, the Arrhenius pre-exponential factor A can be written in terms of $\Delta S^{\ddagger}$,

$$A = \frac{k_b T}{h} e^{n} e^{\frac{\Delta S^{\ddagger}}{R}} \qquad (1.1)$$

where k_b is Boltzmann's constant, T is temperature, h is Planck's constant, n is the molecularity of the reaction (n = 2 for a bimolecular process), R is the gas constant and $\Delta S^{\ddagger}$ is the entropy of activation. When it comes to a bond scission reaction in a gas-phase ion, $\Delta S^{\ddagger}$ can be measured directly from the temperature dependence of the dissociation. However, due to the large binding energies typical of gas-phase ions and the low pressures in mass spectrometers, it is difficult to sufficiently heat an ion to its dissociation threshold for kinetics measurements. Black-body infrared dissociation (BIRD) is the only practical method for directly measuring the temperature dependence of ion decomposition.[27, 28] The entropy of activation for a bond cleavage reaction can also be obtained by fitting experimental dissociation versus internal energy data. Threshold photoelectron photoion coincidence (TPEPICO) $k(E)$ vs. E data can be modelled directly with RRKM theory to

extract $\Delta S^{\ddagger}$.[29, 30] Threshold collision-induced dissociation (CID) or surface-induced dissociation (SID) experiments can also include $\Delta S^{\ddagger}$ in the modelling of ion dissociation curves.[31, 32]

The kinetic method, originally developed by Cooks, can also be used for estimating $\Delta S^{\ddagger}$ in the dissociation of electrostatically bound complexes.[33] This method is based on the rates of two competitive dissociation channels of mass-selected cluster ions and uses tandem mass spectrometry to extract thermochemical information such as proton affinities. The original implementation of the kinetic method assumed that $\Delta S^{\ddagger}$ for the two competing channels were the same and thus their difference, $\Delta(\Delta S^{\ddagger}) = 0$. In accordance with these assumptions, the following expression was derived:

$$\ln\left(\frac{k_1}{k_2}\right) = \frac{PA\,(B_1) - PA\,(B_2)}{RT_{eff}} \qquad (1.2)$$

where $PA(B_1)$ and $PA(B_2)$ are the proton affinities of B_1 and B_2, respectively, R is the gas constant and T_{eff} is the effective temperature. To examine systems in which entropy effects did not cancel out, modifications were made to the original method[34-38] so that $\Delta(\Delta S^{\ddagger})$ could be obtained from experiments performed at different center-of-mass collision energies. Information about the individual dissociation channel $\Delta S^{\ddagger}$ values cannot be obtained with either the original or extended methods. Cooks and co-workers later introduced an entropy-corrected version of the kinetic method[39] in which the entropy term is explicitly rewritten as $\Delta(\Delta S^{\ddagger})/R = \Delta S_2^{\ddagger}/R - \Delta S_1^{\ddagger}/R$ giving:

$$\ln\left(\frac{k_1}{k_2}\right) - \frac{\Delta S_1}{R} = \frac{PA(B_1) - PA(B_2)}{RT_{eff}} + \frac{\Delta S_2}{R} \qquad (1.3)$$

assuming that $\Delta(\Delta S)$, the relative reaction entropies, and $\Delta(\Delta S^{\ddagger})$ are very similar. The (k_1/k_2) ratio for each pair of compounds is corrected by the entropy term of the reference base. This approach can be used to obtain $\Delta S_2^{\ddagger}$ provided the entropy effect for the competing reaction $(\Delta S_1^{\ddagger})$ is known.

The final experimental method (to be brought to the reader's attention) that is used in the determination of $\Delta(\Delta S^{\ddagger})$ for proton-bound pairs is that of kinetic energy release distribution (KERD).[40] This method, used in conjunction with finite heat bath theory analysis, allows the relative proton affinities of monomeric species to be determined. To obtain $\Delta(\Delta S^{\ddagger})$, experimental KERDs are first fit to yield transition state temperatures according to the equation $p(\varepsilon) = \varepsilon^{l} \exp(-\varepsilon/k_B T^{\ddagger})$ where ε is the kinetic energy release, l is a parameter experimentally fit to range between 0 and 1; k_B is Boltzmann's constant and $T^{\ddagger}$ is the transition state temperature defined by the average kinetic energy passing through the transition state.[41] The following equation is then used to determine $\Delta(\Delta S^{\ddagger})$ from the experimental branching ratio and the two transition state temperatures:

$$\ln\left(\frac{k_1}{k_2}\right) = \frac{\Delta(\Delta S^{\ddagger})}{k_B} + C\ln\left(\frac{T_1^{\ddagger}}{T_2^{\ddagger}}\right) \qquad (1.4)$$

where k_1 and k_2 are the branching ratio for the two monomers, C is the heat capacity of the energized ion, k_B is Boltzmann's constant and $T_1^{\ddagger}$ and $T_2^{\ddagger}$ are the transition state temperatures for the two reactions.

A central question arises when discussing $\Delta S^{\ddagger}$ for a bond cleavage reaction that has no reverse energy barrier and that is the location of the effective transition state. Since there is no saddle point, the rate constant will depend on the molecular configuration corresponding to the minimum sum-of-states along the reaction coordinate. It has been assumed that this variational transition state lies at large internuclear separations and thus $\Delta(\Delta S^{\ddagger})$ is similar to $\Delta(\Delta S)$,[34-39, 42] where ΔS is the thermodynamic reaction entropy change for each of the two competing bond scission reactions. Ervin[43] presented a rigorous analysis of the kinetic method using RRKM theory and placed the effective transition state at the centrifugal barrier to the dissociation and thus $\Delta(\Delta S^{\ddagger})$ was always greater than $\Delta(\Delta S)$ by a relatively small amount, ~ 6 J K^{-1} mol^{-1}. But again, only $\Delta(\Delta S^{\ddagger})$ was investigated, not the $\Delta S^{\ddagger}$ for a single dissociation channel. Drahos and Vekey[42] also assumed very late transition states in their modelling of the kinetic method (and thus $\Delta(\Delta S^{\ddagger}) = \Delta(\Delta S)$). These assumptions will be investigated in this chapter by using microcanonical variational transition state theory (μ-VTST) to model the unimolecular dissociation of a series of proton-bound acetonitrile-alcohol pairs $(CH_3CN)(XOH)H^+$ (where X = CH_3, CH_3CH_2, $CH_3CH_2CH_2$ and $(CH_3)_2CH$) and to extract the entropy of activation for the bond scission reactions. Comparisons will also be made between the differences in thermodynamic entropies, $\Delta(\Delta S)$, of the two dissociation channels for each complex ion as well as the differences in entropies of activation, $\Delta(\Delta S^{\ddagger})$, for the two dissociating pathways.

1.2.3 Role of Excited States in Ion Dissociation

Chapters 5 and 6 will deal with the gas-phase nitrosation of benzene whose chemistry has been the subject of extensive computational[44-46] and experimental investigation.[47-51] Nitrosation, an electrophilic aromatic substitution, can be achieved in solution by a variety of reagents, including nitrous acid, alkyl nitrites, and nitrosyl acetate[52-54] while ICR mass spectrometry has been the principal technique used to investigate the behaviour of nitrosated aromatic ions in the gas phase.[47-49] Aromatic nitrosation occurs via the general equation:

$$XNO^+ + C_6H_6 \rightarrow X + C_6H_6NO^+ \qquad (1.5)$$

where X can be substituents such as *i*-C_3H_7Cl, CH_3O and t-BuO.[47, 49-51] The results of photodissociation experiments on the $(C_6H_6)(NO)^+$ adduct suggest that the product from reaction (1.5) is a π-complex that does not isomerize into a σ-complex or O-protonated nitrosobenzene.[47, 48] Cacace and Ricci[49] have proposed an alternate method of aromatic nitrosation whereby the nitrosation occurs in the ion-neutral complex formed upon addition of a gaseous arenium ion, $RC_6H_5^{+\bullet}$ (R = H,CH_3) to a neutral nitrosating species, XONO (X = H,CH_3). The complex rearranges to form $RC_6H_5(XONO)H^{+\bullet}$ which then loses XOH to form $(RC_6H_5)(NO)^+$. In all of these studies it is assumed (where even mentioned) that the complexes are generated in their ground, singlet spin-state, $(C_6H_6)(NO)^+$. Ionization of the free radical NO in the ion source of a mass spectrometer by electron or photoionization can produce both NO^+ ($X\ ^1\Sigma^+$) and NO^+ ($a\ ^3\Sigma^+$) which could lead to the formation of both singlet

and triplet complexes of $(C_6H_6)(NO)^+$.[50] In addition, the reaction of $C_6H_6^{+\bullet}$ with NO may also lead to triplet-state complexes.

Theoretical studies[44-46, 51] have been done to complement gas-phase experiments and it has been shown that the interconversion of nitrosated benzene into its isomer, protonated nitrosobenzene, $C_6H_5NOH^+$, cannot compete with dissociation on the microsecond time scale. Until now, all theoretical studies have assumed that the nitrosated benzene complex, $(C_6H_6)(NO)^+$, resides in its singlet state. Most studies of ion-molecule reactions assume that the reactant ions are produced in (or quickly relax into) and react from their ground electronic states. The justification for these assumptions typically relies upon the use of gentle ionization techniques and bath gases since direct spectroscopic confirmation is not always feasible.[55, 56] Most electronic excited states have very short radiative lifetimes (<1μs) compared to typical collision times and so one usually assumes that the reactivity of these ions is governed by the properties of their electronic ground state. This assumption fails for several light ions (e.g. NO^+) whose electronic states have much longer radiative lifetimes (> 1ms). The energetically lowest singlet state of NO^+ is the $X\,^1\Sigma^+$ ground state and the lowest triplet state is the $a^3\Sigma^+$ state, which lies 15.66 eV above the ground state.[57] The $a^3\Sigma^+$ state is the first excited state and is metastable by virtue of the spin-selection rule (Δspin=0) with a radiative lifetime of 740 ms.[58, 59] Since this state lies 15.66 eV above the ground state, it is likely to be much more reactive than ground state NO^+ ($X\,^1\Sigma^+$).[60] It has been suggested that ionization, either by electron impact or photoionization, should form significant amounts of $NO^+(a^3\Sigma^+)$ and O'Keefe and McDonald[61] estimate that two-thirds of the total NO^+ ion population formed by 100 eV electron impact will be $NO^+(a^3\Sigma^+)$.

In particular, chapter 5 will describe the investigation of the unimolecular dissociation of the ionic complexes of NO with aromatic molecules (formed by electron ionization at relatively high ion source pressures in a mass spectrometer); evidence was found for the participation of their excited singlet and triplet states. The aromatic molecules studied were benzonitrile (C_6H_5CN), benzene (C_6H_6), pyridine (C_5H_5N), thiophene (C_4H_4S) and furan (C_4H_4O). Calculations of the structure, electron distribution and binding energies of the ground state singlet and lowest energy triplet states have been used to help in the interpretation of the mass spectra. Chapter 6 involves a theoretical assessment that was done to probe which theory and basis set is most appropriate for describing the geometries, zero-point energies (ZPE) and binding energies of the singlet and triplet ionic complexes of NO and benzene. The results were extended to obtain accurate thermochemistry of the ionic complexes of NO with pyridine, furan, thiophene and benzonitrile.

References

1. J. L. Holmes, A. A. Mommers, J. E. Szulejko, and J. K. Terlouw, "Two new stable $C_3H_8O^+$ isomers: the radical cations $C_3H_6OH_2^{+\bullet}$", *J. Chem. Soc. Chem. Comm.*, 165 (1984).
2. G. Bouchoux, N. Choret, and R. Flammang, "Dehydration of ionized propanol in the gas-phase", *Int. J. Mass Spectrom.* **195/196**, 225 (2000).
3. J. L. Holmes and J. K. Terlouw, "Does the unimolecular dissociation of ionized methylacetate produce CH_3O or CH_2OH radicals?" *Org Mass spectrom.* **21**, 776 (1986).

4. N. Heinrich, J. Schmidt, H. Schwarz, and Y. Apeloig, "On the mechanism of $(C,H_3,O)^{\bullet}$ radical loss from ionized methyl acetate. An *ab initio* Molecular Orbital study", *J. Am. Chem. Soc.* **109**, 1317 (1987).

5. S. S. Shaik, H. B. Schlegel, and S. Wolfe, *Theoretical aspects of physical organic chemistry: The S_N2 mechanism*. Wiley & Sons, New York (1992).

6. C. K. Regan, S. L. Craig, and J. I. Brauman, "Steric effects and solvent effects in ionic reactions", *Science* **295**, 2245 (2002).

7. B. D. Wladkowski, J. L. Wilbur, and J. I. Brauman, "Intrinsic structure-reactivity relationships in gas phase S_N2 reactions: Identity exchange of substituted benzyl chlorides with chloride ion", *J. Am. Chem. Soc.* **116**, 2471 (1994).

8. C. Li, P. Ross, J. E. Szulejko, and T. B. McMahon, "High-pressure mass spectrometric investigations of the potential energy surfaces of gas-phase S_N2 reactions", *J. Am. Chem. Soc.* **118**, 9630 (1996).

9. M. J. Pellerite and J. I. Brauman, "Intrinsic barriers in nucleophilic displacements", *J. Am. Chem. Soc.* **102**, 5993 (1980).

10. M. J. Pellerite and J. I. Brauman, "Intrinsic barriers in nucleophilic displacements. A general model for intrinsic nucleophilicity toward methyl centres", *J. Am. Chem. Soc.* **1983**, 2672 (1983).

11. S. Wolfe, D. J. Mitchell, and H. B. Schlegel, "Theoretical studies of S_N2 transition states. 2. Intrinsic barriers, rate-equilibrium relationships and the Marcus equation", *J. Am. Chem. Soc.* **103**, 7694 (1981).

12. B. D. Wladkowski, K. F. Lim, W. D. Allen, and J. I. Brauman, "The S_N2 identity exchange reaction $ClCH_2CN$ + Cl : experiment and theory", *J. Am. Chem. Soc.* **1992**, 9136 (1992).

13. J. Ren and J. I. Brauman, "Energy deposition in S_N2 reaction products and kinetic energy effects on reactivity", *J. Phys. Chem A* **106**, 3804 (2002).

14. W. N. Olmstead and J. I. Brauman, "Gas-Phase nucleophilic displacement reactions", *J. Am. Chem. Soc.* **99**, 4219 (1977).

15. M. L. Chabinyc, S. L. Craig, C. K. Regan, and J. I. Brauman, "Gas-phase ionic reactions: Dynamics and mechanism of nucleophilic displacements", *Science* **279**, 1882 (1998).

16. D. K. Bohme and L. B. Young, "Kinetic studies of the reactions of oxide, hydroxide, alkoxide, phenyl, and benzylic anions with methyl chloride in the gas phase at 22.5degC", *J. Am. Chem. Soc.* **92**, 7354 (1970).

17. D. K. Bohme, G. I. Mackay, and J. D. Payzant, "Activation energies in nucleophilic displacement reactions measured at 296°K in vacuo", *J. Am. Chem. Soc.* **96**, 4027 (1974).

18. J. I. Brauman, W. N. Olmstead, and C. A. Lieder, "Gas-phase nucleophilic displacement reactions", *J. Am. Chem. Soc.* **96**, 4030 (1974).

19. T. D. Fridgen and T. B. McMahon, "Enthalpy barriers for asymmetric S_N2 alkyl cation transfer reactions between neutral and protonated alcohols", *J. Phys. Chem. A* **107**, 668 (2003).

20. J. A. D. McCormack and P. M. Mayer, "Ion/molecule reaction kinetics using a modified Finnigan GCQ ion trap mass spectrometer: the energetics of the dehydration of proton-bound dimers." *Int. J. Mass Spectrom.* **207**, 183 (2001).

21. J. A. D. McCormack and P. M. Mayer, "The energetics of the dehydration of nitrile-alcohol proton-bound dimers from ion/molecule reaction kinetics", *Int. J. Mass Spectrom.* **207**, 195 (2001).

22. R. A. Ochran, A. Annamalai, and P. M. Mayer, "Unimolecular reactions of proton-bound cluster ions: Competition between dissociation and isomerization in the ethanol-acetonitrile dimer", *J. Phys. Chem A* **104**, 8505 (2000).

23. T. D. Fridgen, J. D. Keller, and T. B. McMahon, "Direct experimental determination of the energy barriers for methyl cation transfer in the reactions of methanol with protonated methanol, protonated acetonitrile and protonated acetaldehyde: a low pressure FTICR study", *J. Phys. Chem. A* **105**, 3816 (2001).

24. R. A. Ochran and P. M. Mayer, "Ion rearrangement at the beginning of cluster formation: methyl substitution effects on the internal S_N2 reaction in the proton-bound dimers of acetonitrile and alcohols", *Eur. J. Mass Spectrom.* **7**, 267 (2001).

25. J. W. Larson and T. B. McMahon, "Formation, thermochemistry, and relative stabilities of proton-bound dimers of oxygen n-donor bases from ion cyclotron resonance solvent-exchange equilibria measurements", *J.Am.Chem. Soc* **104**, 6255 (1982).

26. P. M. Mayer, "Structures and binding energies of proton-bound pairs of HCN and CH_3CN with NH_3, H_2O, HF, CH_3NH_2, CH_3OH and CH_3F", *J. Phys. Chem. A* **103**, 5905 (1999).

27. R. C. Dunbar and T. B. McMahon, "Activation of unimolecular reactions by ambient blackbody radiation", *Science* **279**, 194 (1998).

28. R. C. Dunbar, "BIRD (Blackbody infrared radiative dissociation): Evolution, principles and applications", *Mass Spec. Rev.* **23**, 127 (2004).

29. T. Baer, "Dissociation dynamics of energy selected ions", *Adv. Chem. Phys.* **64**, 111 (1986).

30. T. Baer and P. M. Mayer, "Statistical Rice-Ramsperger-Kassel-Marcus-quasiequilibrium theory calculations in mass spectrometry", *J. Am. Soc. Mass Spectrom.* **8**, 103 (1997).

31. P. B. Armentout and M. T. Rodgers, "Threshold collision-induced dissociation", *J. Phys. Chem A.* **104**, 2238 (2000).

32. J. Laskin, T. H. Bailey, and J. H. Futrell, "Fragmentation energetics for angiotensin II and its analogs from time- and energy-resolved surface-induced dissociation studies", *Int. J. Mass Spectrom.* **234**, 89 (2004).

33. S. A. McLuckey, D. Cameron, and R. G. Cooks, "Proton affinities from dissociations of proton-bound dimers", *J. Am. Chem. Soc.* **130**, 1313 (1981).

34. X. Cheng, Z. Wu, and C. Fenselau, "Collision energy dependence of proton-bound dimer dissociation: entropy effects, proton affinities and intramolecular hydrogen-bonding in protonated peptides." *J. Am. Chem. Soc.* **115**, 4844 (1993).

35. Z. Wu and C. Fenselau, "Gas-Phase basicities and proton affinities of lysine and histidine measured from the dissociation of proton-bound dimers", *Rapid Commun. Mass Spectrom.* **8**, 777 (1994).

36. B. A. Cerda and C. Wesdemiotis, "Li^+, Na^+ and K^+ binding to the DNA and RNA Nucleobases. Bond Energies and Attachment sites from the dissociation of metal ion-bound heterodimers." *J. Am. Chem. Soc.* **118**, 11884 (1996).

37. B. A. Cerda, S. Hoyau, G. Ohanessian, and C. Wesdemiotis, "Binding to cyclic and linear dipeptides. Bond energies, entropies of Na^+ complexation and attachment sites from the dissociation of Na^+-bond heterodimers and *ab initio* calculations." *J. Am. Chem. Soc.* **120**, 2437 (1998).

38. B. A. Cerda and C. Wesdemiotis, "Gas Phase copper (I) ion affinities of valine, lysine and arginine based on the dissociation of Cu^+-bound heterodimers at varying internal energies." *Int. J. Mass Spectrom.* **185/186/187**, 107 (1999).

39. X. Zheng and R. G. Cooks, "Thermochemical determinations by the kinetic method with direct entropy correction", *J. Phys. Chem A* **106**, 9939 (2002).

40. J. J. Hache, J. Laskin, and J. H. Futrell, "Relative proton affinities from kinetic energy release distributions for dissociation of proton-bound dimers", *J. Phys. Chem A* **106**, 12051 (2002).

41. C. E. Klotz, *Z. Phys. D* **21**, 335 (1991).

42. L. Drahos and K. Vekey, "Entropy evaluation using the kinetic method: is it feasible?" *J. Mass Spectrom.* **38**, 1025 (2003).

43. K. M. Ervin, "Microcanonical analysis of the kinetic method. The meaning of the "apparent entropy"", *J. Am. Soc. Mass Spectrom.* **13**, 435 (2002).

44. S. Skokov and R. A. Wheeler, "Oxidative aromatic substitutions: Hartree-Fock/Density functional and *ab initio* molecular orbital studies of benzene and toluene nitrosation", *J. Phys. Chem A* **103**, 4261 (1999).

45. S. R. Gwaltney, S. V. Rosokha, M. Head-Gordon, and J. K. Kochi, "Charge-transfer mechanism for electrophilic aromatic nitration and nitrosation via the convergence of *ab initio* molecular orbital and Marcus-Hush theories with experiments", *J. Am. Chem. Soc.* **125**, 3273 (2003).

46. K. Raghavachari, J. Reents, W.D., and R. C. Haddon, "Gas-phase nitrosation of benzene: Theoretical investigations", *J. Computational Chem.* **7**, 265 (1986).

47. J. Reents, W.D. and B. S. Freiser, "Gas-phase nitrosation of benzene. Implications for solution electrophilic aromatic substitution reactions", *J. Am. Chem. Soc.* **102**, 271 (1980).

48. J. Reents, W.D. and B. S. Freiser, "Gas-phase binding energies and spectroscopic properties of NO^+ charge transfer complexes", *J. Am. Chem. Soc.* **103**, 2791 (1981).

49. F. Cacace and A. Ricci, "Gas-phase reaction of nitrous acid and methyl nitrite with arenium ions. A new route to electrophilic aromatic nitrosation", *Chem. Phys. Lett.* **253**, 184 (1996).

50. A. D. Williamson and J. L. Beauchamp, "Ion-molecule reactions of NO^+ with organic molecules by ion cyclotron resonance spectroscopy", *J. Am. Chem. Soc.* **97**, 5714 (1975).

51. N. Dechamps, P. Gerbaux, R. Flammang, G. Bouchoux, P.-C. Nam, and M.-T. Nguyen, "Gas phase nitrosation of substituted benzenes", *Int. J. Mass Spectrom.* **232**, 31 (2004).

52. S. M. Hubig and J. K. Kochi, "Direct observation of the Wheland intermediate in electrophilic aromatic substitution. Reversible formation of nitrosoarenium cations", *J. Am. Chem. Soc.* **122**, 8279 (2000).

53. E. Bosch and J. K. Kochi, "Direct nitrosation of aromatic hydrocarbons and ethers with the electrophilic nitrosium cation", *J. Org. Chem* **59**, 5573 (1994).

54. B. C. Challis, R. J. Higgins, and A. J. Lawson, "The chemistry of nitroso-compounds. Part 11. The nitrosation of substituted benzenes in concentrated acids", *J.Chem. Soc. Perkin Trans. 2*, 1831 (1972).

55. E. Ferguson, "Ion-molecule reactions", *Annu. Rev. Phys. Chem.* **26**, 17 (1975).

56. F. C. Fehsenfeld, "Diagnostics of the flowing afterglow", *Int. J. Mass Spectrom. Ion Phys.* **16**, 151 (1975).

57. D. L. Albritton, A. L. Schmeltekopf, and R. N. Zare, "Potential energy curves for NO^+", *J. Chem. Phys* **71**, 3271 (1979).

58. R. Wester, K. G. Bhushan, N. Altstein, D. Zajfman, O. Heber, and M. L. Rappaport, "Radiative lifetime measurement of the a^3S^+ metastable state of NO^+ using a new type of electrostatic ion trap", *J. Chem. Phys* **110**, 11830 (1999).

59. A. G. Calamai and K. Yoshino, "Radiative lifetimes of the triplet metastable state of NO^+", *J. Chem. Phys* **101**, 9480 (1994).

60. I. Dolan, F. C. Fehsenfeld, and D. L. Albritton, "Rate constants for the reactions of metastable NO^+ (triplet) with SO_2, CO_2, CH_4, N_2, D_2 and O_2 at relative kinetic energies 0.04-2.5eV", *J.Chem. Phys.* **71**, 3280 (1979).

61. A. O'Keefe and J. R. McDonald, "Radiative lifetimes and kinetic studies of metastable NO^+ and O_2^+", *Chem. Phys.* **103**, 425 (1986).

CHAPTER 2

CONCEPTS AND TECHNIQUES EMPLOYED IN THE STUDY OF GASEOUS IONS

2.1 Introduction

This chapter will provide the reader with some background into the field of gas-phase ion chemistry and introduce some of the experimental and theoretical techniques that are employed in the study of gaseous ions. The first part of this chapter will involve a discussion of gas-phase ion chemistry, with a focus on the role of internal energy in ion processes. The second part will comprise a brief discussion of statistical theories (e.g., RRKM and variational transition state theory) and their applications to mass spectrometry. The final component of this chapter will consist of a brief description of computational methods used in the study of gas-phase ions.

2.2 The Role of Internal Energy in Gas-Phase Ion Chemistry

The chemistry of an ion depends on its internal energy. To produce a certain fragmentation product from a precursor ion, the precursor ion must have sufficient internal energy to produce the desired product. To illustrate this fact, consider an ion, M^+, which has an energy P. With this energy, M^+ can only access reaction channels A, B and C (Figure 2.1) since the ion has insufficient internal energy to access the reaction products formed via

channels D and E. The relative importance of A-C will change with internal energy since the rate of each process varies with energy in a unique fashion.

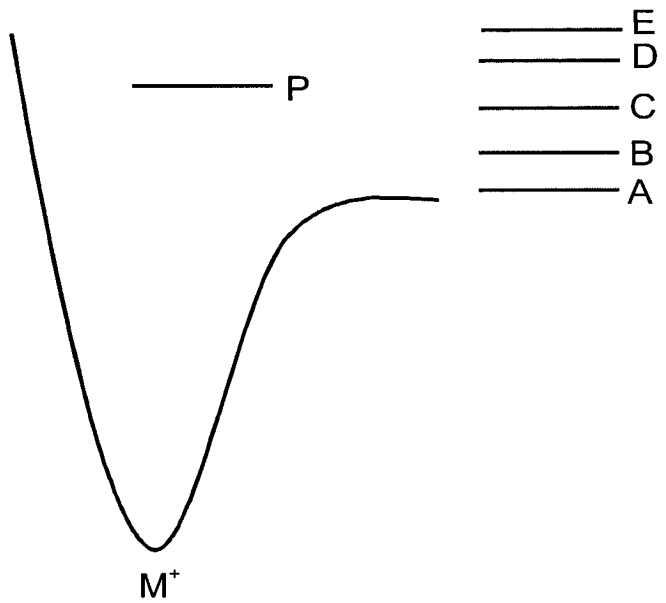

Figure 2.1 Reaction channel accessibility of an ion M^+ with internal energy P as a function of ion internal energy.

2.3 The Isomerization of Gas-Phase Ions

Depending upon the internal energy of an ion, isomerization reactions may also occur since energized molecular and fragment ions are not only limited to decomposition. Upon ionization, a wide range of excess internal energies is transferred to the ion and so it is also possible for an ion to rearrange to various isomeric structures, of classical or non-classical form. These isomerization reactions can greatly complicate the interpretation of mass spectra and thus some understanding of the parameters involved is very important. The relative energy barriers for dissociation (E_{diss}) and isomerization (E_{iso}) are the

parameters that principally determine whether and to what extent an ion A^+ rearranges to an isomeric ion B^+ at a given internal energy E. Several different scenarios are illustrated in Figure 2.2.

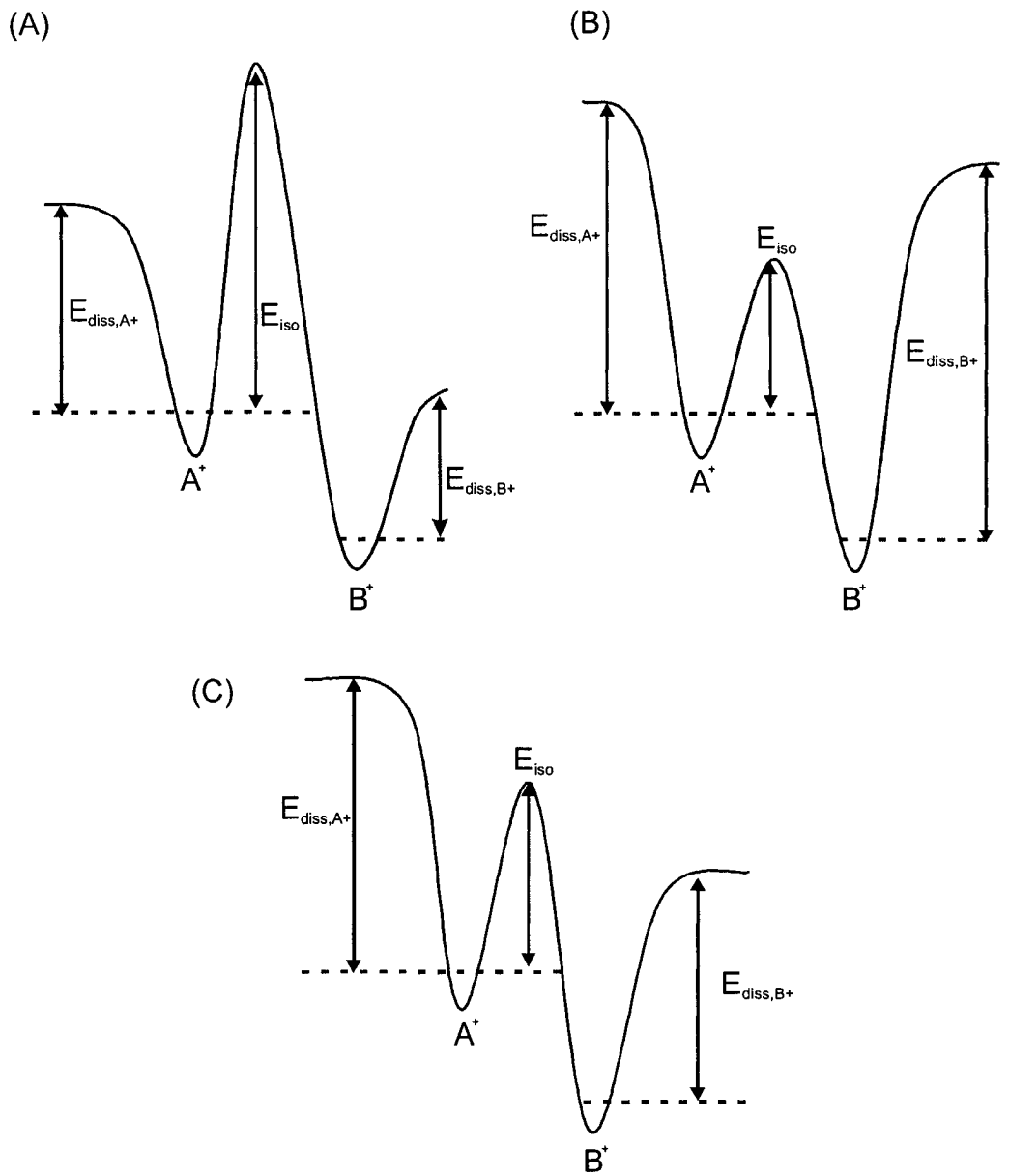

Figure 2.2 Potential Energy Diagrams featuring possible isomerization between ions A^+ and B^+.

In case (a), $E_{iso} >> E_{diss}$ and so no isomerization is possible below the threshold energy for dissociation and in general, even above this threshold, decompositions will occur much faster than isomerization (due to the greater sum-of-states in the corresponding activated complexes). In case (b), where $E_{iso} << E_{diss}$, there will be a mixture of rapidly interconverting structures, A^+ and B^+ at internal energies above E_{iso}. At increased internal energies, decomposition also becomes possible. Since decomposition has been preceded by a number of interconversions, the original connectivity of the atoms with respect to one another may have been altered several times resulting in partial or full randomization of the initial structure. Based on these two cases, isomerization will not hinder the structural elucidation of A^+ and B^+ in case (a) while in case (b), the investigation of the dissociation of these ions will give no information unique to one structure. Intermediate situations between cases (a) and (b) are also possible. In case (c), A^+ must isomerize to B^+ prior to dissociation and thus both A^+ and B^+ will generate similar mass spectral results.

2.4 The Use of RRKM Theory in Mass Spectrometry

We can determine the rate constant at a particular internal energy by modelling the dissociation of an ion using statistical theories; the theory applied in this thesis is the Rice-Rampsberger-Kassel-Marcus quasi-equilibrium theory (RRKM/QET).[1-4] These two theories (i.e., RRKM and QET) were independently developed around the same time and are now accepted to be the same theory. For simplicity, the RRKM/QET theory will simply be referred to as RRKM theory in this thesis. This statistical theory assumes that energy is statistically distributed among all modes throughout the reactions and that the lifetimes of

the intermediates along the reaction path are sufficiently long to allow for the necessary energy redistribution (a more complete description of the assumptions will be provided later). Mass spectrometry is a useful tool for testing the assumptions of this theory since reactions occur in collision-free conditions (isolated reactants and products), and the ionic species can be selected and identified with high specificity.[5]

RRKM theory[6] was developed as a means of calculating the rate constant for a unimolecular reaction for an ion (or molecule) at a given internal energy, E; its rate expression is proportional to the ratio between the number of states in the transition state, $N^{\ddagger}$, above the activation energy, E_0, and the density of states in the reactant at a given energy, $\rho(E)$. Before we get into a derivation of RRKM theory,[7] it seems appropriate to provide the reader with some background information into sums and densities of states so that they may have a clear understanding of these terms. The density of states, $\rho(E)$, is defined as the number of quantum states at energy E per unit energy (expressed in units of energy^{-1}) while the sum-of-states, N(E), is defined as the total number of quantum states having an energy equal to or less than E and bears dimensionless units. Both functions are linked via the relationship, $\rho(E) = dN(E)/dE$. The evaluation of these terms requires knowledge of the vibrational frequencies (and in some treatments, of rotational constants) of the molecular ion and of the transition state. Experimental data are sometimes available for the former but not for the latter. Therefore, the missing information can only be derived from estimates, or more reliably from *ab initio* molecular orbital calculations. With this knowledge of sums and densities of states, we can proceed with the theoretical derivation of RRKM theory.

Let us consider a polyatomic molecular ion with a well-defined internal energy E and assume that its potential energy surface is characterized by a saddle point having the energy E_0. If we analyze the situation when the system has the geometry of the saddle point, the total internal energy E can be partitioned as follows. A certain amount of translational energy ε will be transferred to the reaction coordinate with the remainder, $E-E_0-\varepsilon$, being stored in the subsystem formed by the remaining 3N-7 degrees of freedom, i.e., the transition state (Figure 2.3). This remainder is the energy available to be statistically distributed among the modes of the transition state.

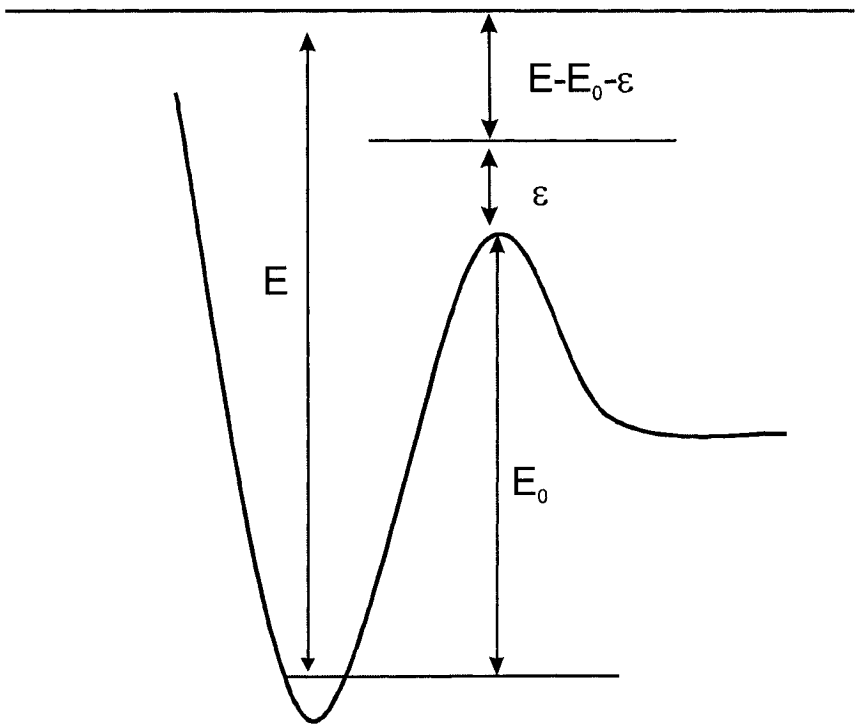

Figure 2.3 Reaction coordinate for a dissociation with a real barrier. E and E_0 are the total ion energy and activation energy. ε is the translational energy in the reaction coordinate. The remaining energy, $E - E_0 - \varepsilon$, is the energy available to be statistically distributed.[6]

If we let ρ_t, $\rho^{\ddagger}$, and ρ respectively represent the density of states associated with the translational motion in the reaction coordinate, the density of states of the transition state and of the reactant, then the number of the molecular ions per cm^{-1} that are apt to react will as a result be equal to $\rho^{\ddagger}(E\text{-}E_0\text{-}\varepsilon)\ \rho_t(\varepsilon)/\ \rho(E)$.[7] In order to obtain a reactive flux, however, this fraction must be multiplied by the frequency of crossing the saddle point region in the direction of reactants to products. The dissociation rate constant, $k(E)$, is then obtained by integrating the reactive flux over all possible values of the translational energy in the reaction coordinate ε, which can vary from zero to its maximum value $E\text{-}E_0$. Hence, the rate constant is equal to[7]

$$k(E) = \frac{\int_0^{E-E_0} \rho^{\ddagger}(E - E_0 - \varepsilon)d\varepsilon}{h\rho(E)} \equiv \frac{\sigma}{h}\frac{N^{\ddagger}(E - E_0)}{\rho(E)} \quad (2.1)$$

In the above equation, σ is the symmetry number, h is Planck's constant, $N^{\ddagger}(E\text{-}E_0)$ is the sum-of-states of the transition state and represents the total number of levels of the transition state having a nonfixed energy less than or equal to $E\text{-}E_0$. In statistical terms, this represents the number of ways the reacting ion can cross the dividing surface to products (i.e., probability that a reaction will proceed to products) and $\rho(E)$, the reactant ion density of states at an energy E, reflects the probability that the energy in the ion will "get lost" among the various rotational-vibrational modes and not find its way into the critical mode responsible for the taking the reaction over the col (i.e., barrier responsible for reaction). As a result, $k(E)$ increases with increasing $N^{\ddagger}$ and decreases with increasing $\rho(E)$.

The reader might raise the question of why the numerator is a sum-of-states while that of the denominator is a density; the reason is the following.[6] At the transition state, a portion of the ion's total energy is channelled into the critical coordinate (e.g., the C—H bond for the dissociation of the benzene ion) responsible for taking the reaction to products. For this bond to dissociate, at least E_0 of energy must be present within this critical C—H bond. If we have just enough energy to pass toward the products, we would have a total energy of E - E_0 left to distribute to the other 29 vibrational modes in the benzene ion. This represents one way to pass through the transition state. We can represent its contribution to the total rate constant by the first term in the following expression:[6]

$$k(E,\varepsilon) = \frac{\rho^{\ddagger}(E-E_0)}{h\rho(E)} + \frac{\rho^{\ddagger}(E-E_0-\varepsilon_1)}{h\rho(E)} + \frac{\rho^{\ddagger}(E-E_0-\varepsilon_2)}{h\rho(E)} + \ldots \quad (2.2)$$

The second and subsequent terms involve passing through the transition state with energy ε above the required minimum energy of E_0. Because the reaction coordinate at the transition state consists of translational energy of the departing fragments, we can also think of this energy ε as the translational energy of the fragments. Thus the total energy of the transition state $E - E_0$ is partitioned between the translational energy ε and the remaining internal energy $E - E_0 - \varepsilon$. If we now add up all of the terms in the numerators of equation (2.2) we will obtain a sum-of-states that is thus the sum of states from 0 to $E - E_0$.

At this time, a description of some of the assumptions behind the formulation of the RRKM theory will be given:[8]

1. The neutral molecule is first ionized to a collection of electronic states of the molecular ion. The population of these excited states is then transferred to the ground state of the molecular ion through very fast radiationless transitions on a time scale of the order of 10^{-14} to 10^{-13} s. After this ultrafast state, the electronic excitation has completely relaxed and the available internal energy is exclusively stored in the vibrational and rotational degrees of freedom of the ground state molecular ion.

2. During the following picoseconds, the anharmonicity of the vibrations lead to further energy transfer among normal modes of the molecular ion. This process, denoted intramolecular vibrational energy redistribution, is assumed to be so efficient that the total internal energy is rapidly fully randomized, i.e., statistically redistributed over the active degrees of freedom. Chemical processes are assumed to occur only after the available internal energy is statistically redistributed.

3. A reaction is assumed to be characterized by the existence of a point of no return, i.e., by a critical configuration for dissociation. This assumption is formulated in terms of a critical hypersurface that divides the phase space of the molecular ion into two regions: one associated with the reactant and the other with the products. Once an ion crosses the dividing surface of the products, it is assumed to never recross it and to asymptotically reach an infinite value of the reaction coordinate, thereby describing the generation of products. The reaction rate is then the outward flux across a critical surface in the direction of the products.

The evaluation of the RRKM expression typically involves extensive *ab initio* calculations. In order to do so, the reaction mechanism must first be determined, followed by the identification of the transition state. Once the transition state has been identified, its energy E_0 needs to be calculated as well as its 3N-7 vibrational frequencies and three rotational constants. Similarly, the 3N-6 frequencies and three rotational constants of the molecular ion must also be determined. Beyer and Swinehart[9] developed an efficient algorithm, known as the direct count method, to carry out a direct count of the harmonic vibrational energy levels. The FORTRAN code for the direct count method may be found in Appendix A of this thesis. Although the programming is quite simple, it had three initial drawbacks that should be mentioned. First, this method is the most time consuming approach, which becomes a problem when dealing with large ions. Second, in most calculations, one is interested in the density or sum-of-states at a few energies that are well above the minimum for dissociation; in the exact count method, however, one is obliged to calculate these functions from 0 up to the maximum energy of interest. Third, each frequency is treated separately so that frequencies cannot be bunched to save time in calculations. Despite the discussed limitations, modern computers have made the limitations of the direct count algorithm relatively unimportant. Two other methods (which are beyond the scope of this thesis) are also used: the Whitten-Rabinovitch method[10, 11] and the method of steepest descent.[12]

2.5 Entropy of Activation

The microcanonical version of transition state theory is often replaced by a canonical expression of the rate constant (i.e., involving a temperature that is arbitrarily equated to 600K, for example) when describing ions that dissociate in a mass spectrometer. This may seem inappropriate since reactions occurring in a mass spectrometer are not thermally activated and are studied under collision-free conditions. However, the advantage is that canonical rate constants can be parameterized through two physically meaningful parameters: the critical energy E_0 and the thermal entropy of activation, $\Delta S^{\ddagger}$. In order to obtain $\Delta S^{\ddagger}$, vibrational frequencies are required for both the molecular ion and the transition state.[6]

The magnitude of $\Delta S^{\ddagger}$ (including the sign) provides a quantitative measure of the degree of tightness or looseness of the transition state and is a convenient way to describe the nature of a reaction.[6] Transition states that are less ordered ("loose") than the reactant ion are characterized by positive $\Delta S^{\ddagger}$ values. Simple bond cleavage reactions typically have loose transition states. Transition states that are more ordered than the reactant ion have negative values of $\Delta S^{\ddagger}$; these "tight" transition states are usually associated with rearrangement processes. If the vibrational frequencies of both the reactant ion and transition state are known, then the nature of the process may be inferred; if however, the nature of the process is known, the transition state frequencies can be estimated (as opposed to being calculated) such that $\Delta S^{\ddagger}$ values of the appropriate sign may be obtained. The entropy of activation is given by the expression

$$\Delta S^{\ddagger} = k_B \ln \frac{Q^{\ddagger}}{Q} + \frac{U^{\ddagger} - U}{T} = k_B \ln \frac{\Pi q_i^{\ddagger}}{\Pi q_i} + \frac{U^{\ddagger} - U}{T} \quad (2.3)$$

where k_B is Boltzmann's constant, U is the average internal energy, T is temperature, Q is the total partition function $q_1q_2q_3...q_n$, and

$$q_i = \frac{1}{1-\exp(-h\nu_i / k_B T)} \qquad (2.4)$$

where h is Planck's constant and ν_i are the vibrational frequencies. The average internal energies can be calculated from the usual formulae by using the vibrational partition functions. Typically, $\Delta S^{\ddagger}$ values are reported at specific temperatures, usually 600 or 1000 K.

The effects of both E_0 and $\Delta S^{\ddagger}$ on the rate constant as a function of energy are complimentary. The E_0 is largely responsible for the magnitude of k(E) (Figure 2.4a) while $\Delta S^{\ddagger}$ is largely responsible for the slope (Figure 2.4b). As observed in Figure 2.4a, the entropy of activation for both channels is the same but the activation energies (E_0) differ with the activation energy of channel A being lower than that of channel B. Tight transition states (such as rearrangement processes) have k(E) curves that increase gradually with increasing energy whereas loose transition states, which are typically bond cleavage processes, have k(E) curves that increase more rapidly. The entropy of activation for a loose transition state is larger than that of a tight transition state. As can be seen in Figure 2.4b, the entropy of activation of channel A is greater than that of channel B, thus inferring that transition state (A) is looser than transition state (B). Sometimes neither E_0 nor the transition state structure is known and so both of these parameters can be adjusted to obtain

(a)

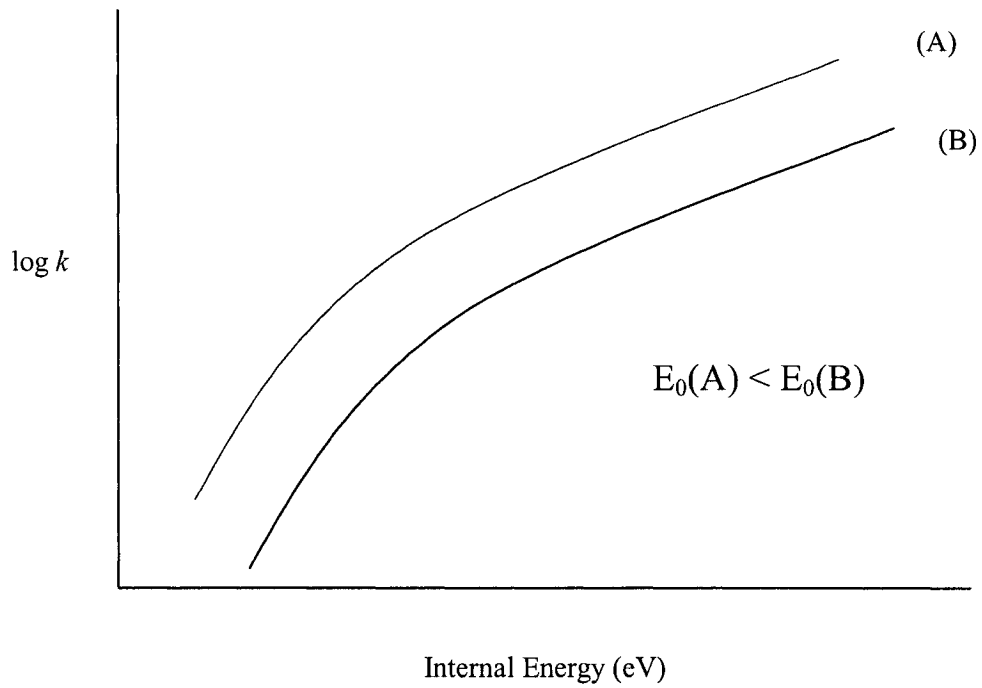

(b)

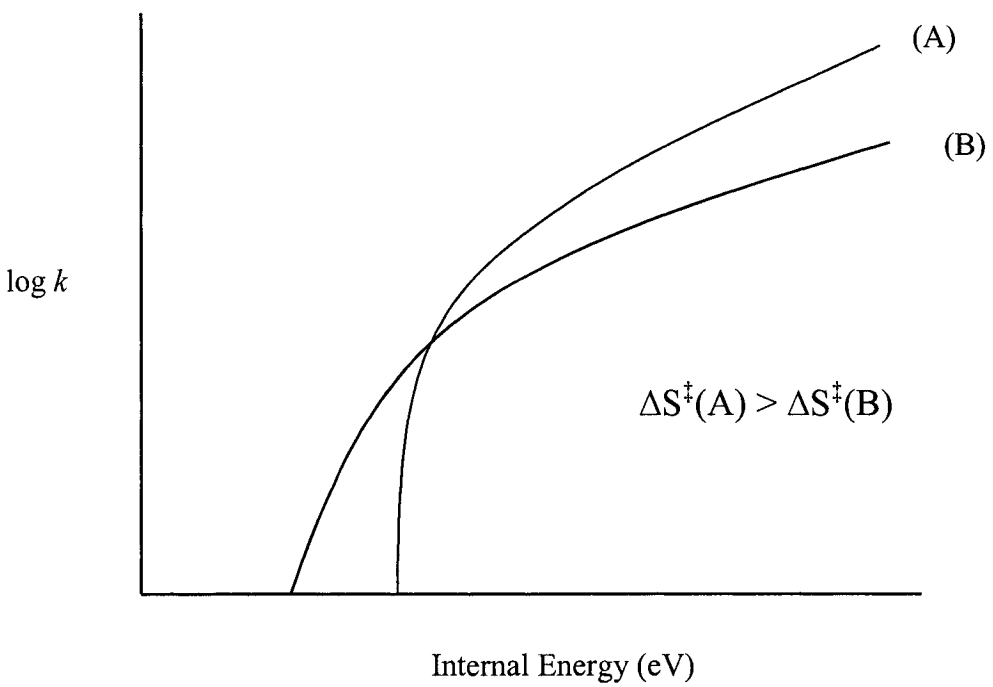

Figure 2.4 Variation of log k(E) with increasing internal energy as (a) E_0 changes and (b) $\Delta S^{\ddagger}$ changes.

an appropriate fit to experimental rate constant versus energy data. Ideally the transition state structure can be calculated by *ab initio* calculations and vibrational frequencies therein obtained. This will fix $\Delta S^{\ddagger}$ leaving only E_0 to be adjusted to fit the experimental data. If necessary, the transition state frequencies may themselves be estimated. The usual technique is to remove one of the reacting ion vibrational frequencies to represent the reaction coordinate and use the remaining reaction ion frequencies as those of the transition state.[6] The transition state can be made loose or tight by scaling the lowest five or six vibrational frequencies (which contribute the most to the calculated sum-of-states) by a common factor (less than 1.0 will produce $\Delta S^{\ddagger}>0$ where greater than 1.0 will produce $\Delta S^{\ddagger}<0$).

2.6 Variational Transition State Theory (VTST)

A unimolecular reaction can be viewed as a reaction flux in phase space. If the energy E is greater than the dissociation energy, E_0, then the molecule has a chance to dissociate and thus reach a part of the hypersurface that is associated with the dividing surface, or transition state. The dividing surface divides reactants and products and once a trajectory passes through it, the reaction will proceed directly to products without returning. The rate of reaction is then related to the total flux of reactants that passes through this dividing surface.[7] At the dividing surface, the molecule is in the process of dissociating along a one-dimensional reaction coordinate, which is the minimum energy reaction path. The minimum rate for a unimolecular reaction, k_{min}, at $E = E_0$ is given by

$$k_{min} = \sigma \frac{1}{h\rho(E_0)} \qquad (2.5)$$

(found by substituting $E = E_0$ into equation (2.1)) and represents the rate constant when there is just one path leading over the transition state region. Transition state theory is exact if the dividing surface is crossed only once by all reactive trajectories. If this is not the case, i.e., if some of the trajectories recross the surface, then the calculated rate constant will be overestimated and so, in principle, the RRKM equation represents an upper bound to the rate constant. With variational transition state theory, the position of the dividing surface is varied so that a better estimate of the rate constant may be obtained.

For reactions with substantial saddle points, the dividing surface is located at the saddle point because energy is a dominating factor in determining the transition state sum-of-states. If, however, no saddle point exists along the reaction path (such as for a unimolecular dissociation), then the position of the dividing surface should be varied until the rate constant reaches a minimum and so it is necessary to search directly for the minimum flux configuration. As such, the transition state can be viewed as the bottleneck for reactive events. The existence of a minimum flux configuration is due to the interplay between the potential energy, V(R), which is constantly rising as the reaction proceeds, and the decrease in the vibrational frequencies for transitional modes which are evolving into product rotations and translations.[2] As the reaction proceeds, the reduction in the available energy tends to reduce the density of states while the lowering of the transitional vibrational frequencies tends to increase the density of states. The two opposing forces result in a

minimum in the density or sum-of-states at some R^* value. The transition state, located at R^*, is the entropic bottleneck (Figure 2.5).

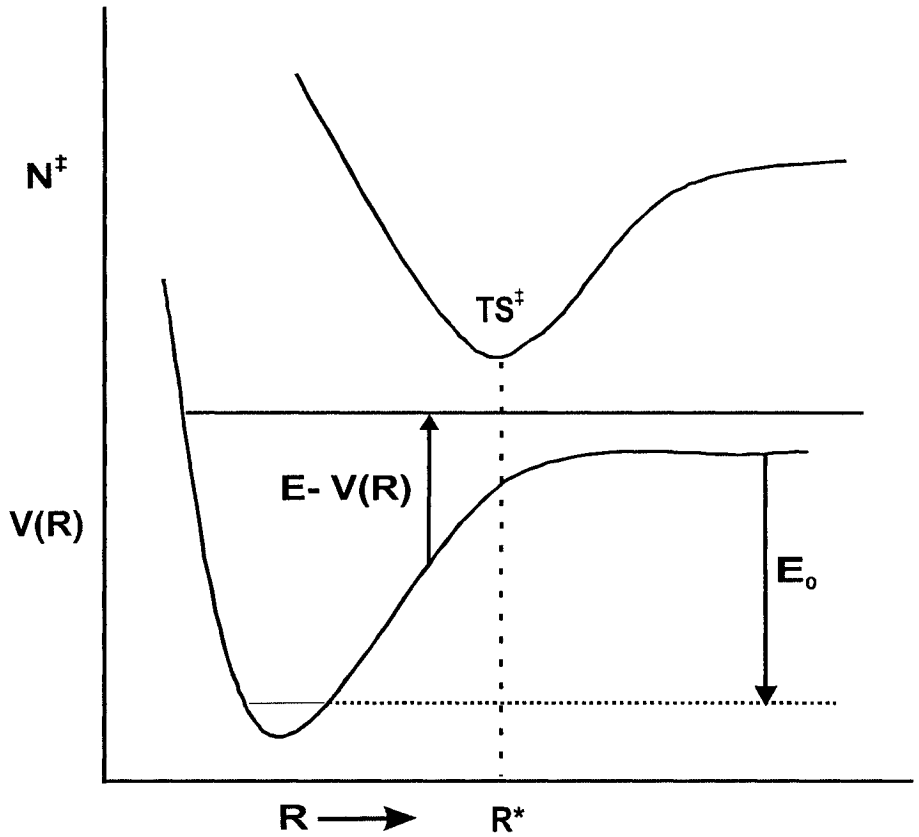

Figure 2.5 The variation of the sum-of-states ($N^{\ddagger}$) with R. The position of the transition state at a given total energy is shown at R = R*.

Two effects have been found to govern the position of the variational transition state.[13] The way the potential energy surface varies along the reaction coordinate leads to an enthalpic effect and so the presence of a saddle point brings a significant contribution to this effect. A second effect is linked to the variation of the density of states, $\rho^{\ddagger}$, along the reaction coordinate. Because the density of states is directly related to the concept of entropy, one usually speaks of an entropic effect. The importance of this entropic effect

increases rapidly with the internal energy E and the angular momentum L. As E and L increase, the variationally selected position moves to smaller values of the reaction coordinate.

2.7 Implications to Metastable Observations on the VG-ZAB

The RRKM equation accounts for an important feature of mass spectrometric observations. Reactions cannot always be studied at their exact threshold since a fragment can only be detected if the parent ion dissociates prior to being mass analysed. Metastable ions (as observed on a VG ZAB sector mass spectrometer such as that used in this thesis work) decompose with rate constants between 10^4 and 10^6 s^{-1} while stable ions decompose at lower rates; the terms "stable" and "metastable" are thereby defined by the timescale of a given instrument wherein a range of rate constants are involved in fragmentations.

With a VG-ZAB sector mass spectrometer, two types of experiments may be performed: MIKES (mass-analysed ion kinetic energy spectrometry) and CID (collision-induced dissociation). MIKES experiments involve the study of metastable ions, i.e., those ions that have sufficient internal energy to spontaneously dissociate in the field-free regions of a sector mass spectrometer, while CID experiments involve the study of higher energy processes. All fragment ions observed via these methods are the result of simple bond cleavage reactions and/or ion rearrangement. If we consider the acetonitrile-methanol proton-bound pair, its MIKES mass spectrum contains two ions: one at m/z 42 (CH_3CNH^+) due to a simple bond cleavage and the other at m/z 56 ($CH_3CNCH_3^+$) due to ion

rearrangement (Figure 2.6). In this mass spectrum, the simple bond cleavage reaction dominates ion isomerization by a factor of 2:1. In the CID experiment, the parent ion is collisionally activated and so higher energy processes may be accessible thereby affecting the relative abundance of the two fragments. In the collision process, a fraction of the ion's kinetic energy is transferred into internal energy, thereby affecting its dissociation into various fragment ions; the extent of fragmentation depends upon the total internal energy of the excited ion. In the CID mass spectrum, m/z 42 increases in intensity while m/z 56 remains largely unaffected (10:1). These results are consistent with m/z 42 being the result of a simple bond cleavage reaction and the production of m/z 56 being due to a rearrangement. Let's now discuss these differences in terms of log k(E) vs. E curves (Figure 2.7).

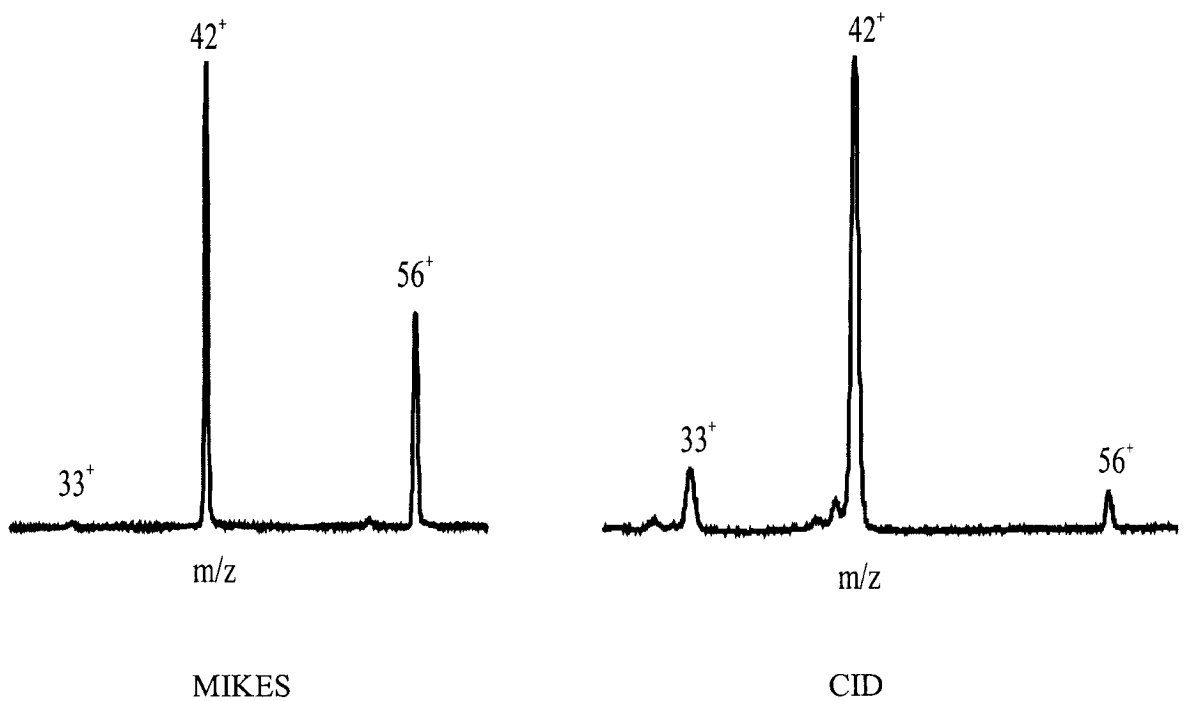

Figure 2.6 MIKES and CID mass spectra of the acetonitrile-methanol proton-bound pair.

Rearrangement reactions generally have low critical energies and low frequency factors due to the unfavourable entropy change necessary to reach the transition state whereas simple bond cleavage reactions often have higher critical energies and higher frequency factors. For ions that dissociate via competitive rearrangement and simple cleavage reactions, their dissociations generally occur via a rearrangement process at low internal energies (due to a lower critical energy) while at higher internal energies, the simple cleavage reaction tends to dominate due to a higher frequency factor. (Figure 2.7) In Figure 2.7, curve (A) refers to the simple bond cleavage reaction while that of (B) represents ion rearrangement. In the metastable window (i.e., 10^4-10^6 s^{-1}), the isomerization pathway (curve B) occupies a larger area under the curve than does the simple bond cleavage. When we go to higher internal energies (as in CID reactions), we can see that curve A (simple bond dissociation) begins to dominate the chemistry.

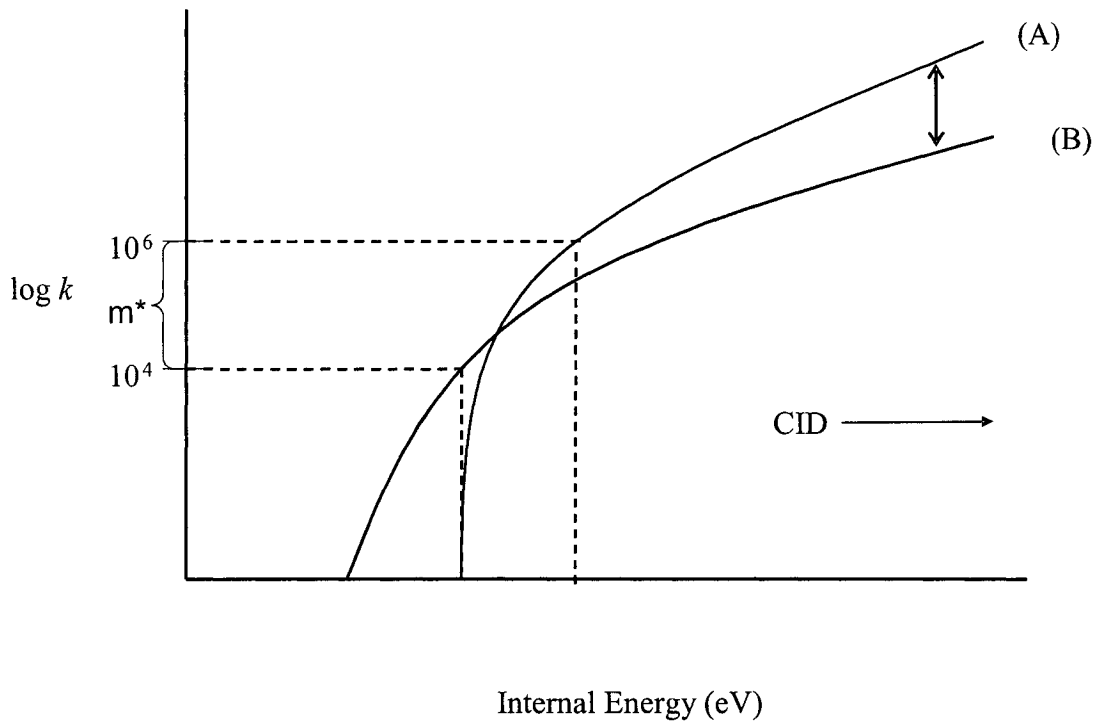

Figure 2.7 Log k(E) vs. E curves for competing rearrangement and dissociation processes.

2.8 Computational Methods

Model chemistries are characterized by the combination of theoretical procedure and basis set. For example, every calculation performed with Gaussian must specify the desired theoretical model in addition to the molecular system and which results to compute. The Gaussian program[14] contains various procedures corresponding to different approximation methods (commonly referred to as different levels of theory). This section will present a brief review of the computational methods referred to in this thesis. It will start with an introduction to Hartree-Fock theory (HF) and continue with Second Order Moller-Plesset perturbation theory (MP2), Coupled Cluster with Single and Double excitations (CCSD), Quadratic Configuration Interaction with Single and Double excitations (QCISD) and lastly, three Density Functional methods, B-LYP, B3-LYP and B3-PW91. The objective here will not be to give detailed derivations, but rather to characterize the various methods and to emphasize their weak and strong points.

2.8.1 *Ab initio* Methods

The first *ab initio* method that will be discussed is the Hartree-Fock Method.[15] Hartree-Fock (HF) theory is very useful for providing initial, first level predictions for many systems. It is also reasonably good at computing the structures and vibrational frequencies of stable molecules and some transition states. The HF theory is a variational method in quantum mechanics in which the n-electron wavefunction of a molecular system is represented as a single determinant wavefunction. An individual molecular orbital (MO),

ψ_j, can be expressed as a linear combination of a finite set of N one electron wavefunctions known as basis functions, φ_1, φ_2..., φ_N. In the case where atomic orbitals of constituent atoms are used as basis functions, one speaks of a linear combination of atomic orbitals (LCAO) theory. The individual orbitals can be written as

$$\Psi_j = \sum_{\mu=1}^{N} c_\mu \varphi_{\mu i} \quad (2.6)$$

where the MO expansion coefficients $c_{\mu i}$ are adjusted to minimize the expectation value of the total energy E. The final value of E will be as close to the exact energy as is possible within the limitations of the HF theory, namely the limitations of a single determinant wavefunction using the particular basis set chosen.

The primary weakness of HF theory is its neglect of electron correlation, a component which generally improves the accuracy of computed energies and molecular geometries.[15] For organic molecules, correlation is an extra correction for very-high accuracy work but is not generally needed to obtain qualitative results; one exception to this rule are compounds exhibiting Jahn-Teller distortions, which often require correlation to give qualitatively correct results. While correlation of the motions of electrons with the same spin is partially taken into account by virtue of the determinant form of the wavefunction, single configuration wavefunctions do not take into account the correlation between electrons with opposite spin. This means that the calculated Hartree-Fock energies will be greater than the exact values and so by convention, the difference between the Hartree-Fock and the exact energies is called the correlation energy.[16]

$$E_{Correlation} = E_{Exact} - E_{Hartree\text{-}Fock}$$

A number of calculations begin with a HF calculation and then correct for correlation. Such methods used in this thesis are the second order Moller-Plesset perturbation theory (MP2), configuration interaction (CI) and coupled cluster (CC) theory. One approach to the electron correlation problem is the Moller-Plesset Perturbation Theory; of all the methods, this method has been used the most extensively in this thesis. Unlike the HF approximation, Moller-Plesset calculations are not variational and so, it is not uncommon to find MP2 calculations that give total energies below the exact total energy. In perturbation theory, the electronic Hamiltonian (H) is divided into a zero order Hamiltonian (H^0) and a perturbation (V) according to:[16]

$$H = H^0 + \lambda V \quad (2.7)$$

The exact or full configuration interaction ground state wavefunction (Ψ_λ) and energy (E_λ) for a system described by the Hamiltonian (H) may now be expanded in powers of λ according to Raleigh-Schrödinger perturbation theory.

$$\Psi_\lambda = \Psi^{(0)} + \lambda\Psi^{(1)} + \lambda^2\Psi^{(2)} + \ldots$$
$$E_\lambda = E^{(0)} + \lambda E^{(1)} + \lambda^2 E^{(2)} + \ldots \quad (2.8)$$

In Moller-Plesset theory, H^0 is taken to be the sum of the one-electron Fock operators. The eigenvalue, E_s, corresponding to a particular determinant, Ψ_s, is the sum of the one-electron

energies for the spin orbitals which are occupied in Ψ_s. Practical perturbation methods may be formulated by truncation of the series in equation (2.8) to various orders and by setting the parameter λ=1. In the literature, these methods are referred to by the highest-order energy term allowed, e.g., truncation after second order is MP2.

A configuration interaction (CI) wavefunction is a multiple-determinant wavefunction, which is constructed by starting with the HF wavefunction and making new determinants by promoting electrons from occupied to unoccupied orbitals.[15] Configuration interaction calculations are classified by the number of excitations used to make each determinant. If only one electron has been moved for each determinant, it is called a configuration interaction single-excitation (CIS) calculation. The configuration interaction calculation with all possible excitations is called a full CI. A full CI calculation that uses an infinitely large basis set will give an exact quantum mechanical result. Despite the accuracy that one can obtain with such a method, one of the drawbacks is the large amount of CPU time required (CISDT calculations have an N^8 time complexity where N is the number of basis functions) and as such, these calculations are rarely done.

Couple cluster (CC) calculations are similar to configuration interaction calculations in that the wavefunction is a linear combination of many determinants. The choice of determinants in a CC calculation is however more complex than that involved in a CI.[15] Like CI, there are various orders of the CC expansion, called CCSD, CCSDT and so on. Coupled cluster calculations give variational energies as long as the excitations are included successively and so CCSD is variational while CCD is not. The accuracy of these two

methods (i.e., CI and CC) is very similar but the advantage of doing coupled cluster calculations is that it is a size extensive method (i.e., gives an energy that is a linear function of the number of electrons). Often, coupled-cluster results are a bit more accurate than those obtained from the equivalent size configuration interaction calculation.

Quadratic configuration interaction calculations (QCI) use an algorithm that is a combination of the CI (configuration interaction) and CC (coupled cluster) algorithms. One of the more popular QCI methods is that involving single and double-excitation calculations, QCISD. A QCISD calculation is an approximation to a CCSD calculation. These calculations are popular since they often give an optimal amount of correlation for high-accuracy calculations for organic molecules while using less CPU time than coupled cluster calculations.

In general, *ab initio* calculations give very good qualitative results and can yield increasingly accurate quantitative results as the molecules in question become smaller. The advantage of *ab initio* methods is that they eventually converge to the exact solution once all the approximations are made sufficiently small in magnitude. Of the methods described above, the relative accuracy of results is the following:

$$HF << MP2 < CISD < CCSD < CCSD(T) < \text{Full CI}$$

The disadvantage of *ab initio* methods is that they are expensive. These methods often take enormous amounts of computer CPU time, memory, and disk space. The HF

method scales at N^2.[15] This means that a calculation twice as big takes 4 times as long to complete. Correlated calculations often scale much worse than this. Minimally correlated methods, such as MP2, are often used when correlation is important to the description of large molecules.

2.8.2 Density Functional Theory

Density functional theory (DFT) has become very popular in recent years.[15] The premise behind DFT is that the energy of a molecule can be determined from the electron density instead of a wavefunction. This theory originated with a theorem by Hohenberg and Kohn[17] and applied only to finding the ground-state electronic energy of a molecule. A practical application of this theory was later developed by Kohn and Sham[18] who formulated a method similar in structure to the Hartree-Fock method.

In density functional theory, the electron density is expressed as a linear combination of basis functions similar in mathematical form to HF orbitals and it is this electron density that is used to compute the energy. A determinant is then formed from these basis functions, called Kohn-Sham orbitals. There has been some debate over the interpretation of these orbitals although it is known that they are not mathematically equivalent to either HF orbitals or natural orbitals from correlated calculations. They do, however, describe the behaviour of electrons in a molecule, just as the other orbitals mentioned do.

A density functional is used to obtain the energy for the electron density. A functional is a function of a function and the exact density functional is not known. The appropriate functionals employed by current DFT methods partition the electronic energy into several terms:

$$E = E^T + E^V + E^J + E^{XC}$$

where E^T is the kinetic energy term (arising from the motion of the electrons), E^V includes terms describing the potential energy of the nuclear-electron attraction and of the repulsion between pairs of nuclei, E^J is the electron-electron repulsion term (it is also described as the Coulomb self-interaction of the electron density) and E^{XC} is the exchange-correlation term and includes the remaining part of the electron-electron interactions.

A popular gradient-corrected exchange functional was proposed by Becke in 1988;[19] a widely used gradient corrected correlational functional is the LYP functional of Lee, Yang and Parr.[20] The combination of these two forms gives the B-LYP method.[21] Perdew and Wang also proposed some important gradient-corrected functionals, e.g., Perdew-Wang 86. There are also several hybrid functionals which define the exchange functional as a linear combination of Hartree-Fock, local, and gradient-corrected exchange terms. This exchange functional is then combined with local and/or gradient-corrected correlation functionals; one of the best known of these hybrid functionals is Becke's three-parameter formulation where hybrid functionals based on it are available in Gaussian via the B3-LYP and B3-PW91 keywords.

Some functionals were developed by parametrizing functions to best reproduce experimental results. Thus, there are in essence *ab initio* and semiempirical versions of DFT. DFT tends to be classified either as an *ab initio* method or in a class by itself. The advantage of using electron density is that the integrals for Coulomb repulsion need be done only over the electron density, which is a three-dimensional function, thus reducing the scaling (from comparable *ab initio* methods) to N^3. With DFT, at least some electron correlation can be included in the calculation and therefore results in computations that are a bit more accurate. It has been found that the better DFT functionals give results with accuracy similar to that of an MP2 calculation.

2.8.3 Basis Sets

A basis set is the mathematical description of the orbitals within the program used to perform the theoretical calculation. Basis sets assign a group of basis functions to each atom within a molecule so to approximate its orbitals. These basis functions are themselves composed of a linear combination of Gaussian functions; such basis functions are referred to as contracted functions and the component Gaussian functions are referred to as primitives. Larger basis sets more accurately approximate the orbitals by imposing fewer restrictions on the locations of the electrons in space. Standard basis sets for electronic structure calculations use linear combinations of Gaussian functions to form the orbitals. Gaussian offers a wide range of pre-defined basis sets, which are classified by the number and types of basis functions that they contain.

The first way that a basis set can be made larger is to increase the number of basis functions per atom. Split valence basis sets, such as 6-31G, have two (or more) sizes of basis function for each valence orbital. Double zeta basis sets form all molecular orbitals from linear combinations of two sizes of functions for each atomic orbital. Similarly, triple split valence basis sets, i.e., 6-311G, use three sizes of contracted functions for each orbital-type. Split valence basis sets allow orbitals to change size, but not shape.[15] This limitation can be removed by using polarized basis sets, which add orbitals with angular momentum beyond what is required for the description of each atom. For example, polarized basis sets add d functions to carbon atoms and f functions to transition metals and some even add p functions to hydrogen atoms. One example of a polarized basis set is 6-31G(d). Its name indicates that it is the 6-31G basis set with d functions added to non-hydrogen atoms. This basis set (also known as 6-31G*) is becoming very common for calculations involving up to medium sized systems. Another popular polarized basis set is 6-31G(d,p) also known as 6-31G** which adds p functions to hydrogen atoms in addition to the d functions on heavy atoms. In addition to polarization, diffuse functions may also be added to a basis set. Diffuse functions are larger-size versions of s- and p-type functions, which allow the orbitals to occupy a larger region of space.[15] Basis sets with diffuse functions are important for systems that need electron density relatively far from the nucleus: molecules with lone pairs, anions and other systems with significant negative charge and systems in their excited states. The 6-31+G(d) basis set is the 6-31G(d) basis set with diffuse functions added to heavy atoms while the double plus version, 6-31++G(d), adds diffuse functions to the hydrogen atoms as well. Diffuse functions on hydrogen atoms seldom make a significant different in accuracy.

2.8.4 Frequency Calculations

Molecular vibrational frequencies depend on the second derivative of the energy with respect to the nuclear positions. Analytic second derivatives in the Gaussian program are available for the HF, MP2, and DFT methods. Frequencies are calculated numerically for CCSD and QCISD methods. Prior to calculating the vibrational frequencies of a structure, the structure must first be optimized. This is done by including both the "opt" and "freq" keywords in the route section of a job, which requests a geometry optimization followed by a frequency calculation. A frequency job must use the same theoretical model and basis set as produced in the optimized geometry.

A frequency job begins by first computing the energy of the structure and then proceeds to calculate the frequencies of that structure. The total energy computed by a geometry optimization corresponds to a minimum on the potential energy surface. A molecule can never have this energy since it must always have some vibrational motion. The Gaussian program computes the zero-point energy correction along with the vibrational frequencies. For accurate work, the scaled zero-point energy correction[22] will be added to the total energy for the optimized geometry. Raw frequency values computed at the Hartree-Fock level contain systematic errors due to the neglect of electron correlation, resulting in overestimates of about 10-12%. Therefore, it is usual to scale frequencies predicted at the Hartree-Fock level by an empirical factor of 0.8929.[22] Use of this factor has been demonstrated to produce very good agreement with experiment for a wide range of systems. Frequencies computed with methods other than Hartree-Fock are also scaled to

eliminate known systemic errors in calculated frequencies. Table 2.1 lists the recommended scale factors for frequencies and zero-point energies of the theories used in this thesis work.

Table 2.1: Recommended scaling factors for frequencies and for zero-point energies[22]

Method	Frequency Scale Factor	Zero-Point Energy Scale Factor
HF/6-31G(d)	0.8929	0.9135
HF/6-31+G(d)	0.8970	0.9153
HF/6-31G(d,p)	0.8992	0.9181
HF/6-311G(d,p)	0.9051	0.9248
MP2/6-31+G(d)	0.9434	0.9670
QCISD/6-31+G(d)	0.9537	0.9776
B-LYP/6-31G(d)	0.9945	1.0126
B3-LYP/6-31G(d)	0.9614	0.9806
B3-PW91/6-31G(d)	0.9573	0.9772

Frequency calculations are also used in determining the nature of a stationary point found by a geometry optimization. Geometry optimizations converge to a structure on the potential energy surface where the forces on the system are essentially zero. The final structure may correspond to a minimum on the potential energy surface or it may represent a saddle point, which is a minimum with respect to some directions on the surface and a maximum in one or more others. First order saddle points, which are a maximum in exactly one degree of freedom and a minimum in all other orthogonal degrees of freedom,

correspond to transition state structures linking two minima. When evaluating potential transition state structures, it is important to examine the number of imaginary frequencies (there should only be one negative listed in the output) and the mode corresponding to the imaginary frequency. By definition, a structure which has n imaginary frequencies is an nth order saddle point and so, ordinary transition structures are usually characterized by one imaginary frequency since they are first-order saddle points.

2.8.5 Intrinsic Reaction Coordinate (IRC) Calculation

An IRC calculation examines the reaction path leading down from a transition state on a potential energy surface and is used to confirm whether the correct transition state has been determined. Such a calculation starts at the saddle point and follows the path in both directions from the transition state, optimizing the geometry of the molecular system at each point along the path. In this way, an IRC calculation definitely connects two minima on the potential energy surface by a path which passes through the transition state between them.

In Gaussian, a reaction path calculation is requested with the IRC keyword. An IRC calculation begins at the transition state and steps along the reaction path a fixed number of times, the default being 6 in the direction toward the two minima that it connects. However, in most cases, it will not step all the way to the minimum on either side of the path and so an optimization will be required after the IRC calculation is complete.

References

1. L. S. Kassel, "Studies in homogeneous gas reactions I", *J. Phys. Chem.* **32**, 1617 (1928).
2. T. Baer and W. L. Hase, *Unimolecular Reaction Dynamics, Theory and Experiments*. Oxford University Press, New York (1996).
3. R. A. Marcus, "Unimolecular dissociations and free radical recombination reactions", *J.Chem. Phys.* **20**, 359 (1952).
4. O. K. Rice and H. C. Ramsperger, "Theories of unimolecular gas reactions at low pressures", *J. Am. Chem. Soc.* **49**, 1617 (1927).
5. K. L. Busch, G. L. Glish, and S. A. McLuckey, *Mass Spectrometry/Mass Spectrometry*. VCH Publishers, New York (1988).
6. T. Baer and P. M. Mayer, "Statistical Rice-Ramsperger-Kassel-Marcus-quasiequilibrium theory calculations in mass spectrometry", *J. Am. Soc. Mass Spectrom.* **8**, 103 (1997).
7. J. C. Lorquet and B. Leyh, *in "Encyclopedia of Mass Spectrometry"* (R. Caprioli, ed.), Vol. 1: Theory and Ion Chemistry, p. 8. Elsevier, 2003.
8. K. G. Kay, "Decomposition of isolated molecules: a transition state treatment", *J. Chem. Phys* **65**, 3813 (1976).
9. T. Beyer and D. R. Swinehart, "Number of multiply-restricted partitions [A1] (Algorithm 448)", *ACM Commun.* **16**, 379 (1973).
10. G. Z. Whitten and B. S. Rabinovitch, "Accurate and facile approximation for vibrational energy-level sums", *J. Chem. Phys* **38**, 2466 (1963).

11. G. Z. Whitten and B. S. Rabinovitch, "Approximation for rotation-vibration energy level sums", *J. Chem. Phys* **41**, 1883 (1964).

12. W. Forst, *Theory of Unimolecular Reactions*. Academic, New York (1973).

13. R. G. Gilbert and S. C. Smith, *Theory of Unimolecular and Recombination Reactions*. Blackwell Scientific Publications, Oxford, U. K. (1990).

14. M. J. Frisch, G. W. Trucks, H. B. Schlegel, G. E. Scuseria, M. A. Robb, J. R. Cheeseman, V. G. Zakrzewski, J. A. Montgomery, R. E. Stratmann, J. C. Burant, S. Dapprich, J. M. Millam, A. D. Daniels, K. N. Kudin, M. C. Strain, O. Farkas, J. Tomasi, V. Barone, M. Cossi, R. Cammi, B. Mennucci, C. Pomelli, C. Adamo, S. Clifford, J. Ochterski, G. A. Petersson, P. Y. Ayala, Q. Cui, K. Morokuma, D. K. Malick, A. D. Rabuck, K. Raghavachari, J. B. Foresman, J. Cioslowski, J. V. Ortiz, B. B. Stefanov, G. Liu, A. Liashenko, P. Piskorz, I. Komaromi, R. Gomperts, R. L. Martin, D. J. Fox, T. Keith, M. A. Al-Laham, C. Y. Peng, A. Nanayakkara, C. Gonzalez, M. Challacombe, P. M. W. Gill, B. Johnson, W. Chen, M. W. Wong, J. L. Andres, C. Gonzalez, M. Head-Gordon, E. S. Replogle, and J. A. Pople, *in* "GAUSSIAN 98 Rev. A.7". Gaussian Inc., Pittsburgh PA, 1998.

15. D. Young, *Computational Chemistry: A practical guided for applying techniques to real world problems*. John Wiley & Sons, Inc.(2001).

16. I. N. Levine, *Quantum Chemistry*. Prentice-Hall Inc., New Jersey (2000).

17. P. Hohenberg and W. Kohn, "Inhomogeneous Electron Gas", *Phys. Rev.* **136**, B864 (1964).

18. W. Kohn and L. J. Sham, "Self-consistent equations including exchange and correlation effects", *Phys. Rev.* **140**, A1133 (1965).

19. A. D. Becke, "Density-functional exchange-energy approximation with correct asymptotic behavior", *Phys. Rev. A* **38**, 3098 (1988).

20. C. Lee, W. Yang, and R. G. Parr, "Development of the Colle-Salvetti correlation-energy formula into a functional of the electron density", *Phys. Rev. B* **37**, 785 (1988).

21. B. Miehlich, A. Savin, H. Stoll, and H. Preuss, "Results obtained with the correlation energy density functionals of becke and Lee, Yang and Parr", *Chem. Phys. Lett.* **157**, 200 (1989).

22. A. P. Scott and L. Radom, "Harmonic vibrational frequencies: An evaluation of hartree-fock, moller-plesset, quadratic configuration interaction, density functional theory and semi-empirical scale factors", *J. Phys. Chem.* **100**, 16502 (1996).

CHAPTER 3

DEVELOPMENT OF AN EMPIRICAL MODEL FOR PREDICTING ISOMERIZATION ENERGETICS OF PROTON-BOUND PAIRS

3.1 Introduction

One class of gas-phase ions that undergo a unimolecular rearrangement is the family of proton-bound pairs of alcohols and nitriles $(RCN)(ROH)H^+$ and $(R'OH)(ROH)H^+$ (where R represents substituents). The mass spectrometry of these proton-bound pairs has been extensively studied in this laboratory,[1-4] and by Fridgen and McMahon[5, 6] and Audier.[7] A feature common to each system is an isomerization reaction (leading to a kinetically unstable isomer that loses water) that competes on the microsecond timescale with the cleavage of the hydrogen bond. The competition between the two reaction channels indicates that a fine balance exists between the relative energy barriers for dissociation and isomerization.

The isomerization mechanism of a proton-bound pair involving nitriles and alcohols consists of an internal S_N2-type rearrangement with the initial isomerization of the molecular pair to an intermediate ion complex (IC) through a transition state (TS_a) followed by the stretching of the C–O bond in this ion (via TS_b) to form a thermodynamically stable isomer, which then dissociates to lose water (Figures 1.5 and 3.1). The isomerization mechanism for

the $(CH_3CN)(CH_3OH)H^+$ proton-bound pair is shown in Figure 3.1. The mechanism and surface are analogous to that determined for $(ROH)(R'OH)H^+$.

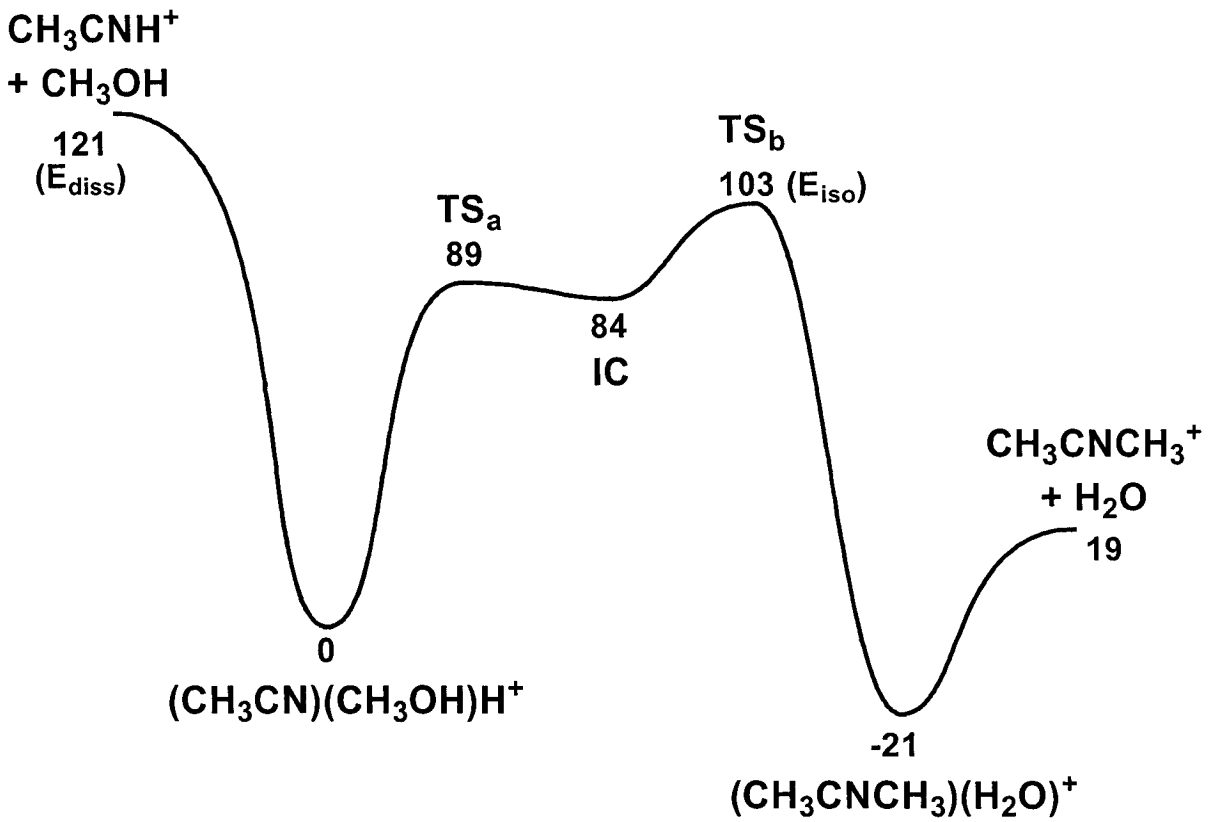

Figure 3.1 MP2/6-31+G(d) potential energy diagram for the unimolecular process of the proton-bound pair consisting of acetonitrile and methanol.[1] The labels E_{diss} and E_{iso} refer to the two energy levels used in the peak intensity ratio vs. ΔE modelling.

This mechanism was deduced from the combination of mass spectrometry (the dissociation of metastable and collisionally activated cluster ions together with isotopic labelling) and *ab initio* molecular orbital calculations.[2] Computationally, it has been found that methyl substitution of the central carbon of the intermediate nitrile-alcohol complex (IC) will stabilize this ion and the transition states TS_a and TS_b.[3] RRKM modelling of the kinetics on

the reaction surface has shown that even though it is lower in energy, TS_a can play an important role in determining the fraction of ions that undergo isomerization.[8]

Empirical relationships[9,10] exist indicating that the key factor in determining the strength of the hydrogen bonds in these ions is the difference in proton affinity (PA) of the two molecules. This chapter addresses the unimolecular S_N2 reaction by first examining the relationship between the energetics and relative peak intensities in tandem mass spectra and then by deriving empirical formulae for predicting the energies of the IC and transition states, thereby allowing the entire potential energy surface to be mapped out without experimental or computational input.

3.2 Experimental Procedures in Brief

The experiments were performed on a modified VG ZAB-2HF mass spectrometer, which incorporates a magnetic sector followed by two electrostatic analysers (BEE geometry)[11]. Protonated cluster ions were generated in the chemical ionization ion source of the instrument. The pressures in the ion source chamber, read with an ionization gauge located above the ion source diffusion pump, were typically between 10^{-5} and 10^{-4} Torr (the pressure in the ion source itself being approximately two orders of magnitude higher). The accelerating voltage was held constant at 8kV. Metastable ion kinetic energy (MIKES) mass spectra were recorded in the usual manner in the second field-free region (2FFR) of the mass spectrometer. All chemicals were commercially obtained and used without further purification.

3.3 Computational Procedures in Brief

Standard *ab initio* molecular orbital calculations[12] were performed using the Gaussian 98 suite of programs.[13] Geometries were optimized at the MP2/6-31+G(d) level of theory since previous work from this group has shown that relative energies on these surfaces are adequately described at this level of theory.[14] When compared with G3 energies for the $(CH_3CN)(CH_3OH)H^+$ proton-bound pair, we expect these MP2 energies to be accurate within ± 10 kJ mol^{-1}. Vibrational frequency analysis was done to ensure that transition states and minima were obtained. The zero-point energies were scaled by a factor of 0.967 recommended by Scott and Radom.[15] Transition state structures were confirmed by the intrinsic reaction coordinate (IRC) method in Gaussian 98.

Microcanonical rate constants were calculated using the RRKM expression: [16]

$$k(E) = \frac{\sigma}{h}\frac{N^{\ddagger}(E - E_0)}{\rho(E)} \qquad (3.1)$$

where σ is the reaction symmetry number, h is Planck's constant, $N^{\ddagger}(E\text{-}E_0)$ is the sum-of-states for the transition state and $\rho(E)$ is the density of states of the reacting ion. Sums and densities of states were calculated using the direct count algorithm of Beyer and Swinehart.[17]

3.4 Results and Discussion

3.4.1 General Mechanistic Features

The surface presented in Figure 3.1 has features that are common with and distinct from the gas-phase bimolecular S_N2 reaction. The most obvious similarity is TS_b, which resembles the transition state shown in the bimolecular S_N2 reaction. The main distinctions are in the initial isomerization step from the proton-bound pair to the IC via TS_a. It has been shown that the bimolecular reaction of CH_3CNH^+ with neutral methanol skips the proton-bound pair and forms the IC directly before crossing TS_b.[5] The long lifetime (and lower internal energy) of metastable ions means that any IC formed will rearrange back to the proton-bound pair prior to dissociation.

3.4.2 Peak Height Ratio vs. ΔE

The chemistry of two families of proton-bound pairs was examined: proton-bound nitrile-alcohol pairs and alcohol-alcohol pairs. Characteristic MIKES spectra for the acetonitrile-alcohol proton-bound pairs involving methanol, ethanol, 1- and 2-propanol are shown in Figure 3.2.

The chemistry of the family of proton-bound alcohol-alcohol pairs is remarkably similar to that of the proton-bound nitrile-alcohol pairs in that both families rearrange via an internal S_N2-type mechanism to lose water. A representative MIKES mass spectrum of the methanol-methanol proton-bound pair is shown below in Figure 3.3. Two peaks are observed in this mass spectrum: one at m/z 33 ($CH_3OH_2^+$, due to a simple hydrogen bond cleavage) and another at m/z 47 ($(CH_3)_2OH^+$, due to water loss).

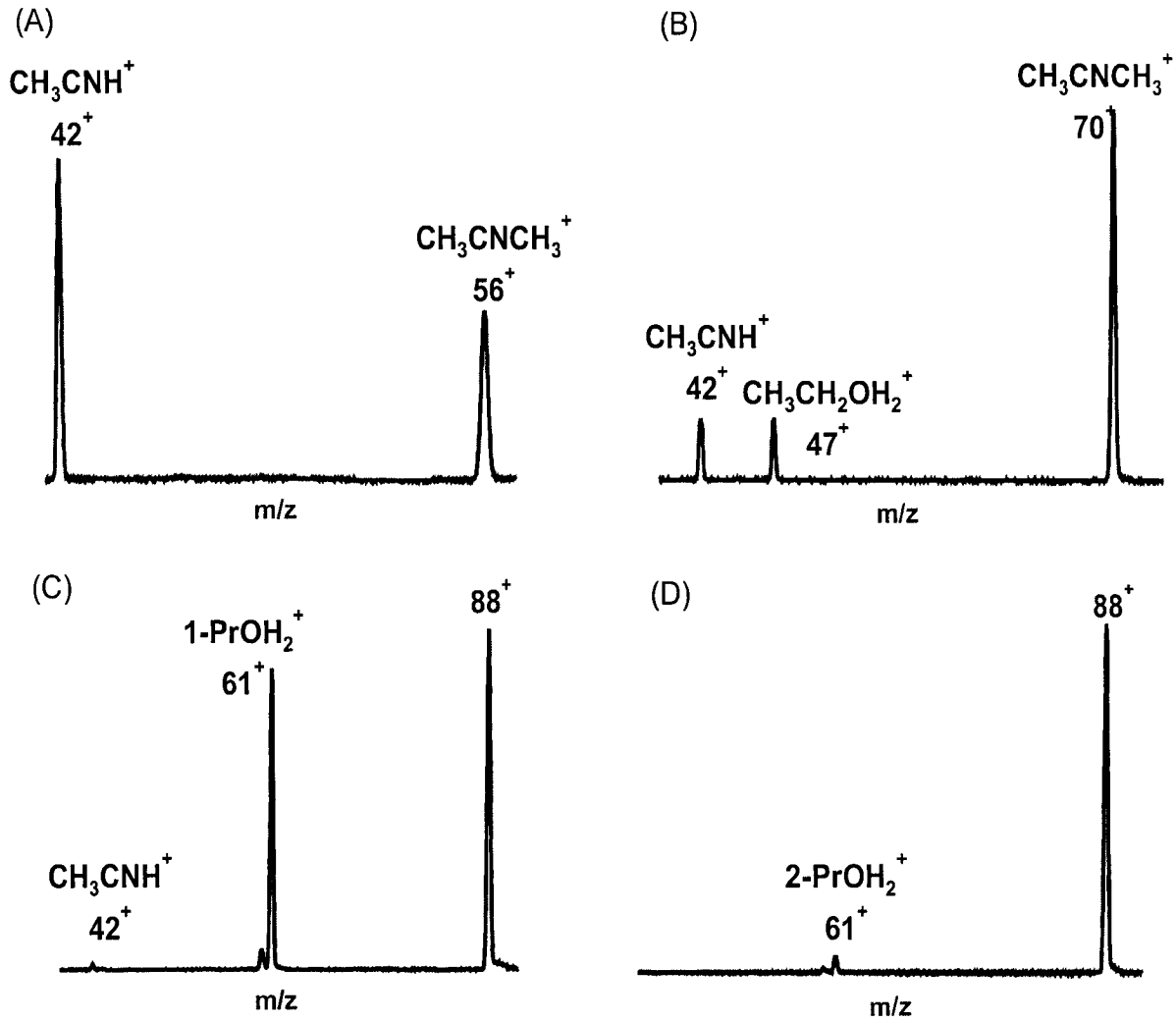

Figure 3.2 Representative MIKES mass spectra of the proton-bound pairs: (a) $(CH_3CN)(CH_3OH)H^+$,(b) $(CH_3CN)(CH_3CH_2OH)H^+$, (c) $(CH_3CN)(CH_3CH_2CH_2OH)H^+$ and (d) $(CH_3CN)((CH_3)_2CHOH)H^+$.

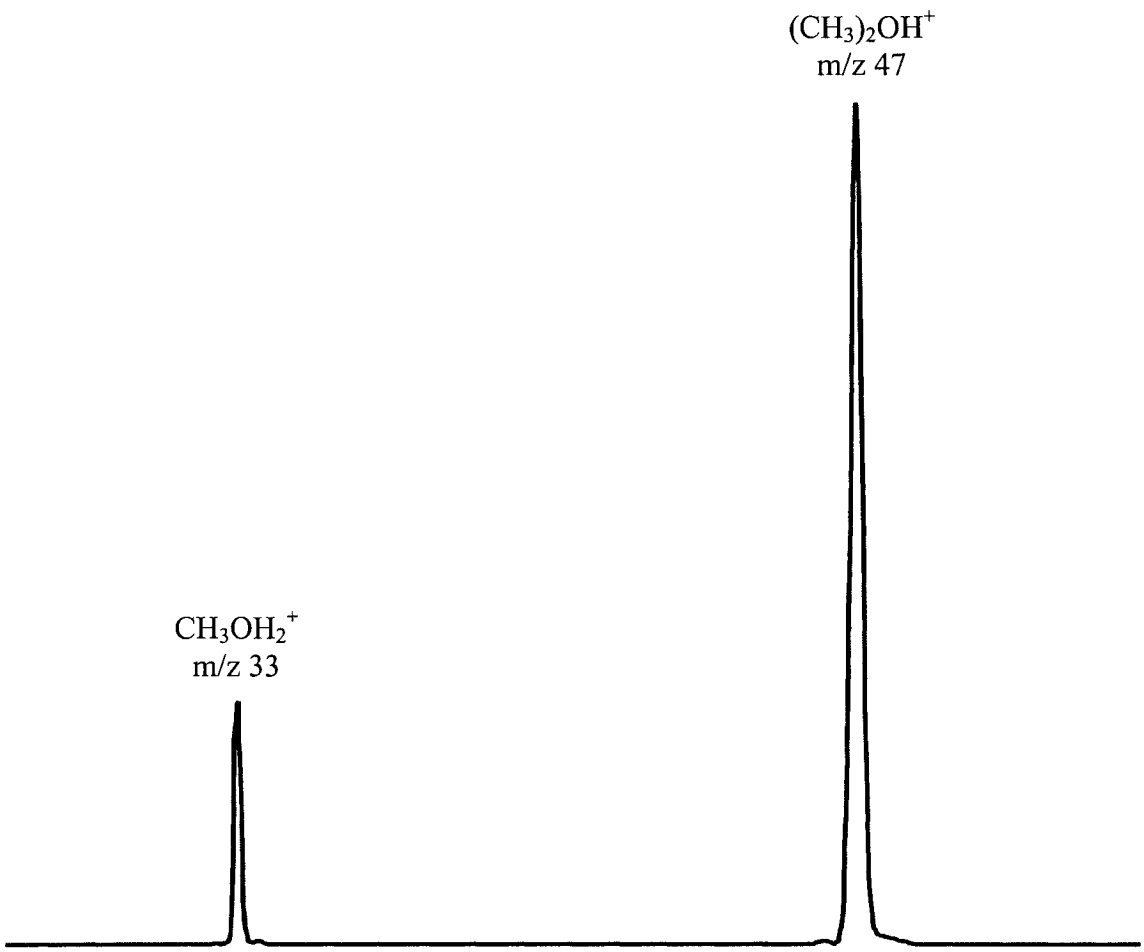

Figure 3.3 MIKES mass spectrum of the methanol-methanol proton-bound pair.

It is tempting to simplify the potential energy surface from that shown in Figure 3.1 to a single well surface whose product channels are simple hydrogen bond cleavage and isomerization through the high energy transition state, TS_b leading to water loss (Figure 3.4).

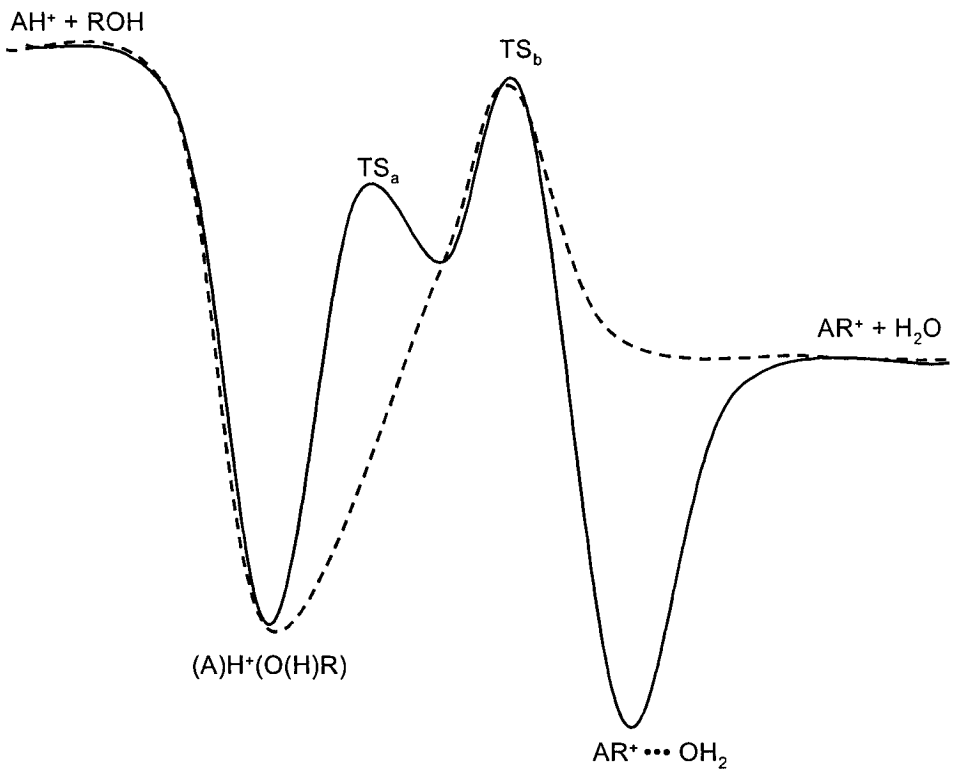

Figure 3.4 Simplified single well, two product surface where the solid line is the original potential energy surface and the dotted line is the simplified surface. "A" in this scheme may represent either an alcohol or a nitrile group.

This simplification of the potential energy surface is based upon two assumptions: (1) the intermediate complex (IC), once formed, will return to the reactant proton-bound pair and (2) the thermodynamically stable isomer of the reactant ion, $(AR)(H_2O)^+$, will directly proceed to products. The simplification makes sense when the rate constants for the fundamental processes in Figure 3.1 are compared (Figure 3.5).

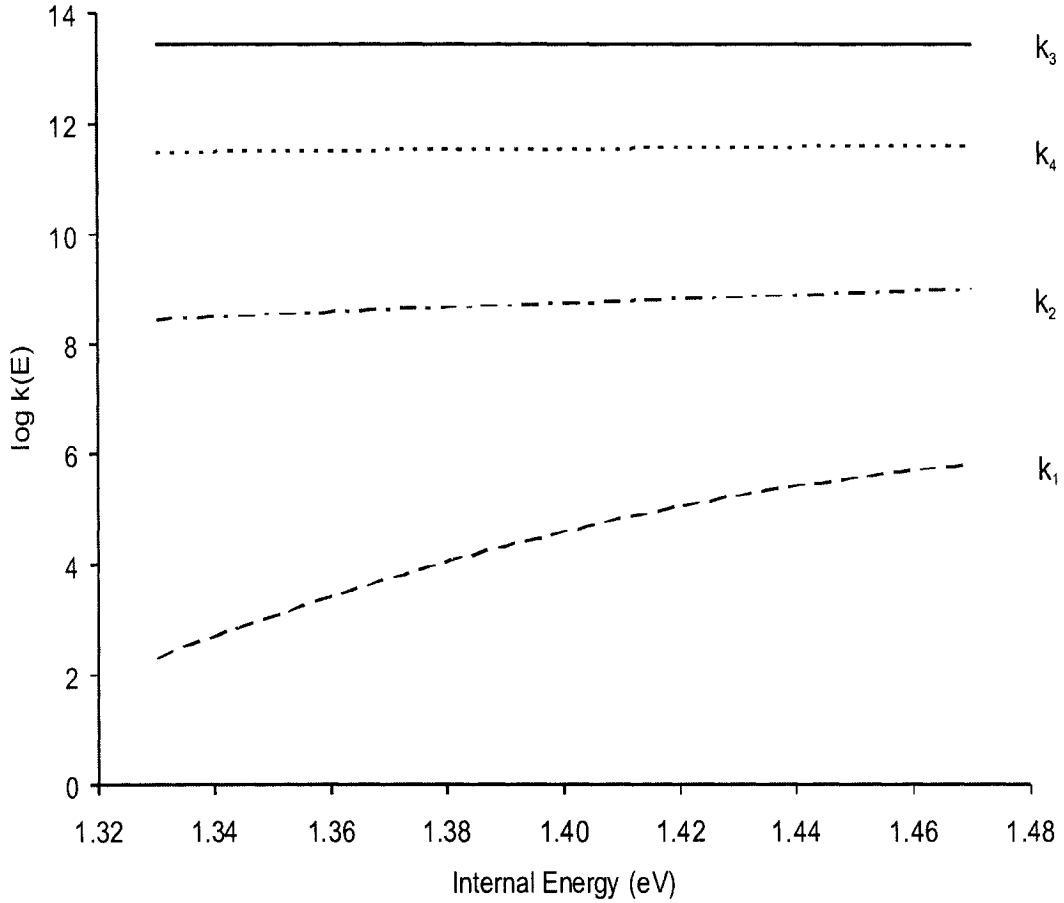

Figure 3.5 RRKM rate constants k(E) of the four elementary processes in the S_N2 mechanism for $(CH_3CN)(CH_3OH)H^+$. k_1 = dissociation of $(CH_3CN)(CH_3OH)H^+$ to $CH_3CNH^+ + CH_3OH$, k_2 = $(CH_3CN)(CH_3OH)H^+$ to IC via TS_a, k_3 = IC to $(CH_3CN)(CH_3OH)H^+$ via TS_a and k_4 = IC to $(CH_3CNCH_3)(H_2O)^+$ via TS_b.

The rate constant (at 1.40 eV) for k_3 is approximately 6 orders of magnitude faster than that of k_2 (10^{14} vs. 10^8 s^{-1}) thus justifying the approximation that once the intermediate complex is formed it returns to the proton-bound pair. The rate constant for k_4 (complex-to-products) is on the order of 10^{12} s^{-1}. The log k(E) vs. E curves suggest that the IC will not have a significant lifetime and may be considered, to a first approximation, as kinetically irrelevant. With this simplification, there should be a relationship between the ratios of the

intensities of the peaks in the MIKES mass spectra for the two processes and the relative barrier heights, similar to the commonly used kinetic method[18]:

$$\ln\left(\frac{k_{diss}}{k_{iso}}\right) = \ln\left(\frac{I_{diss}}{I_{iso}}\right) = \ln\left(\frac{A_{diss}}{A_{iso}}\right) - \frac{\Delta E}{RT} \quad (3.2)$$

where k_{diss} and k_{iso} are the rate constants for the dissociation and isomerization of the proton-bound pair, I_{diss} and I_{iso} are the ion peak intensities measured in the mass spectrum of metastable proton-bound pairs, A_{diss} and A_{iso} are the pre-exponential factors, ΔE is the difference between the calculated barrier heights to dissociation and isomerization (which consist of the difference between the energy of the proton-bound pair and the lowest energy dissociation products (E_{diss}) and the high energy transition state, TS_b (E_{iso})), R is the gas constant and T is the temperature. By plotting the natural logarithm of the ratio of peak intensities, ln (I_{diss}/I_{iso}), against the difference in the calculated barrier heights, a linear relationship is obtained (Figure 3.6). The equation of the line was determined to be ln (I_{diss}/I_{iso}) = -0.42ΔE + 10. This relationship is based upon the calculated relative energies for the proton-bound pairs of acetonitrile with methanol, ethanol, 1-propanol, 2-propanol, 1-butanol and 2-butanol, but extends to proton-bound pairs involving propionitrile suggesting that this equation can be used to determine the barrier height ratio between the two channels for any alkylnitrile-alcohol pair. Thus, by measuring the relative peak intensities in the MIKES mass spectra of proton-bound pairs involving alkylnitriles and alcohols, the difference in the barrier heights for the two dissociation channels may be obtained (Table 3.1).

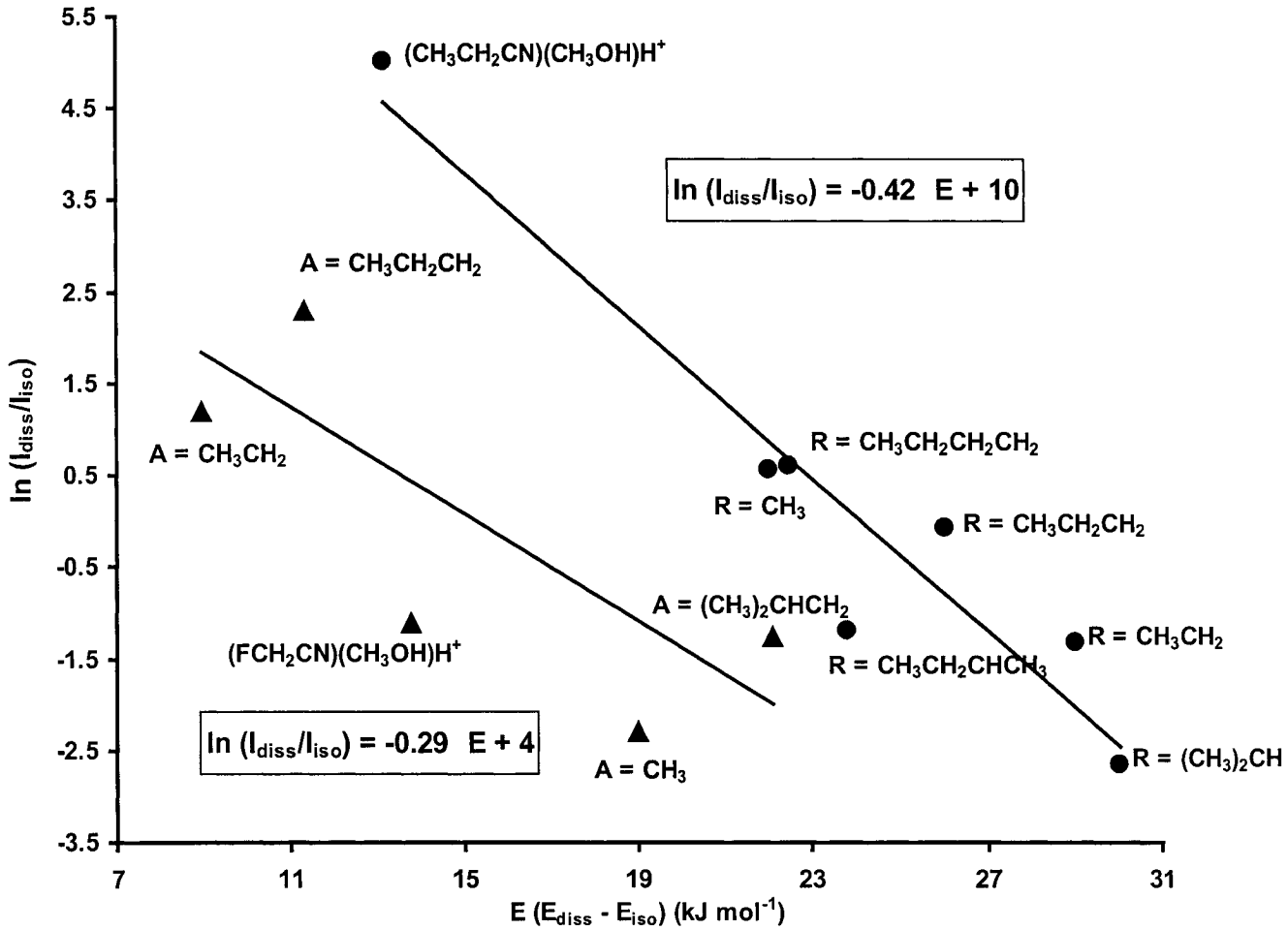

Figure 3.6 Plot of ln (I_{diss}/I_{iso}) vs ΔE for the following proton-bound pairs: (•) $(CH_3CN)(ROH)H^+$ unless otherwise noted and (▲) $(ClCH_2CN)(AOH)H^+$ unless otherwise noted. MP2 energy differences are believed to be within ± 10 kJ mol^{-1} (see Computational Procedures).

Table 3.1 Isomerization energies (TS_b) determined from mass spectrometric peak intensity ratios for the proton-bound pairs between the indicated nitrile and alcohols.[a]

	I_{diss}	I_{iso}	ΔE^c	E_{diss}[b]	E_{iso}
CH_3CH_2CN					
methanol	100.00	0.67	12	115	103
ethanol	100.00	12.67	19	120	102
1-propanol	100.00	40.00	22	123	101
2-propanol	1.00	100.00	35	125	90
1-butanol	81.56	100.00	24	124	99
2-butanol	0.67	100.00	36	120	84
2-methylpropanol	5.33	100.00	31	125	94
1,1-dimethylethanol	0.67	100.00	36	123	87
$CH_3CH_2CH_2CN$					
methanol	100.00	0.00	-	114	-
ethanol	100.00	2.67	15	119	104
1-propanol	100.00	11.33	19	122	103
2-propanol	2.67	100.00	32	124	91
1-butanol	100.00	52.00	22	123	100
2-butanol	1.57	100.00	34	121	87
2-methylpropanol	26.67	100.00	27	124	97
1,1-dimethylethanol	2.00	100.00	33	124	91
$(CH_3)_2CHCN$					
methanol	100.00	0.00	-	112	-
ethanol	100.00	0.67	12	118	106
1-propanol	100.00	2.33	15	121	106
2-propanol	6.67	100.00	30	122	92
1-butanol	100.00	8.67	18	121	103
2-butanol	13.73	100.00	29	122	93
2-methylpropanol	100.00	94.00	24	122	99
1,1-dimethylethanol	2.67	100.00	32	125	92

[a] All reactions lead to H_2O loss and involve the nitrile migrating to the backside of the protonated alcohol. Values in kJ mol^{-1}.
[b] Derived employing the relationship $E_{diss} = -0.26|\Delta PA| + 125$ kJ mol^{-1} [10].
[c] All MP2/6-31+G(d) energies are within ± 10 kJ mol^{-1} (see Computational Procedures).

Coupled with the empirical expression for E_{diss}[10] (see below), E_{iso} can be extracted (Table 3.1). The slope (1/RT) of 0.42 mol kJ^{-1} yields a temperature of 286 K. This "effective" temperature has been discussed in relation to the kinetic method[18-21] and has been found to be related to the internal energy content of dissociating proton-bound pairs.[22]

The relationship described above will provide the relative energetics of the two reaction channels however in order to determine the absolute isomerization energy of a proton-bound pair, its dissociation energy is first required. The dissociation energies used in this work were obtained by using a relationship derived by Mayer,[10] which correlates the binding energy (BE) of nitrile-containing proton-bound pairs with the differences in their proton affinities (ΔPA). The expression derived in Mayer's work is BE (in kJ mol^{-1}) = -0.26|ΔPA| + 125. Therefore, by knowing the proton affinities of the two species in the proton-bound pair, the dissociation energy can be obtained. The dissociation energies obtained from Mayer's relationship are in agreement with values calculated at the MP2/6-31+G(d) level of theory and so, this relationship was therefore used to obtain the dissociation energy of the proton-bound pairs. By employing Mayer's empirical relationship to determine the dissociation energy (E_{diss}), the isomerization energy of any nitrile-alcohol pair can be found. The mass spectrometry of the alkylnitrile-alcohol proton-bound pairs involving CH_3CH_2CN, $CH_3CH_2CH_2CN$ and $(CH_3)_2CHCN$ was investigated in the 2FFR of the mass spectrometer and their relative peak heights and isomerization energies are shown in Table 3.1. Contrary to the observation that dimethyl substitution of the central carbon lowered the energy barrier, alkyl substitution on the nitrile in the proton-bound pair had no visible effect upon the isomerization energy.

The single well approximation breaks down when halogenated nitriles are examined. MP2/6-31+G(d) calculations for $(ClCH_2CN)(CH_3OH)H^+$ showed that chloro-substitution lowered the relative energy of TS_a, but left TS_b unaffected, resulting in a more abundant isomerization reaction compared to $(CH_3CN)(CH_3OH)H^+$.[8] Plotting ln (I_{diss}/I_{iso}) vs. ΔE for the proton-bound pairs $(ClCH_2CN)(AOH)H^+$ and $(FCH_2CN)(CH_3OH)H^+$ (where A = CH_3, CH_3CH_2, $CH_3CH_2CH_2$ and $(CH_3)_2CH$)) results in a displaced line with ln (I_{diss}/I_{iso}) = -0.29ΔE + 4. The lower PAs of the halogenated alkylnitriles (745.7 kJ mol^{-1} for $ClCH_2CN$ vs 779.2 kJ mol^{-1} for CH_3CN) make it easier for them to migrate to the backside of the alcohol moiety, resulting in a lower energy for TS_a. This slope yields an effective temperature of 414 K, which means that these dissociating ions may have a broader internal energy distribution than those for the alkyl nitriles discussed above. As with the previous relationship, one could take the tandem mass spectrum of similar halonitrile-alcohol pairs and obtain its isomerization energy.

Clearly, two main factors in determining the energetics of the species in this rearrangement reaction are the stabilization of the charge in TS_b and the proton affinity of the migrating moiety. These two parameters are employed below to produce more general relationships for the energetics of the S_N2 rearrangement.

3.4.3 Empirical Relationships

The preceding discussion clearly illustrates the relationship between the peak heights observed in mass spectra and their barrier heights calculated with theory. Although this

method for extracting energetics is simple to use, it has the drawback that only the energy of TS_b is found and that considerable mass spectrometric and theoretical work must be done to establish the initial linear relationships. More desirable would be the ability to predict the energies of TS_a, TS_b and IC without the use of mass spectrometry or theory. The MP2/6-31+G(d) relative energies of TS_a, TS_b and IC for the proton-bound pairs were calculated for $(CH_3CN)(ROH)H^+$, $(CH_3CH_2CN)(CH_3OH)H^+$, $(ClCH_2CN)(AOH)H^+$ and $(FCH_2CN)(CH_3OH)H^+$ (where R = CH_3, CH_3CH_2, $CH_3CH_2CH_2$, $(CH_3)_2CH$, $CH_3CH_2CH_2CH_2$, $CH_3CH_2CHCH_3$ and A = CH_3, CH_3CH_2, $CH_3CH_2CH_2$, $(CH_3)_2CH$)). Using $(CH_3CN)(CH_3OH)H^+$ as the base system, the data provides the following empirical corrections to the relative energies of TS_a, TS_b and IC:

$$E(TS_a) = 87- 9(n) -0.33(\Delta PA)$$

$$E(IC) = 83 - 9(n) - 0.33\ (\Delta PA)$$

$$E(TS_b) = 107 - 9(n) - 0.10(\Delta PA)$$

Similar results are obtained when the family of alcohol proton-bound pairs are investigated (here the base system is $(CH_3OH)_2H^+$). For these ions, one alcohol migrates to the back of the protonated alcohol resulting in the formation of an isomer consisting of a protonated ether bound to H_2O:

$$E(TS_a) = 98 - 9(n) - 0.33(\Delta PA)$$

$$E(IC) = 94 - 9(n) - 0.33(\Delta PA)$$

$$E(TS_b) = 121 - 9(n) - 0.10(\Delta PA)$$

PA effects were probed in the latter series using $(CF_3OH)(CH_3OH)H^+$ and $(CF_3OH)(CH_3CH_2OH)H^+$ and alkyl substitution with $(CH_3OH)(ROH)H^+$ (where R = CH_3, CH_3CH_2, $CH_3CH_2CH_2$, $(CH_3)_2CH$). The first number in each equation is the energy calculated for the reference proton-bound pair, namely $(CH_3CN)(CH_3OH)H^+$ and $(CH_3OH)_2H^+$. The n term represents the number of alkyl substituents on the central S_N2 carbon (e.g., n = 0, 1 and 2 for methyl, ethyl/1-propyl and 2-propyl, respectively) and the 9 kJ mol^{-1} was deduced by comparing the relative energies for TS_a, TS_b and IC among pairs having a constant migrating group (i.e. $(CH_3CN)(ROH)H^+$ and $(CH_3OH)(ROH)H^+$). The ΔPA term is the difference between the proton affinities of the migrating moieties (e.g. for $(ClCH_2CN)(CH_3OH)$, $\Delta PA = PA(CH_3CN) - PA(ClCH_2CN)$). The n term is identical for the equations due to the fact that alkyl substitution of the alcohol results in alkyl substitution of the charge-bearing site in all three species, the central carbon in the S_N2 process (see Figure 3.1). In the proton-bound pair, however, this alkyl substitution is not at the charge-bearing site (the proton), but remote from it. Thus, TS_a, TS_b and IC are stabilized to a greater extent than the original proton-bound pair by approximately 9 kJ mol^{-1} per alkyl group. This is comparable to that found in covalently bound ions. Let us consider alkyl substitution on $CH_3CH_2OH^{+\bullet}$ (Δ_fH = 775 kJ mol^{-1}). If the H on the charge bearing oxygen is replaced with a methyl group to form the methyl ethyl ether ion ($CH_3CH_2OCH_3^{+\bullet}$), the heat of formation decreases by 54 kJ mol^{-1} to 721 kJ mol^{-1}. Similarly, if a methyl group hydrogen is replaced instead to form the n-propanol ion, the heat of formation decreases by only 44 kJ mol^{-1} to 731 kJ mol^{-1}, a difference of 10 kJ mol^{-1} with the previous case. So it can be reasonably inferred that substituents that stabilize or destabilize charge in conventional ions will also do so to the same extent in the species in this S_N2 mechanism.

The second parameter which influences the relative energy of TS_a, TS_b and IC is the proton affinity of the migrating molecule. A slightly larger proton affinity effect is observed for TS_a and IC than TS_b. To rearrange to IC via TS_a the migrating molecule must break a hydrogen bond whereas for the second transition state, TS_b, no migration is involved. The larger the proton affinity of the migrating species, the stronger the hydrogen bond to the proton and thus the higher the energy barrier. For example, the relative energies of TS_a, TS_b and IC for $(CH_3OCH_2CN)(CH_3OH)H^+$ are 82, 106 and 78 kJ mol^{-1}, respectively. The difference between these values and those for the $(CH_3CN)(CH_3OH)H^+$ base system are 5, 1 and 5 kJ mol^{-1}, in agreement with the predictions from the empirical equations of 7, 2 and 7 kJ mol^{-1} (the PA of CH_3OCH_2CN is 758.1 kJ mol^{-1}).[19] In general, there is excellent agreement between the original calculated MP2/6-31+G(d) relative energies and those derived from the empirical equations described above (Figure 3.7). All data used in the formulation of these empirical equations may be found in Table 3.2.

Base systems for other proton-bound pairs between different migrating molecules and methanol (all resulting in H_2O loss) are listed below in Table 3.3. Note that the empirical formulae can only be used within a particular family of proton-bound molecular pairs (e.g. nitriles with alcohols or any nitroalkane with any alcohol). The relative energy values for TS_a, TS_b and IC can be used in conjunction with the correction factors described earlier to provide a wide range of isomerization energies.

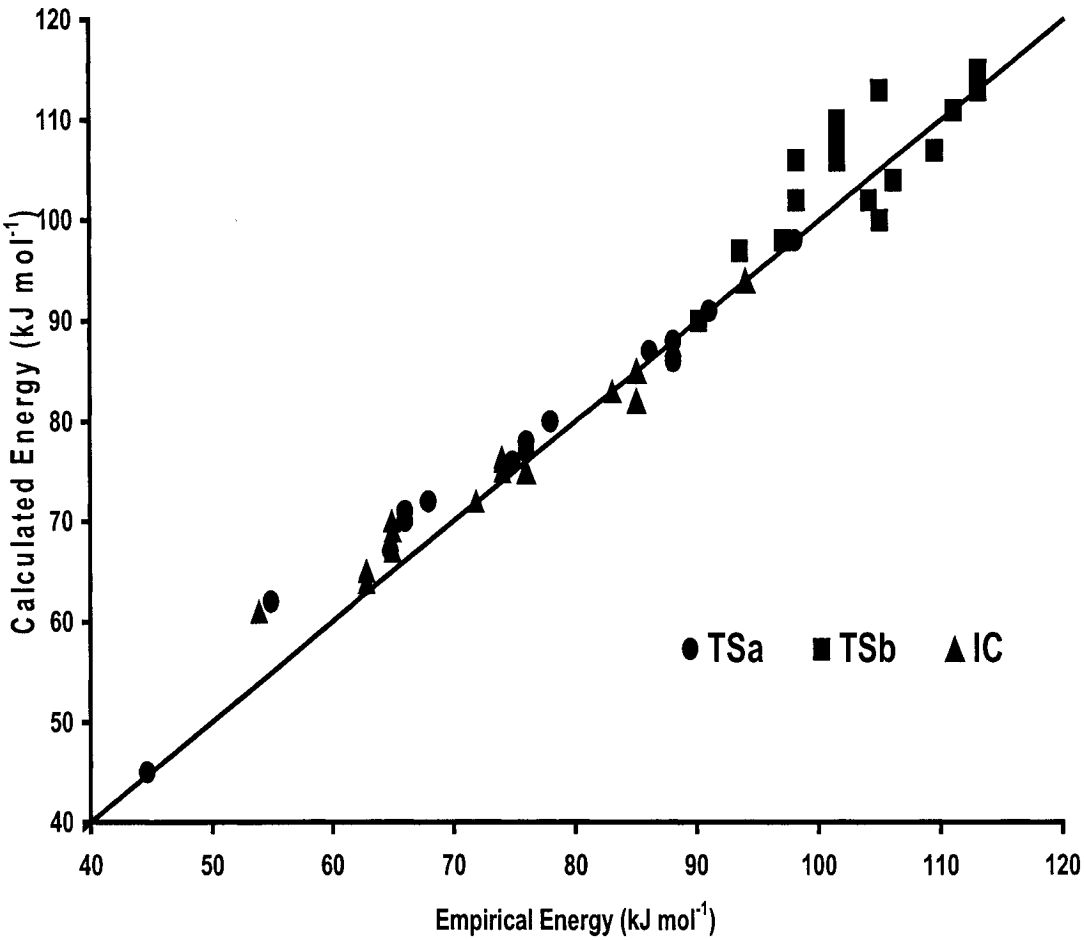

Figure 3.7 Plot of the MP2/6-31+G(d) calculated relative energies for TS_a, TS_b and IC vs. those obtained from the empirical relationships outlined in the text.

Table 3.2: MP2/6-31+G(d) relative energies (as compared to the respective proton-bound pairs, ABH^+). Molecule A migrates in the S_N2 mechanism in each case.[a]

A	B	PA(A)[b]	PA(B)[b]	E_{diss}	TS_a	IC	TS_b
CH_3CN	CH_3OH	779.2	754.3	129	87	83	107
CH_3CN	CH_3CH_2OH	779.2	776.4	139	77	75	110
CH_3CN	$CH_3CH_2CH_2OH$	779.2	786.5	132	77	76	106
CH_3CN	$(CH_3)_2CHOH$	779.2	793	127	70	69	97
CH_3CN	$CH_3CH_2CH_2CH_2OH$	779.2	789.2	130	78	76	108
CH_3CN	$CH_3CH_2CH(OH)CH_3$	779.2	815.0	121	71	67	97
$ClCH_2CN$	CH_3OH	745.7	754.3	123	76	72	104
$ClCH_2CN$	CH_3CH_2OH	745.7	776.4	115	67	65	106
$ClCH_2CN$	$CH_3CH_2CH_2OH$	745.7	786.5	113	67	64	102
$ClCH_2CN$	$(CH_3)_2CHOH$	745.7	793	112	62	61	90
FCH_2CN	CH_3OH	725.0	754.3	116	72	70	102
CH_3CH_2CN	CH_3OH	794.1	754.3	124	91	88	111
CH_3OCH_2CN	CH_3OH	758.1	754.3	124	82	78	106
CH_3OH	CH_3OH	754.3	754.3	139	98	94	121
CH_3OH	CH_3CH_2OH	754.3	776.4	131	88	85	115
CH_3OH	$CH_3CH_2CH_2OH$	754.3	786.5	129	86	82	113
CH_3OH	$(CH_3)_2CHOH$	754.3	793	122	80	75	100
CF_3OH	CH_3OH	594.3	754.3	57	45	39	113
CF_3OH	CH_3CH_2OH	594.3	776.4	60	40	35	98
CH_3CHO	CH_3OH	768.5	754.3	121	86	82	112
CH_3NO_2	CH_3OH	754.6	754.3	125	80	63	99

[a] All values in kJ mol^{-1} at 0 K.

[b] All proton affinities obtained from the NIST database. Reference 23

Table 3.3 Calculated relative energies of TS_a, TS_b and IC for four base system proton-bound pairs involving the listed migrating molecule and methanol. The S_N2 reaction leads to water loss in each case.[a]

Migrator	PA[b]	TS_a	IC	TS_b
CH_3OH	754.3	98	94	121
CH_3CN	779.2	87	83	107
CH_3CHO	768.5	86	82	112
CH_3NO_2	754.6	80	63	99

[a] Values in kJ mol^{-1} and are relative to the proton-bound pair.
[b] Reference [23]

3.5 Conclusions

A relationship has been demonstrated between relative peak intensities measured in metastable ion mass spectra and calculated barrier heights to dissociation and isomerization reactions in gas-phase proton-bound pairs. A series of empirical relationships have been derived for the energetics of S_N2 reaction surfaces involving alcohol-alcohol and alcohol-acetonitrile proton-bound pairs. The relative energies of the species involved in the isomerization reactions are lowered by charge stabilizing substituents at the S_N2 carbon. The PA of the migrating molecule in the mechanism can cause the relative energy of the first barrier and the intermediate complex in the mechanism to be raised or lowered. By calculating the first member in a family of proton-bound pairs, the three empirical equations can be used to determine the energetics of other members of the series. The family of nitroalkane proton-bound pairs have been recently studied in our group and they have been

found to also undergo the internal S_N2 rearrangement to lose nitrous acid, HONO. It is reasonable to conclude that all proton-bound pairs obey the S_N2-type mechanism, the observation of the products simply being determined by the energetics.

References

1. P. M. Mayer, "Unimolecular reactions of proton-bound cluster ions: Competition between dissociation and isomerization in the methanol-acetonitrile dimer", *J. Phys. Chem A* **103**, 3687 (1999).
2. R. A. Ochran, A. Annamalai, and P. M. Mayer, "Unimolecular reactions of proton-bound cluster ions: Competition between dissociation and isomerization in the ethanol-acetonitrile dimer", *J. Phys. Chem A* **104**, 8505 (2000).
3. R. A. Ochran and P. M. Mayer, "Ion rearrangement at the beginning of cluster formation: methyl substitution effects on the internal S_N2 reaction in the proton-bound dimers of acetonitrile and alcohols", *Eur. J. Mass Spectrom.* **7**, 267 (2001).
4. J. A. D. McCormack and P. M. Mayer, "Ion/molecule reaction kinetics using a modified Finnigan GCQ ion trap mass spectrometer: the energetics of the dehydration of proton-bound dimers." *Int. J. Mass Spectrom.* **207**, 183 (2001).
5. T. D. Fridgen, J. D. Keller, and T. B. McMahon, "Direct experimental determination of the energy barriers for methyl cation transfer in the reactions of methanol with protonated methanol, protonated acetonitrile and protonated acetaldehyde: a low pressure FTICR study", *J. Phys. Chem. A* **105**, 3816 (2001).

6. T. D. Fridgen and T. B. McMahon, "Experimental determination of activation energies for gas-phase ethyl and n-propyl cation transfer reactions", *J. Phys. Chem. A* **106**, 9648 (2002).

7. H. E. Audier, C. Monteiro, P. Mourgues, and D. Robin, "Isomerization of proton-bound alcohol dimers", *Rapid Commun. Mass Spectrom.* **3**, 84 (1989).

8. R. A. Ochran and P. M. Mayer, "How does chlorine substitution on acetonitrile affect the internal S_N2 isomerization of proton-bound pairs $(ClCH_2CN)(ROH)H^+$ (R = CH_3, C_2H_5, C_3H_7)?" *Int. J. Mass Spectrom.* **227**, 471 (2003).

9. J. W. Larson and T. B. McMahon, "Formation, thermochemistry, and relative stabilities of proton-bound dimers of oxygen n-donor bases from ion cyclotron resonance solvent-exchange equilibria measurements", *J.Am.Chem. Soc* **104**, 6255 (1982).

10. P. M. Mayer, "Structures and binding energies of proton-bound pairs of HCN and CH_3CN with NH_3, H_2O, HF, CH_3NH_2, CH_3OH and CH_3F", *J. Phys. Chem. A* **103**, 5905 (1999).

11. J. L. Holmes and P. M. Mayer, "Combined mass spectrometric and thermochemical examination of the C_2H_2N family of cations and radicals", *J. Phys. Chem.* **99**, 1366 (1995).

12. W. J. Hehre, L. Radom, P. v. R. Schleyer, and J. A. Pople, *Ab Initio Molecular Orbital Theory*. John Wiley & Sons, New York (1986).

13. M. J. Frisch, G. W. Trucks, H. B. Schlegel, G. E. Scuseria, M. A. Robb, J. R. Cheeseman, V. G. Zakrzewski, J. A. Montgomery, R. E. Stratmann, J. C. Burant, S. Dapprich, J. M. Millam, A. D. Daniels, K. N. Kudin, M. C. Strain, O. Farkas, J.

Tomasi, V. Barone, M. Cossi, R. Cammi, B. Mennucci, C. Pomelli, C. Adamo, S. Clifford, J. Ochterski, G. A. Petersson, P. Y. Ayala, Q. Cui, K. Morokuma, D. K. Malick, A. D. Rabuck, K. Raghavachari, J. B. Foresman, J. Cioslowski, J. V. Ortiz, B. B. Stefanov, G. Liu, A. Liashenko, P. Piskorz, I. Komaromi, R. Gomperts, R. L. Martin, D. J. Fox, T. Keith, M. A. Al-Laham, C. Y. Peng, A. Nanayakkara, C. Gonzalez, M. Challacombe, P. M. W. Gill, B. Johnson, W. Chen, M. W. Wong, J. L. Andres, C. Gonzalez, M. Head-Gordon, E. S. Replogle, and J. A. Pople, *in* "GAUSSIAN 98 Rev. A.7". Gaussian Inc., Pittsburgh PA, 1998.

14. P. M. Mayer, "Binding energies of nitrile containing proton-bound clusters: The performance of HF, MP2 and B3-LYP vs. G2", *Chem. Phys. Lett.* **314**, 311 (1999).

15. A. P. Scott and L. Radom, "Harmonic Vibrational Frequencies: An evaluation of hartree-fock, moller-plesset, quadratic configuration interaction, density functional theory and semi-empirical scale factors", *J. Phys. Chem.* **100**, 16502 (1996).

16. T. Baer and W. L. Hase, *Unimolecular Reaction Dynamics, Theory and Experiments*. Oxford University Press, New York (1996).

17. T. Beyer and D. R. Swinehart, "Number of multiply-restricted partitions [A1] (Algorithm 448)", *ACM Commun.* **16**, 379 (1973).

18. S. A. McLuckey, D. Cameron, and R. G. Cooks, "Proton affinities from dissociations of proton-bound dimers", *J. Am. Chem. Soc.* **130**, 1313 (1981).

19. X. Zheng and R. G. Cooks, "Thermochemical determinations by the kinetic method with direct entropy correction", *J. Phys. Chem A* **106**, 9939 (2002).

20. X. Cheng, Z. Wu, and C. Fenselau, "Collision energy dependence of proton-bound dimer dissociation: entropy effects, proton affinities and intramolecular hydrogen-bonding in protonated peptides." *J. Am. Chem. Soc.* **115**, 4844 (1993).

21. Z. Wu and C. Fenselau, "Gas-Phase basicities and proton affinities of lysine and histidine measured from the dissociation of proton-bound dimers", *Rapid Commun. Mass Spectrom.* **8**, 777 (1994).

22. L. Drahos and K. Vekey, "How closely related are the effective temperature and the real temperature?" *J. Mass Spectrom.* **34**, 79 (1999).

23. P. J. Linstrom and W. G. Mallard, *NIST Chemistry WebBook, NIST Standard Reference Database Number 69.* National Institute of Standards and Technology, Gaithersburg, MD (March 2003).

Supplemental Material: Optimized geometries of proton-bound pairs, TS_a, TS_b and intermediate complexes used in derivation of empirical formulae.

$(CH_3CN)(ROH)H^+$	Proton-Bound Pair	TS_a	IC	TS_b
$R = CH_3$	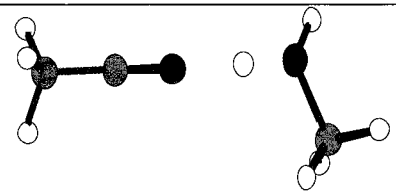	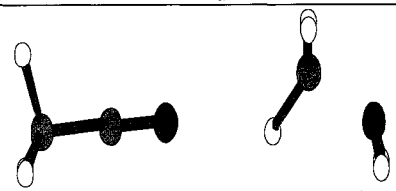	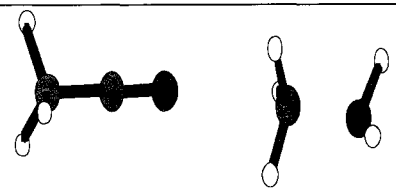	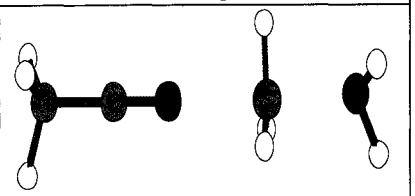
$R = CH_3CH_2$	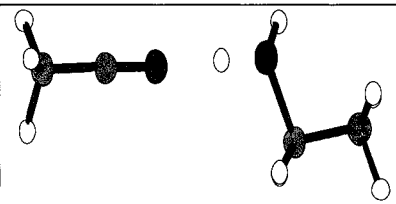	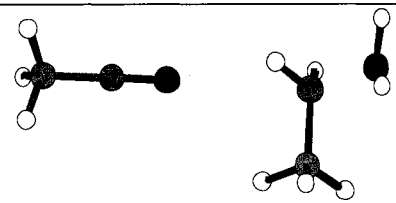	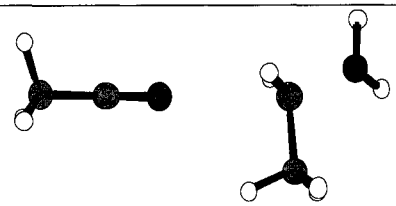	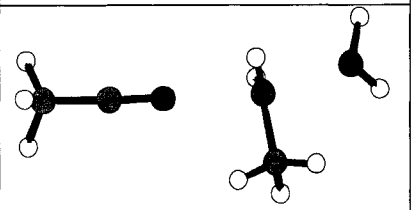
$R = CH_3CH_2CH_2$	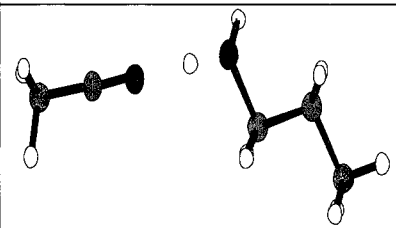	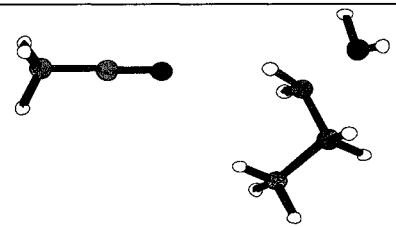	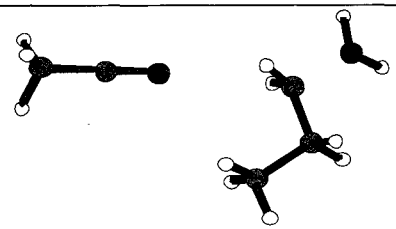	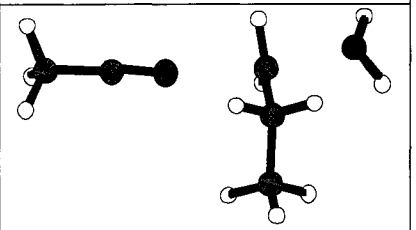
$R = (CH_3)_2CH$	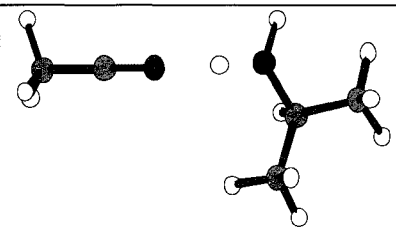	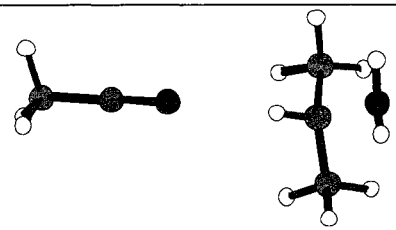	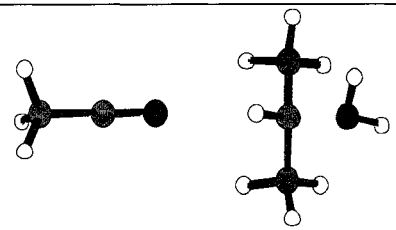	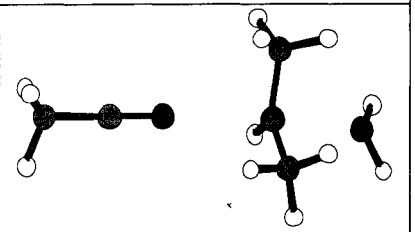

	Proton-Bound Pair	TS_a	IC	TS_b
$R = CH_3CH_2CH_2CH_2$	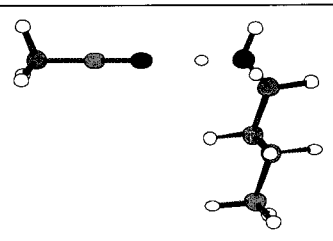	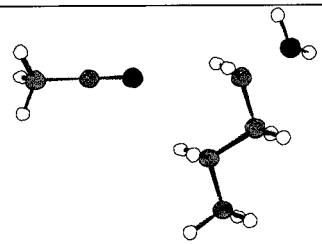	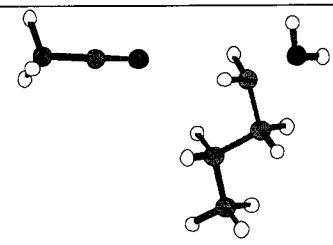	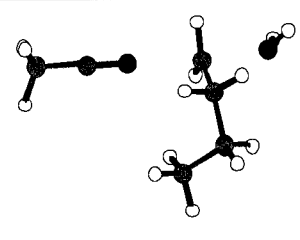
$R = (CH_3)_2CHCH_2$	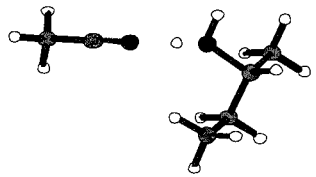	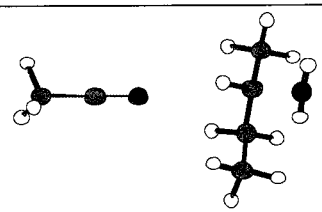	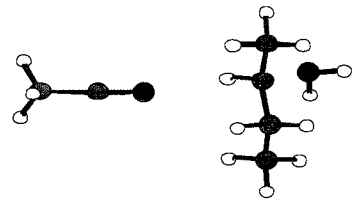	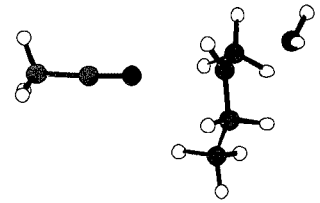
$(CH_3CH_2CN)(CH_3OH)H^+$	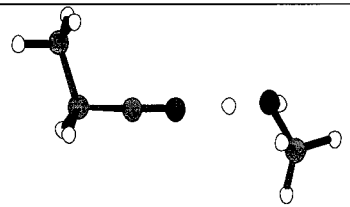	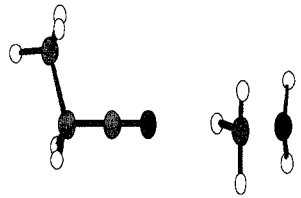	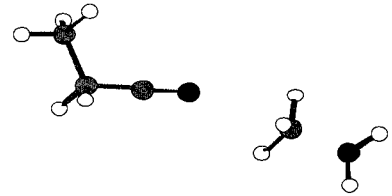	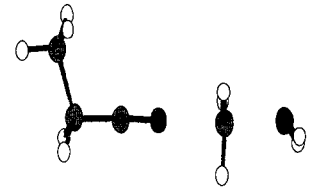
$(CH_3NO_2)(CH_3OH)H^+$	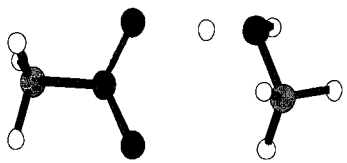	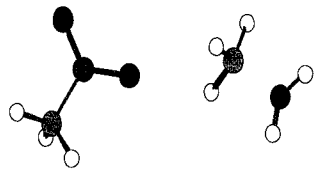	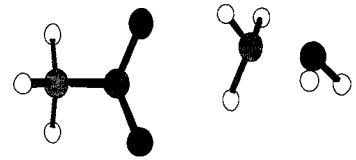	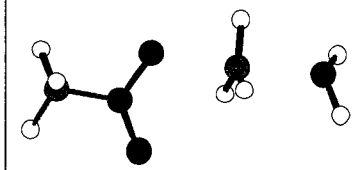

$(ClCH_2CN)(ROH)H^+$	Proton-Bound Pair	TS_a	IC	TS_b
R = CH_3	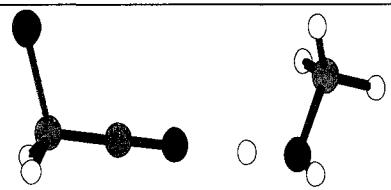	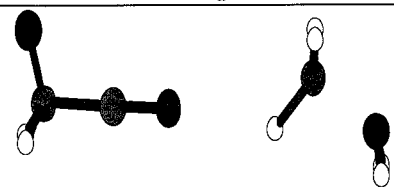	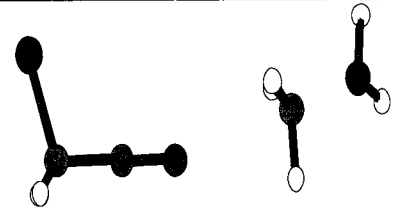	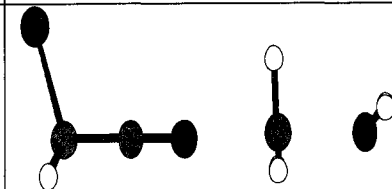
R = CH_3CH_2	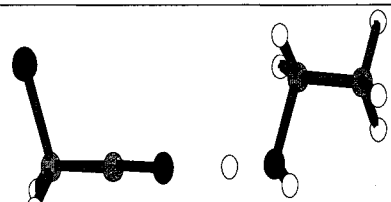	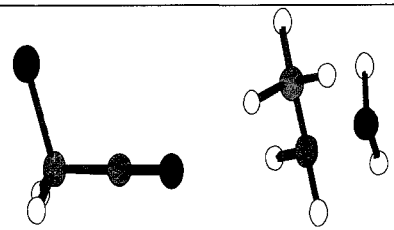	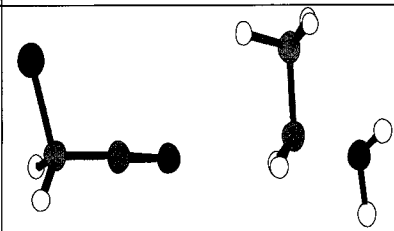	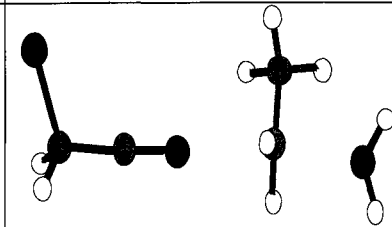
R = $CH_3CH_2CH_2$	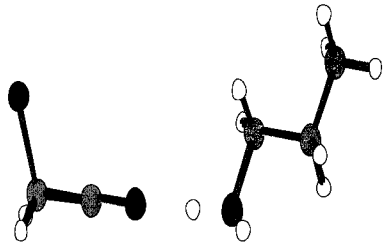	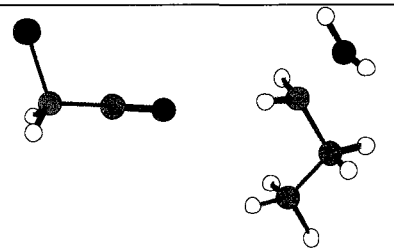	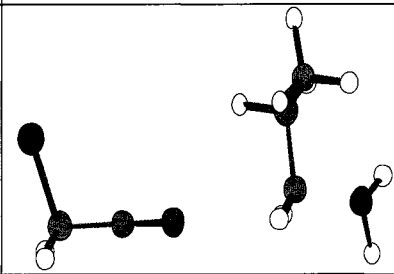	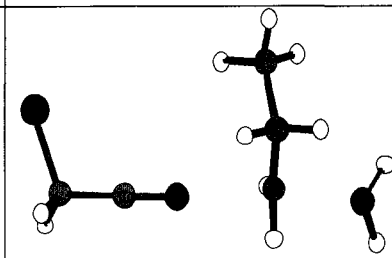
R = $(CH_3)_2CH$	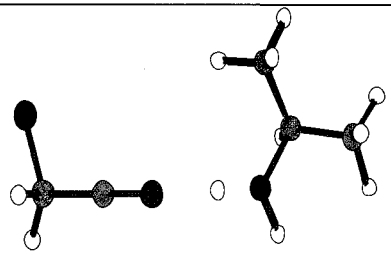	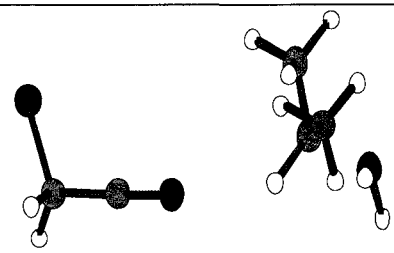	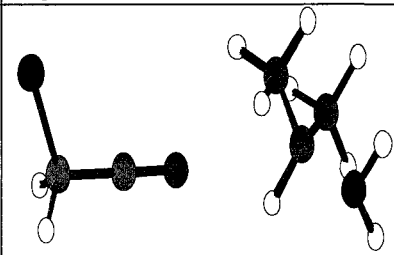	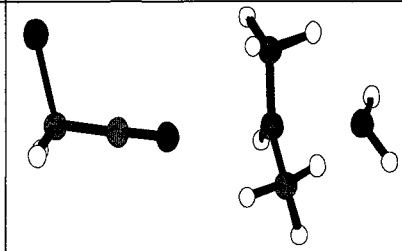

$(CH_3OH)(ROH)H^+$	Proton-Bound Pair	TS_a	IC	TS_b
$R = CH_3$	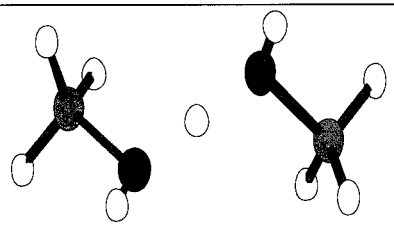	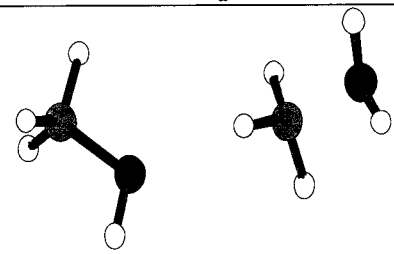	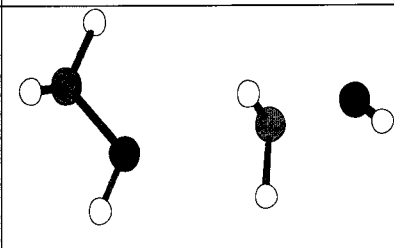	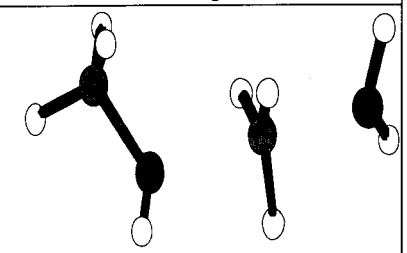
$R = CH_3CH_2$	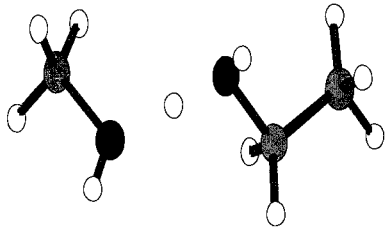	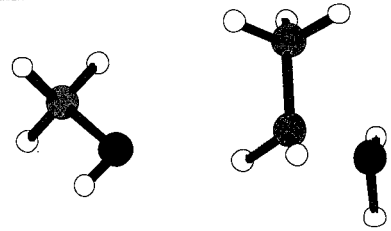	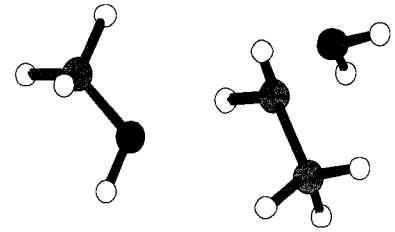	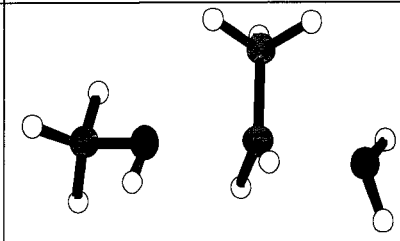
$R = CH_3CH_2CH_2$	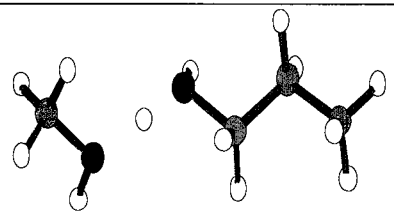	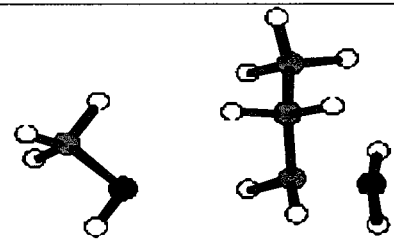	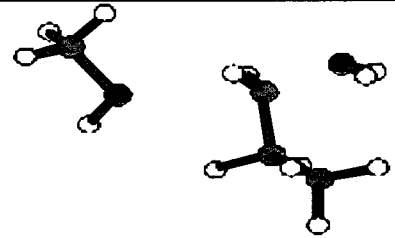	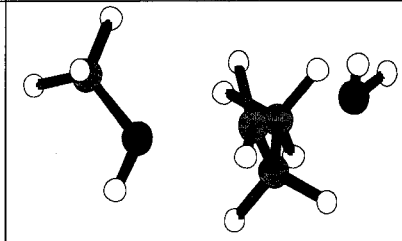
$R = (CH_3)_2CH$	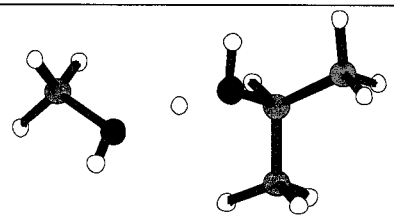	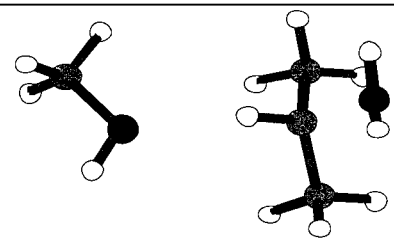	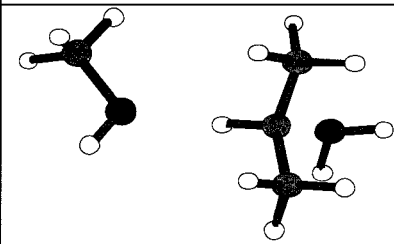	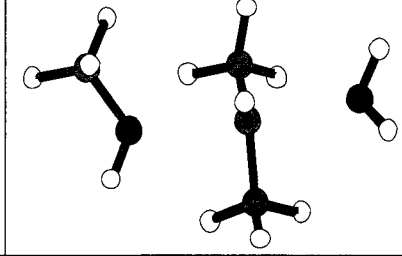

	Proton-Bound Pair	TS_a	IC	TS_b
$(CF_3OH)(CH_3OH)H^+$	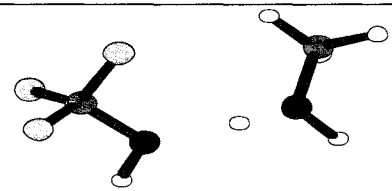	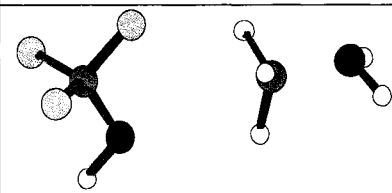	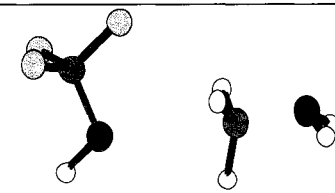	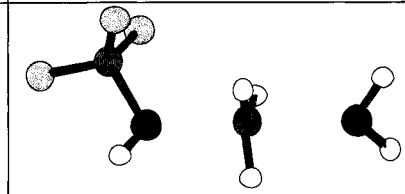
$(CF_3OH)(CH_3CH_2OH)H^+$	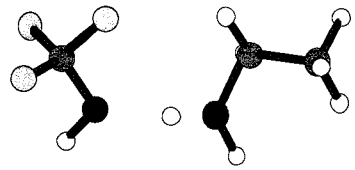	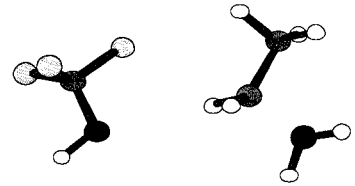	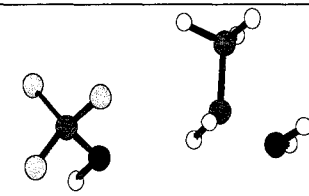	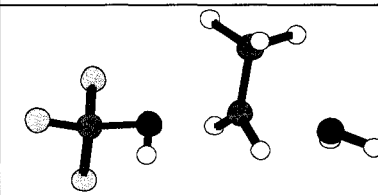
$(FCH_2CN)(CH_3OH)H^+$	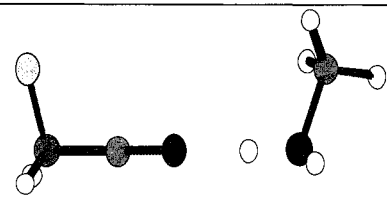	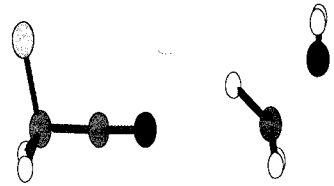	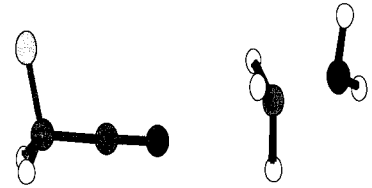	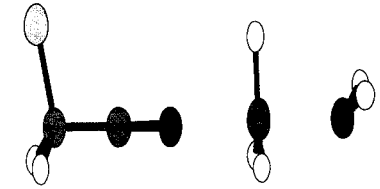
$(CH_3CHO)(CH_3OH)H^+$	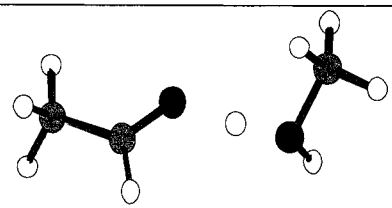	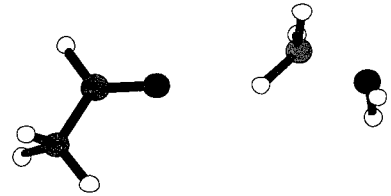	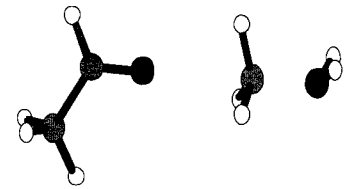	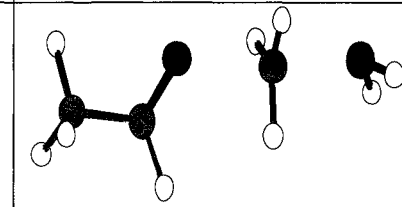

CHAPTER 4

ENTROPY CHANGES IN THE DISSOCIATION OF PROTON-BOUND COMPLEXES: A VARIATIONAL RRKM STUDY

4.1 Introduction

In this chapter, microcanonical variational transition state theory (μ-VTST) is used to model the unimolecular dissociation of a series of proton-bound acetonitrile-alcohol pairs $(CH_3CN)(XOH)H^+$ (where X = CH_3, CH_3CH_2, $CH_3CH_2CH_2$ and $(CH_3)_2CH$) so as to extract the entropy of activation ($\Delta S^{\ddagger}$) for the bond scission reactions. In particular, $\Delta S^{\ddagger}$ for a single dissociation channel will explicitly be determined and the manner in which it changes with molecular functionality will be explored. In addition to examining how $\Delta S^{\ddagger}$ changes systematically, the entropies of activation and thermodynamic entropies for the dissociation of proton-bound pairs into CH_3CNH^+ + ROH and $CH_3CN + ROH_2^+$ will be compared.

4.2 Computational Procedures

Ab initio molecular orbital calculations were carried out using the Gaussian 98 suite of programs.[1] Geometries were optimized and harmonic vibrational frequencies were calculated, at the MP2/6-31+G(d) level of theory. All vibrational frequencies were scaled by the factor of 0.9434 recommended by Scott and Radom[2] prior to use.

Variational transition state theory was used to model the unimolecular dissociation of the proton-bound complex according to the following expression:[3-6]

$$k(E) = \frac{\sigma}{h} \frac{N^{\ddagger}(E, E_0, R^*)}{\rho(E)} \quad (4.1)$$

where $k(E)$ is the unimolecular rate constant at an ion internal energy, E, σ is the reaction symmetry number, h is Planck's constant, E_0 is the 0 K activation energy, $\rho(E)$ is the reactant ion density of states and $N^{\ddagger}(E,E_0,R^*)$ is the sum-of-states for the fragmentation bottleneck located at an intracluster separation R^*. The density and sum-of-states were calculated by the direct count method of Beyer and Swinehart.[7]

Two methods (approximate and detailed) were used to determine the entropies of activation, $\Delta S^{\ddagger}$, for the dissociation of four acetonitrile-alcohol proton-bound pairs, $(CH_3CN)(ROH)H^+$, (where R = CH_3, C_2H_5, C_3H_7 and $(CH_3)_2CH$) into CH_3CNH^+ + ROH and CH_3CN + ROH_2^+. Since the dissociation reaction into CH_3CNH^+ and neutral alcohol proceeded in a straightforward manner with the two separating moieties simply getting farther apart, an approximate method was employed. This method first involved calculating the energy of each proton-bound pair ABH^+ for several intracluster separations, R, (without optimization) ranging from the equilibrium value to 12 Å. An example is shown below in Figure 4.1 for $(CH_3CN)(CH_3OH)H^+$. The reaction path of a dissociation process does not have a reaction barrier and so a unique transition state cannot be obtained with *ab initio* MO calculations. The transition state responsible for the simple bond cleavage of the proton-

bound pair was therefore located by finding the intracluster separation, R*, having the lowest sum-of-states and thus responsible for the minimum reaction flux. The normal modes of ABH^+ were assigned to frequencies of either one of the dissociation products AH^+ or B (common modes) or to one of the six modes that are converted to translational and rotational degrees of freedom of the products (the vanishing modes) by comparing their calculated atomic displacements. This process is uncomplicated since the six vanishing modes are the only ones for which all of the atoms in ABH^+ are displaced. For the common modes the transition state frequencies were chosen to be the average of their values in the complex and in the free product and hence were the same for every configuration along the curve in Figure 4.1. Of the six vanishing modes, the lowest frequency mode was a torsion mode and was treated as a free rotor in the RRKM calculations[3] while the highest frequency mode was the intracluster stretching frequency representing the reaction coordinate for the cleavage of the complex. The four remaining frequencies were then scaled according to the following equation:[3, 8, 9]

$$\nu'(R) = \nu(R_{eq})e^{-\alpha(R-R_{eq})} \qquad (4.2)$$

where $\nu'(R)$ is the value of the frequency at an intracluster separation R, R_{eq} is the equilibrium hydrogen bond distance and α is an adjustable parameter. This equation is based on the assumption that the four modes will vanish exponentially to zero along the reaction coordinate.[8, 9] The parameter α is adjustable and was determined by comparing the four vanishing frequencies of each molecular system with those calculated for the optimized AH^+—B structures having intracluster separations of 5.0 Å and 8.0 Å. The value of α used

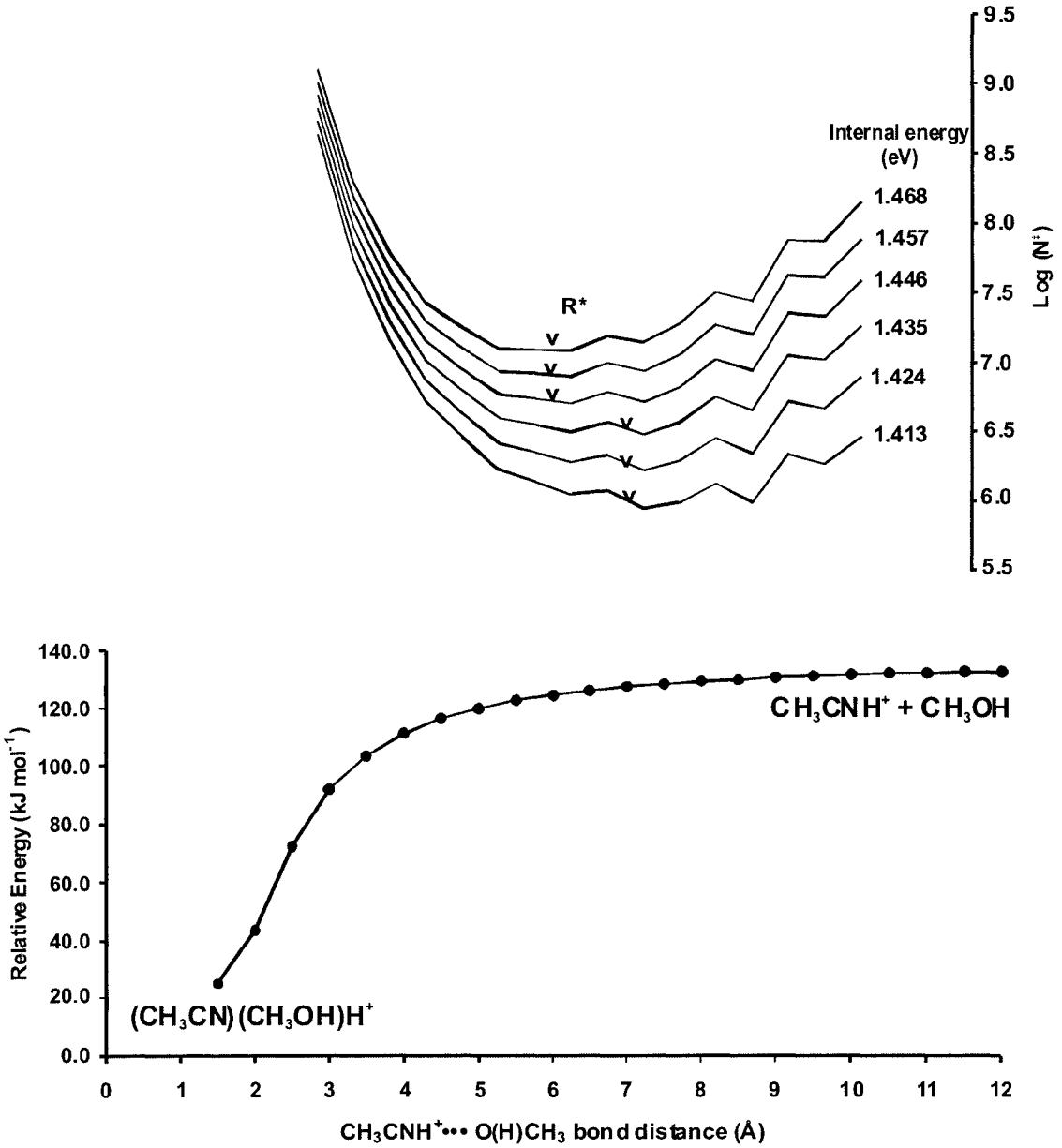

Figure 4.1 Plot of the relative energy vs. $CH_3CNH^+\bullet\bullet\bullet O(H)CH_3$ bond distance in the $(CH_3CN)(CH_3OH)H^+$ complex at the MP2/6-31+G(d) level of theory. Superimposed on the figure is the calculated sum-of-states, $\log(N^{\ddagger})$ as a function of R at various internal energies and the locations, R*, of the variational transition state.

to calculate the new frequencies at each R-value was an average of the α values obtained at intracluster separations of 5.0 and 8.0 Å. The four α values derived for each of the four complexes as well as all vibrational frequencies used in the RRKM treatment are listed in Table 4.1. The logarithm of the sum-of-states, log ($N^{\ddagger}$), was then calculated as a function of R.

This approach to locating the minimum in $N^{\ddagger}$ is, of course, only approximate. It is impossible to determine how approximate unless a fully optimized dissociation reaction coordinate is obtained (and avoid the use of equation (4.2)). Even then, however, it is uncertain how accurately most modest computational levels of theory can model a dissociation reaction coordinate. In light of this fact, all computational approaches to this problem will yield only estimates of the true entropy of activation. By treating all of the systems in the same manner, it is hoped that at least the relative $\Delta S^{\ddagger}$ values will be reliable. We estimated the uncertainty in the $\Delta S^{\ddagger}$ values, using the spread in the α-values obtained for the 5.0 and 8.0 Å geometries, to be ± 3 J K^{-1} mol^{-1}.

The dissociation of the proton-bound pairs into neutral acetonitrile and protonated alcohol was not as straightforward as the pathway to CH_3CNH^+ and neutral alcohol and so, the approximate method described above could not be incorporated (see Results and Discussion). Instead, full geometry optimizations (and frequency analyses) were required for all structures along the dissociation pathways. The N—H bond was stretched (by 0.5 Å increments), held fixed at each point and the rest of the geometric parameters optimized

Table 4.1 Information used in the determination of $\Delta S^{\ddagger}$ for the dissociation of proton-bound pairs into CH_3CNH^+ and neutral alcohol.

	Harmonic Frequencies (cm^{-1})[a]
$(CH_3CN)(CH_3OH)H^+$	67, 80, 129, 147, 260, 329, 331, 517, 882, 908, 964, 1013, 1015, 1098, 1160, 1290, 1374, 1417, 1417, 1419, 1451, 1454, 1665, 1943, 2155, 2943, 2983, 3039, 3040, 3103, 3117, 3470
CH_3CNH^+	322, 322, 541, 541, 866, 1008, 1008, 1362, 1394, 1394, 2183, 2927, 3029, 3029, 3486
CH_3OH	313, 1004, 1028, 1129, 1306, 1437, 1464, 1473, 2908, 2977, 3045, 3562
Transition state (common)	325, 327, 415, 711, 725, 984, 1010, 1011, 1063, 1209, 1233, 1265, 1368, 1405, 1406, 1428, 1459, 1462, 2169, 2714, 2935, 2946, 3034, 3034, 3047, 3074, 3516
Transition state (vanishing)[b]	67, 80, 129, 147
α values ($Å^{-1}$)	0.46, 0.44, 0.20, 0.20
Rotational Constant for rotor (GHz)	23.3
Moment of Inertia (10^{-47} kg m^2)	360, 643, 667 for $(CH_3CN)(CH_3OH)H^+$ 5.39, 99.4, 99.4 for CH_3CNH^+ 6.61, 34.3, 35.5 for CH_3OH
$(CH_3CN)(CH_3CH_2OH)H^+$	36, 51, 88, 125, 207, 251, 328, 329, 408, 512, 783, 790, 900, 950, 970, 1014, 1015, 1066, 1157, 1223, 1268, 1369, 1374, 1396, 1418, 1419, 1446, 1456, 1473, 1664, 2144, 2159, 2937, 2943, 2991, 3019, 3039, 3039, 3040, 3073, 3455
CH_3CNH^+	322, 322, 541, 541, 866, 1008, 1008, 1362, 1394, 1394, 2183, 2927, 3029, 3029, 3486
CH_3CH_2OH	225, 279, 401, 794, 871, 1009, 1058, 1140, 1214, 1248, 1362, 1404, 1445, 1461, 1490, 2896, 2930, 2939, 3014, 3026, 3546
Transition state (common)	265, 325, 326, 404, 527, 587, 792, 827, 989, 883, 1011, 1011, 1062, 1103, 1149, 1219, 1258, 1366, 1368, 1400, 1406, 1406, 1446, 1459, 1481, 2164, 2823, 2934, 2935, 2965, 2984, 3017, 3033, 3034, 3034, 3501
Transition state (vanishing)[b]	36, 51, 88, 125
α values ($Å^{-1}$)	0.27, 0.31, 0.25, 0.25
Rotational Constant for rotor (GHz)	19.7
Moment of Inertia (10^{-47} kg m^2)	42.6, 1030, 1050 for $(CH_3CN)(CH_3CH_2OH)H^+$ 5.39, 99.4, 99.4 for CH_3CNH^+ 24.2, 89.3, 103 for CH_3CH_2OH
$(CH_3CN)(CH_3CH_2CH_2OH)H^+$	33, 40, 86, 111, 121, 186, 225, 286, 328, 329, 434, 511, 746, 825, 864, 893, 903, 969, 1013, 1015, 1017, 1087, 1158, 1204, 1247, 1279, 1310, 1374, 1375, 1395, 1419, 1419, 1456, 1461, 1466, 1472, 1663, 2146, 2193, 2926, 2936, 2943, 2979, 2989, 3019, 3032, 3040, 3040, 3063, 3452

CH_3CNH^+	322, 322, 541, 541, 866, 1008, 1008, 1362, 1394, 1394, 2183, 2927, 3029, 3029, 3486
$CH_3CH_2CH_2OH$	115, 225, 246, 265, 439, 741, 865, 872, 1003, 1036, 1051, 1144, 1205, 1220, 1269, 1299, 1383, 1400, 1458, 1462, 1468, 1487, 2883, 2917, 2927, 2934, 2979, 3000, 3005, 3542
Transition state (common)	122, 210, 265, 319, 320, 417, 561, 617, 740, 791, 865, 895, 928, 986, 1017, 1018, 1048, 1145, 1188, 1241, 1284, 1306, 1371, 1377, 1398, 1428, 1428, 1461, 1464, 1470, 1477, 1638, 2118, 2567, 2938, 2943, 2966, 2993, 3013, 3034, 3036, 3036, 3058, 3218, 3461
Transition State (vanishing)[b]	33, 40, 86, 111
α values ($Å^{-1}$)	0.13, 0.09, 0.03, 0.08
Rotational Constant for rotor (GHz)	10.6
Moment of Inertia (10^{-47} kg m^{-2})	78.8, 1460, 1510 for $(CH_3CN)(CH_3CH_2CH_2OH)H^+$ 5.39, 99.4, 99.4 for CH_3CNH^+ 31.7, 220, 236 for $CH_3CH_2CH_2OH$
$(CH_3CN)((CH_3)_2CHOH)H^+$	36, 47, 89, 116, 197, 219, 265, 329, 330, 352, 388, 449, 510, 706, 875, 898, 916, 920, 954, 1014, 1015, 1064, 1109, 1175, 1235, 1308, 1355, 1374, 1395, 1396, 1419, 1420, 1438, 1446, 1456, 1464, 1671, 2141, 2348, 2930, 2937, 2943, 2980, 3015, 3026, 3031, 3036, 3039, 3040, 3445
CH_3CNH^+	322, 322, 541, 541, 866, 1008, 1008, 1362, 1394, 1394, 2183, 2927, 3029, 3029, 3486
$(CH_3)_2CHOH$	216, 266, 290, 350, 398, 465, 799, 902, 925, 938, 1054, 1117, 1157, 1226, 1326, 1350, 1378, 1391, 1444, 1446, 1458, 1467, 2883, 2912, 2925, 2991, 3007, 3012, 3020, 3529
Transition state (common)	225, 267, 320, 320, 347, 349, 371, 438, 657, 809, 887, 892, 907, 936, 995, 1017, 1018, 1095, 1166, 1215, 1311, 1353, 1377, 1394, 1399, 1428, 1428, 1440, 1450, 1461, 1468, 1642, 2116, 2859, 2934, 2940, 2943, 3000, 3020, 3027, 3035, 3035, 3036, 3043, 3457
Transition state (vanishing)[b]	36, 47, 89, 116
α values ($Å^{-1}$)	0.13, 0.17, 0.05, 0.09
Rotational Constant for rotor (GHz)	7.0
Moment of Inertia (10^{-47} kg m^{-2})	120, 1130, 1200 for $(CH_3CN)((CH_3)_2CHOH)H^+$ 5.3, 99.4, 99.4 for CH_3CNH^+ 96.9, 104, 176 for $(CH_3)_2CHOH$

[a] vibrational frequencies calculated at the MP2/6-31+G(d) level of theory, scaled by 0.9434
[b] frequencies which are varied according to equation (4.2).

prior to performing vibrational frequency analyses. Geometry optimizations were done on each structure beginning with the equilibrium geometry and ending with the configuration at a distance of 17 Å for the $(CH_3CN)(CH_3OH)H^+$ and 13 Å for the ethanol, n-propanol and isopropanol containing proton-bound pairs. The calculated vibrational frequencies were then used to determine the configuration representing the minimum in the sum-of-states (the effective transition state), and therefore $\Delta S^{\ddagger}$.

According to statistical thermodynamics, the translational entropy (S_{trans}), rotational entropy (S_{rot}) and vibrational entropy (S_{vib}) of a nonlinear molecule in a canonical ensemble can be written as follows:

$$S_{trans} = \frac{5}{2} L_N k_B + L_N k_B \ln\left(\left(\frac{2\pi M k_B T}{L_N h^2}\right)^{3/2}\left(\frac{k_B T}{p_0}\right)\right) \tag{4.3}$$

$$S_{rot} = \frac{3}{2} L_N k_B + L_N k_B \ln\left(\frac{\pi^{1/2}}{\sigma}\left(\frac{8\pi^2 k_B T}{h^2}\right)^{3/2}(I_A I_B I_C)^{1/2}\right) \tag{4.4}$$

$$S_{vib} = L_N k_B \sum_{j=1}^{3n-6}\left(\frac{(h\nu_j / k_B T)e^{-h\nu_j/k_B T}}{1-e^{-h\nu_j/k_B T}} - \ln(1-e^{-h\nu_j/k_B T})\right) \tag{4.5}$$

where L_N, k_B and h are Avogadro's number, Boltzmann's constant and Planck's constant respectively; M is the molar mass; P_0 is 101325 Pa; σ is the symmetry number; I_A, I_B and I_C

are the three principal moments of inertia; ν_j is the vibration frequency associated with the jth normal mode. All entropy values were calculated at 600 K.

4.3 Results and Discussion

4.3.1 Dissociation of $(CH_3CN)(ROH)H^+$ into CH_3CNH^+ and ROH (Channel A)

The dissociation of the four proton-bound pairs to form CH_3CNH^+ + ROH occurs by breaking the O—H hydrogen bond in the starting geometry. This process is the lowest energy pathway for the dissociation of the $(CH_3CN)(CH_3OH)H^+$ and $(CH_3CN)(CH_3CH_2OH)H^+$ proton-bound pairs. Throughout this thesis, this channel shall be referred to as channel A. When the geometric parameters (and related vibrational frequencies) of the complexes are compared to those of the free products (Figure 4.2) differences are observed between the two smaller complexes $(CH_3CN)(CH_3OH)H^+$ and $(CH_3CN)(CH_3CH_2OH)H^+$ and the two propanol-containing complexes. The N—H bond length in free CH_3CNH^+ is 1.016 Å however as the size of the alcohol chain within the complex increases, the N—H distance increases therefore bringing the proton closer to the alcohol group. The proton in $(CH_3CN)(CH_3OH)H^+$ and in $(CH_3CN)(CH_3CH_2OH)H^+$ sits closer to the alcohol moiety with O—H and N—H bond lengths of 1.075 and 1.474 Å in $(CH_3CN)(CH_3OH)H^+$ and 1.060 and 1.519 Å, respectively, in $(CH_3CN)(CH_3CH_2OH)H^+$ despite acetonitrile having a significantly higher proton affinity (ΔPA = 24.9 kJ mol^{-1}) than methanol and a slightly higher proton affinity than ethanol (ΔPA = 2.8 kJ mol^{-1}).[10] It might have been expected that the proton should lie closer to the species with the higher proton

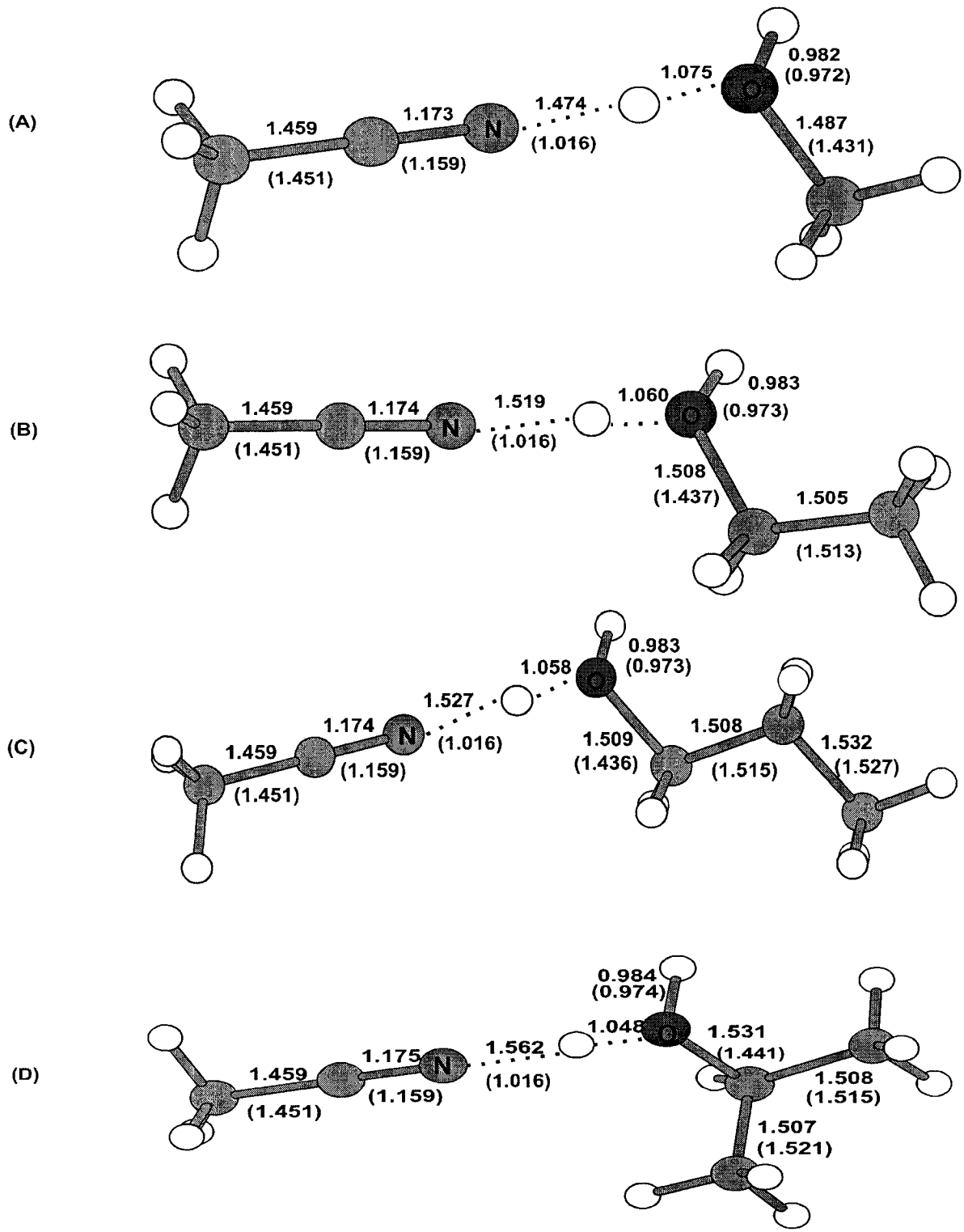

Figure 4.2 Selected optimized geometric parameters for the four proton-bound complexes obtained at the MP2/6-31+G(d) level of theory. Values corresponding to the free products are in parentheses (CH_3CNH^+ + ROH).

affinity. Fridgen et al [11] attribute the position of the proton in the two complexes to the ion-dipole interaction. The dipole moments of acetonitrile and methanol are 3.92 D and 1.70 D, respectively, and the minimum energy structure of the complex has a calculated dipole moment of 1.60 D. They found that by stretching and freezing the O—H bond at 1.5 Å the N—H bond shortens to 1.094 Å, the energy of the system increases by 22 kJ mol^{-1} and the value of dipole moment increases to 3.41 D. They proposed that increasing the magnitude of the ion-dipole interaction in the complex (by associating the proton with the lower dipole moment moiety) would contribute to lowering the energy of the complex since this would lower its overall dipole moment. Consistent with this explanation, the proton resides nearer the higher PA (and lower dipole moment) moiety in the two propanol-containing complexes.

In $(CH_3CN)(CH_3OH)H^+$, the C—C and C—N bonds of free acetonitrile are 1.451 and 1.159 Å; these bond lengths increase mildly to 1.459 and 1.173 Å in the proton-bound complex. The bonds have similar lengths in the other three complexes since all complexes dissociate to form CH_3CNH^+ and their respective neutral alcohol. In $(CH_3CN)(CH_3OH)H^+$, the C—O bond length goes from 1.487 Å in the complex to 1.431 Å in the free product while a more significant change is observed in the C—O bond length of the other three complexes. This bond length decreases from 1.508 Å in the $(CH_3CN)(CH_3CH_2OH)H^+$ and $(CH_3CN)(CH_3CH_2CH_2OH)H^+$ complexes to 1.437 Å in the free moiety. The greatest difference occurs in the isopropanol complex where the C—O bond length increases from 1.441 Å in the free isopropanol to 1.531 Å in the proton-bound complex. Even with such large bond length changes, however, the ∠HOC angle in methanol decreases by only 3° (from 112° to 109° upon dissociation) and the ∠OCC angle increases from 106° to 112°.

Similarly in the ethanol complex, the ∠HOC angle decreases from 111° to 109° while the ∠OCC angle increases from 106° to 107° upon dissociation. Whereas ∠OCC angle increased in size upon dissociation for the methanol and ethanol-containing systems, these angles decreased for the two propanol-containing complexes. The ∠OCC angle in n-propanol decreased from 109° to 108° upon dissociation while in isopropanol, it decreased from 106° to 105°. The ∠HOC angles in both propanol systems decreased from 113° in the complex to 109° in the free moiety. Such minor geometry changes result in only small changes in the vibrational frequency of each common mode during the dissociation. Indeed, if the vibrational frequencies of the vanishing modes are fixed at their respective values in the equilibrium complexes, the calculated $\Delta S^{\ddagger}$ values are very small in magnitude, with some values being tight.

The α values of the four vanishing modes were found to be unique (Table 4.1). If we consider the first bending mode, the α value is 0.46 $Å^{-1}$ for $(CH_3CN)(CH_3OH)H^+$, 0.27 $Å^{-1}$ for $(CH_3CN)(CH_3CH_2OH)H^+$ and finally stabilizes to 0.13 $Å^{-1}$ for $(CH_3CN)(CH_3CH_2CH_2OH)H^+$ and $(CH_3CN)((CH_3)_2CHOH)H^+$. The four α values for $(CH_3CN)(CH_3OH)H^+$ range from 0.46 and 0.44 $Å^{-1}$ for the first and second modes to 0.20 $Å^{-1}$ for the third and fourth modes. For $(CH_3CN)(CH_3CH_2OH)H^+$, the α values were more consistent, averaging around 0.25 $Å^{-1}$. The α values for $(CH_3CN)(CH_3CH_2CH_2OH)H^+$ and $(CH_3CN)((CH_3)_2CHOH)H^+$ were comparable to each other while being much smaller than the values obtained for the other two pairs (largest $\alpha = 0.17$ $Å^{-1}$). The α values obtained for the four disappearing modes in $(CH_3CN)(CH_3CH_2CH_2OH)H^+$ and $(CH_3CN)((CH_3)_2CHOH)H^+$ are more similar to those found in ion-radical dissociation

reactions ($(CH_3)_2NH_2^+ + {}^{\bullet}CH_2N(H)CH_3$, $\alpha = 0.08$ $Å^{-1}$)[12] and ion-molecule reactions ($Li^+ + H_2O$, $\alpha = 0.1$ $Å^{-1}$).[13] This would suggest that the acetonitrile-propanol proton-bound pairs contain more ionic character while the larger α values observed with the methanol and ethanol containing pairs suggest more covalent character within the complex. This does not necessarily correlate with a stronger bond as the bond dissociation energies (calculated at the MP2/6-31+G(d) level of theory) are 129, 139, 132 and 127 kJ mol^{-1} for X = CH_3, CH_3CH_2, $CH_3CH_2CH_2$ and $(CH_3)_2CH$), respectively. All values of α for the four complexes are much less than the α values found in bond scission reactions of neutral molecules (for CH_3-CH_3, $\alpha = 0.92$ $Å^{-1}$)[14] or in the dissociation of bromobenzene ions ($\alpha = 1$ and 2 $Å^{-1}$).[6] The bottleneck of the dissociation reaction was found to move to lower values of R as the internal energy of the ion increased as is expected from variational TST.

The log $k(E)$ vs. E curves (Figure 4.3) for the two propanol containing complexes show that the rate constants accessible on the metastable time frame (10^4 s^{-1} to 10^6 s^{-1}) corresponding to the dissociation of metastable ions in our VG ZAB mass spectrometer occur over an internal energy range of 2.1 to 2.6 eV. The internal energy range for the methanol and ethanol systems is narrower, 1.38 to 1.41 eV for methanol and 1.58 to 1.76 eV for ethanol due to the smaller density of states in these latter two systems. For $(CH_3CN)(CH_3CH_2CH_2OH)H^+$, R* remained constant at 8.5 Å while for the other three systems, a small range of R* values was observed. For $(CH_3CN)(CH_3OH)H^+$ and $(CH_3CN)(CH_3CH_2OH)H^+$, R* occurred within the respective ranges of 6.5-7.5 Å and 6.0-7.0 Å, while for $(CH_3CN)((CH_3)_2CHOH)H^+$, the R* value ranged from 7.0 to 7.5 Å.

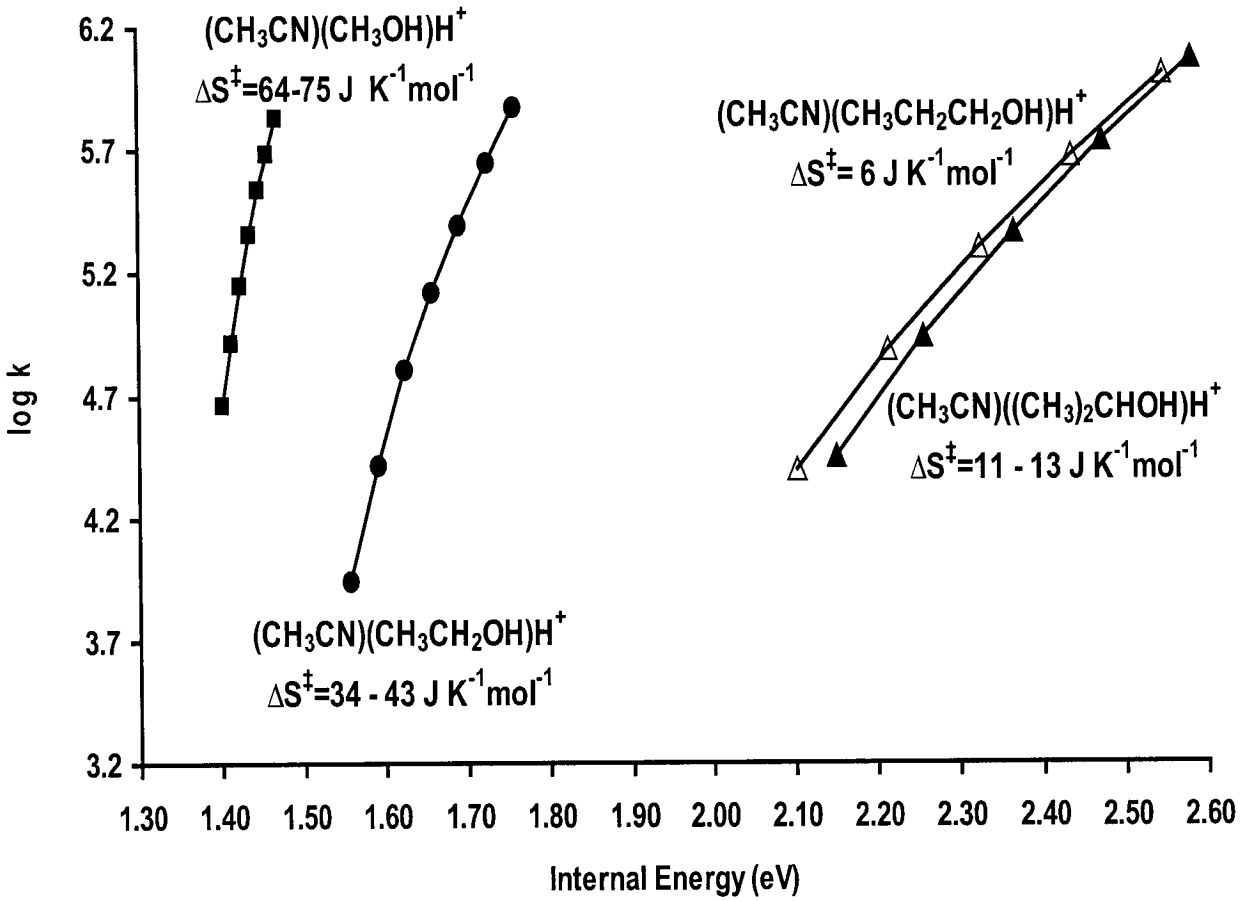

Figure 4.3 Calculated log $k(E)$ vs. E curves for the dissociation of the four proton-bound complexes.

These values of R* are consistent with the calculated α values. The larger α values for $(CH_3CN)(CH_3OH)H^+$ and $(CH_3CN)(CH_3CH_2OH)H^+$ mean that the frequencies of the vanishing vibrational modes decrease rapidly with increasing R, pulling the variational transition state closer to the equilibrium configuration than in the case of $(CH_3CN)(CH_3CH_2CH_2OH)H^+$ and $(CH_3CN)((CH_3)_2CHOH)H^+$. Larger decreases in the vanishing mode frequencies for the smaller complexes at the transition state result in larger entropies of activation. The values of $\Delta S^{\ddagger}$ ranged from 64 - 75 J K^{-1} mol^{-1} for $(CH_3CN)(CH_3OH)H^+$, 34 - 43 J K^{-1} mol^{-1} for $(CH_3CN)(CH_3CH_2OH)H^+$, 6 J K^{-1} mol^{-1} for $(CH_3CN)(CH_3CH_2CH_2OH)H^+$ and 11 - 13 J K^{-1} mol^{-1} for $(CH_3CN)((CH_3)_2CHOH)H^+$. The ranges in $\Delta S^{\ddagger}$ stem from the ranges in R* obtained over the internal energy window of interest.

4.3.2 Dissociation of $(CH_3CN)(ROH)H^+$ into CH_3CN and ROH_2^+ (Channel B)

The dissociation of proton-bound acetonitrile-alcohol pairs to form CH_3CN and protonated alcohol does not involve a direct bond cleavage from its starting geometry as did channel A but rather a rotation of the protonated alcohol moiety with respect to the nitrile (Figure 4.4). This dissociation channel is the lowest energy pathway for the dissociation of the two propanol-containing complexes.

In the $(CH_3CN)(CH_3OH)H^+$ proton-bound pair, the C—C and C—N bonds in acetonitrile slightly increase in length from 1.459 and 1.173 Å respectively in the complex to 1.464 and 1.181 Å in the free product (Figure 4.5). A more significant increase in bond

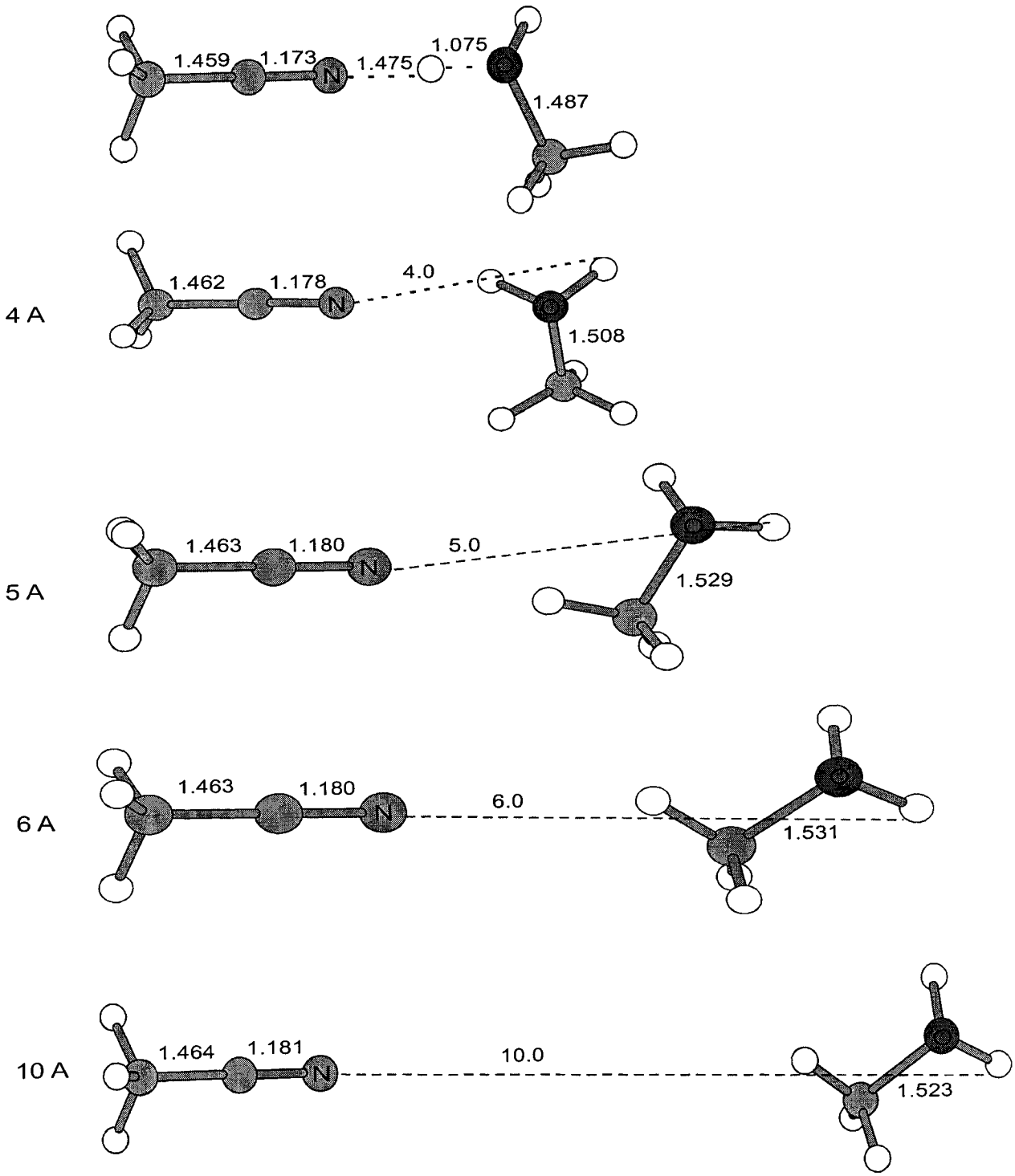

Figure 4.4 Optimized geometries of the $(CH_3CN)(CH_3OH)H^+$ proton-bound pair at a series of bond distances.

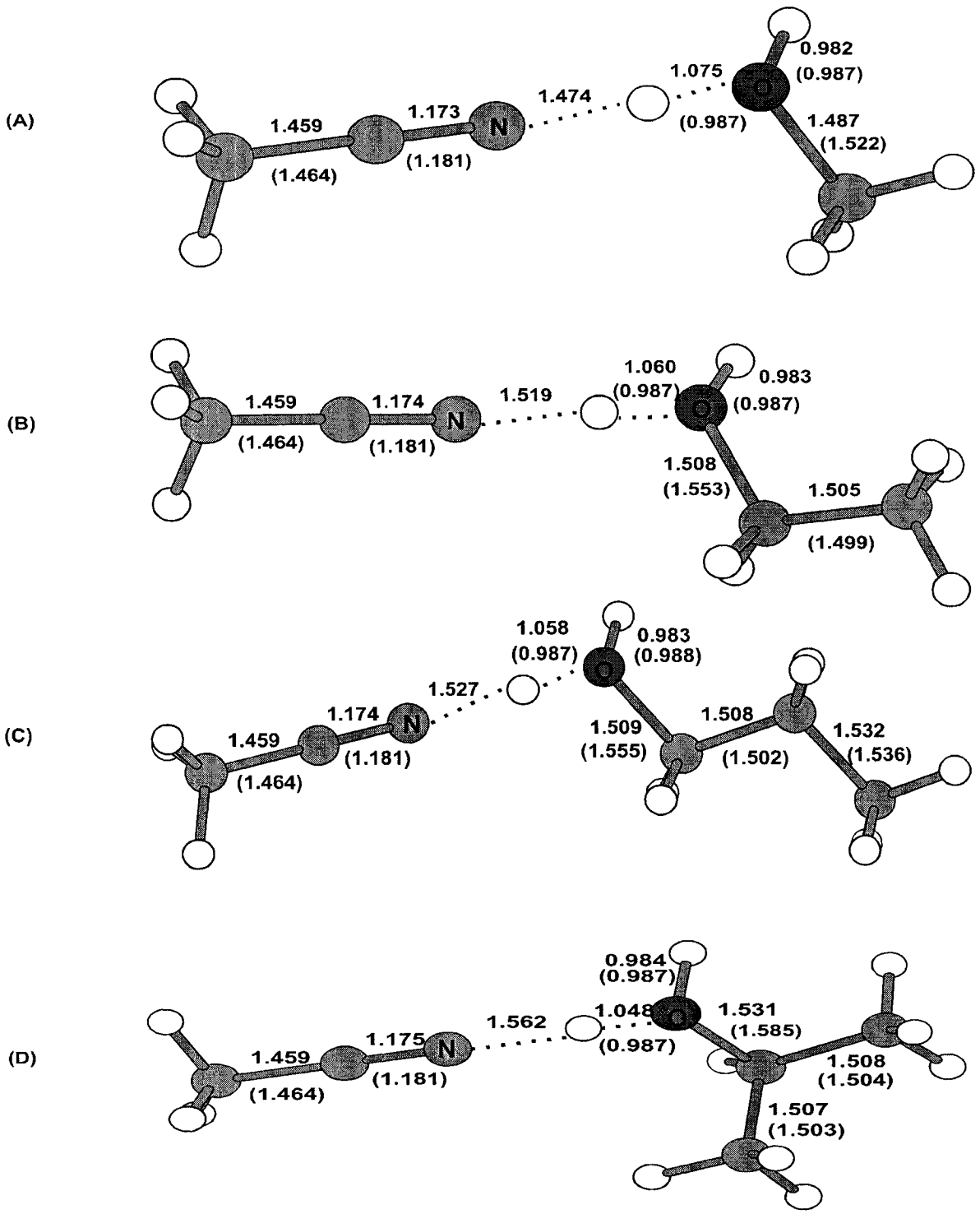

Figure 4.5 Selected optimized geometric parameters for the four proton-bound complexes obtained at the MP2/6-31+G(d) level of theory. Values corresponding to the free products are in parentheses ($CH_3CN + ROH_2^+$).

length was observed in the methanol moiety with the C—O bond distance increasing from 1.487 Å in the optimized geometry to 1.522 Å in free $CH_3OH_2^+$. This is in contrast with the previous channel where the C—N and C—O bond lengths decreased upon dissociation to free CH_3CNH^+ and CH_3OH (to 1.159 and 1.431 Å, respectively). The C—C and C—N bonds of acetonitrile in the ethanol, n-propanol and isopropanol-contaning complexes similarly increase in length from 1.459 and 1.174 Å in the optimized geometry to 1.464 and 1.181 Å in free acetonitrile. These values were expected to be similar as both proton-bound pairs are dissociating to form neutral acetonitrile and a protonated alcohol. In $(CH_3CN)(CH_3CH_2OH)H^+$, the C—C bond decreased slightly from 1.505 to 1.499 Å while the C—O bond increased from 1.508 to 1.555 Å. Similarly, in the propanol pairs, the C—O bond length increases upon dissociation, with the C—O bond in isopropanol increasing in length from 1.531 in the complex to 1.585 Å in free protonated isopropanol.

In all of the four optimized proton-bound pairs, the bulk of the positive charge (+0.68) resides on the proton while acetonitrile carries +0.10 charge and the remaining +0.22 being on the alcohol. The geometries of these proton-bound pairs (shown in Figures 4.2 and 4.5) are such that the hydroxyl functionality of the alcohol sits closest to the proton (a net negative charge sits on the OH group). With this configuration, the optimized proton-bound pair can be thought of as an acetonitrile dipole interacting with the central proton which then interacts with the negative charge of the hydroxyl group in the alcohol. During the dissociation of these proton-bound pairs to form CH_3CN and protonated alcohol, the alcohol group rotates with respect to the nitrile to form configurations as shown in Figure 4.4. The charges observed on the CH_3 and OH_2 groups of protonated methanol were found

to be +0.55 and +0.42, respectively, at 16.5 Å. These values are virtually identical to those found in solitary $CH_3OH_2^+$. Similar charge distributions are encountered in the dissociating configurations for the ethanol, n- and isopropanol-containing complexes with the charge distribution in the protonated alcohol moiety being identical to that found in the free product. At long range (11.0 Å), the ethanol group has rotated such that the CH_3CH_2 group (+0.57 charge) now lies closest to the CH_3CN moiety and so this geometry can be thought of as an ion-dipole complex between CH_3CN and protonated ethanol. The charges on the propanols are +0.59 and +0.40 on the $CH_3CH_2CH_2$ and OH_2 parts of protonated n-propanols (at 12.0 Å) while those on isopropanol (at 12.5 Å) are +0.58 and +0.42, respectively. All of these configurations can as such be summarized as ion-dipole complexes between CH_3CN and protonated alcohol.

The internal energy ranges for this dissociation channel in the methanol, ethanol, n- and isopropanol containing pairs are 1.52-1.56, 1.46-1.55, 1.52-1.63 and 1.46-1.56 eV, respectively. The effective transition states for the dissociation of the four proton-bound pairs into $CH_3CN + CH_3OH_2^+$, $CH_3CN + CH_3CH_2OH_2^+$, $CH_3CN+ + CH_3CH_2CH_2OH_2^+$ and $CH_3CN + (CH_3)_2CHOH_2^+$ were located at 16.5, 11.0, 12.0 and 12.5 Å, respectively. These effective transition states, located at large internuclear distances, indicate that the dividing surface for these reactions is situated near the products (Figure 4.6). All systems examined had a concrete minimum in the sum-of-states except for the $(CH_3CN)(CH_3OH)H^+$ proton-bound pair. For this pair, the minimum was taken at a point where the entropies of activation had converged.

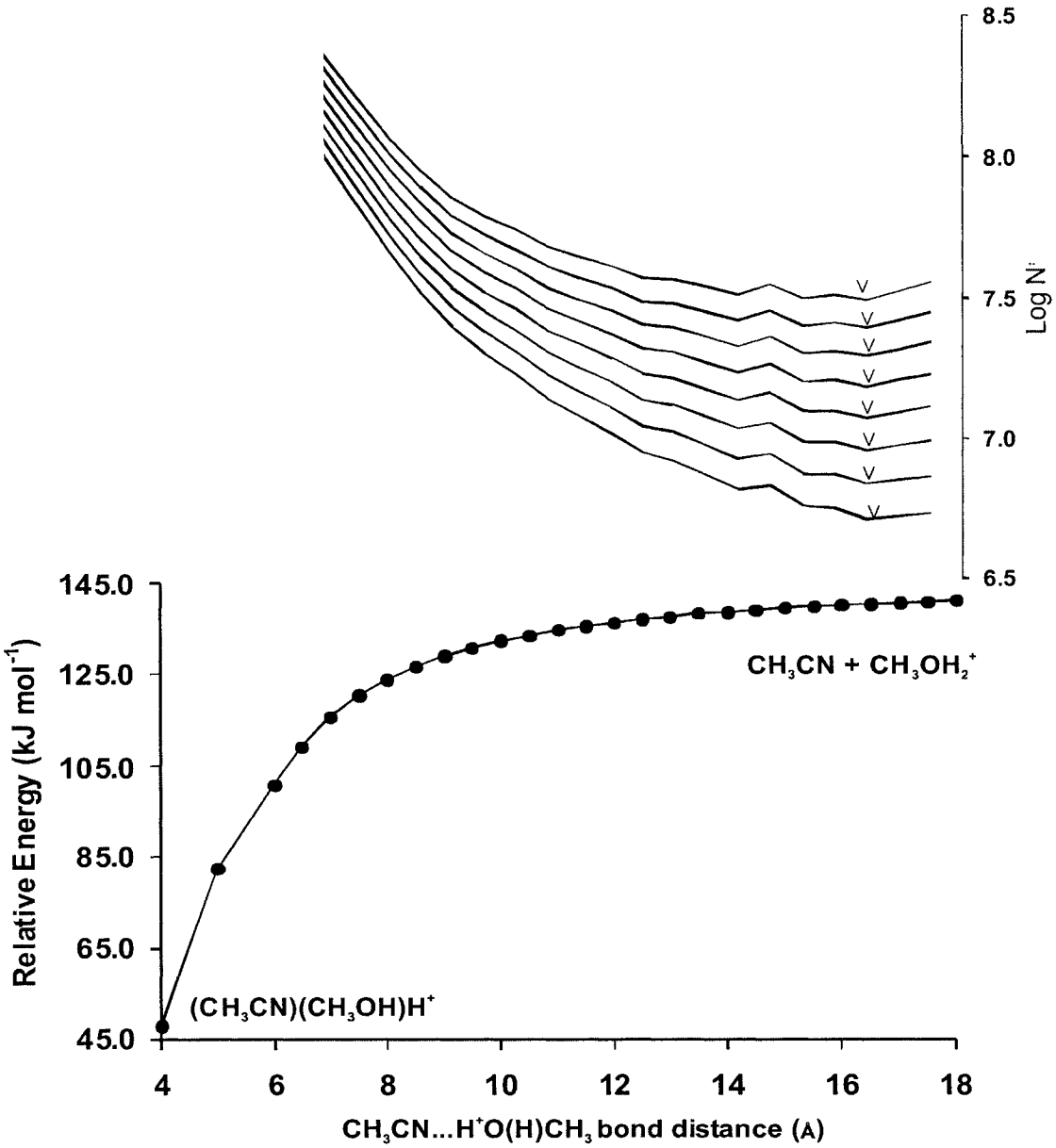

Figure 4.6 Plot of the relative energy vs. $CH_3CN\bullet\bullet\bullet H^+O(H)CH_3$ bond distance in the $(CH_3CN)(CH_3OH)H^+$ complex at the MP2/6-31+G(d) level of theory. Superimposed on the figure is the calculated sum-of-states, log $N^{\ddagger}$, as a function of R at various internal energies.

To facilitate a comparison between the two channels, the vibrational frequencies at these R* values were used to calculate the alpha values for the four disappearing modes of channel B. The four alpha values for the methanol-acetonitrile proton-bound pair were calculated to be 0.14, 0.11, 0.14 and 0.15 $Å^{-1}$ (Table 4.2); these values are smaller than those determined for the lower energy channel A (0.46, 0.44, 0.20 and 0.20 $Å^{-1}$, respectively). Similar alpha values were calculated for the ethanol system (0.12, 0.11, 0.15 and 0.17 $Å^{-1}$); as with the methanol system, these values are smaller than those determined for the lower energy channel A (0.27, 0.31, 0.25 and 0.25 $Å^{-1}$). The four alpha values of each of the two propanol-containing systems were found to be similar with n-propanol and isopropanol having values of 0.16, 0.11, 0.14, 0.17 $Å^{-1}$ and 0.14, 0.14, 0.14, 0.17 $Å^{-1}$, respectively. These values are larger than those calculated for channel A (0.13, 0.09, 0.03 and 0.08 for n-propanol and 0.13, 0.17, 0.05, 0.09 $Å^{-1}$ for isopropanol).

The $\Delta S^{\ddagger}$ for the dissociation of $(CH_3CN)(CH_3OH)H^+$ via channel B is 67 J K^{-1} mol^{-1} ,which is within error to that found for channel A (Table 4.3). A similar result is obtained for $(CH_3CN)(CH_3CH_2OH)H^+$. As a result, the difference in $\Delta S^{\ddagger}$ for the two competing dissociation channels, $\Delta(\Delta S^{\ddagger})$, is approximately zero. Comparable channel B $\Delta S^{\ddagger}$ values were determined for $(CH_3CN)(CH_3CH_2CH_2OH)H^+$ and $(CH_3CN)((CH_3)_2CHOH)H^+$, 51 and 54 J K^{-1} mol^{-1}, respectively; while these channel B values are similar to those obtained for $(CH_3CN)(CH_3OH)H^+$ and $(CH_3CN)(CH_3CH_2OH)H^+$ they are significantly larger than those values obtained for channel A (Table 4.3). So, according to the present treatment, $\Delta(\Delta S^{\ddagger})$ for the competing dissociations of the two propanol-containing proton-bound pairs are not zero.

Table 4.2 Information used in the determination of $\Delta S^{\ddagger}$ for the dissociation of proton-bound pairs into CH_3CN and ROH_2^+.

	Harmonic Vibrational Frequencies (cm^{-1})
$(CH_3CN)(CH_3OH)H^+$	67, 80, 129, 147, 260, 329, 331, 517, 882, 908, 964, 1013, 1015, 1098, 1160, 1290, 1374, 1417, 1417, 1419, 1451, 1454, 1665, 1943, 2155, 2943, 2983, 3039, 3040, 3103, 3117, 3470
CH_3CN	311, 311, 886, 1020, 1020, 1379, 1437, 1437, 2091, 2942, 3032, 3032
$CH_3OH_2^+$	252, 727, 792, 909, 1128, 1241, 1422, 1439, 1442, 1637, 2991, 3126, 3133, 3364, 3453
Transition State (at 16.5 Å)	8, 14, 14, 15, 255, 313, 313, 727, 791, 885, 909, 1020, 1020, 1128, 1241, 1379, 1422, 1436, 1436, 1439, 1441, 1637, 2090, 2942, 2991, 3032, 3032, 3126, 3133, 3364, 3453
α values ($Å^{-1}$)	0.14, 0.11, 0.14, 0.15
Rotational Constant for rotor (GHz)	23.3 for the reactant ion, 31.7 for the transition state
Moment of Inertia (10^{-47} kg m^2)	360, 643, 667 for $(CH_3CN)(CH_3OH)H^+$ 5.291, 92.9, 92.9 for CH_3CN 8.132, 40.0, 41.6 for $CH_3OH_2^+$
$(CH_3CN)(CH_3CH_2OH)H^+$	36, 51, 88, 125, 207, 251, 328, 329, 408, 512, 783, 790, 900, 950, 970, 1014, 1015, 1066, 1157, 1223, 1268, 1396, 1418, 1419, 1446, 1456, 1473, 1664, 2144, 2159, 2937, 2943, 2991, 3019, 3039, 3039, 3040, 3073, 3455
CH_3CN	311, 311, 886, 1020, 1020, 1379, 1437, 1437, 2091, 2942, 3032, 3032
$CH_3CH_2OH_2^+$	200, 257, 359, 676, 724, 800, 905, 942, 1115, 1174, 1245, 1357, 1389, 1439, 1455, 1466, 1621, 2937, 3005, 3019, 3044, 3092, 3358, 3455
Transition State (at 11.0 Å)	11, 17, 20, 20, 169, 259, 314, 314, 356, 675, 738, 775, 884, 901, 934, 1020, 1020, 1092, 1195, 1273, 1340, 1380, 1388, 1435, 1435, 1440, 1452, 1463, 1635, 2091, 2933, 2943, 3012, 3018, 3033, 3033, 3034, 3095, 3364, 3459
α values ($Å^{-1}$)	0.13, 0.13, 0.17, 0.20
Rotational Constant for rotor (GHz)	19.7 for the reactant ion, 12.8 for the transition state
Moment of Inertia (10^{-47} kg m^2)	42.6, 1030, 1050 for $(CH_3CN)(CH_3CH_2OH)H^+$ 5.291, 92.9, 92.9 for CH_3CN 2.735, 9.823, 11.3 for $CH_3CH_2OH_2^+$

$(CH_3CN)(CH_3CH_2CH_2OH)H^+$	33, 40, 86, 111, 121, 186, 225, 286, 328, 329, 434, 511, 746, 825, 864, 893, 903, 969, 1013, 1015, 1017, 1087, 1158, 1204, 1247, 1279, 1310, 1374, 1375, 1395, 1419, 1419, 1456, 1461, 1466, 1472, 1663, 2146, 2193, 2926, 2936, 2943, 2979, 2989, 3019, 3032, 3040, 3040, 3063, 3452
CH_3CN	311, 311, 886, 1020, 1020, 1379, 1437, 1437, 2091, 2942, 3032, 3032
$CH_3CH_2CH_2OH_2^+$	123, 196, 230, 245, 399, 724, 734, 756, 866, 887, 955, 1009, 1131, 1171, 1235, 1289, 1302, 1366, 1401, 1466, 1467, 1475, 1482, 1614, 2940, 2950, 2995, 3006, 3038, 3049, 3084, 3374, 3470
Transition State (at 12 Å)	6, 12, 20, 20, 119, 187, 222, 241, 314, 314, 395, 705, 721, 755, 862, 881, 884, 950, 1002, 1020, 1020, 1126, 1164, 1224, 1277, 1294, 1358, 1380, 1394, 1435, 1435, 1454, 1459, 1460, 1471, 1616, 2091, 2932, 2941, 2943, 2993, 2997, 3028, 3033, 3033, 3038, 3082, 3357, 3455
α values ($Å^{-1}$)	0.16, 0.11, 0.14, 0.17
Rotational Constant for rotor (GHz)	10.7 for reactant ion, 8.3 for transition state
Moment of Inertia (10^{-47} kg m^{-2})	78.8, 1460, 1510 for $(CH_3CN)(CH_3CH_2CH_2OH)H^+$ 5.291, 92.9, 92.9 for CH_3CN 34.4, 235, 252 for $CH_3CH_2CH_2OH_2^+$
$(CH_3CN)((CH_3)_2CHOH)H^+$	36, 47, 89, 116, 197, 219, 265, 329, 330, 352, 388, 449, 510, 706, 875, 898, 916, 920, 954, 1014, 1015, 1064, 1109, 1175, 1235, 1308, 1355, 1374, 1395, 1396, 1419, 1420, 1438, 1446, 1456, 1464, 1671, 2141, 2348, 2930, 2937, 2943, 2980, 3015, 3026, 3031, 3036, 3039, 3040, 3445
CH_3CN	311, 311, 886, 1020, 1020, 1379, 1437, 1437, 2091, 2942, 3032, 3032
$(CH_3)_2CHOH_2^+$	184, 232, 268, 346, 354, 426, 607, 742, 857, 894, 919, 926, 1082, 1157, 1196, 1313, 1351, 1393, 1402, 1443, 1454, 1465, 1471, 1614, 2937, 2941, 3019, 3024, 3029, 3039, 3050, 3370, 3469
Transition State (at 12.5 Å)	8, 11, 19, 20, 161, 226, 264, 314, 314, 343, 350, 424, 590, 731, 854, 884, 889, 914, 922, 1020, 1020, 1073, 1152, 1192, 1302, 1346, 1380, 1387, 1395, 1430, 1436, 1436, 1441, 1453, 1460, 1619, 2091, 2928, 2932, 2943, 3010, 3013, 3019, 3031, 3033, 3033, 3039, 3357, 3459
α Values ($Å^{-1}$)	0.14, 0.14, 0.14, 0.17
Rotational Constant for rotor (GHz)	7.0 for reactant ion, 7.3 for transition state
Moment of Inertia (10^{-47} kg m^{-2})	120, 1130, 1200 for $(CH_3CN)((CH_3)_2CHOH)H^+$ 5.291, 92.9, 92.9 for CH_3CN 108, 109, 188 for $(CH_3)_2CHOH$

Table 4.3 Thermodynamic and activation entropies for the two dissociation channels of four acetonitrile-alcohol proton-bound pairs.[a]

	$\Delta S^{\ddagger}$ [b]		ΔS		$\Delta(\Delta S)^{\ddagger}$	$\Delta(\Delta S)$
	CH_3CNH^+ + ROH	CH_3CN + ROH_2^+	CH_3CNH^+ + ROH	CH_3CN + ROH_2^+		
$(CH_3CN)(CH_3OH)H^+$	70 ± 8	67	92	90	3 ± 11	2
$(CH_3CN)(CH_3CH_2OH)H^+$	39 ± 4	43	103	100	-4 ± 7	3
$(CH_3CN)(CH_3CH_2CH_2OH)H^+$	6	51	94	91	-45 ± 6	3
$(CH_3CN)((CH_3)_2CHOH)H^+$	12 ± 4	54	100	101	-42 ± 7	-1

[a] in J $K^{-1}mol^{-1}$.

[b] ± 3 J K^{-1} mol^{-1} unless otherwise stated.

Two factors are at play in determining $\Delta S^{\ddagger}$ for these dissociation reactions. One is the location of the dividing surface and the other is how "fast" the four vanishing modes go to zero over the course of the dissociation (as exemplified by the α values that can be derived from equation 4.2). A dissociation in which the vibrational frequencies go to zero rapidly with increasing separation of the products, and for which the dividing surface lies close to the products will have a large $\Delta S^{\ddagger}$ value. If the dividing surface of this system moves towards the reactant, the $\Delta S^{\ddagger}$ value will drop since the values of the four vanishing vibrational frequencies will become more reactant–like. When the transition state frequencies for the four vanishing modes for each channel in $(CH_3CN)(CH_3OH)H^+$ and $(CH_3CN)(CH_3CH_2OH)H^+$ are compared to their respective values in the equilibrium structures, the average deviations are similar, resulting in $\Delta(\Delta S^{\ddagger}) \approx 0$. For example, in

$(CH_3CN)(CH_3OH)H^+$, R* for channel B is located at 16.5 Å while that for channel A is 7.0 Å. The resulting α values for the four vanishing modes produce transition state vibrational frequencies that differ from the equilibrium values (differences of 4, 5, 35 and 40 for channel A and 8, 14, 14 and 15 for channel B) with similar average deviations of 17 and 13 cm^{-1}, for channels A and B, respectively. For $(CH_3CN)(CH_3CH_2CH_2OH)H^+$, the combination of the location of the dividing surface and the α values result in quite different average deviations in the transition state frequencies for the two competing channels in each case: 57 cm^{-1} for channel A and 22 cm^{-1} for channel B. A similar result is obtained for $(CH_3CN)((CH_3)_2CHOH)H^+$. Thus, $\Delta(\Delta S^{\ddagger})$ is not zero for these two proton-bound molecular pairs.

4.3.3 Thermodynamic ΔS and Δ(ΔS)

Thermodynamic entropy changes for the dissociations of $(CH_3CN)(CH_3OH)H^+$, $(CH_3CN)(CH_3CH_2OH)H^+$, $(CH_3CN)(CH_3CH_2CH_2OH)H^+$ and $(CH_3CN)((CH_3)_2CHOH)H^+$ are listed in Table 4.3. For their respective dissociations via channel A, ΔS values were calculated to be 92, 103, 94, and 100 J K^{-1} mol^{-1}, respectively. These values were nearly identical to those determined for channel B (90, 100, 91, 101 J K^{-1} mol^{-1}, respectively) as expected for simple molecular systems and Δ(ΔS) are zero.

The values of $\Delta S^{\ddagger}$ for the bond cleavage reactions are clearly different from those calculated for ΔS. There is a definite trend in the $\Delta S^{\ddagger}$ values for channel A with the values decreasing as the alcohol side chain lengthens, due to the migration of the variational

transition state farther away from the reactant complex. This trend is absent in the $\Delta S^{\ddagger}$ values for channel B as well as in the thermodynamic ΔS. There is a greater absolute change in magnitude in $\Delta S^{\ddagger}$ of channel A in going from X = CH_3 to X = $CH_3CH_2CH_2$ (~ 70 J $K^{-1}mol^{-1}$) than there is variation in $\Delta S^{\ddagger}$ of channel B (24 J $K^{-1}mol^{-1}$) or the thermodynamic ΔS (12 J K^{-1} mol^{-1}) in addition to greater relative changes (factor of ~ 11 for $\Delta S^{\ddagger}$ to 1.6 for channel B and 1.1 for ΔS) (Table 4.3). The entropies of activation calculated for the methanol and ethanol-containing complexes were identical, resulting in a $\Delta(\Delta S^{\ddagger})$ of zero while for the propanol-containing complexes, a substantial difference existed (40 - 45 J K^{-1} mol^{-1}). In light of these different trends, it may be wise to be careful assigning $\Delta(\Delta S^{\ddagger})$ = $\Delta(\Delta S)$ in the competitive dissociation reactions of proton-bound pairs, even when the two components of the complex are structurally related.

4.4 Conclusions

The entropies of activation for the dissociation of a series of acetonitrile-alcohol proton-bound pairs, $(CH_3CN)(CH_3OH)H^+$, $(CH_3CN)(CH_3CH_2OH)H^+$, $(CH_3CN)(CH_3CH_2CH_2OH)H^+$ and $(CH_3CN)((CH_3)_2CHOH)H^+$, were compared for two dissociation pathways (CH_3CNH^+ + ROH and CH_3CN + ROH_2^+) using microcanonical variational transition state theory. The dissociation of the proton-bound pairs via channel A to form CH_3CNH^+ and neutral alcohol occurred by simple bond dissociation in which the two departing fragments simply get farther apart. Over the course of dissociation by channel B the departing protonated alcohol moiety rotates to produce a more favourable interaction with the dipole of the neutral acetonitrile. The absolute $\Delta S^{\ddagger}$ values for each dissociation

pathway were found to be determined by the combination of the location of the dividing surface and the rapidity with which the four key vanishing modes in each dissociation tended to zero as a function of increasing separation of the products. $\Delta(\Delta S^{\ddagger})$ values for methanol and ethanol-containing complexes were approximately zero while a considerable difference was observed for the two propanol-containing pairs. It was also found that the changes in $\Delta S^{\ddagger}$ in going from $(CH_3CN)(CH_3OH)H^+$ to $(CH_3CN)((CH_3)_2CHOH)H^+$ were not quantitatively mirrored in the thermodynamic ΔS values for the four dissociation reactions. Little change was observed in the thermodynamic entropies of the two dissociation channels for the four systems, thus resulting in $\Delta(\Delta S) = 0$.

References

1. M. J. Frisch, G. W. Trucks, H. B. Schlegel, G. E. Scuseria, M. A. Robb, J. R. Cheeseman, V. G. Zakrzewski, J. A. Montgomery, R. E. Stratmann, J. C. Burant, S. Dapprich, J. M. Millam, A. D. Daniels, K. N. Kudin, M. C. Strain, O. Farkas, J. Tomasi, V. Barone, M. Cossi, R. Cammi, B. Mennucci, C. Pomelli, C. Adamo, S. Clifford, J. Ochterski, G. A. Petersson, P. Y. Ayala, Q. Cui, K. Morokuma, D. K. Malick, A. D. Rabuck, K. Raghavachari, J. B. Foresman, J. Cioslowski, J. V. Ortiz, B. B. Stefanov, G. Liu, A. Liashenko, P. Piskorz, I. Komaromi, R. Gomperts, R. L. Martin, D. J. Fox, T. Keith, M. A. Al-Laham, C. Y. Peng, A. Nanayakkara, C. Gonzalez, M. Challacombe, P. M. W. Gill, B. Johnson, W. Chen, M. W. Wong, J. L. Andres, C. Gonzalez, M. Head-Gordon, E. S. Replogle, and J. A. Pople, *in* "GAUSSIAN 98 Rev. A.7". Gaussian Inc., Pittsburgh PA, 1998.

2. A. P. Scott and L. Radom, "Harmonic Vibrational Frequencies: An evaluation of hartree-fock, moller-plesset, quadratic configuration interaction, density functional theory and semi-empirical scale factors", *J. Phys. Chem.* **100**, 16502 (1996).

3. T. Baer and W. L. Hase, *Unimolecular Reaction Dynamics, Theory and Experiments*. Oxford University Press, New York (1996).

4. P. Pechukas, "Transition state theory", *Annu. Rev. Phys. Chem.* **32**, 159 (1981).

5. D. G. Truhlar and B. C. Garrett, "Variational transition-state theory", *Acc. Chem. Res.* **13**, 440 (1980).

6. C. Lifshitz, F. Louage, V. Aviyente, and K. Song, "Transition-state switchings for single potential well ionic dissociations", *J. Phys. Chem.* **95**, 9298 (1991).

7. T. Beyer and D. R. Swinehart, "Number of multiply-restricted partitions [A1] (Algorithm 448)", *ACM Commun.* **16**, 379 (1973).

8. W. L. Hase, "Theoretical critical configuration for ethane decomposition and methyl radical recombination", *J. Chem. Phys* **57**, 730 (1972).

9. M. Quack and J. Troe, "Specific rate constants of unimolecular processes", *J. Ber. Bunsen-Ges. Phys. Chem.* **78**, 240 (1974).

10. P. J. Linstrom and W. G. Mallard, *NIST Chemistry WebBook, NIST Standard Reference Database Number 69*. National Institute of Standards and Technology, Gaithersburg, MD (March 2003).

11. T. D. Fridgen, J. D. Keller, and T. B. McMahon, "Direct experimental determination of the energy barriers for methyl cation transfer in the reactions of methanol with protonated methanol, protonated acetonitrile and protonated acetaldehyde: a low pressure FTICR study", *J. Phys. Chem. A* **105**, 3816 (2001).

12. P. M. Mayer, J. W. Keister, T. Baer, M. Evans, C. Y. Ng, and C.-W. Hsu, "The dimethylamine dimer ion is an ion-radical complex: a combined TPEPICO, variational RRKM and *ab initio* study of the fragmentation of ionized dimers of diemthylamine", *J. Phys. Chem. A* **101**, 1270 (1997).

13. W. L. Hase, "Properties of variational transition states for association reactions", *Chem. Phys.Lett.* **139**, 389 (1987).

14. W. L. Hase, "The criterion of minimum state density in unimolecular rate theory. An application to ethane dissociation", *J.Chem. Phys.* **64**, 2442 (1976).

CHAPTER 5

EVIDENCE FOR THE PARTICIPATION OF EXCITED ELECTRONIC STATES IN THE UNIMOLECULAR DISSOCIATION REACTIONS OF IONIC COMPLEXES BETWEEN NO AND AROMATIC COMPOUNDS

5.1 Introduction

This chapter describes the investigation of the unimolecular dissociation of the ionic complexes of NO with aromatic molecules (formed by electron ionization at relatively high ion source pressures in a mass spectrometer) and evidence that was found for the participation of their excited singlet and triplet states. The aromatic molecules studied were benzonitrile (C_6H_5CN), benzene (C_6H_6), pyridine (C_5H_5N), thiophene (C_4H_4S) and furan (C_4H_4O). Calculations of the structure, electron distribution and binding energies of the ground state singlet and lowest energy triplet states have been used to help in the interpretation of the mass spectra.

5.2 Procedures in Brief

The experiments were performed on a modified VG ZAB sector mass spectrometer,[1] which incorporates a magnetic sector followed by two electrostatic sectors (BEE geometry). A "high-pressure" ion source was used to generate the cluster ions by introducing nitric oxide gas into the ion source via the chemical ionization (CI) gas inlet and aromatic

compounds via the liquid septum inlet.[2] A lower pressure ion source (operated in CI mode) was used to generate protonated nitrosobenzene, $C_6H_5NOH^+$. The pressures in the ion source chamber, read with an ionization gauge located above the ion source diffusion pump, were typically between 10^{-5} and 10^{-4} Torr. The pressure in the "high-pressure" ion source is approximately three orders of magnitude higher (up to 0.1 Torr) while that inside the lower pressure source is approximately two orders of magnitude higher.[2] The accelerating voltage was held constant at 8 kV and metastable ion (MIKES) and collision-induced dissociation (CID) mass spectra were recorded in the usual manner in the second and third field-free regions of the mass spectrometer (see chapter seven for further details).[3] All chemicals were commercially obtained and used without further purification.

Standard *ab initio* molecular orbital calculations[4] were performed using the Gaussian 98 suite of programs.[5] Geometries were optimized at the B3-LYP/6-31+G(d) and B3-LYP/6-311++G(3df,2p) levels of theory, except for the complex involving benzene, which was also explored at the HF/6-31+G(d), MP2/6-31+G(d), QCISD/6-31+G(d) and CCSD/6-31+G(d) levels of theory. Vibrational frequency analysis was used to confirm that equilibrium structures were obtained. Scaling factors for zero-point energies (ZPE) were chosen from the study by Scott and Radom.[6] Orbital assignments were determined using the Pop = reg keyword in Gaussian 98 on the B3-LYP/6-31+G(d) optimized structures. G3 single-point energy calculations were carried out on the optimized B3-LYP/6-31+G(d) geometries of all complexes, and on the MP2/6-31+G(d) and CCSD/6-31+G(d) geometries of the (benzene)$(NO)^+$ complex. G3 theory[7] approximates the energy of a species at the QCISD(T)/G3large level of theory by a series of additive corrections to a base MP4/6-

31G(d) energy. The G3large basis set is a modified version of the standard 6-311+G(3df,2p) basis set in which more polarization functions are added to first row elements (3d2f), fewer on second row elements (2df) and core polarization functions are included. Details of the properties of the G3large basis set can be found in the original publication by Curtiss et al. [7]

RRKM calculations[8] employed the standard expression for the unimolecular dissociation rate constant, $k(E)$ as a function of internal energy, E:

$$k(E) = \frac{\sigma N^{\ddagger}(E - E_0)}{h\rho(E)} \qquad (5.1)$$

where σ is the symmetry number, h is Planck's constant, $N^{\ddagger}$ is the transition state sum-of-states at an internal energy E-E_0, E_0 is the 0 K activation energy and ρ is the reactant density-of-states at an internal energy E. Sums and densities of states were calculated with the direct count algorithm. [9]

5.3 Results and Discussion

The binding energies of the various ionic complexes $(A)(NO)^+$ investigated in this work (Figure 5.1), relative to $A + NO^+ (X\ ^1\Sigma^+)$, are listed in Table 5.1 (A = C_6H_5CN, C_6H_6, C_5H_5N, C_4H_4S and C_4H_4O). While the details of each system will be discussed in detail below, some preliminary general comments are worthwhile. It is seen that the density

functional treatment B3-LYP/6-311++G(3df,2p) uniformly predicts complexes (singlet and triplet) that are more strongly bound than the composite G3 approach (based on B3-LYP/6-31+G(d) geometries) by ~ 40 – 50 kJ mol^{-1}. The electron correlation treatment used in optimizing the structure of the complexes is not a factor since the G3 binding energies calculated for $(C_6H_6)(NO)^+$ are the same regardless whether MP2, B3-LYP or CCSD (all with the 6-31+G(d) basis set) geometries are employed (145, 145 and 143 kJ mol^{-1}, respectively).

Table 5.1 G3 and B3-LYP/6-311++G(3df,2p) 0 K binding energies for singlet and triplet $(A)(NO)^+$ where A= benzene, pyridine, furan, thiophene and benzonitrile.

A	Binding Energies					
	singlet				triplet	
	π-complex		n-complex			
	G3[a]	B3-LYP[b]	G3[a]	B3-LYP[b]	G3[a]	B3-LYP[b]
benzene	143	189	--	--	17	70
pyridine	108	151	210	247	3	75
furan	149[c]	190[c]	--	--	42	105
thiophene	153[d]	198[d]	--	--	-44	106
benzonitrile	--	141	--	177	--	32

[a] Based on B3-LYP/6-31+G(d) geometries and scaled ZPEs, in kJ mol^{-1}.

[b] B3-LYP/6-311++G(3df,2p) energies and scaled ZPEs, in kJ mol^{-1}.

[c] For the π-complex (a) in Figure 5.1.

[d] For the π-complex (b) in Figure 5.1.

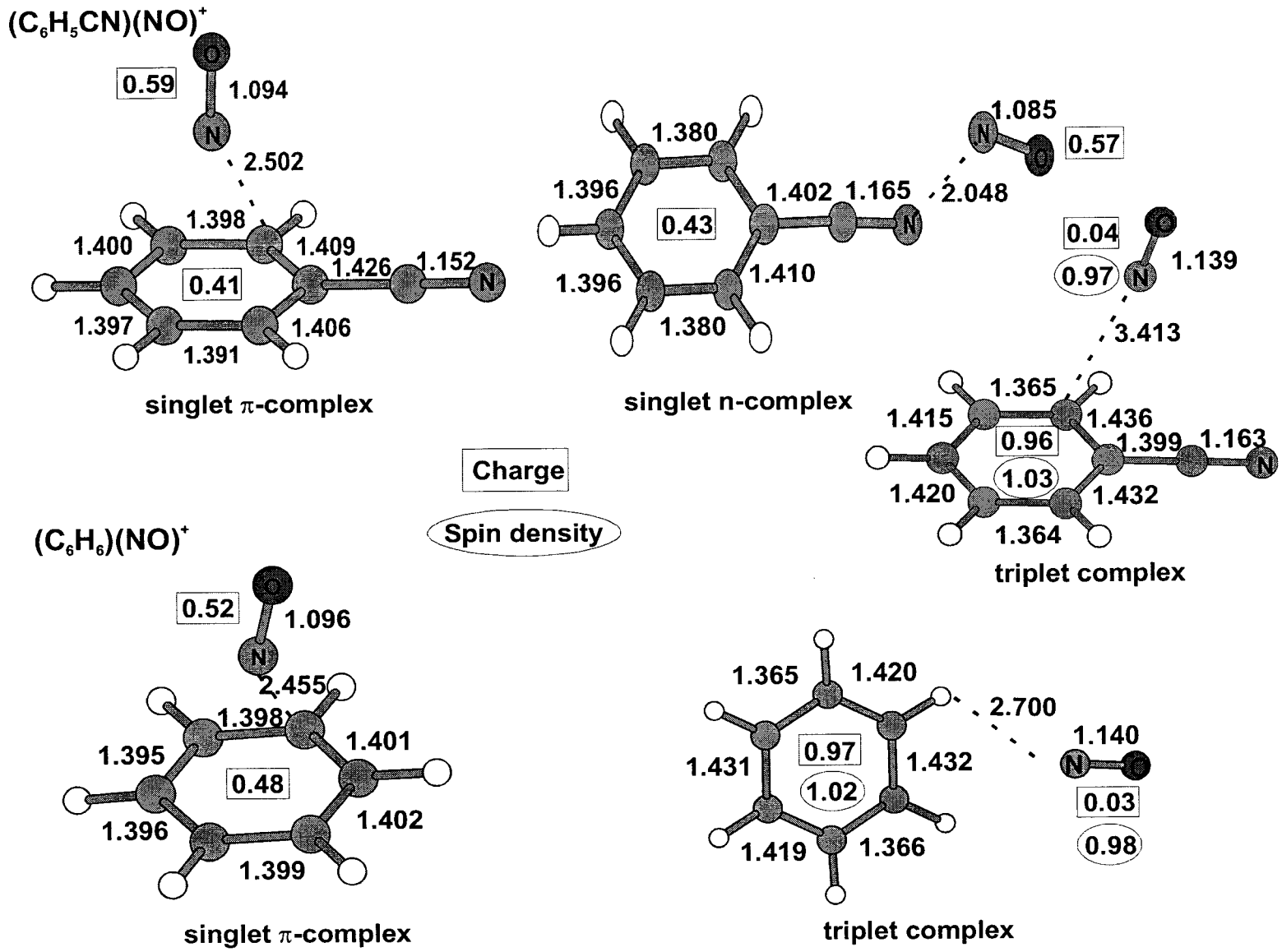
(C6H5CN)(NO)+
0.59
1.094
2.502
1.398
1.400
1.409
1.426
1.152
0.41
1.397
1.406
1.391
singlet π-complex
1.380
1.396
1.402
1.165
0.43
1.396
1.410
1.380
1.085
0.57
2.048
0.04
0.97
1.139
3.413
singlet n-complex
1.365
1.415
1.436
0.96
1.399
1.163
1.03
1.420
1.432
1.364
triplet complex
Charge
Spin density
(C6H6)(NO)+
0.52
1.096
2.455
1.398
1.401
1.395
0.48
1.396
1.402
1.399
singlet π-complex
1.365
1.420
2.700
1.140
0.97
1.431
1.432
1.02
0.03
0.98
1.419
1.366
triplet complex

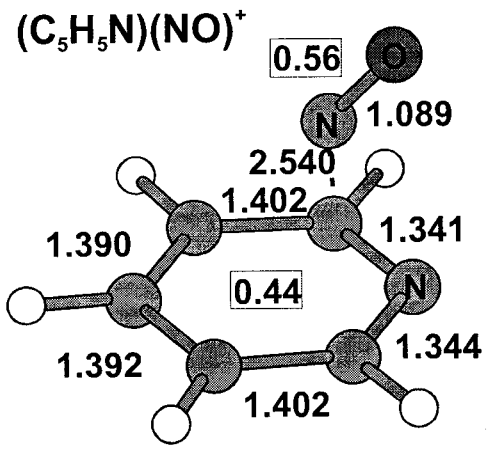

singlet π-complex

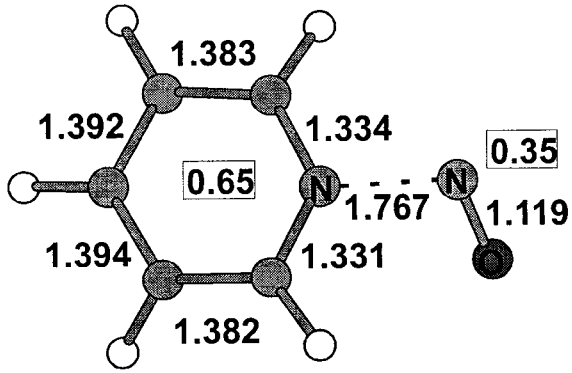

singlet n-complex

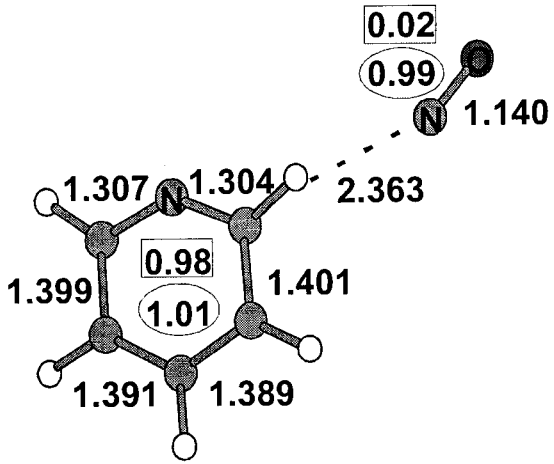

triplet complex

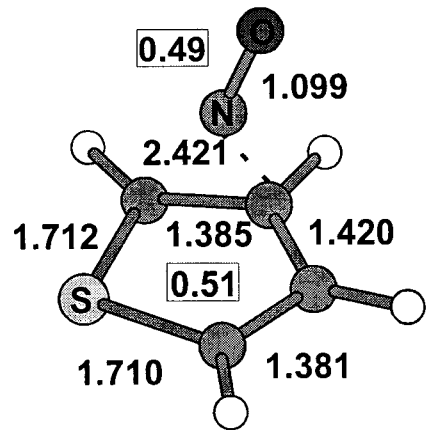

singlet π-complex (a)

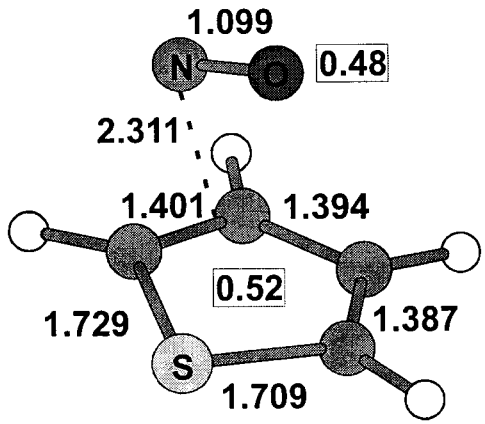

singlet π-complex (b)

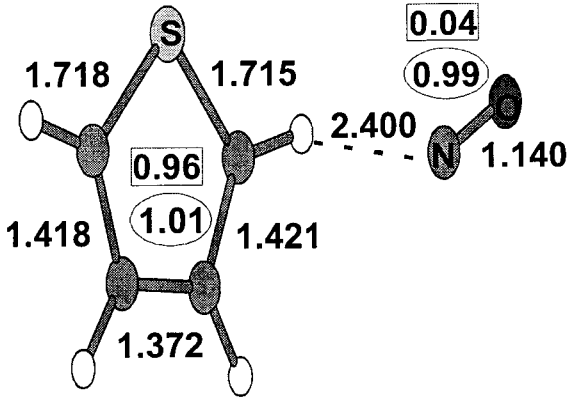

triplet complex

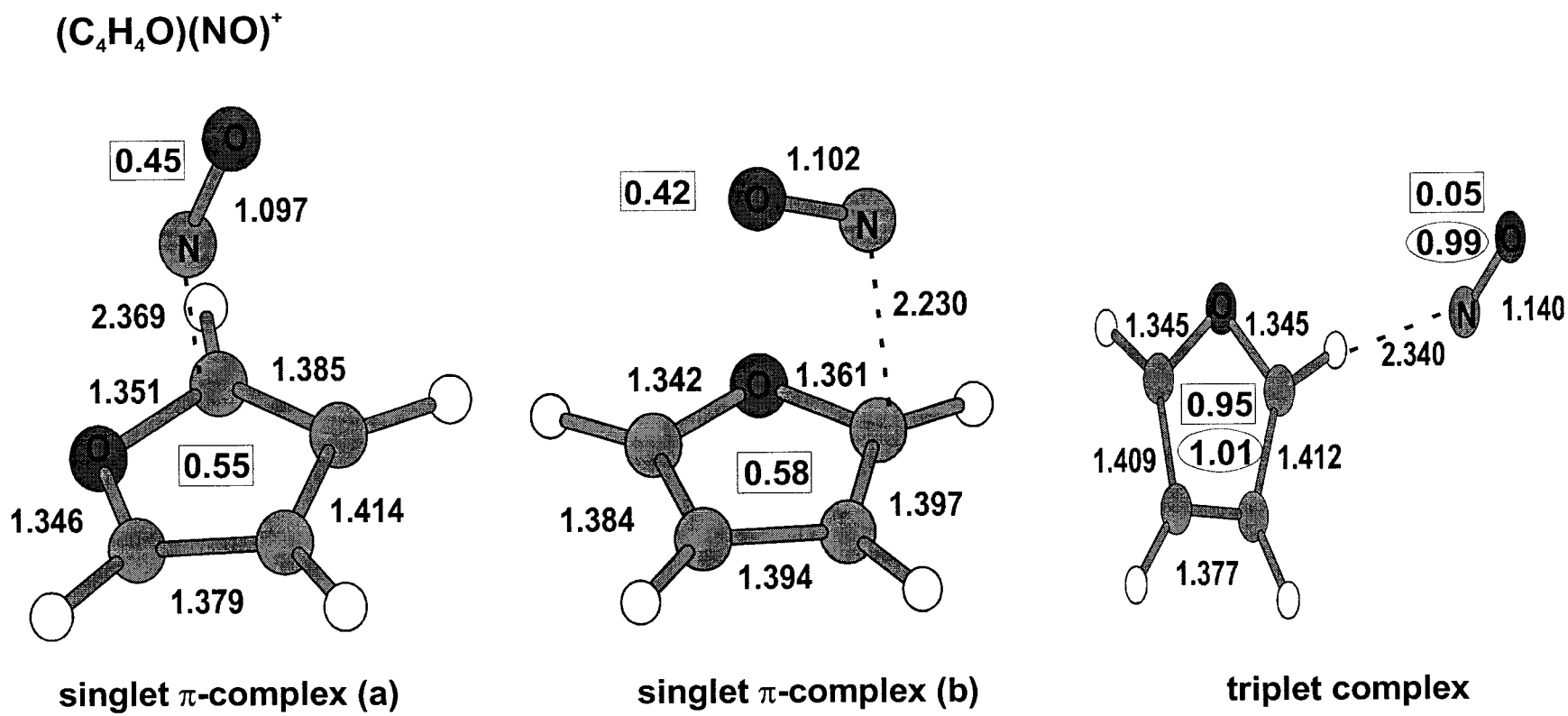

Figure 5.1. Optimized geometries of singlet and triplet $(A)(NO)^+$ complexes for A = benzonitrile (a), benzene (b), pyridine (c), thiophene (d) and furan (e). Calculated at the B3-LYP/6-311++G(3df,2p) level of theory. All bond lengths given in Å.

The basis set used in the geometry optimization is also not critical as B3-LYP/6-311++G(3df,2p) single-point energy calculations on the above MP2, B3-LYP and CCSD geometries produce binding energies (185, 188 and 186 kJ mol^{-1}) that are close to the fully optimized B3-LYP/6-311++G(3df,2p) value, 189 kJ mol^{-1}. The reason for the difference between the two sets of values lies in the calculated ionization energy of NO. The B3-LYP/6-311++G(3df,2p) value is 9.72 eV, which is 0.46 eV higher than the experimental value of 9.26. The G3 value (based on the B3-LYP/6-31+G(d) geometry) for NO is much better, 9.28 eV. While the poor B3-LYP/6-311++G(3df,2p) value can be due to either a poor energy for NO or NO^+, the trend of high binding energies means the problem lies with the energy of NO^+. So, it is likely that all of the B3-LYP/6-311++G(3df,2p) values presented in Table 5.1 are too high by ~ 44 kJ mol^{-1}. Taking that into account, there is generally good agreement between G3 and B3-LYP/6-311++G(3df,2p) values.

5.3.1 $(C_6H_5CN)(NO)^+$

The mass spectrum of metastable $(C_6H_5CN)(NO)^+$ ions changes as a function of NO pressure (Figure 5.2). The ionization energy of C_6H_5CN (9.62 eV) is considerably higher than that of NO (9.26 eV).[10] The lowest energy singlet spin-state of the complex will have the $(C_6H_5CN)(NO^+)$ electron distribution and will adiabatically dissociate into NO^+ + C_6H_5CN. This is consistent with what is observed at low NO ion source pressures (1 x 10^{-5} mbar), Figure 5.2a. At medium NO pressures (5 x 10^{-5} mbar), three peaks are observed in the MIKES mass spectrum (Figure 5.2b): m/z 30 (NO^+), 103 ($C_6H_5CN^{+\bullet}$) and a fragment of ionized benzonitrile, m/z 76 ($C_6H_4^+$). In this mass spectrum, the appearance of $C_6H_5CN^{+\bullet}$

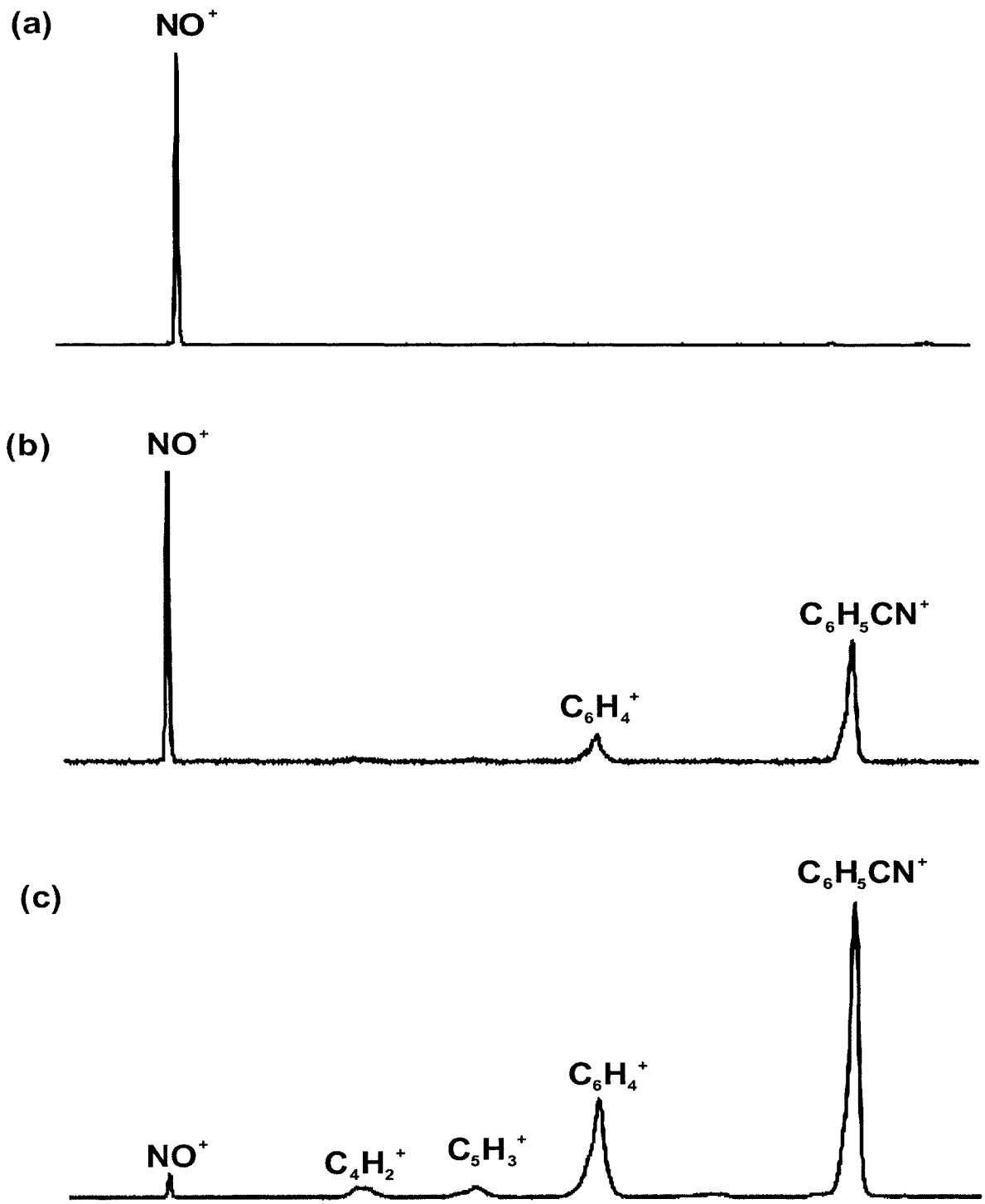

Figure 5.2 MIKES mass spectra of $(C_6H_5CN)(NO)^+$ complexes, m/z 133 at (a) low NO pressure (1 x 10^{-5} mbar), (b) medium NO pressure (5 x 10^{-5} mbar) and (c) high NO pressure (1 x 10^{-4} mbar).

ions indicates that either an excited singlet-state or triplet-state complex is being co-generated in the ion source. At high NO pressures (1 x 10^{-4} mbar), the largest peak in the mass spectrum is that due to ionized benzonitrile (Figure 5.2c) and there are now several observed fragmentation products from the ionized benzonitrile (in fact, these fragment ions are all observed in the CID mass spectrum of ionized benzonitrile). Since the binding energy of either the first excited singlet-state complex or the lowest energy triplet-state complex (both from the reaction of $C_6H_5CN^{+\bullet}$ with NO in the ion source) will be positive with respect to $C_6H_5CN^{+\bullet}$ + NO, they would be expected to dissociate at threshold only to $C_6H_5CN^{+\bullet}$. The production of ionized benzonitrile with enough internal energy to itself decompose can only be due to the formation of either higher excited singlet-states or, perhaps more likely, the formation of an excited triplet-state from the reaction between NO^+ (a $^3\Sigma^+$) and C_6H_5CN in the ion source. Electron-impact ionization with 70 eV electrons is known to produce a large distribution of NO^+ singlet and triplet states.[11] The initial state populations of NO^+ are ~ 33% singlet (15% X $^1\Sigma^+$ and 18% A $^1\Pi$) and 67 % triplet.[11] The A $^1\Pi$ state radiatively relaxes back to the X $^1\Sigma^+$, and has a lifetime of only 55 ns.[12] So in the ion source, most, if not all, of the singlet NO^+ will be in the lowest electronic state. Triplet states decay to the lowest energy a $^3\Sigma^+$ state within 100μs,[13] while the radiative lifetime of the a $^3\Sigma^+$ state is 1.45 s.[11] The reactants NO^+ (a $^3\Sigma^+$) + C_6H_5CN lie 617 kJ mol^{-1} above NO^+ (X $^1\Sigma^+$) + C_6H_5CN.[14] So, generation of the excited state triplet complex having the configuration $(C_6H_5CN)(NO^+)$ would result in the complex having sufficient internal energy to form $C_6H_5CN^{+\bullet}$ product ions which themselves have enough internal energy to undergo further dissociation (the appearance energy for $C_6H_4^{+\bullet}$ from $C_6H_5CN^{+\bullet}$ is 403 kJ mol^{-1},[10] much lower than the 617 kJ mol^{-1} available). Increasing the pressure in the ion source increases the rate at which

complexes are formed, allowing more of the excited state complex to be made prior to the decay/quenching of the NO^+ (a $^3\Sigma^+$) state. It also means that the above formed triplet-state complex must have a lifetime on the order of tens of microseconds.

The structures of the lowest singlet and triplet-state complexes were optimized at the B3-LYP/6-311++G(3df,2p) level of theory and are shown in Figure 5.1. Due to the extensive computational demands, G3 binding energies could not be obtained for these complexes, so only the B3-LYP/6-311++G(3df,2p) values are listed in Table 5.1. The singlet-state complex has two low energy isomers: the higher energy of the two corresponding to a π-complex (binding energy of 141 kJ mol^{-1} relative to $NO^+ + C_6H_5CN$) and the lower energy structure an n-complex in which the NO is bound electrostatically to the CN functionality (binding energy of 177 kJ mol^{-1} relative to $NO^+ + C_6H_5CN$). This difference of 36 kJ mol^{-1} is qualitatively similar to the results obtained by Dechamps et al. at the B3-LYP/6-311++G(d,p) and CCSD(T)/6-311++G(d,p) levels of theory (31 and 28 kJ mol^{-1}, respectively).[15] Even though the IE of benzonitrile is 0.36 eV greater than that of NO, both singlet complexes exhibit charge distributions that are split between the two moieties (B3-LYP/6-311++G(3df,2p) values are 0.60 of a charge on NO and 0.40 on benzonitrile in the π-complex and 0.58 on NO and 0.42 on benzonitrile in the n-complex). The molecular orbitals of the ground state encompass both moieties and the simple picture of the electron distribution presented earlier is not sufficient to describe these complexes (how much this would change in going away from a single-determinant wavefunction is not known). The calculations for the lowest energy triplet-state place NO above the plane of the aromatic ring, near the CN substituent. The charge and spin-distributions indicate a $(C_6H_5CN^{+\bullet})(NO^{\bullet})$

electron distribution. It is calculated to be bound by only 32 kJ mol^{-1}, which is expected to be ~ 44 kJ mol^{-1} too high (see above). So this lowest triplet-state is only nominally bound with respect to the formally spin forbidden dissociation products $C_6H_5CN + NO^+$ (but will be bound with respect to $C_6H_5CN^{+\bullet} + NO^{\bullet}$).

5.3.2 $(C_6H_6)(NO)^+$

The mass spectrum of metastable $(C_6H_6)(NO)^+$ cluster ions (MIKES mass spectrum) is shown in Figure 5.3a. Two signals are observed at m/z 78 and 30 corresponding to $C_6H_6^{+\bullet}$ and NO^+. When magnified more than 100 times, a small peak with m/z 51 is observed, due to the dissociation of benzene ions. This peak is so small that it could be due to residual collisions with the background gas in the 2FFR ($2x10^{-8}$ Torr). If, as in the case of benzonitrile, the peak is due to the formation of the excited-state complex between NO^+ (a $^3\Sigma^+$) and benzene, it can be concluded that there is an insignificant amount of this complex generated in the ion source.

The metastably generated m/z 78 was transmitted to the third field-free region (3FFR) and subjected to collision-induced dissociation (CID). The resulting CID mass spectrum (Figure 5.4a) is virtually identical to that of the benzene ion generated in the ion source in the absence of NO (Figure 5.4b). These results are consistent with the formation of a π-complex between NO and benzene. In addition to forming a π-complex with benzene, NO^+ may be inserted into one of the C—H bonds of the benzene ring to form protonated nitrosobenzene,

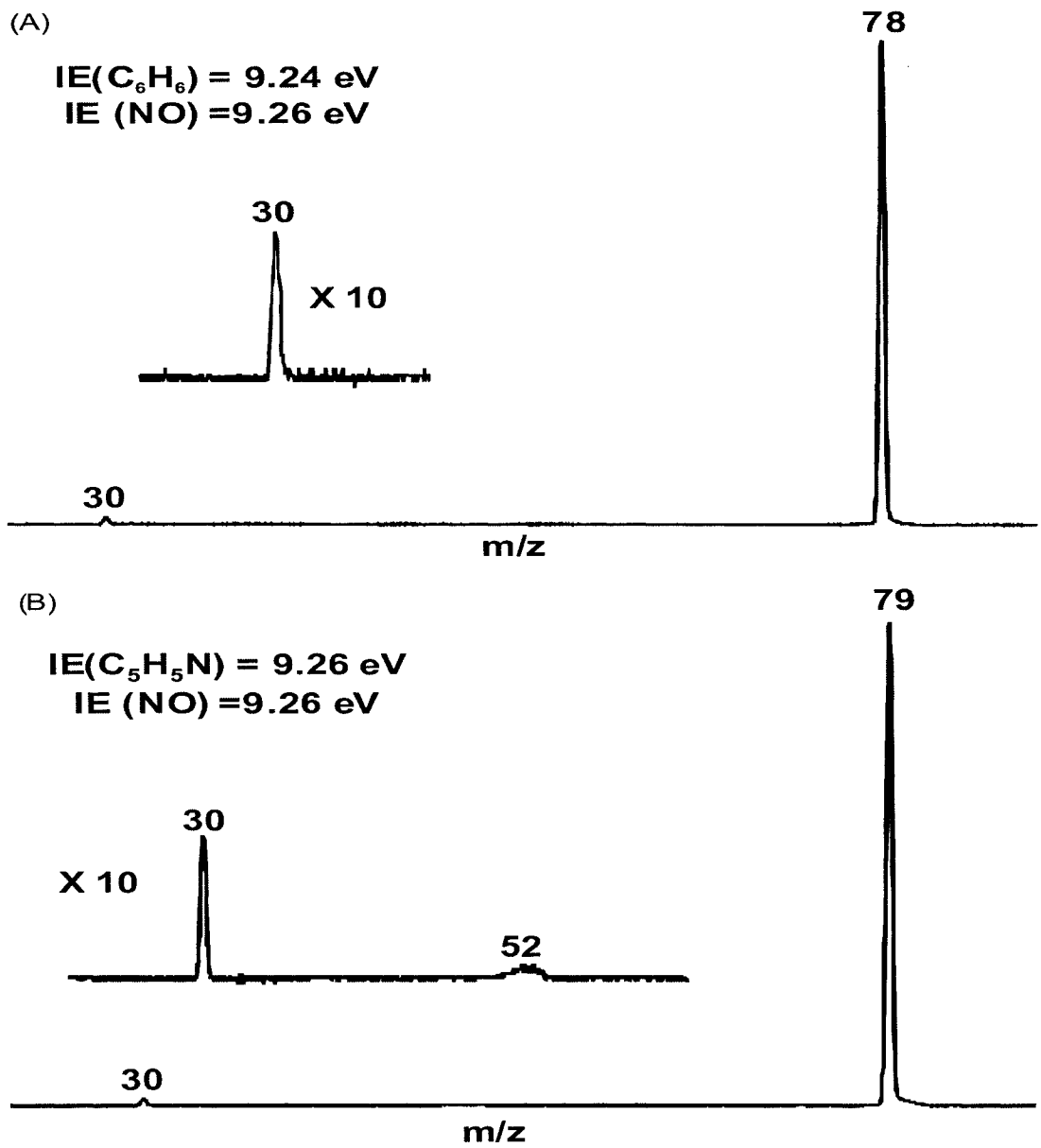

Figure 5.3 Metastable ion mass spectra for the $(A)(NO)^+$ complexes: a) $(C_6H_6)(NO)^+$, m/z 108 and b) $(C_5H_5N)(NO)^+$, m/z 109.

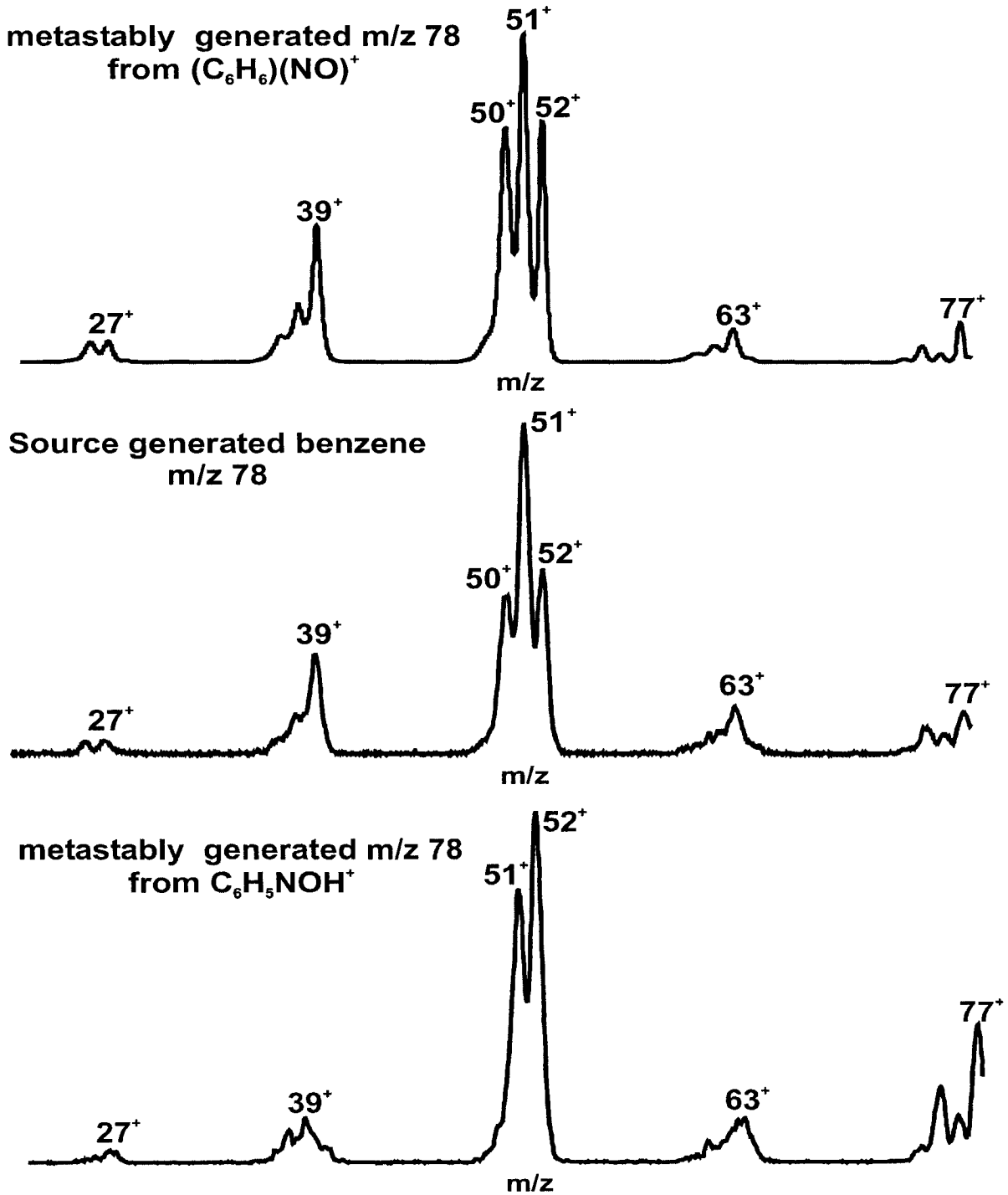

Figure 5.4 CID mass spectra of a) metastably generated m/z 78 ions from $(C_6H_6)(NO)^+$, b) source generated benzene and c) metastably generated m/z 78 ions from protonated nitrosobenzene.

$C_6H_5NOH^+$. The MIKES mass spectrum of protonated nitrosobenzene, $C_6H_5NOH^+$ exhibits only one product ion at m/z 78. The CID mass spectra of $C_6H_5NOH^+$ and $(C_6H_6)(NO)^+$ were found to be closely similar. Previous work on these two isomers[16] has shown that the π-complex and protonated nitrosobenzene have similar CID mass spectra with the exception of a charge stripping peak (m/z 54) present in that of $C_6H_5NOH^+$. We did not observe this doubly-charged ion in the CID mass spectrum of $C_6H_5NOH^+$. The CID mass spectrum of the metastably generated m/z 78 ion from protonated nitrosobenzene (Figure 5.4c) is not ionized benzene, and so it is clear that these two isomers do not interconvert on the microsecond timescale and our experiments are only dealing with a π-complex formed in the ion source. This is in agreement with previous experimental and theoretical work on these two isomers. Reents and Freiser[16] produced a π-complex by reacting C_6H_6 with different nitrating agents (CH_2ONO^+, CH_3ONOH^+ and CH_3ONONO^+) as well as by reacting $C_6H_6^{+\bullet}$ with CH_3ONO. Their ICR results showed that $(C_6H_6)(NO)^+$ and $C_6H_5NOH^+$ do not interconvert on the μs timescale. Raghavachari et al.[17] were the first to theoretically address the possible interconversion of the $(C_6H_6)(NO)^+$ complex into its $C_6H_5NOH^+$ isomer and in a recent paper Gwaltney et al.[18] found that isomerization from $(C_6H_6)(NO)^+$ to $C_6H_5NOH^+$ occurs over a barrier of 247 kJ mol^{-1} (CCSD(T)/6-31G**), which lies 96 kJ mol^{-1} above the $C_6H_6 + NO^+$ dissociation products of $(C_6H_6)(NO)^+$.

Ground state singlet $(C_6H_6)(NO)^+$ should have the nominal electron distribution $(C_6H_6^{+\bullet})(NO^\bullet)$ since the IE of benzene, 9.24 eV, is 0.02 eV lower than that of NO. This structure will adiabatically dissociate to $C_6H_6^{+\bullet}$ + NO. When the structure of the singlet complex was optimized at a variety of levels of theory from HF, MP2 and B3-LYP to QCISD and CCSD, the charge is observed to be almost equally split between the benzene

ring and the NO moiety (the CCSD/6-31+G(d) values are 0.38 of a charge on benzene and 0.62 on NO, while the B3-LYP/6-311++G(3df,2p) values are 0.48 and 0.52, respectively). Even when the distance between the two molecules was increased by 2 Å, the charge remained split between them. Increasing the distance further causes the electron density to move to the departing NO moiety to form $C_6H_6^{+\bullet}$ + NO. One driving force for the charge to be on NO when it is near the aromatic ring is that a complex involving the interaction of the quadrupole moment on benzene with a small point-like charge on NO would be preferred to one in which a more diffuse charge on benzene interacts with the dipole moment of NO. So, adiabatically, the ground state will dissociate to form only m/z 78. The charge distribution and molecular orbitals from the theoretical calculations suggest that an electron is spread over both molecules in the complex. If the electron transfer between NO and benzene was fast (compared to the microsecond timescale of the metastable dissociations probed here), the two product ions would then have nearly equal intensities since the two dissociation thresholds differ by only 2 kJ mol^{-1}. Another possibility is that some of the ionic complexes were generated in their ground triplet $(C_6H_6^{+\bullet})(NO^{\bullet})$ state. Dissociation of this state to form NO^+ ($X\ ^1\Sigma^+$) is spin forbidden,[19] but might be allowed via an avoided crossing with an excited state. Calculations on the lowest energy triplet-state at the B3-LYP/6-311++G(3df,2p) level of theory yield charge and spin distributions indicative of the above electron distribution. Therefore, from the combined experimental and theoretical data, the mass spectrum of the $(C_6H_6)(NO)^+$ complex suggests either a) there is slow intracluster electron transfer in the complex or b) that a significant population of the lowest energy triplet-state complex is made in the ion source. The relative ionization cross-sections for NO and C_6H_6 (at 70 eV) are 3 $Å^2$ and 13 $Å^2$,[20] resulting in a greater abundance of ionized benzene

than ionized NO which would make the formation of the triplet complex just as likely as the singlet complex. Since the number of stabilizing collisions that the two spin-state complexes undergo in the ion source is the same, the initial populations of the two should also be approximately equal. Their respective contributions to the MIKES mass spectrum will then largely be determined by the internal energy of each dissociating complex.

To investigate this further, binding energies of the singlet and triplet complexes were calculated relative to $C_6H_6 + NO^+$ ($X\ ^1\Sigma^+$) (Table 5.2). The optimized geometry of the singlet complex is a π-complex in which the nitrogen atom of the NO moiety lies closest to the ring (Figure 5.1). This structure is 48 kJ mol^{-1} lower in energy than the one in which the oxygen atom of the NO moiety faces the ring (calculated at the B3-LYP/6-31+G(d) level of theory), in reasonable agreement with the difference of 38 kJ mol^{-1} calculated at the MP2/6-31+G* level of theory by Gwaltney et al.[18] Note that the charge is also distributed equally on both molecules in this higher energy complex, so the experimentally observed peak ratios are not due simply to the presence of this isomer. DFT and HF treatments produced a structure with C_1 symmetry while MP2, QCISD and CCSD yield a complex with C_s symmetry. These results are consistent with those reported by other groups.[18, 21] The binding energy of the singlet $(C_6H_6)(NO)^+$ π-complex relative to $NO^+ + C_6H_6$ has been experimentally determined to be 163-205 kJ mol^{-1},[16, 22] which are in reasonable agreement with theoretical values of 220, 195 and 151 kJ mol^{-1} [15, 18, 21] obtained at the B3-LYP/6-31G(d), B3-LYP/6-31+G(d,p) and CCSD(T)/6-31G** levels of theory, respectively. The experimental upper limit of 205 kJ mol^{-1} was obtained from the threshold photodissociation of $(C_6H_6)(NO)^+$ ($(C_6H_6)(NO)^+ + h\nu \rightarrow C_6H_6^{+\bullet} + NO^\bullet$)[16] and the lower limit of 163 kJ mol^{-1} was based upon the reaction

Table 5.2 Binding Energies for singlet and triplet $(C_6H_6)(NO)^+$ as a function of level of theory

	Binding Energy [a]	
	singlet	triplet
HF/6-31G(d)	95	165
HF/6-31+G(d)	88	153
HF/6-31G(d,p)	95	166
HF/6-31+G(d,p)	87	153
HF/6-311G(d,p)	86	140
HF/6-311+G(d,p)	91	138
HF/6-311+G(2df,p)	85	132
MP2/6-31+G(d)	171	n/a[b]
B-LYP/6-31+G(d)	238	98
B3-LYP/6-31+G(d)	206	96
B3-PW91/6-31+G(d)	204	83
QCISD/6-31+G(d)	131	n/a[b]
CCSD/6-31+G(d)	132	n/a[b]
G3[c]	143	17
B3-LYP/6-311++G(3df,2p)	189	67
Experimental Value[d]	165-205	

[a] In kJ mol^{-1} at 0 K. Binding energy calculated relative to $NO^+ + C_6H_6$.

[b] we were unable to successfully optimize the triplet structure at this level of theory.

[c] Based on B3-LYP/6-31+G(d) geometries and ZPEs.

[d] from Reference 4.

$C_2H_5ONOH^+ + C_6H_6 \rightarrow C_2H_5OH + (C_6H_6)(NO)^+$ (and employed the binding energy between NO^+ and ethanol).[23] As the level of theory is improved, the binding energy of the singlet complex seems to converge to a value around 145 kJ mol^{-1} (Table 5.2) which is 20 kJ mol^{-1} lower than the reported lower experimental estimate. The best DFT value (B3-LYP/6-311++G(3df,2p)), 189 kJ mol^{-1}, lies in between the two experimental results (but is expected to be ~ 44 kJ mol^{-1} too high as mentioned previously).

At the HF level of theory the triplet complex is ~ 80 kJ mol^{-1} more stable than the singlet complex (Table 5.2). This trend is reversed at the density functional and G3 levels of theory. The optimized triplet structure has the NO group lying to the side of the benzene ring rather than sitting above the ring (to form a π-complex) (Figure 5.1). The NO bond length and the charge and spin distributions indicate that the complex is best described as a $C_6H_6^{+\bullet}$ ion interacting with a neutral NO molecule, $(C_6H_6^{+\bullet})(NO^{\bullet})$. There is an asymmetry in the charge on the benzene ion moiety in the complex that creates a dipole with which NO can interact. The two highest levels of theory, G3 calculations on the B3-LYP/6-31+G(d) geometry and B3-LYP/6-311++G(3df,2p) give values of 17 and 67 kJ mol^{-1}, respectively, for the 0 K binding energy. Clearly, the singlet state complex has a greater density-of-states than the triplet complex, resulting in the latter having a larger unimolecular dissociation rate constant, $k(E)$. A plot of $k(E)$ vs. E for the two spin-state complexes (employing a 0 K activation energy, E_0, of 145 kJ mol^{-1} for the singlet complex and 70 kJ mol^{-1} for the triplet) shows that at this lower limit for the difference in the two binding energies, the internal energy range responsible for dissociations in the 2FFR of the instrument (10^4 $s^{-1} < k < 10^6$ s^{-1}) is 34 kJ mol^{-1} for the singlet complex and 5 kJ mol^{-1} for the triplet complex. So, these

thermochemical and kinetic results suggest that the triplet-state complex should not be participating to a large extent in the 2FFR observations, which in turn means that proposal (b) is responsible for the appearance of the MIKES mass spectrum: electron transfer in the ground state singlet complex is slower than metastable dissociation.

5.3.3 $(C_5H_5N)(NO)^+$

The MIKES mass spectrum of the $(C_5H_5N)(NO)^+$ ion (Figure 5.3b) is similar to that observed for the $(C_6H_6)(NO)^+$ ion. The CID mass spectrum of the metastably generated m/z 79 was identical to that of ionized pyridine and so no rearrangement of the pyridine moiety has taken place. In addition to ionized pyridine, we observe a small abundance of $C_4H_4^+$ ions (m/z 52) in the MIKES mass spectrum due to metastable loss of HCN from ionized pyridine (in fact, this fragment ion is the main peak observed in the MIKES mass spectrum of ionized pyridine). The intensity of the signal is too large to be due to residual collisions in the 2FFR of the instrument. As in the case for benzonitrile, the production of ionized pyridine with enough internal energy to decompose is likely due to the formation of a small amount of excited triplet-state from the reaction between NO^+ (a $^3\Sigma^+$) and C_5H_5N in the ion source. The ionization energies of NO and pyridine are virtually identical (both are listed as 9.26 eV),[10] and so one cannot *a priori* associate the ground singlet-state with either the $(C_5H_5N^{+\bullet})(NO^{\bullet})$ or $(C_5H_5N)(NO^+)$ electron distributions. The reality will be a mixture of the two. If the electron transfer between the two molecules in the complex is fast (compared to the microsecond timescale of the experiment), such mixing should result in the singlet-state

complex dissociating into equal amounts of NO^+ and $C_5H_5N^{+\bullet}$ due to their identical thermochemical thresholds.

The lowest energy singlet complex is not a π-complex but rather an n-complex (NO bound to the N atom in pyridine) with the NO moiety interacting with the N atom in the pyridine ring (Figure 5.1). This complex has a binding energy with respect to $C_5H_5N + NO^+$ ($X\ ^1\Sigma^+$) of 247 kJ mol^{-1} at the B3-LYP/6-311++G(3df,2p) level of theory, compared to the 151 kJ mol^{-1} for the π-complex (in which the N atom in NO is directed towards the π-system of the pyridine ring, Figure 5.1). This difference (96 kJ mol^{-1}) is identical to that reported by Dechamps et al. at the B3-LYP/6-311++G(d,p) level of theory.[15] The binding energies calculated with G3 theory are 108 and 210 kJ mol^{-1}, respectively. In the n-complex, the NO group lies in the plane of the pyridine ring at a distance from the pyridine nitrogen of 1.767 Å (B3-LYP/6-311++G(3df,2p)). A π-complex with the O atom in NO facing the pyridine ring lies 42 kJ mol^{-1} higher than that having an N – ring interaction (at the B3-LYP/6-31+G(d) level of theory). As was the case for A = benzene, the triplet complex involves a neutral NO molecule hydrogen bonding in the plane of an ionized aromatic ring (Figure 5.1) with a binding energy of only 75 kJ mol^{-1} at the B3-LYP/6-311++G(3df,2p) level of theory and 3 kJ mol^{-1} at the G3 level of theory.

The calculated charge distributions in the equilibrium n- and π-complexes reflect the similar IE values, the positive charge being split roughly equally between NO and pyridine. However, as the NO (in the n-complex) is pulled away from the N atom in pyridine, the charge migrates to the NO moiety so that at an N—N distance of 6 Å NO carries a single

positive charge (B3-LYP/6-311++G(3df,2p)). This is likely due to the increased attractive potential of a point-like NO ion interacting with the dipole of pyridine than if a more diffuse positive charge on the aromatic ring interacts with the small dipole of NO. So, theory predicts that $(C_5H_5N)(NO^+)$ should dissociate adiabatically to $C_5H_5N + NO^+$, but the experimental result shows the opposite behaviour. The only other rationalization for the experimental observation is the participation of the lowest energy triplet-state complex formed when $C_5H_5N^{+\bullet}$ reacts with NO in the ion source, for which $C_5H_5N + NO^+$ are formally spin-forbidden products. However the binding energy of the triplet-state is too low for it to compete effectively with the ground singlet-state on the microsecond timescale (as mentioned earlier for A = benzene), and so the calculated charge distribution along the dissociation reaction coordinate must not reflect the adiabatic channel.

5.3.4 $(C_4H_4S)(NO)^+$ and $(C_4H_4O)(NO)^+$

The MIKES mass spectra of the $(C_4H_4S)(NO)^+$ and $(C_4H_4O)(NO)^+$ cluster ions each display only one peak corresponding to ionized thiophene and furan, respectively (identities of the product ions were confirmed as described above). This is expected since both aromatic molecules have significantly lower ionization energies (8.86 eV and 8.88 eV for thiophene and furan, respectively)[10] than nitric oxide (9.26 eV). The CID mass spectra of the complexes contain small amounts of NO^+ indicating that this dissociation channel is available. The ground singlet-state of both of these complexes should be $(C_4H_4S^{+\bullet})(NO^\bullet)$ and $(C_4H_4O^{+\bullet})(NO^\bullet)$ due to the low IE of the aromatic ring. In the case of $(C_4H_4S)(NO)^+$, the lowest energy singlet-state structure (at the B3-LYP/6-311++G(3df,2p) level of theory)

corresponds to a π-complex in which the N atom in the NO moiety is directed toward the π-system of the aromatic ring (π-complex (a) in Figure 5.1) with a G3 binding energy with respect to $C_4H_4S + NO^+$ ($X\ ^1\Sigma^+$) of 153 kJ mol^{-1}. This structure sits 13 kJ mol^{-1} lower in energy than the isomeric π-complex (b) in which the NO sits parallel to the ring. The lowest energy singlet-state structure for $(C_4H_4O)(NO)^+$ corresponds to a complex in which the NO moiety lies parallel to the plane of the furan ring with the two oxygen atoms facing each other (π-complex (b) in Figure 5.1). This complex sits 4 kJ mol^{-1} lower in energy than π-complex (a) with a G3 binding energy relative to $C_4H_4O + NO^+$ ($X\ ^1\Sigma^+$) of 149 kJ mol^{-1}. Similar geometries were obtained by Dechamps et al.[15] The charge distributions in these complexes indicate significant mixing of the two electron distributions $(A^{+\bullet})(NO^\bullet)$ and $(A)(NO^+)$ with the charge being roughly equally split between the two moieties (Figure 5.1). Even so, ionized thiophene and furan will be the only dissociation products observed due to their lower thermochemical thresholds for formation. The lowest energy triplet-states of the two complexes (Figure 5.1) have the NO group interacting with H atoms in the plane of the ring. The spin and charge distributions are both consistent with only the $(C_4H_4S^{+\bullet})(NO^\bullet)$ and $(C_4H_4O^{+\bullet})(NO^\bullet)$ electron distributions. The binding energies of the two triplet-state complexes are 105 and 106 kJ mol^{-1}, respectively, at the B3-LYP/6-311++G(3df,2p) level of theory. The values decrease to 42 and -44 kJ mol^{-1}, respectively, at the G3//B3-LYP/6-31+G(d) level of theory. All components of the G3 calculation predict a triplet $(C_4H_4S)(NO)^+$ complex that is higher in energy than $NO^+ + C_4H_4S$. This was originally thought to be due to a large geometry change between B3-LYP/6-31+G(d) and the *ab initio* methods; however, when optimized at the MP2/6-31+G(d) level of theory, the complex was found to be 8 kJ mol^{-1} higher than the above dissociation products. This difference is greater

than the previously discussed problem with the B3-LYP/6-311++G(3df,2p) IE of NO. There must be a significant barrier to dissociation to the formally spin-forbidden $NO^+ + C_4H_4S$ products that allows an equilibrium triplet structure to be found in this case.

5.4 Conclusions

NO chemical ionization of aromatic compounds in a high-pressure ion source of a mass spectrometer can form excited-state ionic complexes as evidenced from their unimolecular dissociation chemistry and *ab initio* calculations of their structure and electron distributions. The unimolecular dissociation of metastable ionic complexes of NO and benzonitrile can only be explained by the participation of an excited-state complex formed when NO^+ (a $^3\Sigma^+$) binds to benzonitrile that can dissociate to form high internal energy ionized benzonitrile. A similar result is observed when A = pyridine, but the amount of this excited triplet-state complex formed in the ion source is small. The calculated dissociation reaction coordinate for the ground singlet-state complex suggests that it adiabatically forms NO^+, in contrast to the experimental observation of primarily ionized pyridine. When A = benzene, the MIKES mass spectrum is dominated by ionized benzene, a result that is consistent with the adiabatic dissociation of the ground singlet-state of the complex, provided electron transfer between the two molecules in the complex is slow compared to the microsecond timescale of the experiment. If fast electron transfer does occur, then the lowest energy triplet-state must be co-produced in the ion source. The MI mass spectra of the complexes involving furan and thiophene are consistent with the dissociation of the lowest energy singlet-states.

References

1. J. L. Holmes and P. M. Mayer, "Combined mass spectrometric and thermochemical examination of the C_2H_2N family of cations and radicals", *J. Phys. Chem.* **99**, 1366 (1995).
2. E. E. Rennie and P. M. Mayer, "Confirmation of the "long-lived" tetra-nitrogen (N_4) molecule using neutralization-reionization mass spectrometry and *ab initio* calculations", *J. Chem. Phys* **120**, (2004).
3. K. L. Busch, G. L. Glish, and S. A. McLuckey, *Mass Spectrometry/Mass Spectrometry*. VCH Publishers, New York (1988).
4. W. J. Hehre, L. Radom, P. v. R. Schleyer, and J. A. Pople, *Ab Initio Molecular Orbital Theory*. John Wiley & Sons, New York (1986).
5. M. J. Frisch, G. W. Trucks, H. B. Schlegel, G. E. Scuseria, M. A. Robb, J. R. Cheeseman, V. G. Zakrzewski, J. A. Montgomery, R. E. Stratmann, J. C. Burant, S. Dapprich, J. M. Millam, A. D. Daniels, K. N. Kudin, M. C. Strain, O. Farkas, J. Tomasi, V. Barone, M. Cossi, R. Cammi, B. Mennucci, C. Pomelli, C. Adamo, S. Clifford, J. Ochterski, G. A. Petersson, P. Y. Ayala, Q. Cui, K. Morokuma, D. K. Malick, A. D. Rabuck, K. Raghavachari, J. B. Foresman, J. Cioslowski, J. V. Ortiz, B. B. Stefanov, G. Liu, A. Liashenko, P. Piskorz, I. Komaromi, R. Gomperts, R. L. Martin, D. J. Fox, T. Keith, M. A. Al-Laham, C. Y. Peng, A. Nanayakkara, C. Gonzalez, M. Challacombe, P. M. W. Gill, B. Johnson, W. Chen, M. W. Wong, J. L. Andres, C. Gonzalez, M. Head-Gordon, E. S. Replogle, and J. A. Pople, *in* "GAUSSIAN 98 Rev. A.7". Gaussian Inc., Pittsburgh PA, 1998.

6. A. P. Scott and L. Radom, "Harmonic vibrational frequencies: An evaluation of Hartree-Fock, Moller-Plesset, quadratic configuration interaction, density functional theory and semi-empirical scale factors", *J. Phys. Chem.* **100**, 16502 (1996).

7. L. A. Curtiss, K. Raghavachari, P. C. Redfern, V. Rassolov, and J. A. Pople, "Gaussian-3 (G3) theory for molecules containing first and second row atoms", *J. Chem. Phys* **109**, 7764 (1998).

8. T. Baer and W. L. Hase, *Unimolecular Reaction Dynamics, Theory and Experiments*. Oxford University Press, New York (1996).

9. T. Beyer and D. R. Swinehart, "Number of multiply-restricted partitions [A1] (Algorithm 448)", *ACM Commun.* **16**, 379 (1973).

10. P. J. Linstrom and W. G. Mallard, *NIST Chemistry WebBook, NIST Standard Reference Database Number 69*. National Institute of Standards and Technology, Gaithersburg, MD (March 2003).

11. A. O'Keefe and J. R. McDonald, "Radiative lifetimes and kinetic studies of metastable NO^+ and O_2^+", *Chem. Phys.* **103**, 425 (1986).

12. J. E. Hesser, "Absolute transition probabilities in ultraviolet molecular spectra", *J. Chem. Phys.* **48**, 2518 (1968).

13. W. B. Maier II and R. F. Holland, "Emission from long-lived states in ion beams. New Band Systems of NO+", *J. Chem. Phys.* **54**, 2693 (1971).

14. D. L. Albritton, A. L. Schmeltekopf, and R. N. Zare, "Potential energy curves for NO^+", *J. Chem. Phys* **71**, 3271 (1979).

15. N. Dechamps, P. Gerbaux, R. Flammang, G. Bouchoux, P.-C. Nam, and M.-T. Nguyen, "Gas-phase nitrosation of substituted benzenes", *Int. J. Mass Spectrom.* **232**, 31 (2004).

16. J. Reents, W.D. and B. S. Freiser, "Gas-phase nitration of benzene. Implications for solution electrophilic aromatic substitution reactions", *J. Am. Chem. Soc.* **102**, 271 (1980).

17. K. Raghavachari, J. Reents, W.D., and R. C. Haddon, "Gas-phase nitrosation of benzene: Theoretical investigations", *J. Computational Chem.* **7**, 265 (1986).

18. S. R. Gwaltney, S. V. Rosokha, M. Head-Gordon, and J. K. Kochi, "Charge-transfer mechanism for electrophilic aromatic nitration and nitrosation via the convergence of *ab initio* molecular orbital and Marcus-Hush theories with experiments", *J. Am. Chem. Soc.* **125**, 3273 (2003).

19. G. Herzberg, *Molecular Spectra and Molecular Structure III: Electronic Spectra and Electronic Structure of Polyatomic Molecules*. Van Nostrand Reinhold Co., New York (1966).

20. Y.-K. Kim, K. K. Irikura, M. E. Rudd, M. A. Zucker, J. S. Coursey, K. J. Olsen, and G. G. Wiersma, *Electron-Impact Ionization Cross Section Database*. National Institute of Standards and Technology, Gaithersburg, MD. (2000).

21. S. Skokov and R. A. Wheeler, "Oxidative Aromatic Substitutions: Hartree-Fock/Density Functional and *ab initio* molecular orbital studies of benzene and toluene nitrosation", *J. Phys. Chem A* **103**, 4261 (1999).

22. J. Reents, W.D. and B. S. Freiser, "Gas-phase binding energies and spectroscopic properties of NO^+ charge transfer complexes", *J. Am. Chem. Soc.* **103**, 2791 (1981).

23. R. Farid and T. B. McMahon, "Gas-phase ion-molecule reactions of alkylnitrites by ion cyclotron resonance spectroscopy", *Int. J. Mass Spectrom. Ion Phys.* **27**, 163 (1978).

CHAPTER 6

THEORETICAL ASSESSMENT OF SINGLET AND TRIPLET SPIN-STATE IONIC COMPLEXES OF NITRIC OXIDE AND BENZENE

6.1 Introduction

This chapter involves a theoretical assessment of the performance of a variety of levels of *ab initio* and density functional theories to describe the geometries, zero-point energies (ZPE), ionization energies (IE), and binding energies (BE) of the singlet and triplet-state ionic complexes of nitric oxide and benzene. A discussion of the binding energies of $(NO)(aromatic)^+$ cluster ions involving benzene, pyridine, furan, thiophene and benzonitrile will also be given.

6.2 Computational Procedures in Brief

Standard *ab initio* molecular orbital calculations[1] were performed using the Gaussian 98 suite of programs.[2] Geometries were optimized with a variety of basis sets at the HF level of theory. Geometries were also obtained at the MP2, B-LYP, B3-LYP, B3-PW91, QCISD, and CCSD levels of theory using the 6-31+G(d) basis set. Vibrational frequency analysis was used to confirm that equilibrium structures were obtained, although for the QCISD and CCSD methods, frequency analysis was impossible due to the lack of sufficient computational resources. Scaling factors for zero-point energies (ZPE) were chosen from

the study by Scott and Radom.[3] G3 level[4, 5] single-point energy calculations were performed on B3-LYP/6-31+G(d), MP2/6-31+G(d) and CCSD/6-31+G(d) optimized geometries.

6.3 Theoretical investigation of ion and neutral geometries.

This section includes a discussion of the geometries of $NO^{\bullet}$, $NO^{+}(X^{1}\Sigma^{+})$, $NO^{+}(a^{3}\Sigma^{+})$, C_6H_6, $C_6H_6^{+\bullet}$, $(C_6H_6)(NO)^{\bullet}$, $(C_6H_6)(NO)^{+}$ $(X^{1}A)$ and $(C_6H_6)(NO)^{+}$ $(a^{3}A)$ as a function of electron correlation and basis set.

6.3.1 $NO^{\bullet}$

At the UHF level of theory, the bond length of the $NO^{\bullet}$ molecule remains constant at 1.127 Å until a triple zeta basis set is used (Table 6.1). The use of a triple zeta basis set reduced the bond length by 0.01 Å while incorporating polarization and diffuse functions into a double zeta basis set had no effect. Extending the basis set to 6-311+G(2df,p) further lowers the bond length, but by only 0.002 Å. With the 6-31+G(d) basis set, MP2 theory produced a bond length of 1.143 Å, slightly longer than the values obtained with HF theory. Higher levels of electron correlation (QCISD and CCSD) increase the N—O bond length to 1.174 Å and 1.166 Å, respectively. B3-LYP and B3-PW91 theories produced similar bond lengths (1.158 and 1.154 Å respectively) while the B-LYP bond length was 0.2 Å longer (1.175 Å). MP2, B3-LYP and B3-PW91 methods produced bond lengths intermediate to HF and QCISD and CCSD, with the B3-PW91 value being closest in agreement to the

Table 6.1 Optimized geometric parameters for neutral and ionized NO, benzene and complex.[a]

Method	$NO^{\cdot}$	NO^{+} ($X\ ^1\Sigma^+$)	NO^{+} ($a\ ^3\Sigma^+$)	(C_6H_6)		$(C_6H_6)^{+\cdot}$				$(C_6H_6)(NO)^{\cdot}$			$(C_6H_6\text{-}NO)^{+}$ (^1X)			$(C_6H_6\text{-}NO)^{+}$ (a^3A)	
Effect of Basis Set	N-O	N-O	N-O	C-C	C-H	C-C	C-C'	C-H	C'-H	N-O	N-Ring	<ONCC	N-O	N-Ring	<ONCC	N-O	N-Ring
HF/6-31G(d)	1.127	1.041	1.251	1.386	1.076	1.383	1.445	1.074	1.073	1.127	3.735	0.0	1.059	2.554	0.0	1.123	3.689
/6-31+G(d)	1.127	1.040	1.252	1.389	1.076	1.384	1.445	1.075	1.073	1.127	4.051	-6.6	1.052	2.628	0.0	1.123	3.775
/6-31G(d,p)	1.127	1.041	1.251	1.386	1.076	1.382	1.444	1.075	1.073	1.127	3.736	1.6	1.056	2.552	0.0	1.123	3.680
/6-31+G(d,p)	1.127	1.040	1.252	1.388	1.076	1.384	1.445	1.075	1.073	1.127	4.051	-6.6	1.053	2.626	0.0	1.123	3.760
/6-311G(d,p)	1.117	1.029	1.181	1.386	1.076	1.381	1.444	1.075	1.073	1.117	3.906	0.0	1.040	2.641	0.0	1.113	3.674
/6-311+G(d,p)	1.118	1.029	1.183	1.386	1.076	1.382	1.444	1.075	1.073	1.118	4.008	0.0	1.044	2.601	0.0	1.114	3.734
/6-311+G(2df,p)	1.115	1.026	1.178	1.383	1.075	1.382	1.444	1.075	1.073	1.115	3.990	0.0	1.035	2.676	0.0	1.111	3.749
B3-LYP/6-31+G(d)	1.158	1.073	1.170	1.399	1.087	1.373	1.433	1.088	1.086	1.158	3.490	-2.7	1.114	2.447	112.6	1.154	3.505
/6-311++G(3df,2p)	1.145	1.056	1.158	1.391	1.082	1.365	1.426	1.083	1.081	1.145	3.494	-2.6	1.096	2.455	112.5	1.140	3.606
Effect of Electron Correlation																	
HF	1.127	1.040	1.252	1.389	1.076	1.384	1.445	1.075	1.073	1.127	4.051	-6.6	1.052	2.628	0.0	1.123	3.775
MP2	1.143	1.103	1.194	1.399	1.088	1.376	1.429	1.088	1.086	1.144	3.098	-3.3	1.147	2.509	115.4		
B-LYP	1.175	1.088	1.188	1.409	1.095	1.385	1.443	1.095	1.093	1.176	3.455	-1.4	1.135	2.478	112.7	1.170	3.568
B3-LYP	1.158	1.073	1.170	1.399	1.087	1.373	1.433	1.088	1.086	1.158	3.490	-2.7	1.114	2.447	112.6	1.154	3.505
B3-PW91	1.154	1.071	1.166	1.396	1.088	1.371	1.430	1.088	1.086	1.154	3.794	2.7	1.111	2.416	112.0	1.154	3.632
QCISD	1.174	1.084	1.182	1.400	1.090	1.381	1.410	1.090	1.087				1.109	2.524	116.4		
CCSD	1.166	1.080	1.182	1.400	1.088	1.408	1.411	1.084	1.084				1.123	2.480	116.2		
Best MO Value [e]	1.178	1.094	1.256	1.406	1.089	1.410	1.412	1.084	1.084	1.156[f]	3.159[f]	3.3[f]	1.140	2.528	116.4		
Experimental Value	1.151[b]	1.063[b]		1.399[c]	1.091[c]								1.13[d]	2.44[d]	117.8[d]		

[a] Bond lengths in Å, bond angles in degrees.

[b] from Reference 6.

[c] from Reference 7.

[d] from Reference 12.

[e] values obtained via additivity: CCSD/6-311+G(2df,p) unless otherwise stated.

[f] values obtained via additivity: MP2/6-311+G(2df,p)

experimental value of 1.15 Å.[6] A best MO value of 1.178 Å was obtained using additivity to create a CCSD/6-311+G(2df,p) basis set.

6.3.2 NO^+ ($X^1\Sigma^+$) and NO^+ ($a^3\Sigma^+$)

The bond length of the triplet state ion is on average 0.2 Å longer than that of the singlet state at HF, but only ~0.1 Å longer at the other levels of theory (Table 6.1). For $NO^+(X^1\Sigma^+)$, the bond length at HF with a double zeta basis set is 1.040 Å, but the bond length decreases to 1.029 Å with the use of a triple zeta basis set. The bond length of NO^+ ($X^1\Sigma^+$) increases to 1.103 Å in going from HF/6-31+G(d) to MP2/6-31+G(d), but decreases again with respect to QCISD and CCSD results (1.084 Å and 1.080 Å, respectively). B3-LYP and B3-PW91 produced similar bond lengths (1.073 Å and 1.071 Å, respectively), while B-LYP is slightly higher at 1.088 Å and has a result comparable to QCISD and CCSD theories. B3-LYP, when used with an extended basis set, produced the bond length (1.056 Å) closest in agreement with the experimental result of 1.063 Å.[6] In the case of $NO^+(a^3\Sigma^+)$, a larger variation in bond length was observed between basis sets at the HF level of theory. The use of a triple zeta basis set reduces the bond length from 1.251 to 1.181 Å and incorporation of more polarization reduces the bond length further to 1.178 Å. B3-LYP and B3-PW91 produced N—O bond lengths in excellent agreement for NO^+ ($a^3\Sigma^+$) (1.170 and 1.164 Å) while B-LYP produced a slightly higher N—O bond length of 1.188 Å. The bond lengths obtained at the QCISD and CCSD are both 1.182 Å.

6.3.3 C_6H_6

Both density functional theory and the QCISD and CCSD calculations placed neutral benzene in a conformation with D_{6h} symmetry while MP2 produced C_s symmetry. Hartree-Fock (HF) theory generated the desired D_{6h} symmetry with larger basis sets but failed with the 6-31G(d), 6-31+G(d) and 6-31G(d,p) basis sets. For neutral benzene, HF theory showed little variation in the C—C and C—H bond lengths (1.386 Å and 1.076 Å, respectively) with basis set. MP2, QCISD and CCSD theories produced a C—C bond length of 1.400 Å and a C—H bond length of 1.088 Å. Some variation in bond length was observed within the density functional methods. B3-LYP and B3-PW91 theories produced values similar to those at QCISD and CCSD while B-LYP produced the longest bond lengths for benzene (C—C bond length and C—H bond lengths of 1.409 and 1.095 Å respectively). The best MO values generated via additivity (1.406 and 1.089Å for C—C and C—H bond lengths, respectively) were in reasonable agreement with experiment although theoretical calculations at the QCISD/6-31+G(d) level of theory agree best with the experimental C—C and C—H bond lengths of 1.399 and 1.091 Å, respectively.[7]

6.3.4 $C_6H_6^{+\cdot}$

Hartree-Fock theory, irrespective of basis set used, failed to generate the desired D_{2h} symmetry and placed the benzene cation in a configuration with C_1 symmetry. MP2, QCISD, CCSD and density functional theory produced an ion with D_{2h} symmetry. There is virtually no variation in the geometry as a function of basis set at HF (Table 6.1), the values obtained with the largest basis set being 1.382 and 1.444 Å for the two types of C—C bonds and 1.075 and 1.073 Å for the two types of C—H bonds. B3-LYP and B3-PW91 theories yield values similar to MP2 while B-LYP yields values ~0.01 Å larger than the other two

DFT methods. QCISD/6-31+G(d) and CCSD/6-31+G(d) produce slightly different C—C bond lengths with the QCISD bond length 0.02 Å lower at 1.381 Å.

6.3.5 $(C_6H_6)(NO)^{\bullet}$

All theories and basis sets examined produced a complex with C_1 symmetry. The bond length of the NO in the complex is similar to that of free neutral NO molecules (Table 6.1). The geometry of the neutral cluster has the NO moiety parallel to the plane of the benzene ring (Figure 6.1) as shown by the ONCC dihedral angles in Table 6.1. Since neither benzene nor NO possess significant dipole moments ($\mu(C_6H_6) = 0$ D; $\mu(NO) = 0.14$ D), the interaction between neutral NO and benzene can be attributed to the interaction of the quadrupole moment of the two molecules. The N—Ring distance was identified by the distance between the nitrogen atom in the NO moiety to the nearest carbon in the ring. HF/6-31G(d) produced an N—O bond length of 1.127 Å while the shortest N—Ring distance was found to be 3.735 Å. Upon the addition of a diffuse function, the N—Ring distance increases to 4.051 Å while the N—O bond length remains unaffected. Addition of polarization functions to the hydrogen in the basis set had no effect on either parameter, which makes sense since the C—H bonds are not involved in the interaction; however changing from a double zeta to a triplet zeta basis set caused the N—O bond length to shrink from 1.127 Å to 1.117 Å (exactly the same effect as for the lone $NO^{\bullet}$ molecule) and the N—Ring distance to increase from 3.736 Å to 3.906 Å. In the case of MP2/6-31+G(d), the NO bond length increased to 1.144 Å whereas the N—Ring distance decreased from 4.051 Å at the HF/6-31+G(d) level to 3.098 Å at the MP2/6-31+G(d). Due to the open-shell nature of

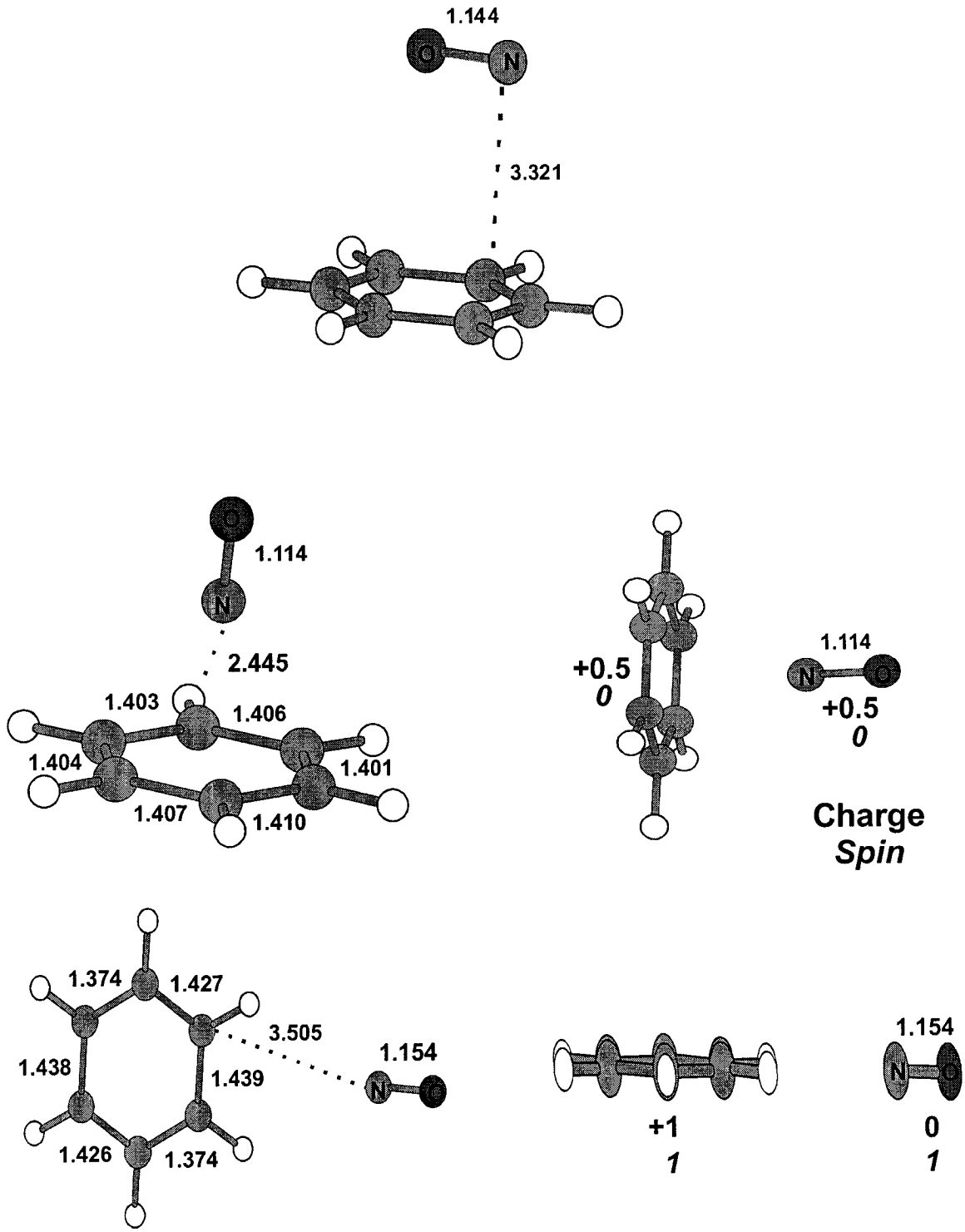

Figure 6.1 Optimized geometries of $(C_6H_6)(NO)^{\bullet}$, $(C_6H_6)(NO)^{+}$ (X^1A) and $(C_6H_6)(NO)^{+}$ (a^3A) calculated with the B3-LYP/6-31+G(d) level of theory. All bond lengths given in Å.

the complex and resulting increase in demand for computational resources, we were unable to optimize the complex at QCISD or CCSD. The B-LYP level of DFT theory produced a geometry different from the other two DFT methods. The N—O bond length increases by ~0.02 Å to 1.176 Å in going from HF/6-31+G(d) to B-LYP /6-31+G(d). In terms of the N—Ring distance, the B3-PW91 method is the anomalous one with a value of 3.794 Å.

6.3.6 $(C_6H_6)(NO)^+$ (X^1A)

The singlet $(C_6H_6)(NO)^+$ ion can best be described as a singlet NO^+ ion interacting with a neutral C_6H_6 molecule (Figure 6.1). The optimized geometry is one in which the nitrogen atom of the NO moiety lies closest to the ring. This structure (calculated at the B3-LYP/6-31+G(d) level of theory) is 48 kJ mol^{-1} lower in energy than the conformation in which the oxygen in the NO moiety faces the ring. This value is in reasonable agreement with the value of 38 kJ mol^{-1} calculated at the MP2/6-31+G* level of theory by Gwaltney et al.[8] DFT and HF theories produced a structure with C_1 symmetry in which a $NO^+(X^1\Sigma^+)$ ion interacts with the π-system of a neutral benzene molecule. A higher level of symmetry (C_s) was obtained with MP2, QCISD and CCSD theories. These results are consistent with those reported by other groups.[8, 9] Due to its symmetry, benzene does not possess a permanent dipole moment, and so the $NO^+(X^1\Sigma^+)$ ion interacts with the quadrupole moment of benzene, similar to that observed for metal ions.[10] Calculations done at the HF level of theory resulted in a structure whereby the NO moiety lies parallel to the plane of the benzene ring while calculations done with MP2, QCISD, CCSD and DFT theories placed the NO moiety slightly tilted from the normal to the plane of the benzene ring; such a geometry avoids an

unstable symmetrical pyramidal arrangement[11] which could cause a degeneracy in the electronic configuration. A Jahn-Teller-type distortion leads to a stabilized structure having a lower symmetry. HF theory places the positive charge on the nitrogen atom in the NO moiety of the complex while the DFT methods with a 6-31+G(d) basis set place the bulk of the positive charge on the oxygen atom. As the basis set is extended (i.e., at the B3-LYP/6-311++G(3df,2p) level of theory), the positive charge moves to the nitrogen atom. MP2 theory splits the charge between the N and O with a slight emphasis of charge on the N while CCSD and QCISD place a slight emphasis of the positive charge on the oxygen atom. The N—O bond distances at the HF level of theory were consistently ~0.01Å longer than that for the free $NO^+(X^1\Sigma^+)$ ion and greater variation was observed between basis sets at the HF level of theory for the ion than the neutral. HF/6-31G(d) calculations produced an N—O bond distance of 1.059 Å and an N-Ring distance of 2.554 Å. When diffuse functions were added, the NO bond distance decreases from 1.059 Å to 1.052 Å while the N—Ring distance increased from 2.554 Å to 2.628 Å (i.e., as the NO moves farther away from the ring, it more closely resembles free $NO^+(X^1\Sigma^+)$). Adding polarization to H in the basis set at the HF level of theory had very little effect upon the distances and bond lengths in the complex since the C—H bonds are not involved in the interaction. The NO bond distance in the complex decreased to 1.040 Å when the basis set was changed from a double zeta to a triple zeta basis set; this change also caused the N—Ring distance to increase by 0.1 Å in the absence of diffuse functions but to decrease slightly when they are employed. MP2/6-31+G(d) gave the longest N—O bond (1.147 Å) and one of the shorter N—Ring distances (2.509 Å). Both QCISD and CCSD gave similar results with the complex 2.5 Å apart and an N—O bond of 1.1 Å. Among DFT methods, B3-LYP and B3-PW91 theories were

comparable to each other with distances of 1.11 Å for the N—O bond and 2.447 and 2.416 Å respectively for the N—Ring distance. The results obtained at the B3-LYP/6-31+G(d) level of theory agree best with the experimental results (N—O bond length of 1.13 Å and N—Ring distance of 2.44 Å).[12]

6.3.7 $(C_6H_6)(NO)^+$ (a^3A)

The optimized triplet structure has the NO group lying to the side of the benzene ring rather than sitting above the ring to form a π-complex as in the case of the singlet structures. The NO bond length in the triplet complex is comparable to that observed in the neutral complex; thus the complex is best described as a $C_6H_6^{+\bullet}$ ion interacting with a neutral NO molecule. There exists an asymmetry in the charge on the benzene ion in the complex and this asymmetry in charge distribution creates a dipole with which NO can interact (Figure 6.1). At the HF/6-31+G(d) level of theory, the NO bond length and N—Ring distances are 1.123 Å and 3.689 Å respectively. The addition of a diffuse function had no effect upon the NO bond length however the N—Ring distance was elongated to 3.775 Å. The use of polarization on non-heavy atoms had no effect on either parameter. In going from a double zeta to a triple zeta basis set, the NO bond decreased by 0.01 Å while the N—Ring lengths increased by 0.13 Å in the absence of a diffuse function while it decreased by 0.01 Å in its presence. HF theory calculated the triplet form of the complex to be lower in energy than the singlet form while DFT calculated the singlet form to be energetically more stable. The triplet complex's open-shell nature and increased demand for computational resources made it impossible to optimize the complex at QCISD or CCSD.

6.4 Ion and neutral zero-point and ionization energies

Incorporated into any determination of relative and absolute energies are the zero-point vibrational energies (ZPE) of the species under consideration. All values presented in Table 6.2 have been scaled by the factors recommended by Scott and Radom.[3] Most of the values are well behaved across basis sets and methods for inclusion of electron correlation. The notable exception is the known poor performance of MP2 for calculating vibrational frequencies (and hence ZPEs) for NO and ionized benzene. The vibrational frequency for NO is twice as large as the other values owing to a vibrational frequency at 3854 cm^{-1}, which is double that calculated at the other levels of theory. HF calculations indicate that the ZPE of singlet NO^+ is twice as large as that of the triplet form, which is due to the stronger shorter bond (Table 6.1); however, once electron correlation is incorporated into the theory, the bonds become more similar and thus so do the ZPE values. ZPE values for neutral benzene average about 258 kJ mol^{-1}; for the ion, they were found to be slightly less (252 kJ mol^{-1}). For the $(C_6H_6)(NO)$ complex, HF and DFT theories yielded little variation in ZPE values, with values of 267 and 271 kJ mol^{-1}, respectively. For the singlet complex, little variation was observed in the ZPE calculated with HF and DFT methods, with both theories yielding values of 279 kJ mol^{-1}. The ZPE at MP2 increases to 279 kJ mol^{-1} for $^2(C_6H_6)(NO)$ but lowers to 274 kJ mol^{-1} for the singlet ion. ZPE values for the triplet at the HF level of theory resemble the neutral form of the complex more than the singlet form. ZPE values of 265 kJ mol^{-1} were obtained for the triplet complex at the HF level of theory with slight variability observed in the first decimal place. DFT produced ZPE values

Table 6.2 Scaled Zero-Point Energies for NO, NO^+ ($X^1\Sigma^+$), NO^+ ($a^3\Sigma^+$), C_6H_6, $C_6H_6^{+\bullet}$, $(C_6H_6)(NO)$, $(C_6H_6)(NO)^+$ (X^1A) and $(C_6H_6)(NO)^+$ (a^3A).[a]

	Scaled ZPE							
Geometry	$NO^\bullet$	NO^+ ($X^1\Sigma^+$)	NO^+ ($a^3\Sigma^+$)	C_6H_6	$C_6H_6^{+\bullet}$	$(C_6H_6)(NO)$	$(C_6H_6)(NO)^+$ (X^1A)	$(C_6H_6)(NO)^+$ (a^3A)
HF/6-31G(d)	12.1	15.6	8.6	258.2	251.9	266.4	278.6	265.5
HF/6-31+G(d)	12.1	15.6	8.6	258.4	251.9	266.7	278.3	265.5
HF/6-31G(d,p)	12.2	15.7	7.1	258.7	252.1	266.9	279.0	265.8
HF/6-31+G(d,p)	12.1	15.7	7.1	258.3	251.6	266.7	278.2	265.2
HF/6-311G(d,p)	12.4	15.9	7.3	258.7	251.9	267.4	278.7	265.9
HF/6-311+G(d,p)	12.3	15.8	7.2	258.6	251.4	267.1	279.0	265.7
HF/6-311+G(2df,p)	12.3	15.7	7.3	258.4	251.8	267.5	278.9	265.7
MP2/6-31+G(d)	22.3	12.2	10.3	252.4	395.3	279.0	274.4	
QCISD/6-31+G(d)	11.3	13.9	10.3					
CCSD/6-31+G(d)	11.2	14.1	10.2					
B-LYP/6-31+G(d)	11.2	14.1	10.5	259.4	251.7	271.5	278.7	264.2
B3-LYP/6-31+G(d)	11.6	14.5	10.8	258.9	252.2	271.4	278.9	265.7
B3-PW91/6-31+G(d)	11.7	14.6	7.7	258.8	252.2	271.1	278.9	265.5
B3-LYP/6-311++ G(3df,2p)	11.6	14.6	10.8	257.1	249.9	269.9	273.7	263.5

[a] In kJ mol^{-1}. Scaling factors taken from Scott and Radom (Reference 3).

ranging from a value of 263 kJ mol^{-1} for B-LYP to 265 kJ mol^{-1} for B3-LYP and B3-PW91. The ionization energies of nitric oxide, benzene and $(NO)(C_6H_6)$ are listed in Table 6.3. Fortuitously, the ionization energy of NO calculated at the HF/6-31G(d) level of theory has been found to agree best with the experimentally determined value of (9.2642 ± 0.00002) eV.[13] The closest accurate theoretical values to agree with experimental work are QCISD and CCSD, which gave values of 9.16 eV. Aside from some fortuitous agreement at the HF level of theory for the two molecules (i.e., NO and benzene), it is clear that the G3 level of theory is necessary to obtain reliable IE values. The next best level of theory is B3-LYP/6-311++G(3df,2p), but one can expect errors of up to 0.5 eV with this method. A theoretical value for the singlet cluster ion at the HF level of theory was found to range from 7.9- 8.4 eV depending on the basis set. At the HF/6-31+G(d) level of theory, an ionization energy of 8.41 eV was obtained for the complex. The addition of a diffuse function to a double zeta basis set resulted in an increase in ionization energy to 8.48 eV, while the addition of polarization to heavy atoms had virtually no effect upon the ionization energy. By changing the basis set from a double zeta to a triple zeta basis set, the ionization energy of the complex decreased from 8.41 to 8.32 eV while increasing the basis set with a diffuse function resulted in the decrease of the ionization energy by 0.20 eV to 8.29 eV from 8.49 eV. DFT yielded values lower than HF with B3-LYP and B3-PW91 methods producing values of 7.79 eV and 7.73 eV, respectively. B-LYP produced a value lower than the other two DFT methods (7.25 eV). MP2 theory yielded a value of 6.94 eV. Ionization energies could not be determined for the cluster ion at the QCISD and CCSD levels of theory due to insufficient computational resources available to perform geometry optimization and vibrational frequency analysis on the open-shell cluster ion.

Table 6.3 Ionization energies of NO, C_6H_6 and the $(C_6H_6)(NO)$ complex. [a]

	Ionization Energy		
Level of theory	IE (NO)	IE(C_6H_6)	IE(complex)[b]
HF/6-31G(d)	9.24	7.56	8.41
HF/6-31+G(d)	9.27	7.71	8.48
HF/6-31G(d,p)	9.24	7.56	8.41
HF/6-31+G(d,p)	9.27	7.71	8.49
HF/6-311G(d,p)	9.08	7.68	8.32
HF/6-311+G(d,p)	9.12	7.72	8.29
HF/6-311+G(2df,p)	9.04	7.71	8.26
MP2/6-31+G(d)	8.60	10.65	6.94
QCISD/6-31+G(d)	9.16	8.74	
CCSD/6-31+G(d)	9.16	8.73	
B-LYP/6-31+G(d)	9.72	8.77	7.25
B3-LYP/6-31+G(d)	9.92	8.98	7.79
B3-PW91/6-31+G(d)	9.84	9.03	7.73
B3-LYP/6-311++G(3df,2p)	9.72	9.06	7.76
G3 (B3-LYP)	9.28	9.30	7.78
Experimental Value[c]	9.2642 ± 0.00002	9.24378 ± 0.00007	

[a] In kJ mol^{-1}.

[b] Ionization of the doublet neutral cluster results in the formation of the singlet ion. So IE (complex) = E($(C_6H_6)(NO)^+$ (X^1A)) - E($(C_6H_6)(NO)$).

[c] From reference 13.

6.5 Binding energies of singlet and triplet state $(A)(NO)^+$ complexes (A = benzene, pyridine, thiophene, furan and benzonitrile).

The binding energies for a series of complexes between NO and aromatics optimized at the B3-LYP/6-311++G(3df,2p) and G3 levels of theory are listed below in Table 6.4. The assessment discussed in this chapter found that the B3-LYP/6-311++G(3df,2p) level of theory was sufficient to describe the behaviour of the electrons in aromatic cluster ions formed with nitric oxide.

Table 6.4 G3 and B3-LYP/6-311++G(3df,2p) 0 K binding energies for singlet and triplet $(A)(NO)^+$ where A = benzene, pyridine, furan, thiophene and benzonitrile.

A	Binding Energies					
	singlet				triplet	
	π-complex		n-complex			
	G3[a]	B3-LYP[b]	G3[a]	B3-LYP[b]	G3[a]	B3-LYP[b]
benzene	143	189	--	--	17	70
pyridine	108	151	210	247	3	75
furan	149	190[c]	--	--	42	105
thiophene	153	198[d]	--	--	-44	106
benzonitrile		141		177		32

[a] Based on B3-LYP/6-31+G(d) geometries and scaled ZPEs, in kJ mol^{-1}.

[b] B3-LYP/6-311++G(3df,2p) energies and scaled ZPEs, in kJ mol^{-1}.

The binding energies for the π-structures of singlet $(C_6H_6)(NO)^+$, $(C_5H_5N)(NO)^+$, $(C_4H_4S)(NO)^+$, $(C_4H_4O)(NO)^+$ and $(C_6H_5CN)(NO)^+$ ions at the B3-LYP/6-311++G(3df,2p) level of theory are 189, 151, 186, 198 and 141 kJ mol^{-1}, respectively. The G3 values for the first four cluster ions in the series are lower at 143, 108, 153 and 139 kJ mol^{-1}; a G3 value for singlet $(C_6H_5CN)(NO)^+$ could not be obtained due to insufficient computational resources. Their structures are similar to that calculated for the singlet $(C_6H_6)(NO)^+$ complex with the NO group sitting above the plane of the benzene ring and with nitrogen facing the ring. When calculated (at the B3-LYP/6-31+G(d) level of theory) with the oxygen atom sitting closest to sitting closest to the aromatic ring, the structures were found to lie higher in energy by 42, 51, 55, 37 and 45 kJ mol^{-1} for the singlet complexes between NO and benzene, pyridine, furan, thiophene and benzonitrile. Since these structures were not the lowest energy conformations, their chemistry was not further explored. The σ-conformation of the singlet $(C_5H_5N)(NO)^+$ complex (at the B3-LYP/6-311++G(3df,2p) level of theory) was found to sit 95 kJ mol^{-1} lower in energy than the π-structure, a result consistent with the work of Dechamps et al.[14] In this geometry, the NO group lies in the plane of the pyridine ring at a distance from the nitrogen in the pyridine ring of 1.723 Å. The binding energies calculated at the B3-LYP/6-311++G(3df,2p) level of theory for the triplet complexes (a^3A), $(C_6H_6)(NO)^+$, $(C_5H_5N)(NO)^+$, $(C_4H_4O)(NO)^+$, $(C_4H_4S)(NO)^+$ and $(C_6H_5CN)(NO)^+$ are 70, 75, 105, 106 and 32 kJ mol^{-1}. As with the singlet complexes, G3 theory lowers the value of the binding energies for the triplet complexes to 17, 3, 42, and -44 kJ mol^{-1}; there were insufficient computational resources to obtain a G3 value for the triplet state of $(C_6H_5CN)(NO)^+$. Their structures with the exception of triplet $(C_6H_5CN)(NO)^+$ are similar to the benzene system with the NO moiety lying to the side of the benzene aromatic

ring. The optimized geometry of $(C_6H_5CN)(NO)^+$ (a^3A) was is similar to the singlet π-complex than the other triplet structures.

6.6 Conclusions

A theoretical assessment has been done to probe the chemistry of singlet and triplet state ionic complexes between NO and benzene, and their dissociation products. This assessment concluded that the B3-LYP/6-311++G(3df,2p) basis set was sufficient to describe the electron character of these complexes. In addition to assessing their geometries as a function of theoretical method and basis set, their zero-point energies and ionization energies were investigated; here it was found that G3 calculations were necessary to obtain reliable ionization energies. The work was further extended to obtain theoretical binding energies for a series of aromatic cluster ions with nitric oxide.

References

1. W. J. Hehre, L. Radom, P. v. R. Schleyer, and J. A. Pople, *Ab Initio Molecular Orbital Theory*. John Wiley & Sons, New York (1986).
2. M. J. Frisch, G. W. Trucks, H. B. Schlegel, G. E. Scuseria, M. A. Robb, J. R. Cheeseman, V. G. Zakrzewski, J. A. Montgomery, R. E. Stratmann, J. C. Burant, S. Dapprich, J. M. Millam, A. D. Daniels, K. N. Kudin, M. C. Strain, O. Farkas, J. Tomasi, V. Barone, M. Cossi, R. Cammi, B. Mennucci, C. Pomelli, C. Adamo, S. Clifford, J. Ochterski, G. A. Petersson, P. Y. Ayala, Q. Cui, K. Morokuma, D. K.

Malick, A. D. Rabuck, K. Raghavachari, J. B. Foresman, J. Cioslowski, J. V. Ortiz, B. B. Stefanov, G. Liu, A. Liashenko, P. Piskorz, I. Komaromi, R. Gomperts, R. L. Martin, D. J. Fox, T. Keith, M. A. Al-Laham, C. Y. Peng, A. Nanayakkara, C. Gonzalez, M. Challacombe, P. M. W. Gill, B. Johnson, W. Chen, M. W. Wong, J. L. Andres, C. Gonzalez, M. Head-Gordon, E. S. Replogle, and J. A. Pople, *in* "GAUSSIAN 98 Rev. A.7". Gaussian Inc., Pittsburgh PA, 1998.

3. A. P. Scott and L. Radom, "Harmonic Vibrational Frequencies: An evaluation of hartree-fock, moller-plesset, quadratic configuration interaction, density functional theory and semi-empirical scale factors", *J. Phys. Chem.* **100**, 16502 (1996).

4. L. A. Curtiss, K. Raghavachari, P. C. Redfern, V. Rassolov, and J. A. Pople, "Gaussian-3 (G3) theory for molecules containing first and second row atoms", *J. Chem. Phys* **109**, 7764 (1998).

5. A. G. Baboul, L. A. Curtiss, P. C. Redfern, and K. Raghavachari, "Gaussian-3 theory using density functional geometries and zero-point energies", *J. Chem. Phys* **110**, 7650 (1999).

6. J. Laane and J. R. Ohlsen, *Prog. Inorg. Chem.* **27**, 465 (1980).

7. K. Tamagawa, T. Iijima, and M. Kimura, "Molecular structure of benzene", *J. Mol. Struct.* **30**, 243 (1976).

8. S. R. Gwaltney, S. V. Rosokha, M. Head-Gordon, and J. K. Kochi, "Charge-Transfer Mechanism for Electrophilic Aromatic Nitration and Nitrosation via the Convergence of ab initio molecular orbital and Marcus-Hush Theories with Experiments", *J. Am. Chem. Soc.* **125**, 3273 (2003).

9. S. Skokov and R. A. Wheeler, "Oxidative aromatic substitutions: Hartree-Fock/Density Functional and *ab initio* molecular orbital studies of benzene and toluene nitrosation", *J. Phys. Chem A* **103**, 4261 (1999).

10. J. C. Ma and D. A. Dougherty, "The cation-pi interaction", *Chem. Rev.* **97**, 1303 (1997).

11. G. I. Borodkin and V. G. Shubin, "Nitrosonium complexes of organic compounds. Structure and reactivity", *Russ. Chem. Rev.* **70**, 211 (2001).

12. S. Brownstein, E. F. GabeLee, and A. Piotrowski, *Can. J. Chem.* **64**, 1661 (1986).

13. P. J. Linstrom and W. G. Mallard, *NIST Chemistry WebBook, NIST Standard Reference Database Number 69.* National Institute of Standards and Technology, Gaithersburg, MD (March 2003).

14. N. Dechamps, P. Gerbaux, R. Flammang, G. Bouchoux, P.-C. Nam, and M.-T. Nguyen, "Gas phase nitrosation of substituted benzenes", *Int. J. Mass Spectrom.* **232**, 31 (2004).

CHAPTER 7

METHODS OF STUDY

7.1 Introduction

In this chapter, a description of the mass spectrometer that was used to conduct the experiments described in this thesis will be given as well as a summary of the theory behind the different experiments performed. An overview will also be given of how the theoretical techniques of *ab initio* theory and variational transition state theory were used to investigate the cluster ions described in this thesis.

7.2 The Modified VG ZAB Mass Spectrometer

The mass spectrometer used to conduct all of the experiments described in this thesis is a custom modified VG ZAB triple focussing mass spectrometer.[1] This instrument consists of a reverse-geometry tandem sector mass spectrometer with a BEE configuration (where B and E refer to magnet and electrostatic analysers, respectively). This triple focussing instrument contains an ion source, a magnetic sector, two electrostatic analysers (ESA), three field-free regions (FFR) and three detectors as shown in Figure 7.1. The magnetic analyser acts as a momentum selector by selecting ions according to their momentum while the electrostatic analyser sorts ions according to their kinetic energies. With this instrument, several types of experiments can be done; the two that will be

described in this thesis are mass-analysed ion kinetic energy spectroscopy (MIKES) and collision-induced dissociation (CID).

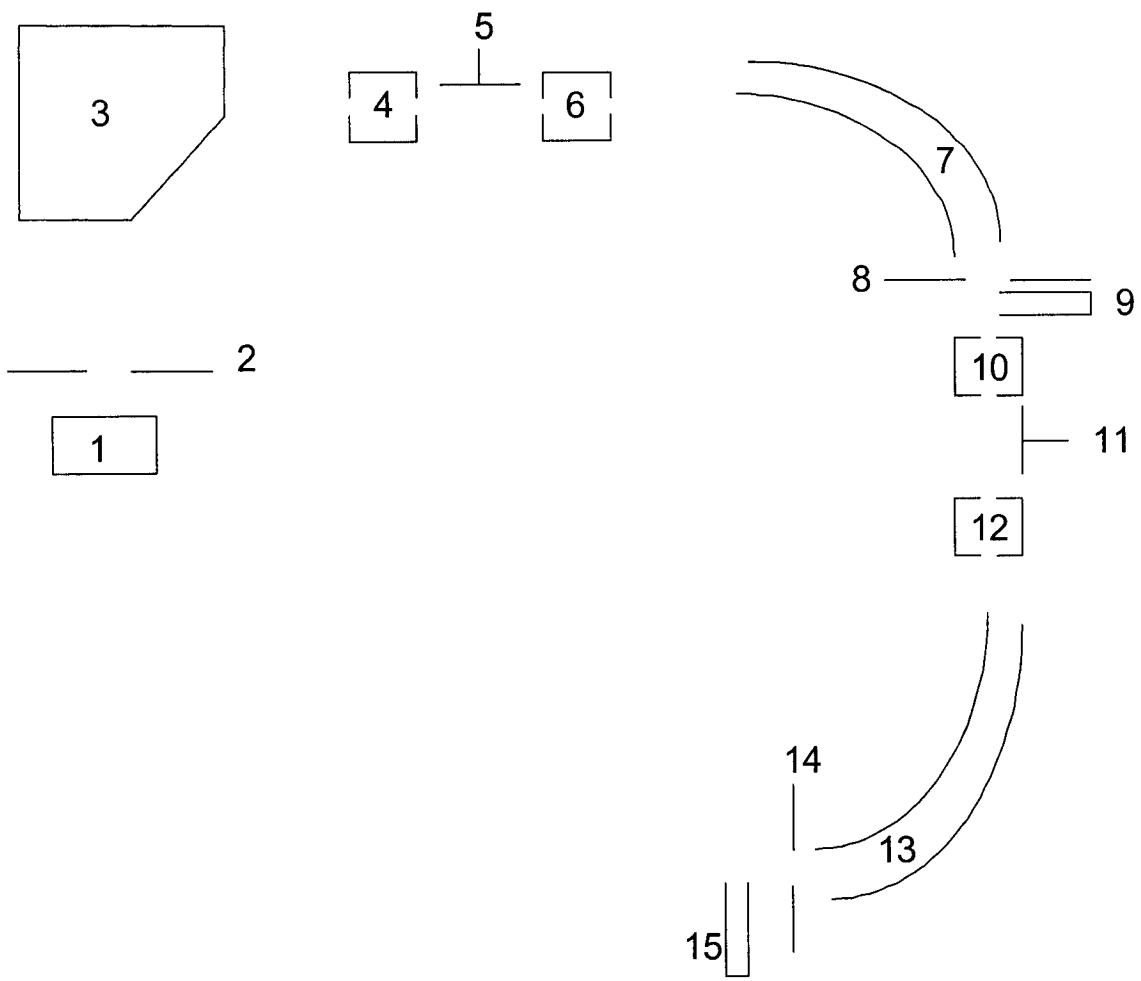

Figure 7.1 Schematic diagram of the modified VG-ZAB mass spectrometer: (1) ion source; (2) slit; (3) magnetic sector; (4) collision cell; (5) deflector electrode; (6) collision cell 2; (7) electric sector 1; (8) collector slit; (9) deflector; (10) collision cell 3; (11) deflector electrode; (12) collision cell 4; (13) electric sector 2; (14) collector slit; (15) detector.

7.2.1 Ion Source

Ions are generated in the ion source of a mass spectrometer by either electron impact or chemical ionization. Chemical ionization involves ionizing molecules via an ion-molecule reaction with a positively charged ion that has been formed as a result of electron ionization. The amount of fragmentation that occurs is in part influenced by the exothermicity of the ion-molecule reaction, i.e., the amount of internal energy present in the initially formed ion. With electron impact (our method of ionization), electrons are generated from a heated helical filament (2.5 to 3.0 A of current are needed to increase the temperature of the filament (> 2000 °C) high enough for the emission of electrons).[2] The electrons are accelerated into the ionization chamber by a potential energy difference between the filament and the electron exit slit which is generally on the order of 70 eV. The electrons that cross the ionization chamber are accelerated toward the trap which sits at a slightly positive potential with respect to the block. In order to keep the electrons on their path, two small magnets are placed in parallel with the electrons' path. Due to the heating of the filament, the source temperature is usually maintained at 150 °C.

Sample is introduced into the ion source via an appropriate inlet system where it is then ionized to make ions. Three different sample inlets exist on the VG-ZAB sector mass spectrometer: a liquid septum inlet, in which a liquid is volatilized in a reservoir and the vapour then leaked into the source via a small capillary; a Granville-Phillips inlet, which is a variable leak valve used for low boiling point liquids that have an appreciable vapour pressure at room temperature; and a solids probe whose tip contains the solid sample held in

a capillary tube. The measured pressure in the ion source chamber, read with an ionization gauge situated above the ion diffusion pump is typically between 10^{-7} and 10^{-6} Torr. The actual pressure in the ion source is approximately two orders of magnitude higher. For the (NO)(aromatic) cluster ion work discussed in chapter 5, a "high-pressure" ion source was used.[3] A regular ion source (which has inlets for gas, liquid and solid samples) was modified for high source pressures by sealing the GC inlets, and mounting an in-house manufactured gas inlet in the solids-probe inlet. The liquid inlet was untouched. This combination allows both gases and liquids simultaneously into the ion source. Two stainless steel plates were spot welded on top of the ion exit plate, so that the plate continued to lie flat on the source block, thus limiting interference with the focusing properties of the source. These plates form a narrow slit 0.015 ± 0.005 mm wide, 8 mm long and 0.02mm deep. These source modifications resulted in a source whose actual pressure is three orders of magnitude higher than that read on the ionization gauge. It is noteworthy to mention that for an effective ion-molecule reaction, it is necessary to maintain a relatively high pressure (i.e., 10^{-5} to 10^{-4} Torr).

Once the ions have been generated, they will fall through a potential gradient (the accelerating voltage, V_{acc}; in the thesis work, this value is 8 kV) as they leave the ion source, such that all ions generated inside the ion source with mass m and charge ze (where z represents the number of charges and e is the fundamental charge on an electron) will leave carrying z x 8keV of kinetic energy according to the following equation:[2]

$$\frac{1}{2} mv^2 = zeV_{acc} \qquad (7.1)$$

Consequently, all ions of the same charge acquire the same kinetic energy, irrespective of their mass. The beam of ions then passes through the source slit and through an assembly of focusing lenses, which consist of a series of shaped plates onto which electric potentials are applied in order to collimate the ion beam in both the y and z directional axes (the x axis being the trajectory direction) in order to maximize both the shape and transmission efficiency of the ion beam. The majority of ions formed by electron ionization are either stable, with insufficient energy to decompose, or unstable, with adequate energy to decompose before leaving the ion source. Ions with a half-life on the order of microseconds are sufficiently long-lived to be accelerated out of the ion source, but decompose in transit to the detector; these ions are called metastable ions. The term metastable applies only to those ions that undergo unimolecular dissociations between the ion source and detector, by virtue of the internal energy that they acquired in the ion source itself (and not as a result of any energy received post-source as in CID mass spectra).[4]

7.2.2 Magnetic Analyzer

The source generated ions pass through a magnetic field (B), produced by an electromagnet. They will follow a circular path with radius (r) through the magnet given by the following equation:[2]

$$\frac{mv}{r} = BzV \qquad (7.2)$$

Equation (7.2) can be rearranged for B (B = mv/zr) so we can see that the magnet is a momentum analyser. For the source generated ions if we substitute equation (7.1) into equation (7.2), we obtain:

$$\frac{m}{z} = \frac{B^2 r^2}{2V_{acc}} \qquad (7.3)$$

Since radius, r, and the accelerating voltage, V_{acc}, are kept constant, it only follows that by varying B, ions can be selected according to their mass to charge ratio.

7.2.3 Electrostatic Analyzer (ESA)

The ESA consists of two curves plates, being a section of a circle with radius r, between which an electric field E can be generated by applying a potential to them. Transmission through the ESA will take place when the centrifugal force on the ion equals the electric field force:[2]

$$\frac{mv^2}{r} = zE \qquad (7.4)$$

Hence the electric sector is a kinetic energy analyzer. For source generated ions, if we substitute equation (7.1) into (7.4), we obtain the following expression:

$$E = \frac{2V_{acc}}{r} \qquad (7.5)$$

If we set the value of the electric field to match the accelerating voltage, this will ensure that any mass selected, source generated ion will be transmitted through the electric sector. If ions are now detected after the electric sector, scanning the magnetic field will produce the double focussing mass spectrum of the sample. In double focussing mode, greater mass resolution can be obtained, because the ESA focuses the small spread in kinetic energies of the ions.

7.2.4 Field Free Region (FFR)

The VG ZAB triple focussing mass spectrometer at the University of Ottawa contains three field free regions: (1) between the source and the magnet; (2) between the magnet and ESA1; and (3) between the two ESA's. The FFR is the main experimental region of the magnetic sector mass spectrometer; it is in these regions that an ion may spontaneously dissociate or dissociate following collisional activation. The second and third FFR house the four collision cells. These cells consist of 2-3 cm long blocks of steel through which a 2mm groove is cut. Cells 1 and 2 sit 10 cm apart, while the distance between cells 3 and 4 is variable, although usually set to 6cm. An assembly of focussing lenses follows cell 2. To each of the collision cells, gas lines are connected. The pressure in the cells is monitored by ionization gauges placed in close proximity. The differential pumping in these regions produces a pressure gradient between the cells and their surroundings, preventing the gas from spreading through the flight tube.

7.2.5 Detectors

The detectors consist of off axis photomultipliers. The detectors are made up of two parts: a conversion dynode and a scintillator. On one side of the ion beam a conversion dynode is placed onto which a high negative potential is applied (ca. 20 kV). The positive ions are attracted toward this dynode, impinge on the central portion of the conversion dynode and secondary electrons are emitted. These electrons are accelerated towards a CaF_2 scintillator, whose produced scintillations are detected by an optically coupled photomultiplier and the signal is amplified.

7.3 Experiments Performed on the VG ZAB

Both MIKES and CID experiments are performed in the following manner. The sole difference is that in a CID experiment a target gas is introduced into one of the collision cells. Sample vapour is first introduced into the ion source (held at the operating potential of the instrument, 8kV) through one of the three inlets described above. The newly formed ions are then pushed out of the source by a repeller electrode through an exit slit and accelerated to the operating kinetic energy of the instrument. A series of ion lenses is used to focus the ion beam onto the entrance aperture of the mass spectrometer. The ions are then momentum selected by the magnetic sector and transmitted into the FFR where they can metastably decompose on the microsecond timescale. The resulting fragment ions are then scanned by the ESA where they are sorted according to their kinetic energy prior to their detection by the detector. I will now take the reader through the theory behind the MIKES and CID experiments and show the differences between the two methods.

7.3.1 Mass-Analysed Ion Kinetic Energy Spectrometry (MIKES)

Every singly charged ion leaving the ion source will have the same translational kinetic energy irrespective of their mass; their ion kinetic energy may be expressed by the following equation:[4]

$$qV_{acc} = \tfrac{1}{2} m_1 v_1^2 = \tfrac{1}{2} m_2 v_2^2 = \tfrac{1}{2} m_n v_n^2$$

where q is the electronic charge, m is the mass, v is the velocity and V_{acc} is the ion source acceleration voltage. A variable magnetic field then separates the ions according to their momentum. If an ion, A^+, with mass m_a metastably dissociates between the magnetic and electric sectors (i.e., in the FFR), the dissociated fragments (ion B^+ with mass m_b and neutral C) have, as a first approximation, the same velocity as the precursor ion (i.e., fragment B will have the velocity v_a.). The kinetic energies, E_{kA} of ion A^+ and E_{kB} of ion B^+, are respectively

$$E_{kA} = eV_s = \frac{m_a v_a^2}{2} \qquad E_{kB} = \frac{m_b v_a^2}{2} \qquad (7.6)$$

We therefore deduce that

$$\frac{E_{kA}}{E_{kB}} = \frac{m_a}{m_b} \qquad (7.7)$$

The ions passing through the electric sector must obey the condition that

$$eE = \frac{mv^2}{r} \qquad (7.8)$$

Normally, the value of E is the same for all the primary ions, because they all have the same kinetic energy. However if we modify the value of E so that

$$eE_a = \frac{m_a v_a^2}{r} \qquad eE_b = \frac{m_b v_a^2}{r} \qquad (7.9)$$

then the value E_b of the metastable ion is observed. Thus,

$$\frac{E_a}{E_b} = \frac{m_a}{m_b} \qquad (7.10)$$

By knowing the ratio E_a/E_b and the value of m_a, the mass m_b of the fragment ion can as a result be obtained. By scanning the ESA to pass ions with lower translational kinetic energies, the fragment ions will sequentially pass through the detector. The final ion abundance versus kinetic energy spectrum is converted to an ion abundance versus fragment m/z spectrum by the above relationship. The result is the mass-analyzed ion kinetic energy spectrum (MIKES). The above analysis supposes that the fragment ion has retained the velocity of the precursor however this is only true if the fragmentation occurs without any release of kinetic energy. Usually the fragmentation goes along with a conversion of part of the internal energy into kinetic energy of the fragments. If the reaction releases kinetic energy δE, then the fragment has a kinetic energy ranging from $(E_{kb} + \delta E)$ to $(E_{kb} - \delta E)$,

depending on whether the orientation of the precursor ion has induced an increase or decrease in the velocity. This variation results in a widening of the peak compared with the width due to the normal dispersion of velocities and to the instrument resolution. The MIKES spectrum is the end result of all low energy unimolecular processes of the selected ions, including isomerization; as a result, the MIKES mass spectra of isomeric ions which interconvert on the microsecond timescale often have closely related or even identical.

7.3.2 Collision-Induced Dissociation (CID) Mass Spectrometry

CID mass spectrometry is a particularly valuable tool for ion structure elucidation and determination. As mentioned above, a CID mass spectrum of mass selected ions is obtained in the same manner as a MIKES mass spectrum except that a target gas is introduced (usually He) into a collision cell located in one of the field-free regions to achieve a 10% reduction in the flux (i.e., single collision conditions).[5] Helium is the most commonly used target gas since it is easy to obtain pure and fast to pump out. The resulting CID mass spectrum contains peaks due to ions formed via all possible unimolecular dissociation processes of the precursor ion. The timescale of the CID fragmentation reactions is quite different from the MIKES spectrum, ranging from the time of the collision event ($t = 10^{-15}$ s) to the time the ions leave the field-free region. As a result, isomerization reactions tend not to play a significant part in collision-induced reactions and thus the CID mass spectra are often characteristic of ion connectivity. Consequently, identical ions generated from a variety of precursor molecules should have indistinguishable CID mass spectra, whereas isomeric ions, in general, will have distinctive CID characteristics. The

effect of internal energy may be best observed when comparing CID mass spectra of both source and metastably generated ions. The two CID mass spectra will be indistinguishable if the structure of the ions is independent of their internal energy content. It is generally accepted that only the metastable reaction channels may depend upon the initial internal energy distribution of the precursor molecules. All other critical energy dissociation channels should be independent of the initial internal energies.

7.4 Theoretical Methods

A combination of theoretical methods was used to complement the mass spectrometric investigation of gas-phase ions. In particular, *ab initio* and density functional methods were used to probe the energetics of ions while variational transition state theory (VTST) was used to model the unimolecular dissociation of proton-bound pairs.

7.4.1 Performing a Theoretical Calculation

The basic steps involved in performing a typical *ab initio* and density functional calculation are very similar and can be treated together. The first task involved in a theoretical calculation is to determine the type of calculation required (i.e., decide on what level of theory and basis set). The software used to perform the theoretical calculations presented in this thesis was Gaussian 98.[6] Gaussian is controlled by specific keywords, which are used to request a certain type of calculation. These keywords are then converted

into internal parameters which then control the execution of the calculation. An example of input data (known as a .com file) for a Gaussian run calculation is shown in Figure 7.2.

%mem = 100Mb	Memory line
%chk = H_3O^+.chk	Checkpoint line
%rwf = a,240Mw,b,240Mw,c,240Mw	Read-write file
# MP2/6-31+ G(d) opt freq	Route line
	Mandatory blank line
Geometry optimization of H_3O^+	Job Title
	Mandatory blank line
1, 1	Charge and Multiplicity
H	Beginning of Z-matrix
O 1 OH	
H 2 OH 1 HOH	
H 2 OH 1 HOH 3 HOHH	
OH = 0.99	
HOH = 111.0	
HOHH = 120.0	End of Z-matrix
	Mandatory blank line

Figure 7.2 Input deck for a geometry optimization of H_3O^+ at the MP2/6-31+G(d) level of theory.

In the filename.com file, the first line indicates how much memory you wish to allocate to the calculation. Line two lists the name of the checkpoint file; this file is useful when a job crashes and can be used to restart the job from that point or to create a new z-matrix using the newzmat command. Line three is reserved for the read-write file and is typically used in split form for larger calculations as a way of increasing the amount of available diskspace for this calculation. It would not be required for H_3O^+ and is therefore only listed for completion. Line four is the route line: it is here that the user specifies the level of theory, basis set and the job commands. In the above example, the level of theory is MP2, the basis set is 6-31+G(d) and the job commands are for a geometry optimization (opt keyword) followed by a frequency calculation (freq keyword). Lines five and seven are mandatory empty spaces while line six is reserved for naming your calculation (you can write whatever you wish). Line eight is reserved for the charge and spin multiplicity of the structure you are studying (for the hydronium ion, these are 1 and 1). The remainder of the .com file consists of the Z-matrix. A blank space after the Z-matrix is also required.

A Z-matrix is a convenient way of specifying the geometry of a molecule by hand because it corresponds to the way that most chemists think about molecular structure: bonds, angles and dihedrals.[7] Let us now examine the Z-matrix in the .com file of H_3O^+ in more detail (Figure 7.3).

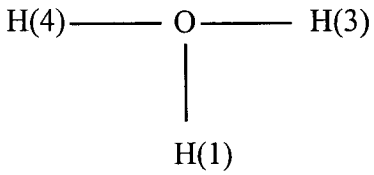


```
H
O     1     OH
H     2     OH    1     HOH
H     2     OH    1     HOH   3     HOHH
```

OH = 0.99

HOH = 90.0

HOHH = 180.0

Figure 7.3 Z-matrix of the hydronium ion.

Each column of the Z-matrix represents a different function: the first column is the element, the second column the atom to which the length refers, the third column the bond length, the fourth column the atom to which the angle refers, the fifth column the angle, the sixth column the atom to which the dihedral angle refers and the seventh column the dihedral angle. This was the easiest way to define a molecule's geometry prior to the development of graphical user interfaces.

Another way to define the geometry of a molecule is as a set of Cartesian coordinates for each atom, which are typically generated by the program. The Cartesian coordinates for the hydronium ion are shown below in Figure 7.4 and could easily be substituted for the Z-matrix in Figure 7.1.

	x	y	z
H	-0.31087	0.047154	-0.91715
O	-0.03912	0.062616	0.036151
H	0.934676	0.222617	0.128528
H	-0.31087	-0.77070	0.499413

Figure 7.4 Cartesian coordinates representation of H_3O^+. The first column is the element and the other columns are the x, y, and z Cartesian coordinates.

It is becoming more common to use programs that have a graphical builder in which the user can essentially draw the molecule they wish to calculate; one such program is GaussView. Graphical interface programs often generate Cartesian coordinates since this is the most convenient way to write those programs.[7] With GaussView, one can build a structure in a Windows type environment where they can specify bond lengths and angles with the click of a mouse. This method is much easier than writing out a complicated Z-matrix as would be required for larger structures like proteins and complex organic molecules. Of the two methods (i.e., Z-matrix or Cartesian coordinates), there is no one best way to specify geometry. A well constructed Z-matrix is usually best for specifying symmetry constraints however Cartesian coordinate optimization may be more efficient than that done with a poorly constructed Z-matrix.

7.4.2 Calculating *k*(E) vs. E Curves using RRKM Theory.

The most accurate method for determining the density and sum of harmonic vibrational states is the direct count method proposed by Beyer and Swinehart.[8] If a system consists of s harmonic oscillators with frequencies of $\omega_i = \nu_i/c$ cm^{-1} where c is the speed of

light, then each will have a series of equally spaced states located at $E_i = n\omega_i$ where n = 0,1,2,.... The zero of energy is the ion's zero point energy and the internal energy is divided into bins of size 1 cm^{-1}. The s frequencies can then be expressed in wavenumbers, rounded off to the nearest wavenumber. The sum-of-states $N^{\ddagger}(E)$ can be obtained either by direct numerical integration of the density of states or computed directly by using the Beyer-Swinehart scheme. In order to perform the above calculation, vibrational frequencies (scaled according to the level of theory used) of the reacting ion and transition state are required. An example of an input deck is shown below in Figure 7.5.

```
Dissociation of the CH3CN-MeOH proton-bound pair at 3A
Title
line
0.952, 1.38, 1.47, 10, 1                    see text for description
 32                                  number of reactant ion vibrational frequencies
  67    80   129   147                 list reactant ion vibrational frequencies
 260   329   331   517
 882   908   964  1013
1015  1098  1160  1290
1374  1417  1417  1419
1451  1454  1665  1943
2155  2943  2983  3039
2943  3103  3117  3470
23.3                                    rotational constant of reactant ion
31                                  number of vibrational frequencies in TS
  28    34    87   100                 list vibrational frequencies in TS
 325   327   415   711
 725   984  1010  1011
1063  1209  1233  1265
1368  1405  1405  1428
1459  1462  2169  2714
2935  2946  3034  3034
3047  3074  3516
23.3                                    rotational constant of TS
```

Figure 7.5 Input information for a log k(E) vs. E calculation

The first line of the input is the title of the calculation; it may be called whatever the user likes. The next line lists the following parameters: Activation energy (in eV), the starting energy value (above E_0) to be printed, the final energy value to be printed, the number of energy values to be printed, and symmetry number. After listing these parameters, the number of vibrational frequencies of the reactant ion are listed followed by the frequencies themselves. On occasion, there will be a hindered internal rotor in the reactant ion frequencies and so this is removed and replaced by the rotational constant as shown in the input deck above. A hindered internal rotor is a hybrid between a free rotor and a vibration and usually sits at a low vibrational frequency, 2-5 cm^{-1}. After the information is listed for the reactant ion, the information is the listed for the transition state.

The output information for the input data given in Figure 7.5 is shown below in Figure 7.6.

Dissociation of the CH_3CN-MeOH proton-bound pair at 3A
entropy of activation at 600K is 25.915 J mol^{-1} K^{-1}

E	RATE	Log10RATE	p	N
1.380	4.75E+07	7.677	1.38E+11	2.19E+08
1.391	5.35E+07	7.728	1.54E+11	2.74E+08
1.402	6.00E+07	7.778	1.72E+11	3.44E+08
1.413	6.72E+07	7.828	1.91E+11	4.29E+08
1.424	7.51E+07	7.876	2.13E+11	5.34E+08
1.435	8.37E+07	7.923	2.37E+11	6.62E+08
1.446	9.31E+07	7.969	2.64E+11	8.20E+08
1.457	1.03E+08	8.014	2.94E+11	1.01E+09
1.468	1.14E+08	8.058	3.26E+11	1.25E+09
1.479	1.26E+08	8.101	3.63E+11	1.53E+09

Figure 7.6 RRKM *k*(E) vs. E output data from the Direct Count method

The output from the calculation not only provides the sum and densities of states, but also rate constant data as a function of internal energy. By plotting the logarithm of the rate constant as a function of internal energy, one can obtain the log k(E) vs. E curves. The entropy of activation for a dissociation or isomerization reaction is also obtained from the output data.

References

1. J. L. Holmes and P. M. Mayer, "Combined mass spectrometric and thermochemical examination of the C_2H_2N family of cations and radicals", *J. Phys. Chem.* **99**, 1366 (1995).
2. R. G. Cooks, J. H. Beynon, R. M. Caprioli, and G. R. Lester, *Metastable Ions*. Elsevier Sci. Pub. Co., Amsterdam (1973).
3. E. E. Rennie and P. M. Mayer, "Confirmation of the "long-lived" tetra-nitrogen (N_4) molecule using neutralization-reionization mass spectrometry and *ab initio* calculations", *J. Chem. Phys* **120**, (2004).
4. J. L. Holmes, *in "Encyclopedia of Mass Spectrometry"* (R. Caprioli, ed.), Vol. 1, p. 91. Elsevier, 2003.
5. J. L. Holmes, "Assigning structures to ions in the gas-phase", *Org Mass spectrom.* **20**, 169 (1985).
6. M. J. Frisch, G. W. Trucks, H. B. Schlegel, G. E. Scuseria, M. A. Robb, J. R. Cheeseman, V. G. Zakrzewski, J. A. Montgomery, R. E. Stratmann, J. C. Burant, S. Dapprich, J. M. Millam, A. D. Daniels, K. N. Kudin, M. C. Strain, O. Farkas, J.

Tomasi, V. Barone, M. Cossi, R. Cammi, B. Mennucci, C. Pomelli, C. Adamo, S. Clifford, J. Ochterski, G. A. Petersson, P. Y. Ayala, Q. Cui, K. Morokuma, D. K. Malick, A. D. Rabuck, K. Raghavachari, J. B. Foresman, J. Cioslowski, J. V. Ortiz, B. B. Stefanov, G. Liu, A. Liashenko, P. Piskorz, I. Komaromi, R. Gomperts, R. L. Martin, D. J. Fox, T. Keith, M. A. Al-Laham, C. Y. Peng, A. Nanayakkara, C. Gonzalez, M. Challacombe, P. M. W. Gill, B. Johnson, W. Chen, M. W. Wong, J. L. Andres, C. Gonzalez, M. Head-Gordon, E. S. Replogle, and J. A. Pople, *in* "GAUSSIAN 98 Rev. A.7". Gaussian Inc., Pittsburgh PA, 1998.

7. D. Young, *Computational Chemistry: A practical guided for applying techniques to real world problems*. John Wiley & Sons, Inc.(2001).

8. T. Beyer and D. R. Swinehart, "Number of multiply-restricted partitions [A1] (Algorithm 448)", *ACM Commun.* **16**, 379 (1973).

Claims to original research

1. The entropy of activation for the dissociation of the series of acetonitrile-alcohol proton-bound pairs ranging from methanol to isopropanol was determined using variational transition state theory (VTST) and it was found that the entropy of activation for the dissociation to CH_3CNH^+ and ROH decreases as a function of increasing alkyl chain.[1] The entropy of activation was found to differ considerably from the thermodynamic entropy. This has been the first explicit study in which individual entropies of activation for the dissociation of proton-bound pairs have been determined.

2. Both high and low energy dissociation channels for the series of acetonitrile-alcohol proton-bound pairs, $(CH_3CN)(ROH)H^+$ (where R = CH_3, C_2H_5, C_3H_7, $(CH_3)_2CH$) were probed using VTST. It was found that the difference between the entropies of activation of the two dissociating channels was zero for R = CH_3 and C_2H_5 while for the two C_3H_7 isomers, the net difference ranged between 40 - 45 J K^{-1} mol^{-1}. The difference in both the thermodynamic entropies, $\Delta(\Delta S)$, of the two channels was found to be zero.[2] This has been the first explicit study to examine the differences between the thermodynamic and activation entropies of two dissociating channels.

3. Empirical relationships for the key features involved in the isomerization of gas-phase ions were derived as means of predicting an ion's tendency for gas-phase rearrangement. Similar empirical equations were established for the families of nitrile-alcohol and

alcohol-alcohol proton-bound pairs.[3] These empirical relationships have been the first derived as means of predicting the energetics of isomerization of proton-bound pairs.

4. Mass Spectrometry and *ab initio* theory were used to investigate ionic complexes formed between NO and benzene, pyridine, furan, thiophene and benzonitrile. Evidence was found for the participation of excited states in the dissociation of these ionic complexes.[4]

[1] J. A. D. Grabowy and P. M. Mayer, "Entropy changes in the dissociation of proton-bound complexes: A variational RRKM study", J. Phys. Chem. A., (2004), 108 (45) 9726-9732.

[2] J. A. D. Grabowy and P. M. Mayer, "$\Delta(\Delta S^{\ddagger})$ and $\Delta(\Delta S)$ for the competing bond cleavage reactions in $(CH_3CN)(ROH)H^+$ (R = CH_3, C_2H_5, C_3H_7, $(CH_3)_2CH$)", J. Am. Soc. Mass Spectrom. (2005), manuscript currently under review.

[3] J. A. D. Grabowy and P. M. Mayer, "The development of an empirical model for predicting the energetics of the internal S_N2 reaction in proton-bound pairs", Can. J. Chem., (2005), accepted for publication.

[4] J. A. D. Grabowy and P. M. Mayer, "Evidence for the participation of excited electronic states in the unimolecular dissociation reactions of ionic complexes between NO and aromatic compounds", Eur. J. Mass Spectrom. (2004), 10(6), 899-907.

Appendix A:

Calculation of Density and Sum of States and Unimolecular Rate Constants
with the use of the Beyer-Swinehart scheme for Direct Count

```
*  This FORTRAN program was adapted from the BASIC version quoted in P.M. Mayer
and T. Baer, J. Am. Soc. Mass Spectrom. 1997, 8, 103-115.
*  by Paul M. Mayer (Chem Dept, U of Ottawa, Ottawa, Canada K1N 6N5)
*   25/7/97
*
* The variables:
* Eo   the activation energy
* MIN and IMIN are the minimum energy for which you want a k printed
* MAX and IMAX are the maximum energy for which you want a k calc and print
* NUM and INUM is the interval you want the k printed at
* Nfreq is the number of vibrational frequencies for both ion and ts
* w(100) is the array into which freqs are put
* p(32000) is the density of states vector in which densities are put
* N(32000) is the sum of states vector in which sums are put
* RATE(32000) is the rate constant vector into which k's are put
* LOGRATE(32000) is the vector into which is put log10(k)
* QMolc, QTs are the ion and ts partition functions at 600K
* UMolc, UTs are the ion and ts internal energies at 600K
*
* The constants:
*  H=3.3364E-11 is Planck's constant in cm-1 sec
*  Kb=1.3807E-23 in Boltzman's constant in J/K
*  Na=6.022E23 is Avogadro's number
*  HJ=6.6262E-34 is Planck's constant in Jsec
*  c=2.9979E10 is the speed of light in cm/sec
*  T is temperature in Kelvin
*
* STEP 1. Variable declaration:
*
      INTEGER IEo,Nfreq,IMIN,INCR,IMAX,ITMAX,J,I,T,v(100)
      REAL w(100),LOGRATE(32000)
      DOUBLE PRECISION p(32000)
      DOUBLE PRECISION N(32000)
      DOUBLE PRECISION RATE(32000)
      REAL Eo,MAX,MIN,NUM,QMolc,UMolc,QTs,UTs,Sts
      REAL H,Kb,Na,HJ,c,Sigma,B
      CHARACTER Title*80,Name*6
*
* STEP 2. Reading in the stuff
*
```

```
      WRITE (*,'("input file name")')
      READ (*,'(a6)') Name
      OPEN (UNIT=8, FILE=Name, STATUS='OLD')
      READ (8,'(a80)') Title
      READ (8,*) Eo,MIN,MAX,NUM,Sigma
      READ (8,*) Nfreq
      READ (8,*) (w(I),I=1,Nfreq)
      READ (8,*) B
*
* STEP 3. Converting input energies to integral wavenumbers
*
      Eo=Eo*8065.5          !converting to cm-1
      IEo=NINT(Eo)          ! converting to an integer
      MAX=MAX*8065.5        ! converting to cm-1
      IMAX=NINT(MAX)        ! converting to an integer
      ITMAX=IMAX-IEo        ! defining transition state maximum energy
      MIN=MIN*8065.5
      IMIN=NINT(MIN)
*
*       Converting input frequencies to integers
*
      DO 20 J=1,Nfreq,1
      v(J)=NINT(w(J))
20    CONTINUE
*
*       Converting rotational constant (GHz) to wavenumbers
*
      Kb=1.3807E-23
      Na=6.022E23
      HJ=6.6262E-34
      c=2.9979E10
      T=600
*
      B=B*(1.0E9/c)
*
* STEP 4. Initializing p and N vectors
*
      DO 40 J=1,32000,1
        p(J)=SQRT(1/(B*J))    !(p with internal rotor densities)
        N(J)=0
40    CONTINUE
*
* STEP 5. Convoluting in the vibrational density of states
*
      DO 200 J=1,Nfreq,1
        DO 100 I=v(J),IMAX,1
```

```
        IF ((I-v(J)) .EQ. 0) THEN
          p(I)=p(I)+0
        ELSE
         p(I) = p(I) + p(I - v(J))
        END IF
100     CONTINUE
200   CONTINUE
*
* STEP 6. Calculating ion partition function and internal energy
*
    QMolc=1
    UMolc=0
    DO 250 I=1,Nfreq,1
      QMolc=QMolc*(1/(1-EXP(-w(I)/417.0)))     !calcing molc partion fcn
      UMolc=UMolc + (w(I)/(EXP(w(I)/417.0)-1)) ! calcing molc int nrg
250   CONTINUE
*
* STEP 7. Calculating sum of states of transition state
*
    READ (8,*) Nfreq
    READ (8,*) (w(I),I=1,Nfreq)
    READ (8,*) B
*
* making TS frequencies integers
*
   DO 270 J=1,Nfreq,1
    v(J)=NINT(w(J))
270   CONTINUE
*
* converting rotational constant to wavenumbers from GHz
*
      B=B*(1.0E9/c)
*
* STEP 7a. Adding to N vector the internal rotor sums
*
    DO 285 J=1,32000,1
      N(J)=N(J)+2*SQRT(J/B)
285   CONTINUE
*
* STEP 7c.  Convoluting in the vibrational sums
*
    DO 400 J=1,Nfreq,1
      DO 300 I=v(J),ITMAX,1
        N(I) = N(I) + N(I-v(J))
300     CONTINUE
400   CONTINUE
```

```
*
* STEP 8. Calculating ts partition function and internal energy at 600K
*
    QTs=1
    UTs=0
    DO 450 I=1,Nfreq,1
      QTs=QTs*(1/(1-EXP(-w(I)/417.0)))     !calcing molc partion fcn
      UTs=UTs + (w(I)/(EXP(w(I)/417.0)-1)) ! calcing molc int nrg
450   CONTINUE
*
* STEP 9. Calculating rate constant at specific intervals
*
    H=3.3364E-11
    DO 500 J=1,ITMAX,1
    RATE(J)=(Sigma*N(J))/(H*p(J+IEo))
    LOGRATE(J) = LOG10(RATE(J))
500   CONTINUE
*
* STEP 10. Calculating entropy of activation at 600K
*
    Sts= ((Kb*LOG(Qts/QMolc)) + (HJ*c*(UTs-UMolc))/T)*Na
*
* STEP 8. Printing it off
*
    PRINT '("RRKM k(E) vs E using the Direct Count method")'
    PRINT 550, Title
550   FORMAT (1X,A80)
    PRINT 560, Sts
560   FORMAT ('entropy of activation (J/K/mol) at 600K is', 1PG15.7E2)
    PRINT 600
600   FORMAT (' E        RATE        Log10RATE      p          N')
*
    INCR=INT((IMAX-IMIN)/(NUM-1))
    DO 800 J=IMIN-IEo,IMAX-IEo,INCR
    PRINT 700, (J+IEo)/8065.5, RATE(J), LOGRATE(J),  p(J+IEo),  N(J)
700   FORMAT (1PG10.4E2,E15.7E2,1PG13.4E2,E20.7E3,E20.7E3)
800   CONTINUE
    END
```

Appendix B: Archive Entries for Calculations

Part 1: Archive entries for the proton-bound pairs, TS_a, IC and TS_b that were used in the formulation of the empirical formulae described in Chapter 3.

$(CH_3CN)(CH_3OH)H^+$ proton-bound pair

1,1\N,-0.5658819691,-0.177910282,0.0188851984\H,0.8843799421,-0.438307408,-0.0398325175\O,1.9424189504,-0.6155037716,-0.1135423189\H,2.2134112001,-1.3103640731,0.5251312041\C,2.7579484141,0.6202818852,0.026607492\H,2.3877364719,1.2884296776,-0.7457339292\H,3.7867903177,0.3294496722,-0.1681746286\H,2.6222151303,1.0311399349,1.0252894915\C,-1.7286445754,-0.0236518402,0.0080946175\C,-3.1740470714,0.1715785721,-0.0022586806\H,-3.4048437852,1.2022548879,0.2767658831\H,-3.6387418198,-0.5121414768,0.7119562131\H,-3.560658809,-0.0303107711,-1.0039201282\\Version=x86-Linux-G98RevA.7\HF=-247.313759\MP2=-248.0507656\

Zero-point correction = 0.111511 (Hartree/Particle)

Frequencies	2.0096	70.7605	84.4840
Frequencies	136.4390	155.6945	275.0719
Frequencies	348.3434	350.9847	547.9922
Frequencies	934.6174	962.3947	1021.3864
Frequencies	1073.7754	1075.4559	1163.4303
Frequencies	1229.2179	1367.0491	1455.9391
Frequencies	1502.1124	1502.2861	1504.5827
Frequencies	1537.5978	1541.5221	1764.9451
Frequencies	2059.0626	2284.2609	3119.4512
Frequencies	3161.8047	3221.7866	3222.1494
Frequencies	3289.3176	3303.6146	3677.9497

TS_a for the $(CH_3CN)(CH_3OH)H^+$ system

1,1\X\X,1,1.\O,2,0.7435,1,90.\N,2,nx,3,a,1,d1,0\C,2,cx,1,90.,3,180.,0\X,4,1.,2,90.,5, 0.,0\C,4,cn,6,cnx,2,cnxx,0\X,7,1.,4,90.,6,0.,0\C,7,cc,8,ccx,4,ccxn,0\H,9,hc,7,hcc,8,hccx,0\H,9,hc2,7,hcc2,10,hcch,0\H,9,hc3,7,hcc3,10,hcch1,0\H,3,oh1,2,ohx,1,ohxx,0\H,3,oh2,2,ohx2,1,ohxx2,0\H,5,ch,2,chx,1,chxx,0\H,5,ch2,2,chx2,15,chxh,0\H,5,ch3,2,chx3,15,chxh1,0\\cx=0.79043854\cnx=87.56902439\cnxx=179.99998499\ccx=89.86630647\ccxn=179.99936397\hccx=1.47927351\d1=-105.44015271\a=150.08427886\cn=1.17977078\cc=1.46262044\hc=1.09217159\hc2=1.09215587\oh1=0.98621953\oh2=0.98621952\ch=1.0857034\ch2=1.0857033\hcc=109.79480377\hcc2=109.81524768\ohx=112.6140149\ohx2=112.61395969\chx=103.75271895\chx2=103.75268931\hcch=119.99280194\hcch1=-119.99337311\ohxx=44.0803922\ohxx2=-193.205847\chxx=15.90601299\chxh=117.31377349\chxh1=-121.34325933\nx=3.75237669\hc3=1.09215532\hcc3=109.81507426\ch3=1.08542701\chx3=109.14641918\\Version=x86-Linux-G98RevA.7\HF=-247.2862028\MP2=-248.0177708\

Zero-point correction = 0.111675 (Hartree/Particle)

Frequencies	-98.9071	1.7070	40.9814
Frequencies	52.2114	65.2933	125.4668
Frequencies	259.9751	347.5279	349.2236

Frequencies	787.7621	813.8586	938.4634
Frequencies	952.4544	1078.8610	1079.6053
Frequencies	172.1231	1310.7725	1461.2702
Frequencies	1493.5176	1514.1299	1514.3474
Frequencies	1520.1246	1531.4075	1735.5831
Frequencies	2226.6713	3121.2107	3176.0796
Frequencies	3219.7482	3219.8264	3324.1850
Frequencies	3330.0876	3579.0048	3675.9712

IC for the $(CH_3CN)(CH_3OH)H^+$ system

1,1\C,1.835580457,-0.070217161,-0.0209379439\H,1.4326350113,-0.5051376733,0.8864401555\H,
1.4356013739,-0.49490124,-0.9334959282\H,1.8349532289,1.0136954193,-0.0301149158\N,-0.81
95802091,0.403868505,0.0364469767\C,-1.9926116588,0.2827665231,0.0194286712\C,-3.4446806
223,0.1120706724,-0.0020238453\H,-3.6862019186,-0.9503313297,-0.0806957957\H,-3.87921795
05,0.5110272342,0.9169703653\H,-3.8685471358,0.6400979277,-0.8587759449\O,3.3405691991,-
0.437293856,-0.0841455839\H,3.8586082211,-0.0815645415,0.6751573387\H,3.4949479849,-1.40
93346909,-0.1362507324\\Version=x86-Linux-G98RevA.7\HF=-247.2876739\MP2=-248.0196048\

Zero-point correction = 0.112022 (Hartree/Particle)

Frequencies --	11.2248	44.7225	49.3396
Frequencies --	121.6311	142.9075	153.9181
Frequencies --	265.5978	344.3183	348.6142
Frequencies --	733.2741	784.8913	939.3552
Frequencies --	944.6107	1078.1026	1079.2885
Frequencies --	1186.7509	1294.2241	1454.7985
Frequencies --	1460.8456	1503.4319	1505.7324
Frequencies --	1512.9859	1514.0406	1731.2247
Frequencies --	2229.7498	3121.4136	3195.1294
Frequencies --	3218.8665	3221.9828	3350.8024
Frequencies --	3356.8775	3585.1941	3686.2139

TS_b for the $(CH_3CN)(CH_3OH)H^+$ system

1,1\C\H,1,R2\H,1,R3,2,A3\H,1,R4,2,A4,3,D4,0\O,1,R5,2,A5,3,D5,0\H,5,R6,1,A6,2,D6,0\H,5,R7,1,
A7,6,D7,0\N,1,R8,2,A8,3,D8,0\C,8,R9,1,179.8,2,D9,0\C,9,R10,8,179.26,1,D10,0\H,10,R11,9,A11,8
,D11,0\H,10,R12,9,A12,11,D12,0\H,10,R13,9,A13,11,D13,0\\R2=1.07763549\R3=1.07792307\R4=
1.07792287\R6=0.97924891\R7=0.97924869\R9=1.17516397\R10=1.46046471\R11=1.09236047\R
12=1.09232593\R13=1.09232338\A3=120.25840164\A4=120.25760519\A5=95.35225303\A6=116.
55209372\A7=116.55365212\A8=87.23230933\A11=109.45808841\A12=109.57769252\A13=109.5
942178\D4=171.28250788\D5=-94.35852041\D6=-63.8487392\D7=127.68249173\D8=85.6380568
9\D9=-175.10325997\D10=1.41035024\D11=-7.12054956\D12=119.97825146\D13=-119.98411615
\R5=1.89532332\R8=2.07399567\\Version=x86-Linux-G98RevA.7\HF=-247.2766636\MP2=-248.0
083692\

Frequencies --	-504.3133	7.2904	60.3912
Frequencies --	62.0226	164.3627	255.8180
Frequencies --	275.4024	284.9564	345.0976
Frequencies --	346.5301	537.9229	718.6289
Frequencies --	936.7643	1074.2800	1074.6428

Frequencies --	1146.9708	1177.9479	1328.7871
Frequencies --	1448.6172	1450.3951	1457.3548
Frequencies --	1505.1943	1505.6588	1706.2728
Frequencies --	2262.9058	3120.2806	3221.9799
Frequencies --	3221.9954	3228.2005	3439.4694
Frequencies --	3443.0398	3660.2523	3786.1407

Zero-point correction = 0.109934 (Hartree/Particle)

$(CH_3CN)(CH_3CH_2OH)H^+$ proton-bound pair

1,1\N,0.5792081431,1.132903371,-0.3513919253\C,1.0207140737,2.2202234887,-0.3315607638\C,
1.564397375,3.5739237649,-0.3058639788\H,0.1037316555,-0.3088184982,-0.4058845182\O,-0.2
112240564,-1.3211261946,-0.4239237493\H,-0.6550404537,-1.5130522553,-1.2798023778\C,-1.08
99652382,-1.6918451774,0.7446861452\C,-1.463949945,-3.143525983,0.6117200105\H,2.5988339
41,3.5441227732,0.0441007686\H,0.9694858784,4.1937943685,0.3687622772\H,1.5334162451,3.9
980780846,-1.3121205246\H,-0.4478024202,-1.4884188968,1.5999049331\H,-1.9426432567,-1.01
12849331,0.7310258166\H,-2.056087113,-3.4273919753,1.4868114951\H,-0.5751095979,-3.77644
64263,0.5778920257\H,-2.0806270218,-3.3245528405,-0.2734449028\\Version=x86-Linux-G98
RevA.7\HF=-286.3588348\MP2=-287.2271223\

Zero-point correction = 0.140865 (Hartree/Particle)

Frequencies --	6.9200	38.3288	54.0294
Frequencies --	93.6091	132.9848	219.0728
Frequencies --	266.1445	347.8703	348.7799
Frequencies --	432.1307	542.9190	829.4480
Frequencies --	837.4250	953.4942	1007.0777
Frequencies --	1027.7500	1074.3221	1075.4611
Frequencies --	1130.2546	1226.9415	1296.2366
Frequencies --	1343.9991	1451.5107	1456.5963
Frequencies --	1480.1353	1503.4966	1503.6870
Frequencies --	1533.1925	1543.3034	1560.9076
Frequencies --	1764.0837	2272.7252	2288.5766
Frequencies --	3113.4043	3119.8564	3170.1441
Frequencies --	3200.5473	3221.7518	3221.7615
Frequencies --	3222.2354	3257.1592	3662.4426

TS_a for the $(CH_3CN)(CH_3CH_2OH)H^+$ system

1,1\X\X,1,1.\O,2,0.7435,1,90.\N,2,R1,3,A1,1,D1,0\C,2,R2,1,90.,3,180.,0\X,4,1.,2,90.,5,0.,0\C,4,R3,
6,A2,2,D2,0\X,7,1.,4,90.,6,0.,0\C,7,R4,8,A3,4,D3,0\H,9,R5,7,A4,8,D4,0\H,9,R6,7,A5,10,D5,0\H,9,
R7,7,A6,10,D6,0\H,3,R8,2,A7,1,D7,0\H,3,R9,2,A8,1,D8,0\H,5,R10,2,A9,1,D9,0\H,5,R11,2,A10,15,
D10,0\C,5,R12,2,A11,15,D11,0\H,17,R13,5,A12,3,D12,0\H,17,R14,5,A13,18,D13,0\H,17,R15,5,A1
4,18,D14,0\\D7=83.42968953\D8=-154.49117012\A2=91.65955951\D2=177.62246076\R7=1.0921
9157\A6=109.80715016\R12=1.49649046\A11=106.54660966\D11=119.97169384\R13=1.0917945
6\R14=1.09374272\R15=1.09430179\A12=111.95309169\D12=-59.23609312\A13=112.06920288\
D13=124.86114264\A14=106.43955078\D14=-118.66471515\R2=0.82336742\A3=89.88354551\D3
=179.98101168\D4=91.20786987\R3=1.18009818\R4=1.46272868\R5=1.09217385\R6=1.0921859
3\R8=0.986388\R9=0.98635801\R10=1.08819919\R11=1.08704568\A4=109.83763996\A5=109.81

458501\A7=112.9061445\A8=111.60757321\A9=101.06725914\A10=106.2914012\D5=120.006468
5\D6=-120.01743153\D9=-18.67227614\D10=-117.47467413\R1=3.78870057\D1=-147.34900218\
A1=149.87227157\\Version=x86-Linux-G98RevA.7\HF=-286.3335907\MP2=-287.1974471\

Zero-point correction = 0.140542 (Hartree/Particle)

Frequencies --	-67.9966	5.0990	42.1326
Frequencies --	51.5889	65.2020	115.5610
Frequencies --	201.1431	260.1754	348.2701
Frequencies --	348.6222	375.2413	686.5807
Frequencies --	783.6917	854.2117	937.5888
Frequencies --	948.4892	995.4153	1079.0860
Frequencies --	1079.2618	1180.6022	1236.1161
Frequencies --	1310.7588	1422.1714	1461.1371
Frequencies --	1466.9422	1514.2094	1514.4054
Frequencies --	1524.3900	1538.6677	1558.4925
Frequencies --	1717.5891	2223.7954	3113.8255
Frequencies --	3120.9777	3198.6396	3204.6126
Frequencies --	3219.3493	3219.5112	3223.2698
Frequencies --	3295.8989	3571.3783	3676.8913

IC for the $(CH_3CN)(CH_3CH_2OH)H^+$ system

1,1\C,1.6273544378,-0.1825707706,-0.0150635893\H,1.1919938826,-0.6096001756,0.8847209503\
H,1.1824111099,-0.5980069737,-0.9141312703\C,1.7810519098,1.3064378115,-0.0149925594\H,2
.282394509,1.6706606729,0.8863686407\H,2.3056862617,1.6556616646,-0.9065141692\H,0.7694
366982,1.7216725767,-0.0220096716\N,-1.2582418347,-0.1114536268,0.0443527347\C,-2.438056
146,-0.104658972,0.0241773438\C,-3.9005229446,-0.0965543433,-0.0004470962\H,-4.274974432
2,-1.1197156781,-0.0768164634\H,-4.2838292458,0.3574279332,0.915988032\H,-4.2531024205,0.
4784857332,-0.8594745988\O,3.0861205927,-0.7684517518,-0.0935900131\H,3.6699444563,-0.41
15449156,0.6163689306\H,3.1098037402,-1.7531737889,-0.0482940115\\Version=SGI-G94RevE.
2\HF=-286.3346016\MP2=-287.1984399\RMSD=2.262e-09\

Zero-point correction = 0.140772 (Hartree/Particle)

Frequencies --	12.8444	47.1359	49.4430
Frequencies --	97.5290	100.0088	114.6333
Frequencies --	208.8289	265.4844	345.8210
Frequencies --	347.6696	376.3926	657.7265
Frequencies --	769.8035	848.2321	936.5349
Frequencies --	944.1871	992.6239	1078.4999
Frequencies --	1078.9279	1173.4136	1232.2195
Frequencies --	1306.7036	1414.5791	1460.1261
Frequencies --	1461.9266	1513.9958	1514.1274
Frequencies --	1531.8491	1535.6519	1544.2498
Frequencies --	1714.9412	2224.4453	3115.5081
Frequencies --	3120.8487	3207.5639	3214.9331
Frequencies --	3219.2965	3219.4956	3224.9509
Frequencies --	3310.9156	3575.0451	3682.8205

TS_b for the $(CH_3CN)(EtOH)H^+$ system

1,1\C\H,1,R2\H,1,R3,2,A3\C,1,r4,2,a4,3,d4,0\O,1,R5,2,A5,3,D5,0\H,5,R6,1,A6,2,D6,0\H,5,R7,1,A7
,6,D7,0\N,1,R8,2,A8,3,D8,0\X,8,1.,1,90.,2,0.,0\C,8,R9,9,A9,1,D9,0\X,10,1.,8,90.,9,0.,0\C,10,R10,11
,A10,8,D10,0\H,12,R11,10,A11,11,D11,0\H,12,R12,10,A12,13,D12,0\H,12,R13,10,A13,13,D13,0\H
,4,r14,1,a14,2,d14,0\H,4,r15,1,a15,16,d15,0\H,4,r16,1,a16,16,d16,0\\r4=1.48791136\a4=122.473700
82\d4=175.79512091\r14=1.09336725\r15=1.0914193\r16=1.08998578\a14=108.99432613\a15=10
9.31055308\a16=112.21055512\d14=126.47079461\d15=116.02559076\d16=-122.63091821\R2=1.
07846476\R3=1.08071074\R6=0.97830625\R7=0.9784176\R9=1.17690002\R10=1.4609248\R11=1.
09233527\R12=1.09233761\R13=1.09234268\A3=117.41169942\A5=89.49577619\A6=117.930043
58\A7=117.93507195\A8=82.61324408\A11=109.59595091\A12=109.60602088\A13=109.6026045
5\D5=-86.55674317\D6=-69.71478704\D7=129.79489465\D8=80.7881031\D9=178.32622108\D10
=180.25442638\D11=-38.77341408\D12=119.99818153\D13=-119.98205274\R5=2.02736457\R8=
2.17894822\A9=88.65725847\A10=90.16303423\\Version=x86-Linux-G98RevA.7\HF=-286.32262
74\MP2=-287.1825178

Zero-point correction = 0.137862 (Hartree/Particle)

Frequencies --	-409.3408	9.1595	51.8258
Frequencies --	56.3082	87.4976	157.2736
Frequencies --	185.1775	218.3663	260.7082
Frequencies --	329.3148	338.4053	372.0499
Frequencies --	471.8797	616.4244	847.9324
Frequencies --	932.1015	1004.7472	1057.2980
Frequencies --	1074.5615	1075.6175	1077.0329
Frequencies --	1250.3330	1266.6553	1451.8986
Frequencies --	1457.6877	1506.7039	1506.9847
Frequencies --	1518.6351	1522.1013	1549.5523
Frequencies --	1701.6001	2248.5840	3120.1144
Frequencies --	3127.5525	3212.5350	3221.1523
Frequencies --	3221.2651	3243.3784	3284.2794
Frequencies --	3414.2827	3668.3771	3797.2271

$(CH_3CN)(CH_3CH_2CH_2OH)H^+$ proton-bound pair

1,1\H,-0.6819575983,-0.4353942827,0.229316881\O,0.1689924335,-1.0602215794,0.1653696766\
H,0.2757855174,-1.5562542585,1.0075104998\C,1.4304867879,-0.3098892267,-0.1851728492\H,
1.5429397891,0.4905158544,0.5493494804\H,1.2034691823,0.0981751428,-1.1696776027\C,2.58
43857703,-1.2809722198,-0.2002697779\H,2.7153636244,-1.7172563686,0.7979237879\H,2.3612
670371,-2.0939588518,-0.8981757812\C,3.869159755,-0.5580735632,-0.6161534703\H,4.7041951
349,-1.261662237,-0.6222736514\H,4.1173152767,0.249889482,0.0780878259\H,3.7788000818,-
0.1377006633,-1.6216969401\N,-1.9089770837,0.4713210576,0.2858488256\C,-2.8932585677,1.1
10823869,0.2859847967\C,-4.1149395368,1.9086233214,0.2914105078\H,-4.4976199457,1.98271
38158,1.3118932173\H,-3.8994104226,2.9093437907,-0.0898713082\H,-4.8642528113,1.43104071
81,-0.3440808432\\Version=x86-Linux-G98RevA.7\HF=-325.3952558\MP2=-326.3954055\

Zero-point correction = 0.170198 (Hartree/Particle)

Frequencies --	3.2437	34.8355	42.4309
Frequencies --	90.9794	117.2079	128.0272
Frequencies --	197.2850	238.1913	302.6854
Frequencies --	347.7629	348.2442	460.0194
Frequencies --	541.4112	791.2363	875.0206

Frequencies --	916.2337	946.7374	957.1660
Frequencies --	1026.6279	1074.0729	1075.9830
Frequencies --	1078.1678	1152.2464	1227.9461
Frequencies --	1275.8303	1321.4425	1355.2200
Frequencies --	1388.3863	1456.5375	1457.9513
Frequencies --	1479.0929	1503.8248	1504.0206
Frequencies --	1543.1815	1548.9225	1553.4543
Frequencies --	1560.3585	1762.4405	2275.1396
Frequencies --	2324.9158	3101.6431	3111.8247
Frequencies --	3120.0054	3157.7561	3168.0231
Frequencies --	3200.5200	3213.9343	3221.9234
Frequencies --	3222.2066	3246.3783	3659.4761

TS_a for the $(CH_3CN)(CH_3CH_2CH_2OH)H^+$ system

1,1\X\X,1,1.\O,2,0.7435,1,90.\N,2,R1,3,A1,1,D1,0\C,2,R2,1,90.,3,180.,0\X,4,1.,2,90.,5,0.,0\C,4,R3,
6,A2,2,D2,0\X,7,1.,4,90.,6,0.,0\C,7,R4,8,A3,4,D3,0\H,9,R5,7,A4,8,D4,0\H,9,R6,7,A5,10,D5,0\H,9,
R7,7,A6,10,D6,0\H,3,R8,2,A7,1,D7,0\H,3,R9,2,A8,1,D8,0\H,5,R10,2,A9,1,D9,0\H,5,R11,2,A10,15,
D10,0\C,5,R12,2,A11,15,D11,0\H,17,R13,5,A12,3,D12,0\H,17,R14,5,A13,18,D13,0\C,17,R15,5,A1
4,18,D14,0\H,20,R16,17,A15,5,D15,0\H,20,R17,17,A16,21,D16,0\H,20,R18,17,A17,21,D17,0\\R16
=1.09383476\R17=1.09222878\R18=1.0923903\A15=111.13711194\A16=109.25474561\A17=111.
33635263\D15=61.72164984\D16=119.19809568\D17=-121.06186505\R13=1.09455276\R14=1.09
691117\R15=1.53607364\A12=109.92275122\D12=-55.82145395\A13=110.18041683\D13=119.5
0176926\A14=108.69598176\D14=-120.70981702\D7=95.9975228\D8=-142.18216939\A2=93.419
83999\D2=175.64291935\R7=1.09219149\A6=109.84671412\R12=1.50061233\A11=106.97766985
\D11=120.25743866\R2=0.82334689\A3=89.97715395\D3=180.02255877\D4=107.50424069\R3=1
.18031931\R4=1.4628605\R5=1.09219348\R6=1.09218316\R8=0.98679237\R9=0.98635162\R10=1
.08838792\R11=1.08763567\A4=109.81709862\A5=109.83627478\A7=112.47877081\A8=111.657
35482\A9=101.34622783\A10=105.98450221\D5=120.00204603\D6=-119.99675954\D9=-31.359
3337\D10=-115.93543265\R1=3.72459633\D1=-110.02494536\A1=142.20650871\\Version=x86-
Linux-G98RevA.7\HF=-325.3697689\MP2=-326.3656496

Zero-point correction = 0.169829 (Hartree/Particle)

Frequencies --	-48.0643	4.4414	21.2767
Frequencies --	48.2250	51.7739	105.4626
Frequencies --	123.5103	196.3465	237.7114
Frequencies --	253.8195	347.0717	347.4485
Frequencies --	416.4281	728.5278	779.8155
Frequencies --	803.1736	910.1590	933.1186
Frequencies --	937.7850	1003.2776	1064.6698
Frequencies --	1078.7500	1079.0725	1189.4290
Frequencies --	1229.2812	1300.1218	1352.8372
Frequencies --	1371.8942	1445.3624	1461.1126
Frequencies --	1477.2524	1514.4763	1514.6419
Frequencies --	1533.6675	1541.4157	1545.2323
Frequencies --	1560.3869	1711.6968	2221.6921
Frequencies --	3103.4139	3115.4559	3120.8346
Frequencies --	3168.5086	3199.1493	3207.3559
Frequencies --	3217.7919	3219.1128	3219.1501
Frequencies --	3291.5253	3568.1132	3673.5430

IC for the $(CH_3CN)(CH_3CH_2CH_2OH)H^+$ system

1,1\C,-1.5459464798,-0.3546582981,-0.01993419\N,1.4860871561,-0.5318063896,-0.1016617123\
C,2.6638518386,-0.4919529378,-0.0340814723\C,4.1230016651,-0.4382368816,0.0551943039\H,
4.4839303703,0.5133878703,-0.3410908145\H,4.4331881201,-0.5317273515,1.0982830023\H,4.56
08084328,-1.2551260885,-0.5225552428\H,-0.9431604977,-0.6623392311,0.8302206085\H,-1.065
4921849,-0.62697824,-0.9581032372\O,-2.7868174918,-1.3039444192,0.1119363717\H,-2.547969
9197,-2.2575736546,0.0292103364\H,-3.4816331458,-1.0989819927,-0.5574444328\C,-2.0714328
302,1.0496618489,0.0510888211\H,-2.7576829881,1.2397906972,-0.7836667448\H,-2.6206860829
,1.1890602398,0.9873794839\C,-0.8945024716,2.0332252716,-0.0252324633\H,-0.2015586393,1.8
822445045,0.8052439848\H,-1.2773247422,3.0546549789,0.0262632479\H,-0.340319213,1.91955
43297,-0.9598091753\\Version=x86-Linux-G98RevA.7\HF=-325.3695799\MP2=-326.3656646\

Zero-point correction = 0.169975 (Hartree/Particle)

Frequencies --	3.3652	34.3799	46.0655
Frequencies --	53.6892	63.8956	104.2629
Frequencies --	132.2578	199.7245	239.5653
Frequencies --	252.6480	346.5292	347.1234
Frequencies --	416.8018	723.2246	773.2040
Frequencies --	799.6558	907.3526	933.0069
Frequencies --	937.1729	1000.4918	1066.8481
Frequencies --	1078.6360	1078.9825	1187.0717
Frequencies --	1228.5319	1295.6759	1353.1767
Frequencies --	1370.9955	1439.7969	1461.0379
Frequencies --	1476.7649	1514.4505	1514.8109
Frequencies --	1527.6660	1538.6215	1543.1649
Frequencies --	1559.0319	1710.0302	2221.1506
Frequencies --	3101.3539	3120.7333	3121.2129
Frequencies --	3168.6331	3201.6370	3216.6045
Frequencies --	3218.6781	3219.3329	3219.6147
Frequencies --	3297.3537	3568.9784	3675.5412

TS_b for the $(CH_3CN)(CH_3CH_2CH_2OH)H^+$ system

1,1\C\H,1,R2\H,1,R3,2,A3\C,1,r4,2,a4,3,d4,0\O,1,R5,2,A5,3,D5,0\H,5,R6,1,A6,2,D6,0\H,5,R7,1,A7
,6,D7,0\N,1,R8,2,A8,3,D8,0\X,8,1.,1,90.,2,0.,0\C,8,R9,9,A9,1,D9,0\X,10,1.,8,90.,9,0.,0\C,10,R10,11
,A10,8,D10,0\H,12,R11,10,A11,11,D11,0\H,12,R12,10,A12,13,D12,0\H,12,R13,10,A13,13,D13,0\H
,4,r14,1,a14,2,d14,0\H,4,r15,1,a15,16,d15,0\C,4,r16,1,a16,16,d16,0\H,18,r17,4,a17,1,d17,0\H,18,r18
,4,a18,19,d18,0\H,18,1.0938288,4,a19,19,d19,0\\r17=1.09475432\r18=1.09237205\a17=111.746044
69\a18=110.20497978\a19=110.87586092\d17=59.71162842\d18=119.57876303\d19=-120.910275
16\r16=1.52465333\a16=114.01611721\d16=-124.39282022\r4=1.48953271\a4=121.84525437\d4=
174.04091094\r14=1.09711405\r15=1.09440048\a14=106.87229817\a15=107.26378381\d14=121.4
0140426\d15=111.80361129\R2=1.08030362\R3=1.08184356\R6=0.97837212\R7=0.97873262\R9
=1.17728127\R10=1.4610405\R11=1.09233947\R12=1.09235216\R13=1.09235047\A3=117.41864
908\A5=89.57210489\A6=117.65125994\A7=117.35016517\A8=82.33745758\A11=109.60133721\
A12=109.63398469\A13=109.62150423\D5=-86.7791694 4\D6=-67.60576511\D7=128.64168783\D
8=80.9706743\D9=175.67658178\D10=180.41307878\D11=-9.31791847\D12=120.00847628\D13=
-119.99397224\R5=2.02120472\R8=2.19467236\A9=90.62844277\A10=89.92823322\\Version=x86
-Linux-G98RevA.7\HF=-325.3590361\MP2=-326.3519305

Zero-point correction = 0.167099 (Hartree/Particle)

Frequencies --	-397.7833	6.0719	46.7782
Frequencies --	55.6688	71.6775	130.1537
Frequencies --	172.5921	187.7118	212.9172
Frequencies --	246.5882	337.6641	342.2347
Frequencies --	381.0279	407.7558	483.6033
Frequencies --	620.2998	776.1621	906.1000
Frequencies --	935.4041	961.4676	1037.9701
Frequencies --	1074.5509	1076.4440	1086.7093
Frequencies --	1103.8149	1199.0041	1256.7217
Frequencies --	1316.5906	1418.9190	1457.6666
Frequencies --	1476.2778	1506.8782	1507.1643
Frequencies --	1507.4502	1522.5917	1545.4005
Frequencies --	1551.5319	1701.1647	2245.4821
Frequencies --	3106.1706	3115.5911	3119.9607
Frequencies --	3162.5726	3192.8806	3210.4791
Frequencies --	3220.7794	3220.9384	3267.8938
Frequencies --	3396.8196	3665.5203	3794.2672

$(CH_3CN)((CH_3)_2CHOH)H^+$ proton-bound pair

1,1\H,-0.2475864796,-0.5524912922,-0.3029933705\N,-1.6102273209,0.1800749488,-0.0857593806\C,-2.6554782933,0.7097907209,-0.0067487055\C,-3.9540093061,1.3677529874,0.0971138784\H,-4.1010496049,2.0226856388,-0.7647446115\H,-4.7440522975,0.6135859866,0.1183556497\H,-3.9921948107,1.959644889,1.0144067001\O,0.6611747572,-1.0537066861,-0.4481486546\H,0.5289116428,-2.0067211657,-0.2428053146\C,1.8005583938,-0.4633296369,0.3865933758\H,1.4168082556,-0.4355187014,1.4103113824\C,2.960834432,-1.414744718,0.2393540852\H,3.8039289336,-1.0272155626,0.8185195562\H,2.7293729525,-2.4110874846,0.6298158979\H,3.2679137017,-1.4915448924,-0.8068596982\C,2.0219184792,0.9169783657,-0.1771994409\H,2.8181607421,1.4007284976,0.3960904519\H,2.3325170459,0.8597293515,-1.2234132822\H,1.1265208732,1.5386472677,-0.0958576187\\Version=x86-Linux-G98RevA.7\HF=-325.4024427\MP2=-326.4050361\

Zero-point correction = 0.169692 (Hartree/Particle)

Frequencies --	6.3571	37.7692	49.5096
Frequencies --	94.6144	122.6368	208.9361
Frequencies --	231.7473	281.2352	348.2339
Frequencies --	349.8369	373.5297	411.5780
Frequencies --	476.2485	540.7085	748.7306
Frequencies --	927.4983	952.2805	971.2900
Frequencies --	974.6742	1011.3555	1074.8139
Frequencies --	1076.0388	1128.0442	1175.2224
Frequencies --	1246.3214	1309.1149	1386.9947
Frequencies --	1436.5278	1456.8916	1478.7123
Frequencies --	1479.2772	1504.4992	1504.7856
Frequencies --	1524.0460	1532.7400	1543.7165
Frequencies --	1551.4644	1770.9926	2269.9454
Frequencies --	2488.9614	3106.0660	3114.0461
Frequencies --	3119.9779	3158.6739	3196.2463
Frequencies --	3207.1872	3213.0665	3218.3293

Frequencies -- 3221.4986 3222.0552 3651.1581

TS_a for the $(CH_3CN)((CH_3)_2CHOH)H^+$ system

1,1\O\H,1,B1\H,1,B2,2,A1\C,1,B3,2,A2,3,D1,0\H,4,B4,1,A3,2,D2,0\C,4,B5,1,A4,2,D3,0\H,6,B6,4,A5,1,D4,0\H,6,B7,4,A6,1,D5,0\H,6,B8,4,A7,1,D6,0\C,4,B9,1,A8,6,D7,0\H,10,B10,4,A9,6,D8,0\H,10,B11,4,A10,6,D9,0\H,10,B12,4,A11,6,D10,0\N,1,B13,4,A12,6,D11,0\X,14,1.,4,A13,6,D12,0\C,14,B15,15,90.,4,D13,0\X,16,1.,14,90.,15,D14,0\C,16,B17,17,90.,14,D15,0\H,18,B18,16,A16,17,D16,0\H,18,B19,16,A17,19,D17,0\H,18,B20,16,A18,17,D18,0\\B15=1.18014107\B17=1.46283288\B18=1.09219883\B19=1.09218527\B20=1.09218266\A16=109.80556834\A17=109.82136901\A18=109.84981065\D13=-179.71281483\D14=-164.7702429\D15=-180.00144104\D16=-71.25969369\D17=119.98796549\D18=168.74661834\B1=0.986313\B2=0.986204\B3=1.59845\B4=1.089246\B5=1.500417\B6=1.09271\B7=1.094249\B8=1.094749\B9=1.499935\B10=1.094395\B11=1.094237\B12=1.092758\B13=4.432082\A1=107.827933\A2=111.706938\A3=104.016322\A4=104.132418\A5=111.577945\A6=112.387474\A7=107.033923\A8=104.131104\A9=106.962012\A10=112.285102\A11=111.594477\A12=32.039951\A13=80.717096\D1=123.350451\D2=-60.468422\D3=-179.470276\D4=-62.990851\D5=61.238437\D6=178.368945\D7=-122.741336\D8=67.751529\D9=-175.430655\D10=-51.10546\D11=-128.450232\D12=-52.754024\\Version=x86-Linux-G98RevA.7\HF= -325.3799608\MP2=-326.3779009\

Zero-point correction = 0.168690 (Hartree/Particle)

Frequencies --	-49.3105	3.8303	11.6654
Frequencies --	45.3738	51.6717	101.2420
Frequencies --	179.1128	235.0628	273.1391
Frequencies --	343.8018	345.2337	363.4945
Frequencies --	365.4979	452.0592	596.4130
Frequencies --	787.4428	910.7269	929.3158
Frequencies --	937.2973	980.9345	989.8364
Frequencies --	1078.2258	1078.9584	1107.5427
Frequencies --	1244.0678	1259.8371	1358.0132
Frequencies --	1438.3594	1461.0239	1472.5234
Frequencies --	1479.8983	1514.2780	1514.5241
Frequencies --	1516.0200	1530.4035	1535.0166
Frequencies --	1546.0703	1710.3114	2222.7636
Frequencies --	3106.9220	3109.0040	3120.8663
Frequencies --	3195.1280	3197.7609	3209.6562
Frequencies --	3214.1335	3219.1758	3219.2893
Frequencies --	3232.3964	3569.5848	3681.5985

IC for the $(CH_3CN)((CH_3)_2CHOH)H^+$ system

1,1\C,1.4979537396,0.005857724,-0.1131822404\N,-1.5497314458,-0.0429367071,-0.0410926263\C,-2.7288874068,-0.0209946893,-0.088772139\C,-4.1901920003,0.0062793782,-0.1471486848\H,-4.5994038028,0.1054724614,0.8606456904\H,-4.5208766398,0.853191467,-0.7523868839\H,-4.5603731227,-0.9190531779,-0.5939554916\H,0.7773452521,-0.0158265152,-0.9280385129\C,1.4986944155,-1.2443289721,0.7180102923\H,2.2906094175,-1.2309578738,1.4730940162\H,1.5765064651,-2.1502560337,0.1097319826\H,0.5332963623,-1.2809564504,1.2315012663\O,2.8566050901,0.0370419832,-0.9577711202\H,2.9992416382,-0.7968858345,-1.4644455067\H,3.6419967038,0.1717138365,-0.376479663\C,1.4980072152,1.3136033976,0.6215282858\H,2.2670886816,1.3446330848,1.4004929928\H,1.6149493895,2.1595264827,-0.0593198631\H,0.5214432751,1.4011186068

,1.106364236\\Version=x86-Linux-G98RevA.7\HF=-325.3794404\MP2=-326.3779265\

Zero-point correction = 0.168867 (Hartree/Particle)

Frequencies --	7.0139	42.9478	44.3866
Frequencies --	72.1478	86.9735	102.9372
Frequencies --	166.7976	236.3096	272.8700
Frequencies --	347.1432	348.5829	362.9768
Frequencies --	368.0202	444.4462	590.3463
Frequencies --	782.3521	903.7360	930.8622
Frequencies - -	938.0588	963.1923	979.3805
Frequencies --	1078.7349	1078.9305	1133.4238
Frequencies --	1225.4800	1263.3633	1349.6698
Frequencies --	1423.9814	1460.7913	1467.5177
Frequencies --	1468.6752	1513.9962	1514.2550
Frequencies --	1514.2580	1529.8829	1541.1396
Frequencies --	1544.7336	1714.3004	2221.6027
Frequencies --	3103.9053	3106.8895	3120.6780
Frequencies --	3197.8082	3199.2878	3205.6212
Frequencies --	3219.0226	3219.0805	3219.1107
Frequencies --	3245.3843	3569.3756	3681.5634

TS_b for the $(CH_3CN)((CH_3)_2CHOH)H^+$ system

1,1\C\H,1,R2\C,1,R3,2,A3\C,1,r4,2,a4,3,d4,0\O,1,R5,2,A5,3,D5,0\H,5,R6,1,A6,2,D6,0\H,5,R7,1,A7,
6,D7,0\N,1,R8,2,A8,3,D8,0\X,8,1.,1,90.,2,0.,0\C,8,R9,9,A9,1,D9,0\X,10,1.,8,90.,9,0.,0\C,10,R10,11,
A10,8,D10,0\H,12,1.0923,10,A11,11,D11,0\H,12,R12,10,A12,13,D12,0\H,12,R13,10,A13,13,D13,0
\H,4,r14,1,a14,2,d14,0\H,4,r15,1,a15,16,d15,0\H,4,r16,1,a16,16,d16,0\H,3,r17,1,a17,2,d17,0\H,3,r18
,1,a18,19,d18,0\H,3,r19,1,a19,19,d19,0\\r17=1.08877253\r18=1.09427648\r19=1.09751394\a17=112
.91854389\a18=109.49580718\a19=107.22073858\d17=9.50579205\d18=123.46671983\d19=-121.5
0796716\r16=1.08962439\a16=112.76024652\d16=-125.49891472\r4=1.4707637\a4=119.1696965\
d4=177.36392728\r14=1.09350542\r15=1.09768221\a14=110.42625973\a15=106.56544858\d14=14
4.06475702\d15=115.81997223\R2=1.0806923\R3=1.4712578\R6=0.9762067\R7=0.97639677\R9=
1.17913393\R10=1.46171821\R12=1.09229605\R13=1.0922962\A3=119.78763128\A5=81.746927
8\A6=123.89116678\A7=123.37356492\A8=74.86723157\A11=109.70194007\A12=109.72914051\
A13=109.69152838\D5=-92.82474486\D6=-85.59196589\D7=145.95247347\D8=85.24290299\D9=
179.05815253\D10=179.97605276\D11=-291.45947658\D12=120.01862416\D13=-119.98957531\
R5=2.27136716\R8=2.44966309\A9=87.02990111\A10=90.06253827\\Version=x86-Linux-G98Rev
A.7\HF=-325.3751263\MP2=-326.3628344

Zero-point correction = 0.163972 (Hartree/Particle)

Frequencies --	-202.1966	8.6102	45.6741
Frequencies --	47.1738	68.0039	122.2569
Frequencies --	133.5545	137.2564	163.3355
Frequencies --	181.4777	230.0664	325.2346
Frequencies --	339.2345	350.6501	358.7507
Frequencies --	417.3517	445.7429	823.0589
Frequencies --	879.8470	941.6388	956.4079
Frequencies --	972.2395	1076.4551	1076.6483
Frequencies --	1171.8714	1207.0045	1226.7676

Frequencies --	1400.0941	1424.8934	1459.0289
Frequencies --	1484.9236	1492.8498	1498.3364
Frequencies --	1509.8747	1509.9720	1538.0861
Frequencies --	1541.9306	1704.2960	2231.3987
Frequencies --	3099.6659	3103.5393	3120.2574
Frequencies --	3177.6392	3185.5223	3220.1380
Frequencies --	3220.1620	3241.9938	3249.4531
Frequencies --	3340.1117	3693.4233	3821.5663

$(CH_3CN)(n\text{-}BuOH)H^+$ proton-bound pair

1,1\C,0.8599988148,-4.0480779042,1.1663411499\H,1.2331650168,-3.8604575821,2.1757187075\H,1.6979456948,-4.2861382399,0.5071048164\H,0.1638240472,-4.889720581,1.1869177697\C,0.1727005712,-2.8601007191,0.6706367087\N,-0.3830617657,-1.9043288822,0.2750243192\H,-1.0845886473,-0.6748916413,-0.3379463243\O,-1.5692924671,0.1547326147,-0.7684484459\H,-2.4842048099,-0.1066788825,-1.015534025\C,-1.5581153809,1.366067254,0.139360631\H,-2.1419153845,2.1055534592,-0.4100656069\H,-2.0653573995,1.0737544745,1.0611741361\C,-0.1205467528,1.7763728136,0.3341370228\H,0.4279250612,0.9740097132,0.8442989682\H,-0.1447417314,2.6202999587,1.03714944\C,0.593382896,2.1923157639,-0.9522040247\H,0.6053778897,1.3564416231,-1.6612625797\H,0.0293845371,3.0035218702,-1.4300034069\C,2.023591116,2.6514984397,-0.6768909833\H,2.6142611792,1.8492883248,-0.2226088224\H,2.5212234912,2.9496115723,-1.6033253508\H,2.0374055672,3.5093931134,0.0025165846\\Version=x86-Linux-G98RevA.7\HF=-364.4297183\MP2=-365.5635009

Zero-point correction = 0.199532 (Hartree/Particle)

Frequencies --	4.0680	21.4811	54.0954
Frequencies --	80.0235	86.2051	130.0461
Frequencies --	158.8600	249.7685	254.7828
Frequencies --	282.3155	342.9955	348.7406
Frequencies --	351.8163	498.6313	537.3278
Frequencies --	753.6822	820.8015	858.2422
Frequencies --	916.4399	953.4771	994.2438
Frequencies --	1021.0420	1062.3116	1074.8238
Frequencies --	1076.0496	1100.3015	1159.2023
Frequencies --	1177.5398	1261.7802	1306.3811
Frequencies --	1340.2990	1365.7001	1372.8689
Frequencies --	1437.1264	1454.6739	1457.4971
Frequencies --	1472.3702	1503.9469	1504.2891
Frequencies --	1521.7593	1541.6058	1548.1420
Frequencies --	1548.9598	1555.1229	1768.4545
Frequencies --	2271.8497	2404.0701	3089.4510
Frequencies --	3097.5283	3101.1867	3119.7325
Frequencies --	3133.3767	3151.7361	3156.4111
Frequencies --	3186.3743	3199.4065	3221.4281
Frequencies --	3221.8920	3236.7928	3663.0129

TS_a for the $(CH_3CN)(nBuOH)H^+$ system

1,1\O\N,1,B5\C,1,B6,2,A5\C,2,B7,1,A6,3,D5,0\C,4,B8,3,A7,1,D6,0\H,5,B9,4,A8,3,D7,0\H,5,B10,4,A9,3,D8,0\H,5,B11,4,A10,3,D9,0\H,1,0.986792,2,A11,4,D10,0\H,1,B13,2,A12,4,D11,0\H,3,1.0883

88,1,A13,2,D12,0\H,3,1.087636,1,A14,2,D13,0\C,3,B16,1,A15,2,D14,0\H,13,1.094553,3,A16,1,D1
5,0\H,13,1.096911,3,A17,1,D16,0\C,13,B19,3,A18,1,D17,0\H,16,1.093834,13,A19,3,D18,0\H,16,1.
09239,13,A20,3,D19,0\C,16,B1,13,A1,3,D1,0\H,19,1.09469743,16,A2,13,D2,0\H,19,1.09335458,16
,A3,13,D3,0\H,19,1.0946345,16,A4,13,D4,0\\B8=1.46284258\B9=1.09224811\B10=1.09224775\B1
1=1.09226199\A7=176.7109369\A8=109.79740294\A9=109.87225042\A10=109.85028433\D6=12
6.87648712\D7=159.19860858\D8=-80.81427454\D9=39.19280924\B1=1.53451294\A1=109.5278
388\A2=111.25697191\A3=110.46474634\A4=111.33819812\D1=-179.38316814\D2=60.71451154
\D3=-179.69107837\D4=-60.03358138\D5=-155.171425\ D10=11.742023\D11=117.882134\D12=7
8.665621\D13=-37.269812\D14=-161.07695\D15=-55.821417\D16=63.680282\D17=-176.531245\
D18=61.721611\D19=-59.340315\A5=21.76186\A6=169.595096\A11=81.557999\A12=117.599237
\A13=101.34626\A14=105.984537\A15=106.977709\A16=109.922684\A17=110.180411\A18=108.
695999\A19=111.137152\A20=111.33635\B5=4.336133\B6=1.566847\B7=1.180319\B13=0.98635
1\B16=1.500613\B19=1.536073\\Version=x86-Linux-G98RevA.7\HF=-364.3987928\MP2=-365.52
96864\

IC for the $(CH_3CN)(n\text{-}BuOH)H^+$ system

1,1\C,-0.6859754835,0.5572248182,-1.3113935283\N,-0.7380519909,0.5246298046,1.7343046645\
C,-0.5764411442,0.520699467,2.9036307953\C,-0.3713629034,0.5210128024,4.3520669636\H,0.0
640984529,-0.4302347859,4.665707605\H,0.3052980562,1.332481578,4.6290258038\H,-1.326618
3243,0.6623339385,4.8622619383\H,-0.3257345194,1.3374589887,-0.6468191728\H,-1.51726833
35,0.015429891,-0.8626038993\O,-1.3150241678,1.4015959049,-2.476486714\H,-2.0734781686,
1.9573366424,-2.1779113778\H,-1.6221481633,0.8309226141,-3.2199678025\C,0.382078781,-0.2
975585538,-1.9260536509\H,-0.0518431775,-0.9785262016,-2.6707579634\H,1.1219966403,0.335
8922117,-2.427368538\C,1.0680442837,-1.1328314329,-0.8305689766\H,1.482345895,-0.4610170
901,-0.0716722381\H,0.3215670217,-1.757256629,-0.3270323264\C,2.1731949091,-2.007237517,-
1.4188684186\H,2.9475486174,-1.3976004993,-1.8943484231\H,2.6486893561,-2.6000095141,-0.
633209344\H,1.7748732704,-2.7002445182,-2.1664219181\\Version=x86-Linux-98RevA.7\HF=-36
4.4052298\MP2=-365.5338695\

Zero-point correction = 0.198983 (Hartree/Particle)

Frequencies --	3.3757	24.9580	36.7185
Frequencies --	47.6605	57.5571	103.0004
Frequencies --	107.0747	120.2390	164.0072
Frequencies --	211.7538	255.6721	345.6388
Frequencies --	346.4256	382.5693	404.2797
Frequencies --	714.2556	770.7625	772.4281
Frequencies --	835.9170	914.7500	937.1749
Frequencies --	965.2163	993.3860	1078.5093
Frequencies --	1079.1141	1080.1699	1096.7105
Frequencies --	1184.1538	1222.4721	1274.3294
Frequencies --	1326.6316	1341.5374	1362.3802
Frequencies --	1421.5958	1437.4944	1460.9509
Frequencies --	1472.0901	1514.5397	1514.9929
Frequencies --	1524.9346	1540.1836	1545.2466
Frequencies --	1547.3210	1557.7330	1707.8051
Frequencies --	2220.5018	3087.8900	3102.6391
Frequencies --	3112.6404	3120.6427	3152.5032
Frequencies --	3169.2070	3192.7685	3199.3864
Frequencies --	3200.7967	3218.4231	3219.3179

Frequencies -- 3297.4523 3568.1321 3675.2662

TS_b for the $(CH_3CN)(n\text{-}BuOH)H^+$ system

1,1\C\H,1,R2\H,1,R3,2,A3\C,1,r4,2,a4,3,d4,0\O,1,R5,2,A5,3,D5,0\H,5,R6,1,A6,2,D6,0\H,5,R7,1,A7
,6,D7,0\N,1,R8,2,A8,3,D8,0\X,8,1.,1,90.,2,0.,0\C,8,R9,9,A9,1,D9,0\X,10,1.,8,90.,9,0.,0\C,10,R10,11
,a10,8,D10,0\H,12,1.09235439,10,A11,11,D11,0\H,12,1.09238121,10,A12,13,D12,0\H,12,1.092345
49,10,A13,13,D13,0\H,4,1.08522502,1,a14,2,d14,0\H,4,1.08524257,1,a15,16,d15,0\C,4,r16,1,a16,16
,d16,0\H,18,1.09559313,4,a17,1,d17,0\H,18,1.09511878,4,a18,19,d18,0\C,18,r19,4,a19,19,d19,0\H,
21,1.09335327,18,a20,19,d20,0\H,21,1.09455171,18,a21,19,d21,0\H,21,1.0946778,18,a22,19,d22,0\
\a10=90.09228776\A11=109.60113505\A12=109.62829953\A13=109.63374143\D10=180.2489010
1\D11=-52.99097639\D12=119.98345432\D13=-119.97182552\R5=2.03970783\R8=2.18462533\
A5=85.68490615\A8=82.87420589\D5=-89.02387974\D8=79.74036276\r19=1.52741942\a19=113.
4023105\a20=110.36065039\a21=112.32855508\a22=110.99891651\d19=-123.80012584\d20=58.7
1462846\d21=-60.86410001\d22=178.10875218\a17=109.18800492\a18=107.58193153\d17=57.20
12889\d18=115.05321929\r16=1.52938342\a16=114.57060587\d16=-124.25476583\r4=1.48964387
\a4=121.73700479\d4=176.69746744\a14=107.38618949\a15=107.06810082\d14=134.29944856\d1
5=112.20906761\R2=1.08049001\R3=1.08126521\R6=0.97817582\R7=0.97821265\R9=1.1771734
5\R10=1.46093912\A3=117.03354762\A6=119.04999626\A7=117.99591622\D6=-190.43267279\
D7=228.97372119\D9=179.14387663\A9=88.60273497\\Version=x86-Linux-G98RevA.7\HF=-36
4.3935019\MP2=-365.5193536\

Zero-point correction = 0.196231 (Hartree/Particle)

Frequencies --	-399.0419	5.2513	14.3751
Frequencies --	43.3849	65.9100	101.6491
Frequencies --	112.4885	173.1174	178.5981
Frequencies --	224.6533	261.6823	292.2992
Frequencies --	336.2489	340.5908	369.6649
Frequencies --	427.1387	469.7030	599.6993
Frequencies --	760.9932	827.0238	868.0411
Frequencies --	932.8154	982.2328	1027.2866
Frequencies --	1038.4114	1074.6797	1074.8500
Frequencies --	1085.3195	1124.4597	1180.4477
Frequencies --	1240.1030	1287.5661	1335.2519
Frequencies --	1398.7588	1416.8434	1457.3061
Frequencies --	1472.2720	1483.5628	1507.1171
Frequencies --	1507.2388	1518.9337	1540.8339
Frequencies --	1549.6353	1552.7272	1700.9018
Frequencies --	2245.9393	3099.6124	3115.9092
Frequencies --	3119.7296	3160.8714	3186.1256
Frequencies --	3195.4967	3212.4518	3220.4695
Frequencies --	3220.7058	3258.0919	3271.0500
Frequencies --	3397.3479	3670.0296	3799.6275

$(CH_3CN)(2\text{-}BuOH)H^+$ proton-bound pair

1,1\C,2.345001033,-3.3748275849,0.8378515793\H,1.8446229561,-3.6894343881,1.7565079174\
H,3.398716786,-3.1771644656,1.0474595692\H,2.2661471717,-4.1689809838,0.0918275507\C,1.7
131850627,-2.1625023829,0.3266901599\N,1.2080582016,-1.1836735204,-0.0820000392\H,0.506

7295392,0.0605160421,-0.745919281\O,0.0447384692,0.8671665739,-1.2219344544\H,0.7328641
71,1.3717205522,-1.7109702175\C,-0.7143426421,1.7712761756,-0.2449738372\H,-1.1656413518,
2.4992691842,-0.9244511122\C,0.2734906068,2.40571134,0.7051390256\H,-0.2666249337,3.0995
703319,1.3565113017\H,0.7566448176,1.6532461633,1.3347763229\H,1.0387999415,2.983080912
9,0.1767897173\C,-1.7680243906,0.8909689854,0.3888022261\H,-2.3122601381,1.5378134887,1.
0879547152\H,-1.2760526822,0.1256047338,1.0024663645\C,-2.7405297183,0.2616588091,-0.606
6070475\H,-3.2472263564,1.0285789261,-1.2005083919\H,-2.2368019061,-0.4244672258,-1.2925
32381\H,-3.5069128885,-0.3046832738,-0.0718488031\\Version=x86-Linux-98RevA.7\HF=-364.4
369527\MP2=-365.572877\

Zero-point correction = 0.198880 (Hartree/Particle)

Frequencies --	4.6705	26.8823	51.7193
Frequencies --	84.9356	114.1457	124.6281
Frequencies --	226.1588	234.2507	248.9068
Frequencies --	269.1239	349.5279	350.4151
Frequencies --	366.6210	455.4425	482.6939
Frequencies --	536.1838	731.5129	819.9996
Frequencies --	883.0487	951.1270	993.3886
Frequencies --	1007.9399	1032.5676	1074.2273
Frequencies --	1074.3370	1076.8020	1129.5809
Frequencies --	1187.9722	1209.6774	1276.4373
Frequencies --	1351.0100	1366.5278	1396.1850
Frequencies --	1456.6399	1458.5537	1472.5043
Frequencies --	1476.4204	1504.7737	1505.0758
Frequencies --	1522.2898	1534.7163	1539.3192
Frequencies --	1547.6068	1551.0247	1776.1941
Frequencies --	2266.7001	2543.5678	3099.5464
Frequencies --	3104.0294	3109.8245	3119.8029
Frequencies --	3148.0720	3168.3100	3194.3938
Frequencies --	3197.7132	3205.9195	3206.3427
Frequencies --	3221.2717	3221.6734	3657.1246

TS_a for the $(CH_3CN)(2\text{-}BuOH)H^+$ system

1,1\O\N,1,B2\C,1,B3,2,A3\C,2,B4,1,A4,3,D4,0\C,4,B5,2,178.226226,1,D5,0\H,5,1.09224979,4,A6,
2,D6,0\H,5,1.09221819,4,A7,2,D7,0\H,5,1.09221794,4,A8,2,D8,0\H,1,0.986913,2,A9,4,D9,0\H,1,0.
986474,2,A10,4,D10,0\H,3,1.087864,1,A11,2,D11,0\C,3,B12,1,A12,2,D12,0\H,12,B13,3,A13,1,D13
,0\C,3,B14,1,A14,2,D14,0\H,14,B15,3,A15,1,D15,0\H,14,B16,3,A16,1,D16,0\H,14,B17,3,A17,1,D1
7,0\H,12,B18,3,A18,1,D18,0\C,12,B19,3,A19,1,D19,0\H,19,1.09246341,12,A20,3,D20,0\H,19,1.09
865994,12,A21,3,D21,0\H,19,1.09475963,12,A22,3,D22,0\\B2=4.37308182\B3=1.59394618\B4=1.
18042259\A3=34.53895793\A4=171.94234716\D4=-155.86572759\A9=100.16632542\A10=84.81
094551\A11=103.75113448\D9=-42.06334838\D10=65.33402212\D11=17.87301247\B19=1.52953
285\A19=114.22252412\A20=109.95710056\A21=112.83207573\A22=111.12028404\D19=59.5942
706\D20=-190.23390839\D21=-72.89511174\D22=50.69252093\B5=1.46285839\D5=-5.11163626\
A6=109.99700162\D6=-149.46445259\A7=109.67200325\D7=-29.4547809\D8=90.47752831\A8=
109.81259518\D12=-99.46959922\B12=1.504685\A12=104.48768606\B13=1.09611723\A13=109.7
2309137\D13=-66.68306595\B14=1.50098276\A14=104.25927868\D14=137.22605215\B15=1.094
87549\A15=107.20719656\D15=181.42786635\B16=1.094434\A16=112.41320649\D16=-61.24751
417\B18=1.09684276\A18=104.4244335\D18=-181.16115793\B17=1.0926634\A17=111.49725812\
D17=62.72913432\\Version=x86-Linux-G98RevA.7\HF=-364.4153422\MP2=-365.5475881\

Zero-point correction = 0.198062 (Hartree/Particle)

Frequencies --	-42.0758	12.2373	31.2321
Frequencies --	44.5041	60.3967	102.2192
Frequencies --	122.0814	192.7123	237.3955
Frequencies --	252.5977	266.5963	344.1303
Frequencies --	347.9670	356.0049	430.8760
Frequencies --	472.4533	599.5497	790.9887
Frequencies --	815.5962	876.9810	937.1990
Frequencies --	961.6827	995.3765	1028.5885
Frequencies --	1071.2712	1078.5395	1078.9865
Frequencies --	1127.1475	1215.3760	1255.7143
Frequencies --	1317.1170	1361.9521	1384.0096
Frequencies --	1459.6873	1460.8797	1471.5420
Frequencies --	1482.6038	1508.5820	1513.6537
Frequencies --	1514.8550	1530.2143	1534.7052
Frequencies --	1543.7030	1563.9916	1697.6300
Frequencies --	2220.2910	3077.8078	3105.5300
Frequencies --	3110.3366	3120.5239	3157.6116
Frequencies --	3173.3554	3193.3427	3206.7088
Frequencies --	3211.6816	3218.5753	3219.1491
Frequencies --	3238.6026	3562.9138	3671.4011

IC for the $(CH_3CN)(2\text{-}BuOH)H^+$ system

1,1\C,-0.7464416216,-0.8126198351,-0.7928979034\H,-0.734606061,-0.7751822991,0.2955956085
\C,0.6334544084,-0.8563753784,-1.3928326564\O,-1.4258525128,-2.2415305904,-1.0023890067\C
,-1.7269815642,0.1518430435,-1.3930719251\H,0.5627959273,-0.9823419063,-2.4815417403\H,1.
0373928156,0.1473615193,-1.2183855128\H,-0.841775533,-2.9651615212,-0.6731081512\H,-1.60
37899808,-2.4150688372,-1.9570289769\H,-1.7680781671,0.0684702641,-2.4842299109\H,-2.725
9051163,0.0294684023,-0.9682579998\H,-1.3739420155,1.1569575045,-1.1441266436\N,0.344647
6436,1.2724428694,1.1454147122\C,0.6205389065,2.1070740405,1.933338948\C,0.9618420839,3.
1413455006,2.9098057598\H,1.2717929881,4.0518519905,2.3922495267\H,0.0928917164,3.36269
14735,3.5334537432\H,1.7796779675,2.7953707914,3.5456903537\C,1.5634658813,-1.893707881
4,-0.7655393989\H,1.2706417382,-2.9281249746,-0.989199765\H,2.5746862397,-1.7796620232,-
1.1628692584\H,1.6172355113,-1.7668426856,0.3201508512\\Version=x86-Linux-98RevA.7\HF=-
364.4153619\MP2=-365.5476196\

Zero-point correction = 0.197951 (Hartree/Particle)

Frequencies --	4.6039	30.4857	42.6389
Frequencies --	56.1320	74.4694	98.5743
Frequencies --	122.3624	164.5202	240.4331
Frequencies --	247.3135	252.8638	347.5982
Frequencies --	349.5010	356.7272	419.5274
Frequencies --	473.8684	594.3011	776.1928
Frequencies --	823.1372	873.4017	931.9368
Frequencies --	938.0602	997.6696	1025.6186
Frequencies --	1070.7692	1078.7787	1079.0263
Frequencies --	1141.2457	1223.4019	1241.8137
Frequencies --	1320.1277	1359.4276	1368.8692

Frequencies --	1455.6101	1460.8054	1471.5603
Frequencies --	1475.8419	1507.9955	1514.1987
Frequencies --	1514.2651	1528.5948	1535.8328
Frequencies --	1540.1840	1561.2205	1713.5841
Frequencies --	2220.1012	3082.1130	3096.4075
Frequencies --	3105.6039	3120.5381	3157.5132
Frequencies --	3173.2333	3196.9788	3207.7480
Frequencies --	3215.4851	3218.7237	3219.0579
Frequencies --	3231.1337	3565.5527	3675.0835

TS_b for the $(CH_3CN)(2\text{-}BuOH)H^+$ system

1,1\C\H,1,R2\C,1,r3,2,a3\C,1,r4,2,a4,3,d4,0\O,1,r5,2,a5,3,d5,0\H,5,r6,1,a6,2,d6,0\H,5,r7,1,a7,6,d7,0\
N,1,r8,2,a8,3,d8,0\X,8,1.,1,90.,2,0.,0\C,8,r9,9,a9,1,d9,0\X,10,1.,8,90.,9,0.,0\C,10,r10,11,a10,8,d10,0\
H,12,1.0923,10,a11,11,d11,0\H,12,1.09229605,10,a12,13,d12,0\H,12,1.0922962,10,a13,13,d13,0\H,
4,1.09454366,1,a14,2,d14,0\H,4,1.09715229,1,a15,16,d15,0\H,4,1.08954927,1,a16,16,d16,0\H,3,1.0
9980365,1,a17,2,d17,0\H,3,r18,1,a18,19,d18,0\C,3,r19,1,a19,19,d19,0\H,21,1.09131868,1,a20,19,d2
0,0\H,21,1.09136585,1,a21,19,d21,0\H,21,1.09220797,1,a22,19,d22,0\\R2=1.08179342\r3=1.47755
897\a3=118.85238635\r4=1.46872649\a4=118.19756556\d4=170.99621188\r5=2.18961002\a5=84.3
8863065\d5=-96.72252289\r6=0.97719902\a6=121.49929833\d6=-82.68493429\r7=0.97747088\a7
=120.75311062\d7=137.21717992\r8=2.58818653\a8=70.2446034\d8=82.25808738\r9=1.1798146\
a9=83.8344908\d9=180.52063223\r10=1.46207416\a10=90.13624589\d10=179.98906704\a11=109.
7490972\d11=-440.24700713\a12=109.75045171\d12=120.00395151\a13=109.76258479\d13=-120.
00195931\a14=111.4506086\d14=148.50381099\a15=105.64237588\d15=115.90561068\a16=112.6
7575934\d16=-126.25885845\a17=104.95673479\d17=-104.54444388\r18=1.09263151\a18=109.53
629995\d18=115.03140663\r19=1.53621637\a19=114.78512719\d19=-118.71933488\a20=94.66540
193\a21=93.67420907\a22=140.43035412\d20=-91.80110736\d21=-201.55201497\d22=33.389564
66\\Version=x86-Linux-G98RevA.7\HF=-364.4083921\MP2=-365.5309591

Zero-point correction = 0.193776 (Hartree/Particle)

Frequencies --	-200.6153	10.1402	43.3788
Frequencies --	47.1278	61.6765	93.1850
Frequencies --	126.6783	129.0524	135.3020
Frequencies --	190.8764	221.8446	242.3210
Frequencies --	283.2274	346.1742	350.7104
Frequencies --	354.7502	392.2770	492.7275
Frequencies --	521.9376	773.1235	820.2430
Frequencies --	863.3983	939.0848	988.3345
Frequencies --	1026.8421	1051.3739	1076.9028
Frequencies --	1077.2503	1159.5378	1180.7203
Frequencies --	1223.9686	1297.1423	1404.8104
Frequencies --	1413.9520	1454.5534	1459.6260
Frequencies --	1483.3122	1487.7626	1500.6519
Frequencies --	1511.1256	1511.2661	1536.6194
Frequencies --	1550.4794	1557.6714	1700.3936
Frequencies --	2225.9159	3088.4502	3102.0022
Frequencies --	3120.1284	3127.1001	3180.9160
Frequencies --	3181.9001	3219.0978	3219.4311
Frequencies --	3219.4820	3229.7027	3239.0660
Frequencies --	3323.5856	3678.8024	3808.8362

$(CH_3CH_2CN)(CH_3OH)H^+$ proton-bound pair

1,1\C,-1.1059920777,3.1702273548,0.2759100952\H,-1.7129225334,2.7504305313,1.0806412575\H,-0.1248322394,3.4389022753,0.6725714003\H,-1.5924833086,4.0790036848,-0.0846250275\C,-0.9785686023,2.1830326585,-0.8939883881\H,-1.9601747569,1.924060855,-1.3051102774\H,-0.3824162316,2.6064523244,-1.7094367549\C,-0.3338797352,0.9350903069,-0.4847727093\N,0.1858508649,-0.0562826274,-0.1309019012\H,0.838218408,-1.2566052149,0.3579519893\O,1.2995418022,-2.1594644398,0.7439471425\H,2.2651452698,-2.1492391182,0.567404791\C,0.6581499075,-3.4060148676,0.2519887381\H,0.7916903224,-3.481101242,-0.8256833771\H,1.1302614435,-4.2254965513,0.7875250406\H,-0.3880337988,-3.3107263499,0.5286707105\\Version=x86-Linux-G98RevA.7\HF=-286.3507578\MP2=-287.2197001\

Zero-point correction = 0.141004 (Hartree/Particle)

Frequencies --	6.7946	60.8393	75.1299
Frequencies --	128.8354	142.3157	210.6873
Frequencies --	221.9462	276.1098	379.1126
Frequencies --	544.2372	551.1428	804.6180
Frequencies --	868.3410	948.9985	1026.5371
Frequencies --	1043.0747	1118.7787	1139.0204
Frequencies --	1167.2640	1232.8967	1307.6318
Frequencies --	1359.9234	1373.1821	1473.7293
Frequencies --	1501.3008	1511.6237	1538.2300
Frequencies --	1541.6848	1543.4513	1548.5715
Frequencies --	1754.2418	1926.7924	2270.5127
Frequencies --	3119.3619	3124.9439	3160.8070
Frequencies --	3173.9762	3223.0413	3223.5351
Frequencies --	3287.4229	3302.0843	3680.8479

TS_a for the $(CH_3CH_2CN)(CH_3OH)H^+$ system

1,1\O,0.8450367747,3.986731313,0.8386466575\H,0.8450367747,3.986731313,1.8248446575\H,1.7818767363,3.986731313,0.5306112319\C,0.0312679656,2.826791016,0.2499392824\H,-0.9693043619,2.9903497485,0.6383336953\H,0.085694974,2.9913857478,-0.8218498863\H,0.4702154163,1.8862543629,0.5676385718\N,-0.1545104275,-0.2501052225,0.1790792167\C,-0.4097498668,-1.3973206685,0.063465763\C,-0.7108632976,-2.8230120377,-0.1042498287\H,-0.443582768,-3.3335835117,0.826839307\H,-1.7939926357,-2.9239322264,-0.2295296859\C,0.0372472543,-3.4319620965,-1.2967612727\H,1.1182827422,-3.3479704061,-1.1644855451\H,-0.2183137645,-4.490870118,-1.3808578857\H,-0.2420466511,-2.9351874497,-2.2286359019\\Version=x86-Linux-G98RevA.7\HF=-286.3221857\MP2=-287.18558\

Zero-point correction = 0.141456 (Hartree/Particle)

Frequencies --	-100.6634	3.3817	34.6773
Frequencies --	49.0073	59.5938	119.5268
Frequencies --	212.2352	223.5556	259.8096
Frequencies --	379.1734	540.6639	787.7168
Frequencies --	807.8576	813.5267	857.9976
Frequencies --	952.1524	1047.3818	1122.4403
Frequencies --	1140.1061	1171.3763	1310.6056
Frequencies --	1311.7339	1382.2241	1471.7286

Frequencies --	1492.9006	1519.7629	1522.2385
Frequencies --	1531.6065	1544.6656	1550.7139
Frequencies --	1735.5340	2211.3305	3117.4652
Frequencies --	3120.7795	3170.7443	3175.6975
Frequencies --	3214.6568	3215.8661	3324.1468
Frequencies --	3329.6240	3579.3430	3676.3596

IC for the $(CH_3CH_2CN)(CH_3OH)H^+$ system

1,1\C,-0.1719704665,-0.0979499858,-2.5386779135\N,-0.184359291,-0.2154219415,0.150075298\
C,0.2083817575,-0.078991684,1.2551770665\C,0.6972817721,0.1047782095,2.6257164684\H,1.40
60717751,-0.7026131596,2.8372018125\H,1.2599569351,1.0441167431,2.6490609904\H,0.614573
9885,-0.7944072641,-2.2746933426\H,-0.0338427584,0.9007860127,-2.1410859226\O,-0.0653353
856,-0.0023604613,-4.0821756497\H,0.8187348677,0.310346799,-4.3855927314\H,-0.7533446952
,0.5789684253,-4.4824035647\H,-1.1623447217,-0.5064323803,-2.3733347827\C,-0.4352502378,
0.1232969759,3.6590327001\H,-1.1450619575,0.9264742784,3.4493938317\H,-0.9726334564,-0.8
272719886,3.6694349574\H,-0.0095688067,0.2900687207,4.6514069351\\Version=x86-Linux-G98
RevA.7\HF=-286.3233218\MP2=-287.1871244\

Zero-point correction = 0.141805 (Hartree/Particle)

Frequencies --	8.2274	37.5924	43.7622
Frequencies --	117.9819	130.3375	148.4014
Frequencies --	221.9064	226.9268	266.1828
Frequencies --	376.8319	537.7147	733.0758
Frequencies --	785.7411	806.7690	856.7024
Frequencies --	944.2440	1050.9803	1123.3098
Frequencies --	1140.3044	1187.2667	1293.6023
Frequencies --	1313.6738	1383.2129	1454.0640
Frequencies --	1472.4365	1503.5214	1505.3698
Frequencies --	1521.1956	1544.3936	1550.3643
Frequencies --	1731.4443	2212.7578	3117.2653
Frequencies --	3120.8095	3169.4907	3195.0675
Frequencies --	3214.9526	3219.1749	3351.0041
Frequencies --	3355.9274	3585.0672	3685.9962

TS_b for the $(CH_3CH_2CN)(CH_3OH)H^+$ system

1,1\C\H,1,B1\H,1,1.077905,2,120.219\H,1,1.077924,2,120.22,3,170.418,0\O,1,1.887769,2,95.579,3,
-94.78,0\H,5,0.979351,1,116.312,2,-63.563,0\H,5,0.979356,1,116.3,6,127.199,0\N,1,2.08081,2,86.8
98,3,85.18,0\C,8,1.176548,1,179.8,2,-244.258,0\C,9,1.465235,8,179.26,1,-190.954,0\H,10,1.09518,
9,107.304,8,2.551,0\H,10,1.09515,9,107.43,11,115.231,0\C,10,1.535015,9,112.08,11,-122.346,0\H,
13,1.092033,10,111.097,12,180.857,0\H,13,1.092027,10,111.097,12,59.376,0\H,13,1.092188,10,108
.894,12,-59.881,0\\B1=1.077671\\Version=x86-Linux-G98RevA.7\HF=-286.3134519\MP2=-287.17
69846

Zero-point correction = 0.139749 (Hartree/Particle)

Frequencies --	-502.2408	3.3547	47.0153
Frequencies --	58.0182	166.9713	177.1357
Frequencies --	210.8659	257.2931	287.1408

Frequencies --	307.8656	374.5499	534.5331
Frequencies --	547.0432	724.5504	804.9367
Frequencies --	856.0584	1042.6599	1120.0831
Frequencies --	1138.5872	1148.4299	1179.3021
Frequencies --	1309.2728	1327.2702	1377.0151
Frequencies --	1448.5679	1450.5364	1473.5670
Frequencies --	1514.5399	1544.0487	1549.3267
Frequencies --	1706.4303	2245.3897	3119.0848
Frequencies --	3123.4062	3173.5696	3220.3238
Frequencies --	3220.9002	3228.0550	3439.1632
Frequencies --	3442.2672	3658.8836	3784.7243

$(ClCH_2CN)(CH_3CH_2OH)H^+$ proton-bound pair

1,1\N,-0.630525335,0.4644137517,0.2031634141\C,-0.4639045957,0.5099454137,1.3648453212\C,-0.2596607864,0.5666767785,2.8145329481\H,-0.8077701006,0.4156217819,-1.3575891986\O,-0.8952638833,0.389417426,-2.3984762044\H,-1.7189333254,-0.0881415062,-2.6451619368\C,0.3162810491,-0.2107465083,-3.078860321\C,0.0684682528,-0.2063006628,-4.5625561253\H,0.1081448851,1.5599794562,3.0818753501\H,-1.2141802552,0.3861613741,3.3142606071\H,1.1163514302,0.4600054977,-2.7707864665\H,0.4568828435,-1.2052842348,-2.6533078626\H,0.9651816428,-0.5885390224,-5.0595043857\H,-0.1211246935,0.805137735,-4.9269433991\H,-0.7625017658,-0.8619624479,-4.8383730049\Cl,0.9168608371,-0.6592155547,3.3172602997\\Version=x86-Linux-G98RevA.7\HF=-745.2388208\MP2=-746.2374623

Zero-point correction = 0.132770 (Hartree/Particle)

Frequencies --	9.1309	33.2480	40.7720
Frequencies --	87.0578	117.5995	166.0453
Frequencies --	228.8947	266.0286	323.7614
Frequencies --	426.7552	485.8230	532.7688
Frequencies --	792.5122	818.4675	837.3145
Frequencies --	948.3346	961.3206	993.7859
Frequencies --	1023.4293	1117.6038	1218.0637
Frequencies --	1235.2491	1290.3484	1341.0124
Frequencies --	1360.8544	1450.3379	1479.4724
Frequencies --	1499.3735	1532.4240	1543.1849
Frequencies --	1560.1732	1767.6347	2261.5713
Frequencies --	2540.7112	3113.5628	3147.9371
Frequencies --	3172.4988	3200.7763	3214.5755
Frequencies --	3222.2316	3260.0146	3656.6761

TS_a for the $(ClCH_2CN)(CH_3CH_2OH)H^+$ system

1,1\X\X,1,1.\O,2,0.7435,1,90.\N,2,R1,3,A1,1,D1,0\C,2,R2,1,90.,3,180.,0\X,4,1.,2,90.,5,0.,0\C,4,R3,6,A2,2,D2,0\X,7,1.,4,90.,6,0.,0\C,7,R4,8,A3,4,D3,0\H,9,R5,7,A4,8,D4,0\Cl,9,R6,7,A5,10,D5,0\H,9,R7,7,A6,10,D6,0\H,3,R8,2,A7,1,D7,0\H,3,R9,2,A8,1,D8,0\H,5,R10,2,A9,1,D9,0\H,5,R11,2,A10,15,D10,0\C,5,R12,2,A11,15,D11,0\H,17,R13,5,A12,3,D12,0\H,17,R14,5,A13,18,D13,0\H,17,R15,5,A14,18,D14,0\\R7=1.091746\A6=109.404\D3=179.845\D4=338.264\D5=120.156\D6=-119.688\R4=1.464584\R5=1.091758\R6=1.776723\A4=109.396\A5=110.738\R3=1.180524\A2=92.718\D2=188.089\R1=3.821362\D1=-148.22\A3=89.854\A1=150.355\D8=-154.668\R8=0.986532\A7=113.058\

D7=82.935\R12=1.496927\A11=106.545\D11=119.963\R13=1.091826\R14=1.093739\R15=1.0943
2\A12=111.868\D12=-58.906\A13=112.117\D13=124.797\A14=106.579\D14=-118.545\R9=0.986
503\R10=1.088228\R11=1.087141\A8=111.768\A9=101.11\A10=106.21\D9=-18.414\D10=-117.3
7\R2=0.821495\\Version=x86-Linux-G98RevA.7\HF=-745.2163784\MP2= -746.2111953\

Zero-point correction = 0.132092 (Hartree/Particle)

Frequencies --	-62.5170	2.7268	25.5876
Frequencies --	50.3096	62.3326	102.6101
Frequencies --	187.6351	202.8543	261.8972
Frequencies --	325.1314	376.0460	482.9686
Frequencies --	690.6924	781.2258	787.7885
Frequencies --	853.1514	949.9001	954.0905
Frequencies --	959.3854	995.4957	1180.5039
Frequencies --	1235.4709	1237.0139	1311.4071
Frequencies --	1363.5607	1424.1324	1467.3813
Frequencies --	1507.6275	1524.6835	1538.9300
Frequencies --	1558.0560	1717.6017	2213.3395
Frequencies --	3113.8874	3152.6576	3198.5475
Frequencies --	3204.6065	3218.1469	3223.0513
Frequencies --	3294.8465	3569.6325	3674.8422

IC for the $(ClCH_2CN)(CH_3CH_2OH)H^+$ system

1,1\C,-1.0296990956,2.4234849409,-0.9166469971\H,-1.0296990956,2.4234849409,0.1706340029
\H,-0.0209791237,2.4234849409,-1.3191466836\C,-1.967464513,1.450906848,-1.5622187328\H,-
2.982094297,1.5256995216,-1.160585789\H,-1.9810407624,1.5672872672,-2.64766807\H,-1.5926
347636,0.4509436702,-1.3261982204\N,0.6342785015,0.3401750578,0.2711783248\C,1.17926875
44,-0.6220950639,0.6840354273\C,1.8571637649,-1.8151465338,1.1960970222\H,2.7725830657,-
1.9848290484,0.625861679\H,2.1093921936,-1.6655826874,2.2477309438\O,-1.5300492972,3.852
260833,-1.3358496706\H,-2.4830244229,3.9915949075,-1.1233156938\H,-1.0098809025,4.581762
9705,-0.9235274981\Cl,0.8107182066,-3.2432976294,1.0492449472\\Version=x86-Linux-G98Rev
A.7\HF=-745.2171878\MP2=-746.2120706\

Zero-point correction = 0.132304 (Hartree/Particle)

Frequencies --	3.9484	25.9786	51.4074
Frequencies --	86.6194	94.4690	105.1463
Frequencies --	190.4531	210.3951	265.1279
Frequencies --	322.8510	377.6976	484.1725
Frequencies --	667.1611	770.0792	787.9569
Frequencies --	847.7790	945.4912	953.8575
Frequencies --	959.2914	993.1447	1174.2981
Frequencies --	1233.7521	1235.0156	1308.1720
Frequencies --	1363.2974	1418.4444	1462.6145
Frequencies --	1507.4363	1530.5873	1536.7070
Frequencies --	1544.2251	1715.2471	2213.8681
Frequencies --	3115.6593	3152.5783	3206.9129
Frequencies --	3211.6942	3218.1677	3224.7762
Frequencies --	3306.8982	3572.1340	3679.4158

TS_b for the $(ClCH_2CN)(EtOH)H^+$ system

1,1\C\H,1,B1\H,1,B2,2,A1\C,1,B3,2,A2,3,D1,0\O,1,B4,2,A3,3,D2,0\H,5,B5,1,A4,2,D3,0\H,5,B6,1,
A5,6,D4,0\N,1,B7,2,A6,3,D5,0\X,8,1.,1,90.,2,0.000001,0\C,8,B8,9,A7,1,D6,0\X,10,1.,8,90.,9,0.,0\C,
10,B9,11,A8,8,D7,0\Cl,12,B10,10,A9,11,D8,0\H,12,B11,10,A10,13,D9,0\H,12,B12,10,A11,13,D10,
0\H,4,B13,1,A12,2,D11,0\H,4,B14,1,A13,16,D12,0\H,4,B15,1,A14,16,D13,0\\B3=1.48665352\B8=
1.17712647\B9=1.46555351\B10=1.77296753\B11=1.09229602\B12=1.09227289\B13=1.09408703
\B14=1.09153313\B15=1.08971001\A2=122.5392556\A7=86.73079548\A8=90.31964962\A9=110.
31385487\A10=109.07036154\A11=109.07523563\A12=108.70015404\A13=109.58007894\A14=1
12.26795115\D1=176.61225596\D6=185.64465702\D7=-180.03940018\D8=435.25492674\D9=120
.28881673\D10=-120.28479743\D11=117.95166327\D12=115.72702883\D13=-122.11640081\B5=
0.97819392\A4=118.54313806\D3=-65.46287442\B1=1.07885536\B2=1.08100685\B4=2.05080021
\B6=0.97826267\B7=2.17086325\A1=117.29806472\A3=88.58735526\A5=118.58382206\A6=83.2
7872822\D2=-85.47852411\D4=131.10523054\D5=82.41508517\\Version=x86-Linux-G98RevA.7\
HF=-745.2030396\MP2=-746.193861\

Zero-point correction = 0.129267 (Hartree/Particle)

Frequencies --	-400.7830	5.7503	34.2641
Frequencies --	59.5185	86.7787	141.2210
Frequencies --	159.7143	185.7537	234.9515
Frequencies --	260.1395	318.5966	360.0469
Frequencies --	457.7104	479.4344	601.7451
Frequencies --	790.6407	847.5243	947.9355
Frequencies --	949.7276	996.0394	1052.6654
Frequencies --	1074.8732	1234.6826	1249.2920
Frequencies --	1266.3828	1361.0538	1451.6126
Frequencies --	1501.7578	1515.2351	1520.9900
Frequencies --	1550.0482	1702.5968	2238.5475
Frequencies --	3124.7574	3148.7128	3207.4787
Frequencies --	3215.1658	3245.9860	3281.7852
Frequencies --	3411.2384	3670.4338	3798.8187

$(ClCH_2CN)(CH_3CH_2CH_2OH)H^+$ proton-bound pair

1,1\H,0.1397844274,1.0160856958,0.871839118\O,0.0603998639,0.9940706151,1.9114171227\H,0
.9200498414,1.2592591872,2.3093014389\C,-0.3937928141,-0.3503409267,2.4398888312\H,0.289
6111918,-1.0990267998,2.0339392026\H,-1.3876072556,-0.4547618397,2.0057181979\C,-0.40708
38701,-0.2950442084,3.9463490123\H,0.607416653,-0.1094626618,4.3207081929\H,-1.045560495
3,0.5323083027,4.2713284625\C,-0.9260017379,-1.6220501772,4.5095568794\H,-0.930842342349
9,-1.5828345069,5.6007468098\H,-0.2927446774,-2.4610546639,4.2074559835\H,-1.9489353516,
-1.8199571443,4.1774587952\N,0.2218 488642,1.0185855875,-0.7044291304\C,0.2516028252,0.9
990953808,-1.8784347438\C,0.2919959326,0.9784432379,-3.3427984744\Cl,0.4834421031,-0.682
8951757,-3.9290755183\H,-0.6394332442,1.3986981478,-3.7290356016\H,1.1332825335,1.58668
03975,-3.6828788861\\Version=x86-Linux-G98RevA.7\HF=-784.2753287\MP2=-785.4058507\

Zero-point correction = 0.162093 (Hartree/Particle)

Frequencies --	8.4203	27.1841	36.2397
Frequencies --	81.4613	101.8622	127.7725
Frequencies --	160.7031	211.0156	237.9473

Frequencies --	302.0460	323.5665	452.1512
Frequencies --	487.7722	530.6994	791.7382
Frequencies --	792.5929	863.3411	914.5564
Frequencies --	946.1795	948.6055	962.9432
Frequencies --	1013.1690	1076.7335	1140.6344
Frequencies --	1221.1872	1235.3034	1269.4894
Frequencies --	1318.7339	1354.9520	1360.6223
Frequencies --	1386.9741	1456.1550	1479.1293
Frequencies --	1499.6415	1543.0390	1548.7314
Frequencies --	1553.1145	1560.0390	1764.9230
Frequencies --	2260.7020	2572.5700	3102.0512
Frequencies --	3112.5174	3148.1219	3159.9883
Frequencies --	3168.7965	3201.5517	3214.7123
Frequencies --	3214.7940	3249.3107	3653.9356

TS_a for the $(ClCH_2CN)(CH_3CH_2CH_2OH)H^+$

1,1\X\X,1,1.\O,2,0.7435,1,90.\N,2,R1,3,A1,1,D1,0\C,2,R2,1,90.,3,180.,0\X,4,1.,2,90.,5,0.,0\C,4,R3,6,A2,2,D2,0\X,7,1.,4,90.,6,0.,0\C,7,R4,8,A3,4,D3,0\H,9,R5,7,A4,8,D4,0\Cl,9,R6,7,A5,10,D5,0\H,9,R7,7,A6,10,D6,0\H,3,R8,2,A7,1,D7,0\H,3,R9,2,A8,1,D8,0\H,5,R10,2,A9,1,D9,0\H,5,R11,2,A10,15,D10,0\C,5,R12,2,A11,15,D11,0\H,17,R13,5,A12,3,D12,0\H,17,R14,5,A13,18,D13,0\C,17,R15,5,A14,18,D14,0\H,20,R16,17,A15,5,D15,0\H,20,1.09222878,17,A16,21,D16,0\H,20,1.0923903,17,A17,21,D17,0\\A2=103.11522753\D2=172.08075346\R7=1.09172846\A6=109.44047524\A3=89.8681525\D3=180.12320166\D4=80.81672067\R3=1.18070698\R4=1.46453615\R5=1.09172413\R6=1.77699897\A4=109.41945999\A5=110.74174623\D5=120.12497913\D6=-119.73825349\R1=3.76927918\D1=-104.75103583\A1=142.26979456\R16=1.09303522\A15=111.1625481\A16=109.23873042\A17=111.34254642\D15=61.74834763\D16=119.15250181\D17=-121.15123351\R13=1.09454087\R14=1.09686139\R15=1.53612522\A12=109.90393296\D12=-55.72760176\A13=110.16489507\D13=119.5041876\A14=108.69471855\D14=-120.70613304\D7=87.33981213\D8=-150.54434782\R12=1.50086782\A11=107.02651397\D11=120.15302405\R2=0.82174725\R8=0.98691295\R9=0.98647373\R10=1.08865178\R11=1.08786424\A7=112.72980268\A8=111.73083874\A9=101.34433388\A10=106.01805015\D9=-22.52547863\D10=-116.18879154\\Version=x86-Linux-G98RevA.7\HF=-784.2527411\MP2=-785.3795875\

Zero-point correction = 0.161398 (Hartree/Particle)

Frequencies --	-52.6718	5.6296	22.5082
Frequencies --	32.7017	53.0015	94.6025
Frequencies --	120.7186	187.2586	195.1089
Frequencies --	235.9984	253.4520	323.4112
Frequencies --	416.8799	483.1378	731.7120
Frequencies --	778.3382	787.4639	802.7505
Frequencies --	910.8025	934.0490	954.1969
Frequencies --	959.3628	1003.7347	1064.2926
Frequencies --	1189.9340	1229.4442	1235.0922
Frequencies --	1299.7288	1352.9839	1363.5147
Frequencies --	1371.7847	1444.2880	1476.7641
Frequencies --	1507.8276	1537.4780	1541.5954
Frequencies --	1545.2357	1560.2524	1712.0310
Frequencies --	2211.4395	3104.0888	3118.1609
Frequencies --	3152.8077	3169.2248	3196.0638

Frequencies -- 3211.7738 3217.8218 3218.3376
Frequencies -- 3288.6730 3566.5853 3671.6507

IC for the $(ClCH_2CN)(CH_3CH_2CH_2OH)H^+$ system

1,1\C\H,1,R2\H,1,R3,2,A3\C,1,R4,2,A4,3,D4,0\O,1,R5,2,A5,3,D5,0\H,4,R6,1,A6,2,D6,0\H,4,1.0965
3366,1,A7,6,D7,0\H,5,R8,1,A8,2,D8,0\H,5,R9,1,A9,8,D9,0\C,4,R10,1,A10,6,D10,0\H,10,R11,4,A1
1,1,D11,0\H,10,R12,4,A12,11,D12,0\H,10,R13,4,A13,11,D13,0\N,1,R14,2,A14,3,D14,0\C,14,R15,1
,A15,2,D15,0\C,15,R16,14,A16,1,D16,0\H,16,R17,15,A17,14,D17,0\H,16,R18,15,A18,17,D18,0\Cl,
16,R19,15,A19,17,D19,0\\R2=1.0883598\R3=1.087323\R4=1.50029588\R5=1.57288848\R6=1.098
59158\R8=0.98625351\R9=0.98602942\R10=1.52700443\R11=1.09223945\R12=1.09377257\R13=
1.09397207\R14=2.92271956\R15=1.18058838\R16=1.46455155\R17=1.09174976\R18=1.0917557
\R19=1.77679425\A3=111.79985406\A4=115.55581154\A5=105.27898169\A6=109.9387258\A7=1
04.17682158\A8=111.90335369\A9=112.94038459\A10=114.1838798\A11=109.88586181\A12=11
2.38886739\A13=110.80235154\A14=67.76961864\A15=169.21503326\A16=179.95329982\A17=1
09.41418857\A18=109.41009694\A19=110.67865666\D4=133.73790747\D5=-109.20337189\D6=
53.638436\D7=-112.8021114\D8=-66.97374486\D9=122.54027354\D10=126.48925387\D11=177.3
6639492\D12=119.69708323\D13=-119.04467504\D14=50.3009337\D15=123.02151903\D16=-15
9.53784866\D17=-86.17366352\D18=119.73928688\D19=-120.13053243\\Version=x86-Linux-G98
RevA.7\HF=-784.2533322\MP2=-785.3809541\

Zero-point correction = 0.161495 (Hartree/Particle)

Frequencies --	5.5991	20.9060	41.7397
Frequencies --	61.3715	87.2411	103.5298
Frequencies --	150.7794	190.4245	209.0832
Frequencies --	228.5513	322.0454	326.1847
Frequencies --	457.6846	484.3720	659.8498
Frequencies --	762.9281	787.6531	802.3179
Frequencies --	901.8678	936.9352	953.8963
Frequencies --	959.0221	987.3691	1070.1453
Frequencies --	1152.7846	1229.4491	1234.5809
Frequencies --	1274.6179	1326.2647	1363.2224
Frequencies --	1406.3738	1440.6150	1480.1252
Frequencies --	1507.4910	1518.4591	1529.6376
Frequencies --	1548.6030	1552.2487	1712.7988
Frequencies --	2212.5535	3094.2696	3111.1521
Frequencies --	3152.6234	3154.1873	3197.6219
Frequencies --	3198.7788	3211.3489	3218.2392
Frequencies --	3293.2810	3573.5214	3681.7094

TS_b for the $(ClCH_2CN)(CH_3CH_2CH_2OH)H^+$ system

1,1\C\H,1,B1\H,1,B2,2,A1\C,1,B3,2,A2,3,D1,0\O,1,B4,2,A3,3,D2,0\H,5,B5,1,A4,2,D3,0\H,5,B6,1,
A5,6,D4,0\N,1,B7,2,A6,3,D5,0\X,8,1.,1,90.,2,0.,0\C,8,B8,9,A7,1,D6,0\X,10,1.,8,90.,9,0.000001,0\C,
10,B9,11,A8,8,D7,0\H,12,B10,10,A9,11,D8,0\H,12,B11,10,A10,13,D9,0\Cl,12,B12,10,A11,13,D10,
0\H,4,B13,1,A12,2,D11,0\H,4,B14,1,A13,16,D12,0\C,4,B15,1,A14,16,D13,0\H,18,B16 ,4,A15,1,
D14,0\H,18,B17,4,A16,19,D15,0\H,18,1.093829,4,A17,19,D16,0\\B3=1.48762855\B8=1.17736899\
B9=1.46528955\B10=1.09224717\B11=1.09224081\B12=1.77357352\B13=1.09755008\B14=1.094
90323\B15=1.52486094\B16=1.09457987\B17=1.09232141\A2=121.97524973\A7=87.87729556\A
8=90.11636831\A9=109.16018228\A10=109.13700946\A11=110.18878868\A12=106.44719444\A1

3=107.47834889\A14=114.24727517\A15=111.64964656\A16=110.1137794\A17=111.06414201\D1=175.8181893\D6=185.42986875\D7=-179.61590705\D8=558.27060568\D9=119.54429507\D10=-120.23811096\D11=118.3537061\D12=111.49208441\D13=-124.11973992\D14=59.20377761\D15=119.52451926\D16=-121.04016134\B1=1.08070406\B2=1.08200185\B4=2.05210695\B5=0.97810111\B6=0.97840807\B7=2.18334909\A1=117.33665818\A3=88.61374911\A4=118.6189657 1\A5=118.2566939\A6=83.05994993\D2=-85.52863187\D3=-65.75987065\D4=130.64945954\D5=82.51584735\\Version=x86-Linux-G98RevA.7\HF=-784.239758\MP2=-785.3635739

Zero-point correction = 0.158385 (Hartree/Particle)

Frequencies --	-387.5044	8.4358	26.8998
Frequencies --	58.6958	73.0426	121.7571
Frequencies --	134.1972	169.2456	206.7572
Frequencies --	222.8824	240.8399	317.7824
Frequencies --	370.4601	405.0702	458.4449
Frequencies --	480.8090	597.6066	771.7322
Frequencies --	790.1009	904.8499	949.3047
Frequencies --	949.8494	960.5804	1025.3448
Frequencies --	1076.3484	1105.9749	1199.0277
Frequencies --	1233.5556	1253.6913	1315.0230
Frequencies --	1360.7717	1418.2577	1477.0291
Frequencies --	1501.7580	1503.1386	1523.5611
Frequencies --	1545.4147	1551.0787	1701.5855
Frequencies --	2236.4830	3106.9079	3112.3379
Frequencies --	3149.1061	3157.6786	3194.1093
Frequencies --	3210.9669	3215.6386	3266.2967
Frequencies --	3394.8451	3669.4873	3798.0115

$(ClCH_2CN)((CH_3)_2CHOH)H^+$ proton-bound pair

1,1\H,0.7099586672,0.6084128042,-1.1979528235\N,0.7548238188,0.6639538965,0.4103969574\C,0.7870927663,0.6282945839,1.5845656075\C,0.8273128308,0.5881313342,3.0485215371\H,1.7846565136,0.1686807718,3.3660947588\H,0.7296653565,1.605120774,3.435029774\Cl,-0.4957402858,-0.4137293267,3.6714996888\O,0.6686257456,0.5713005853,-2.2322200524\H,0.7758960867,1.4848208315,-2.5822933734\C,-0.628279883,-0.0729729768,-2.7465746397\H,-1.4313046326,0.4862378191,-2.2585690385\C,-0.6200561545,0.1242138365,-4.2406586809\H,-1.528696446,-0.323559623,-4.6535152795\H,-0.6257839335,1.1833678773,-4.5176526116\H,0.2435687319,-0.3705295922,-4.6923139251\C,-0.562036105,-1.5044410404,-2.2806546687\H,-1.4733073046,-2.0142607122,-2.6070465428\H,0.2978387769,-2.0141739006,-2.7223192331\H,-0.5118803811,-1.5781548783,-1.1911696295\\Version=x86-Linux-G98RevA.7\HF=-784.2826827\MP2=-785.415771\

Zero-point correction = 0.161473 (Hartree/Particle)

Frequencies --	10.2136	28.3880	38.4362
Frequencies --	93.4892	103.8764	164.8758
Frequencies --	222.1009	231.2176	280.6554
Frequencies --	324.0348	373.0595	409.6426
Frequencies --	469.1785	487.7241	529.8889
Frequencies --	736.1091	792.2462	924.7323
Frequencies --	949.0899	961.2167	966.9624
Frequencies --	975.0722	998.7410	1123.7313

Frequencies --	1159.0362	1235.0850	1246.0493
Frequencies --	1299.2087	1360.5173	1385.2820
Frequencies --	1436.1331	1478.6980	1479.1178
Frequencies --	1500.1455	1523.3956	1532.3137
Frequencies --	1543.1567	1551.1284	1770.9701
Frequencies --	2255.7121	2699.4202	3106.5303
Frequencies --	3113.8673	3148.4966	3161.1946
Frequencies --	3196.6453	3206.6438	3213.5325
Frequencies --	3215.2571	3218.7697	3647.6322

TS_a for the $(ClCH_2CN)((CH_3)_2CHOH)H^+$ system

1,1\O\C,1,R2\H,1,R3,2,A3\H,1,R4,2,A4,3,D4,0\H,2,R5,1,A5,3,D5,0\C,2,R6,1,A6,5,D6,0\C,2,R7,1,A7,5,D7,0\H,6,R8,2,A8,1,D8,0\H,6,R9,2,A9,8,D9,0\H,7,R10,2,A10,1,D10,0\H,7,R11,2,A11,10,D11,0\H,7,R12,2,A12,10,D12,0\H,6,R13,2,A13,8,D13,0\N,1,R14,2,A14,3,D14,0\C,14,R15,1,173.86,2,D15,0\C,15,R16,14,A16,1,D16,0\H,16,R17,15,A17,14,D17,0\Cl,16,R18,15,A18,17,D18,0\H,16,R19,15,A19,17,D19,0\\R15=1.18062483\R16=1.46452955\R17=1.09173985\R18=1.77708063\R19=1.09172794\A17=109.42872031\A18=110.65950222\A19=109.44840778\D15=318.58837266\D16=-232.28019643\D17=137.18722019\D18=120.11568026\D19=-119.76758224\A16=179.99701922\R7=1.50034729\R8=1.09270188\R9=1.09422574\R10=1.09452705\A7=104.14565836\A8=111.51538444\A9=112.39878142\A10=107.10162261\D7=118.36034251\D8=-62.84126546\D9=124.18495455\D10=-178.69760076\R2=1.59644204\R3=0.98642131\R4=0.98635345\R5=1.08937282\R6=1.50066527\R11=1.09423874\R12=1.0927778\R13=1.09482012\R14=4.43325735\A3=111.88449\A4=112.0337623\A5=103.94053453\A6=104.1553447\A11=112.32371505\A12=111.51356443\A13=107.12206283\A14=31.57624275\D4=121.31207018\D5=-60.81494952\D6=-118.94714642\D11=117.01283811\D12=-118.72775414\D13=-118.59259891\D14=51.42084109\\Version=x86-Linux-G98RevA.7\HF=-784.2626965\MP2=-785.3917893

Zero-point correction = 0.160275 (Hartree/Particle)

Frequencies --	-46.0044	3.9820	16.0847
Frequencies --	20.0101	53.6657	101.2173
Frequencies --	180.8171	181.4176	236.6979
Frequencies --	274.2503	320.7504	363.9921
Frequencies --	366.0322	452.8310	481.7502
Frequencies --	600.8552	784.5759	787.0695
Frequencies --	910.6739	930.5348	953.7613
Frequencies --	959.1612	980.4834	990.1500
Frequencies --	1107.9560	1233.9418	1243.8302
Frequencies --	1259.2142	1360.9516	1363.8099
Frequencies --	1438.7827	1473.0569	1480.1202
Frequencies --	1507.7508	1516.1072	1530.3530
Frequencies --	1535.5493	1546.2061	1710.2642
Frequencies --	2211.9737	3106.7715	3108.7611
Frequencies --	3152.8589	3194.8378	3197.3646
Frequencies --	3209.2823	3214.0047	3218.4910
Frequencies --	3232.1213	3567.9102	3679.7667

IC for the $(ClCH_2CN)((CH_3)_2CHOH)H^+$ system

1,1\O,2.8000884255,-2.2570353998,1.5447086642\H,2.8431301193,-2.326672527,2.5276245221

\H,3.723648704,-2.2939983831,1.2000887695\C,2.0410692146,-0.9374211994,1.0640552519\H,1.0420363434,-1.1583582152,1.4337551514\C,2.6768266565,0.2434020551,1.7393372169\C,2.129263285,-0.9939448279,-0.4329838744\H,3.7014062552,0.4093148073,1.3928431392\H,2.6595372797,0.1609840663,2.8300087612\H,2.078217578,1.1203520239,1.4724066417\H,3.1594831806,-0.8750055237,-0.7851038205\H,1.6990513346,-1.91615691,-0.8291488979\H,1.5468621109,-0.1529746824,-0.8199629524\N,-0.6744966892,0.4317241619,0.7213781579\C,-1.7037940741,0.6316271999,0.1782335138\C,-2.9783217575,0.8651432519,-0.5038327466\Cl,-2.7074770552,1.2682838283,-2.2135863754\H,-3.5899683475,-0.0375106898,-0.4457598831\H,-3.5057851461,1.690576141,-0.0219556382\\Version=x86-Linux-G98RevA.7\HF=-784.2613944\MP2=-785.3910888\

Zero-point correction = 0.160401 (Hartree/Particle)

Frequencies --	6.6793	21.3431	39.4157
Frequencies --	57.0829	70.3001	110.1021
Frequencies --	165.1285	187.5353	237.5809
Frequencies --	273.5561	324.7530	364.3424
Frequencies --	368.2020	445.1749	483.8677
Frequencies --	598.9471	780.0820	786.8749
Frequencies --	904.1977	933.2939	954.7668
Frequencies --	958.8850	965.4902	979.0054
Frequencies --	1133.9143	1227.2905	1235.0138
Frequencies --	1261.3688	1357.1753	1363.4991
Frequencies --	1425.5281	1468.5978	1471.1098
Frequencies --	1507.8676	1513.9437	1528.1533
Frequencies --	1539.8927	1544.1530	1713.6894
Frequencies --	2210.2853	3102.7028	3107.2399
Frequencies --	3152.2797	3196.9602	3199.3422
Frequencies --	3200.3707	3218.0537	3220.6183
Frequencies --	3245.5222	3567.4339	3679.3006

TS_b for the $(ClCH_2CN)((CH_3)_2CHOH)H^+$

1,1\C\H,1,B1\C,1,B2,2,A1\C,1,B3,2,A2,3,D1,0\O,1,B4,2,A3,3,D2,0\H,5,B5,1,A4,2,D3,0\H,5,B6,1,A5,6,D4,0\N,1,B7,2,A6,3,D5,0\X,8,1.,1,90.,2,0.,0\C,8,B8,9,A7,1,D6,0\X,10,1.,8,90.,9,0.,0\C,10,B9,11,A8,8,D7,0\H,12,1.0923,10,A9,11,D8,0\Cl,12,B10,10,A10,13,D9,0\H,12,B11,10,A11,13,D10,0\H,4,B12,1,A12,2,D11,0\H,4,B13,1,A13,16,D12,0\H,4,B14,1,A14,16,D13,0\H,3,B15,1,A15,2,D14,0\H,3,B16,1,A16,19,D15,0\H,3,B17,1,A17,19,D16,0\\B2=1.4655146\B3=1.46619901\B8=1.17954045\B9=1.46501248\B10=1.7748265\B11=1.09204395\B12=1.09361058\B13=1.09955018\B14=1.08938641\B15=1.0888785\B16=1.09379823\B17=1.10032959\A1=119.5922543\A2=118.88750677\A7=90.10068598\A8=90.07254936\A9=109.27830875\A10=110.43871465\A11=109.24817003\A12=110.90151819\A13=105.92144184\A14=112.78023317\A15=113.01013251\A16=110.68551394\A17=105.70086081\D1=178.78167177\D6=170.38777154\D7=179.85901057\D8=-226.7005631\D9=120.20972872\D10=-119.59322088\D11=146.91149868\D12=115.44424216\D13=-126.43734593\D14=16.74957763\D15=125.54544385\D16=-119.51595951\B1=1.08190925\B4=2.34454153\B5=0.97577052\B6=0.97597607\B7=2.48497201\A3=79.38593189\A4=125.8136837\A5=125.31927093\A6=75.66781263\D2=-92.76736823\D3=-103.01690969\D4=155.55968354\D5=85.15682926\\Version=x86-Linux-G98RevA.7\HF=-784.2572132\MP2=-785.3753062\

Zero-point correction = 0.154964 (Hartree/Particle)

Frequencies --	-139.5181	6.5219	28.4128

Frequencies --	48.5528	55.0614	113.7462
Frequencies --	116.6252	122.2239	149.6127
Frequencies --	173.7687	202.7553	228.3761
Frequencies --	301.8751	318.7571	342.5031
Frequencies --	402.0383	423.5570	483.8305
Frequencies --	780.4387	793.2232	842.4133
Frequencies --	952.0876	956.5442	966.2104
Frequencies --	974.9773	1159.7046	1219.9068
Frequencies --	1234.2261	1234.5627	1361.9487
Frequencies --	1396.9851	1414.5554	1477.0866
Frequencies --	1483.8201	1494.3046	1504.6086
Frequencies --	1537.5742	1548.2498	1707.0340
Frequencies --	2220.6119	3083.6853	3092.1052
Frequencies --	3149.3256	3172.0726	3178.2948
Frequencies --	3215.3060	3244.9710	3249.4971
Frequencies --	3330.2591	3700.0313	3826.4705

$(FCH_2CN)(CH_3OH)H^+$ proton-bound pair

1,1\N,-0.0098826155,-0.5100632672,-0.0443693111\H,1.5322563921,-0.6631862138,-0.190951541
1\O,2.5703063502,-0.7418996657,-0.3172212532\H,2.9582787429,-1.2446801807,0.4328957243\
C,3.2354989992,0.5802654713,-0.5155514637\H,2.7447967323,1.0096931785,-1.3841476045\H,4.
2792560055,0.3595005004,-0.7213132495\H,3.1012756506,1.1853583458,0.3787539346\C,-1.172
1321041,-0.379231919,0.049036395\C,-2.6330505347,-0.1808641615,0.1797374719\F,-2.8375642
652,1.1027409998,0.6627670915\H,-3.043519888,-0.9051853028,0.8871121493\H,-3.109435905,
-0.2815454743,-0.7982324523\\Version=x86-Linux-G98RevA.7\HF=-346.1440558\MP2=-347.053
1908\

Zero-point correction = 0.105243 (Hartree/Particle)

Frequencies --	12.3956	51.5609	82.6846
Frequencies --	135.2749	145.8438	198.1550
Frequencies --	275.8444	328.7512	537.7938
Frequencies --	573.5074	914.3129	934.2588
Frequencies --	1000.5491	1047.9067	1094.0777
Frequencies --	1138.4164	1218.7874	1274.2666
Frequencies --	1369.2748	1419.9929	1508.2283
Frequencies --	1532.5553	1535.4713	1539.7187
Frequencies --	1777.7984	2267.5960	2480.3605
Frequencies --	3147.1660	3164.3118	3219.6647
Frequencies --	3294.8460	3307.9427	3667.2125

TS_a for the $(FCH_2CN)(CH_3OH)H^+$ system

1,1\X\X,1,1.\O,2,0.7435,1,90.\N,2,R1,3,A1,1,D1,0\C,2,R2,1,90.,3,180.,0\X,4,1.,2,90.,5,0.,0\C,4,R3,
6,A2,2,D2,0\X,7,1.,4,90.,6,0.,0\C,7,R4,8,ccx,4,ccxn,0\H,9,R5,7,hcc,8,hccx,0\F,9,R6,7,hcf,10,hccf,0\
H,9,R7,7,hcc3,10,hcch1,0\H,3,R8,2,ohx,1,ohxx,0\H,3,R9,2,ohx2,1,ohxx2,0\H,5,R10,2,chx,1,chxx,0\
H,5,R11,2,chx2,15,chxh,0\H,5,R12,2,chx3,15,chxh1,0\\R3=1.17946726\R4=1.4753594\R5=1.09204
551\R6=1.39342353\A2=98.86835837\D2=180.82893446\ccx=90.66877876\ccxn=180.05663965\hc
cx=-302.6762709\hccf=118.84636662\hcch1=-122.30625862\hcc=110.27930294\hcf=108.22783012
\hcc3=110.27801042\D1=-104.3228396\A1=149.69731598\R1=3.80476698\R2=0.78793556\R8=0.

9864528\R9=0.98646274\R10=1.08574646\R11=1.08573298\ohx=112.8290612\ohx2=112.8191809
9\chx=103.82524469\chx2=103.82651765\ohxx=41.82076757\ohxx2=-195.02410118\chxx=17.946
89588\chxh=117.36216945\chxh1=-121.34322558\R7=1.09202468\R12=1.08522816\chx3=108.997
88083\\Version=x86-Linux-G98RevA.7\HF=-346.1202596\MP2=-347.0253276\

Zero-point correction = 0.104616 (Hartree/Particle)

Frequencies --	-90.3336	2.5418	34.0011
Frequencies --	37.0331	65.0119	111.9717
Frequencies --	212.5666	260.7040	326.3093
Frequencies --	565.7250	787.3102	817.3901
Frequencies --	931.2118	954.6168	1050.9215
Frequencies --	1081.5719	1176.1369	1276.0771
Frequencies --	1311.6881	1423.7376	1495.3663
Frequencies --	1521.0117	1530.9840	1540.7836
Frequencies --	1735.6849	2220.5288	3149.0117
Frequencies --	3177.6796	3219.0458	3323.6891
Frequencies --	3332.0872	3576.1507	3672.5770

IC for the $(FCH_2CN)(CH_3OH)H^+$ system

1,1\C,-1.3649452894,1.8253450302,-0.9974071175\H,-1.3687605841,1.818967455,0.0872346957\
H,-0.3735638591,1.8202742108,-1.4352356527\H,-2.0190400531,1.0854873154,-1.4443731875\N,
-0.2370902762,-0.5529931103,-0.1843867463\C,0.4490997181,-1.3852972279,0.2918516072\C,1.3
263690642,-2.4016895525,0.9038959816\H,1.8529972436,-2.9637464056,0.1298305369\F,2.26386
53754,-1.741080775,1.695331499\H,0.7435837373,-3.0744585533,1.5364766614\O,-1.9607896852
,3.1713504219,-1.4610929274\H,-2.8948932491,3.3026553449,-1.1742060996\H,-1.4323031556,3.
9505465053,-1.1683026296\\Version=x86-Linux-G98RevA.7\HF=-346.1220294\MP2=-347.027420
3\

Zero-point correction = 0.104979 (Hartree/Particle)

Frequencies --	9.6675	32.9725	56.8967
Frequencies --	113.1963	127.8282	136.2221
Frequencies --	214.4885	266.2240	324.4882
Frequencies --	567.5365	755.4240	784.3764
Frequencies --	930.4235	949.2410	1050.3715
Frequencies --	1080.9774	1189.4504	1274.9504
Frequencies --	1299.3710	1422.8165	1464.6198
Frequencies --	1507.2500	1509.7076	1540.2888
Frequencies --	1732.0281	2222.9531	3149.8130
Frequencies --	3190.7584	3220.2455	3344.4301
Frequencies --	3350.0299	3580.9190	3680.6991

TS_b for the $(FCH_2CN)(CH_3OH)H^+$ system

1,1\C\H,1,B1\H,1,B2,2,A1\H,1,B3,2,A2,3,D1,0\O,1,B4,2,A3,3,D2,0\H,5,B5,1,A4,2,D3,0\H,5,B6,1,
A5,6,D4,0\N,1,B7,2,A6,3,D5,0\C,8,B8,5,178.566507,1,D6,0\C,9,B9,8,179.26,5,D7,0\F,10,B10,9,A7
,8,D8,0\H,10,B11,9,A8,11,D9,0\H,10,B12,9,A9,11,D10,0\\B1=1.0780393\B5=0.9788765\B6=0.978
87555\B8=1.17415143\B9=1.48032702\B10=1.38676241\B11=1.09247061\B12=1.09247632\A4=1
17.44347126\A5=117.45336355\A7=107.64948082\A8=109.8266454\A9=109.81432722\D3=-64.6

9896296\D4=129.39390587\D6=-347.62468626\D7=-15.40324611\D8=6.02415115\D9=118.9931
5844\D10=-118.98662914\B2=1.07811019\B3=1.07810659\B4=1.93047002\B7=2.04177944\A1=
120.37763256\A2=120.38030922\A3=94.28023444\A6=88.09574412\D1=175.12567305\D2=-92.4
478202\D5=87.58449436\\Version=x86-Linux-G98RevA.7\HF=-346.107079\MP2=-347.0116612\

Zero-point correction = 0.102747 (Hartree/Particle)

Frequencies --	-513.0491	9.3180	48.1892
Frequencies --	66.5686	154.0815	176.0362
Frequencies --	249.9605	267.8020	317.1312
Frequencies --	333.2581	505.7150	562.6324
Frequencies --	692.5243	914.3848	1046.7482
Frequencies --	1093.9064	1145.0418	1171.8618
Frequencies --	1274.5604	1328.5706	1420.7955
Frequencies --	1447.4171	1448.7902	1533.3221
Frequencies --	1706.1265	2259.4473	3146.6759
Frequencies --	3218.9501	3225.5606	3438.4957
Frequencies --	3440.9793	3665.0827	3790.9403

$(CH_3OH)(CH_3OH)H^+$ proton-bound pair

1,1\C,1.8001992309,1.1348231349,-0.6245514487\H,1.3579377245,1.8009680942,0.1116918477\H
,2.8628221055,1.002948127,-0.4335030811\H,1.6092970823,1.4810152711,-1.6394275026\O,1.14
76582981,-0.1720193456,-0.4113118861\H,1.5062957993,-0.854978461,-1.0134407403\H,-0.0632
35251,-0.1692672288,-0.2895007724\O,-1.2320364972,-0.0821237096,-0.0273074441\H,-1.834760
1574,-0.209549625,-0.7880016421\C,-1.6972948198,-0.8199007568,1.1651346753\H,-2.68296540
42,-0.4362949783,1.4183152332\H,-1.7176326681,-1.8878243286,0.9525110642\H,-0.9801601047
,-0.5834066979,1.9468108758\\Version=x86-Linux-G98RevA.7\HF=-230.4212915\MP2=-231.0623
204\

Zero-point correction = 0.116504 (Hartree/Particle)

Frequencies --	24.3652	54.9968	114.8705
Frequencies --	153.1669	158.5338	318.8800
Frequencies --	465.9690	564.5392	667.5951
Frequencies --	976.3088	984.5870	1040.9687
Frequencies --	1113.4610	1199.5570	1201.8842
Frequencies --	1327.6687	1438.3392	1511.9323
Frequencies --	1517.4911	1537.3659	1540.0119
Frequencies --	1543.0789	1546.9685	1564.7376
Frequencies --	1701.6883	3153.7007	3154.7362
Frequencies --	3273.8610	3275.5845	3289.7145
Frequencies --	3291.4041	3713.7116	3717.5510

TS_a for the $(CH_3OH)(CH_3OH)H^+$ system

1,1\C\H,1,B1\H,1,B2,2,A1\H,1,B3,2,A2,3,D1,0\O,1,B4,2,A3,3,D2,0\H,5,B5,1,A4,2,D3,0\H,5,B6,1,
A5,2,D4,0\H,1,B7,2,A6,5,D5,0\O,1,B8,2,A7,5,D6,0\C,9,B9,1,A8,2,D7,0\H,10,B10,9,A9,1,D8,0\H,1
0,B11,9,A10,1,D9,0\H,10,B12,9,A11,1,D10,0\\B4=1.53476478\B5=0.98618078\B6=0.98614686\A3
=103.62375831\A4=112.75129819\A5=112.78899663\D2=-118.68929664\D3=183.30923571\D4=

60.35526308\B1=1.0856706\B2=1.08649445\B3=1.08565931\A1=113.68232275\A2=111.8949717
4\D1=130.28147865\B7=3.57068988\B8=2.93929153\B9=1.44678833\B10=1.08941171\B11=1.09
257999\B12=1.09259775\A6=106.76687893\A7=96.72835241\A8=127.41880681\A9=106.2250846
\A10=110.83469234\A11=110.87061343\D5=157.96912472\D6=149.28782301\D7=-25.39552023\
D8=-12.2499351\D9=106.4091039\D10=-130.94054546\\Version=x86-Linux-G98RevA.7\HF=-230
.39473\MP2=-231.0272268\

Zero-point correction = 0.118992 (Hartree/Particle)

Frequencies --	-92.0216	43.6531	70.4639
Frequencies --	99.9999	120.5387	167.6937
Frequencies --	265.6623	400.6226	784.0830
Frequencies --	809.6777	951.7605	1037.3284
Frequencies --	1100.7028	1168.5618	1194.7603
Frequencies --	1310.2446	1399.1285	1489.0141
Frequencies --	1520.4183	1524.1374	1542.5001
Frequencies --	1546.9552	1563.6908	1735.9010
Frequencies --	3114.3384	3170.7981	3206.7770
Frequencies --	3235.2632	3320.8693	3323.7487
Frequencies --	3579.9393	3676.7353	3755.3688

IC for the $(CH_3OH)(CH_3OH)H^+$ system

1,1\C,-0.6917877719,0.7992375576,-0.3870640029\H,-0.5256949621,0.8669489271,0.680923138\
H,0.2268540209,0.7261418753,-0.9558742745\H,-1.4443349777,0.0717216539,-0.6705054138\O,-
1.2379092193,2.2004294 675,-0.7587302687\H,-2.063944355,2.4379987553,-0.2762069656\H,-1.3
976895583,2.3134206229,-1.7248039691\H,-0.0142325843,-2.3400334704,0.1961154055\O,0.3879
301125,-1.4596048864,0.3045516568\C,1.6876458253,-1.6368021733,0.9166680521\H,2.1124628
186,-0.6392851226,1.025395395\H,1.5929135549,-2.0987965454,1.9021040163\H,2.3383505271,-
2.2393256507,0.278657268\\Version=x86-Linux-G98RevA.7\HF=-230.3963561\MP2=-231.029143
3\

Zero-point correction = 0.119208 (Hartree/Particle)

Frequencies --	42.9037	83.7653	93.8031
Frequencies --	120.7633	147.1161	190.5226
Frequencies --	269.3883	387.4052	734.9920
Frequencies --	774.4098	942.9083	1036.4522
Frequencies --	1103.4338	1186.0644	1193.8415
Frequencies --	1293.0261	1401.6421	1453.4449
Frequencies --	1504.0116	1507.7277	1525.8842
Frequencies --	1546.4881	1563.9970	1731.0160
Frequencies --	3115.0153	3197.0920	3208.9096
Frequencies --	3233.8337	3349.5918	3361.6519
Frequencies --	3584.0648	3684.8149	3756.1695

TS_b for the $(CH_3OH)(CH_3OH)H^+$ system

1,1\C\H,1,R2\H,1,R3,2,A3\H,1,R4,2,A4,3,D4,0\O,1,R5,2,A5,3,D5,0\H,5,R6,1,A6,2,D6,0\H,5,R7,1,
A7,6,D7,0\H,1,R8,2,A8,3,D8,0\O,8,R9,1,A9,2,D9,0\C,9,R10,8,A10,1,D10,0\H,10,R11,9,A11,8,D11

,0\H,10,R12,9,A12,11,D12,0\H,10,R13,9,A13,11,D13,0\\R5=1.87666931\R6=0.97993032\R7=0.979
69557\A5=95.61431027\A6=115.98824545\A7=116.55294873\D5=-94.56144887\D6=-63.8155657
6\D7=127.17984363\R8=2.60045434\R9=0.97768788\R10=1.45850722\R11=1.08855927\R12=1.0
9011326\R13=1.09188759\A8=104.44445263\A9=44.76825545\A10=109.26635718\A11=106.0276
8246\A12=108.98533434\A13=110.65310051\D8=92.71599663\D9=-15.70699115\D10=221.31712
639\D11=-173.51505073\D12=117.83597017\D13=-119.99850192\R2=1.07798529\R3=1.0783054
4\R4=1.07842769\A3=120.60462134\A4=119.47702596\D4=171.05467947\\Version=x86-Linux-
G98RevA.7\HF=-230.3828426\MP2=-231.0176172\

Zero-point correction = 0.117751 (Hartree/Particle)

Frequencies --	-502.8035	63.8332	108.3763
Frequencies --	139.4910	175.0568	276.5913
Frequencies --	288.1322	345.5102	501.4197
Frequencies --	562.9982	734.5709	1006.1750
Frequencies --	1107.4626	1163.8755	1183.4430
Frequencies --	1203.9596	1342.5169	1396.5567
Frequencies --	1452.0633	1453.5736	1519.5193
Frequencies --	1543.2484	1553.4682	1707.8823
Frequencies --	3128.4999	3221.1223	3235.3828
Frequencies --	3258.4369	3430.4082	3434.4551
Frequencies --	3653.9614	3716.4862	3778.2021

$(CH_3OH)(CH_3CH_2OH)H^+$ proton-bound pair

1,1\C,0.218457086,-1.5717828671,-0.3230950793\H,0.1805973689,-1.5887520277,0.7648952697\
H,1.253071082,-1.5941740132,-0.6693698154\O,-0.3312171213,-0.2099579581,-0.6539065182\C,-
0.6596568588,-2.6110315906,-0.9667030423\H,-0.3917035561,-0.0725825158,-1.6241802593\H,0.
1878977128,0.6188292036,-0.160629502\H,-1.6914108053,-2.5222710272,-0.6212209439\H,-0.63
00842731,-2.5472088303,-2.0583676519\H,-0.2858259449,-3.6004012109,-0.6865265682\O,0.773
4960309,1.5864713863,0.6099788478\H,1.5938307393,2.016869989,0.301281881\C,-0.056705057
9,2.5295946719,1.3661818467\H,0.5195547679,2.8907070382,2.2164844992\H,-0.3717732997,3.3
494732508,0.7209232764\H,-0.9149560843,1.9567214329,1.7098288263\\Version=x86-Linux-G98
RevA.7\HF=-269.4671873\MP2=-270.2384469\

Zero-point correction = 0.147349 (Hartree/Particle)

Frequencies --	44.9466	49.3157	81.7597
Frequencies --	115.5595	137.9210	267.0517
Frequencies --	303.7112	393.6995	453.3193
Frequencies --	551.9492	836.2192	837.4241
Frequencies --	976.5766	1016.8414	1035.6491
Frequencies --	1089.4206	1158.0626	1196.5760
Frequencies --	1258.3311	1327.0803	1335.4413
Frequencies --	1426.7831	1456.5035	1482.8659
Frequencies --	1515.2155	1533.1172	1542.3612
Frequencies --	1542.7355	1552.5238	1560.2926
Frequencies --	1702.2849	1845.4015	3113.0579
Frequencies --	3144.9380	3167.8223	3199.8255
Frequencies --	3221.1764	3254.2035	3258.4126
Frequencies --	3274.7011	3677.2290	3740.5034

TS_a for the $(CH_3OH)(CH_3CH_2OH)H^+$ system

1,1\C\H,1,B1\H,1,B2,2,A1\O,1,B3,2,A2,3,D1,0\H,4,B4,1,A3,2,D2,0\H,4,B5,1,A4,2,D3,0\H,1,B6,2,
A5,4,D4,0\O,1,B7,2,A6,4,D5,0\C,8,B8,1,A7,2,D6,0\H,9,B9,8,A8,1,D7,0\H,9,B10,8,A9,1,D8,0\H,9,
B11,8,A10,1,D9,0\C,1,B12,2,A11,8,D10,0\H,13,B13,1,A12,2,D11,0\H,13,B14,1,A13,2,D12,0\H,13,
B15,1,A14,2,D13,0\\B12=1.49718133\B13=1.09174825\B14=1.09464137\B15=1.09396133\A11=1
14.70283113\A12=112.02267234\A13=106.39158843\A14=112.17058314\D10=58.0986081\D11=1
77.10380631\D12=-64.4351718\D13=52.46681342\B1=1.08808352\B2=1.08822594\B3=1.5666473
4\B4=0.98643542\B5=0.98625343\B6=3.59236244\B7=2.97567588\B8=1.4461835\B9=1.08959863
\B10=1.09282693\B11=1.09276015\A1=112.24076898\A2=106.67589059\A3=112.93667077\A4=1
11.83760655\A5=36.97310142\A6=33.75752738\A7=129.32987893\A8=106.21381593\A9=110.89
649205\A10=110.96019736\D1=-109.68895363\D2=53.06427037\D3=-69.18482183\D4=161.9009
7342\D5=184.21148797\D6=94.24401835\D7=-7.98606383\D8=110.69924831\D9=-126.6480799
9\\Version=x86-Linux-G98RevA.7\HF=-269.4420264\MP2=-270.2067401\

Zero-point correction = 0.147770 (Hartree/Particle)

Frequencies --	-54.5515	39.6756	52.9519
Frequencies --	91.4856	97.7286	155.9210
Frequencies --	197.0404	269.5190	375.9119
Frequencies --	401.3477	686.5791	781.7477
Frequencies --	859.9150	948.4368	996.0079
Frequencies --	1038.0533	1099.9599	1178.8914
Frequencies --	1194.3433	1236.1551	1315.5528
Frequencies --	1398.4542	1424.8791	1467.2002
Frequencies --	1522.7859	1527.3995	1541.5575
Frequencies --	1547.4607	1563.2991	1567.7527
Frequencies --	1718.6942	3111.8550	3112.4090
Frequencies --	3192.5652	3200.6142	3204.0739
Frequencies --	3222.3826	3232.6277	3287.6488
Frequencies --	3572.2255	3677.3352	3752.8831

IC for the $(CH_3OH)(CH_3CH_2OH)H^+$ system

1,1\C\H,1,R2\H,1,R3,2,A3\O,1,R4,2,A4,3,D4,0\C,1,R5,2,A5,3,D5,0\H,4,R6,1,A6,2,D6,0\H,4,R7,1,
A7,6,D7,0\H,5,R8,1,A8,2,D8,0\H,5,R9,1,A9,8,D9,0\H,5,R10,1,A10,8,D10,0\H,1,R11,2,A11,3,D11,
0\O,11,R12,1,A12,2,D12,0\C,12,R13,11,A13,1,D13,0\H,13,R14,12,A14,11,D14,0\H,13,R15,12,A15
,14,D15,0\H,13,R16,12,A16,14,D16,0\\R2=1.0855623\R3=1.08664448\R4=1.57169022\R5=1.4984
1658\R6=0.98594211\R7=0.98613869\R8=1.09298902\R9=1.09341013\R10=1.09356175\R11=3.48
141856\R12=0.97410379\R13=1.4465554\R14=1.08979189\R15=1.09271123\R16=1.0927135\A3=
110.52599027\A4=101.71713474\A5=115.98187393\A6=112.35129575\A7=112.48691991\A8=112
.32337569\A9=112.21809704\A10=106.34821143\A11=60.00358465\A12=37.93383664\A13=107.
63703228\A14=106.28433136\A15=110.94778725\A16=110.90801818\D4=-106.70662795\D5=13
3.95570739\D6=-59.57125683\D7=-121.77921031\D8=51.12986916\D9=124.47817807\D10=-118.
07107471\D11=69.86620773\D12=-85.79029657\D13=-181.73873188\D14=-178.74012881\D15=1
18.5981337\D16=-118.68657403\\Version=x86-Linux-G98RevA.7\HF=-269.4417103\MP2=-270.2
064226\

Zero-point correction = 0.147793 (Hartree/Particle)

Frequencies --	18.4579	67.6307	80.7475

Frequencies --	96.1897	104.7280	156.9476
Frequencies --	174.4824	269.6653	374.9587
Frequencies --	397.9670	664.2257	785.1212
Frequencies --	825.7730	936.3449	983.2878
Frequencies --	1036.9913	1101.3668	1157.7724
Frequencies --	1194.0372	1262.3565	1321.2755
Frequencies --	1392.0181	1400.8190	1459.6065
Frequencies --	1524.3200	1534.9236	1536.2072
Frequencies --	1541.9216	1546.5736	1564.0922
Frequencies --	1729.0112	3112.6284	3113.3620
Frequencies --	3205.2145	3208.0805	3213.8135
Frequencies --	3224.8957	3230.7845	3314.0347
Frequencies --	3577.0340	3681.9827	3752.0813

TS_b for the $(CH_3OH)(CH_3CH_2OH)H^+$

1,1\C\H,1,R2\H,1,R3,2,A3\C,1,R4,2,A4,3,D4,0\H,4,R5,1,A5,2,D5,0\H,4,R6,1,A6,5,D6,0\O,1,R7,2,A7,3,D7,0\H,7,R8,1,A8,2,D8,0\H,7,R9,1,A9,8,D9,0\H,1,R10,2,A10,3,D10,0\O,10,R11,1,A11,2,D11,0\C,11,R12,10,A12,1,D12,0\H,12,R13,11,A13,10,D13,0\H,12,R14,11,A14,13,D14,0\H,12,R15,11,A15,13,D15,0\H,1,R16,2,A16,3,D16,0\\R13=1.08892194\R14=1.09060606\R15=1.09208664\R16=2.15113601\A13=106.12488578\A14=109.35811251\A15=110.72517194\A16=95.31831681\D13=-174.33437098\D14=117.99037476\D15=-119.78934199\D16=182.92791991\R2=1.07941751\R3=1.08063237\R4=1.48566598\R5=1.09251158\R6=1.09356053\R7=2.00096946\R8=0.97851341\R9=0.97875212\R10=2.71245818\R11=0.97736347\R12=1.45679417\A3=117.7269471\A4=122.37551459\A5=109.74124975\A6=108.36203167\A7=90.55677059\A8=117.8629068\A9=118.61497583\A10=85.55958703\A11=44.44186185\A12=108.91883954\D4=175.29227361\D5=139.6008993\D6=116.1852454\D7=-87.14163488\D8=-76.67730777\D9=130.85588026\D10=62.28024381\D11=86.68968786\D12=-141.4835552\\Version=x86-Linux-G98RevA.7\HF=-269.4299256\MP2=-270.1930188

Zero-point correction = 0.145519 (Hartree/Particle)

Frequencies --	-426.2898	52.2382	99.6480
Frequencies --	129.7103	140.3707	167.3927
Frequencies --	220.2211	243.5071	291.0221
Frequencies --	353.6435	459.8470	472.6022
Frequencies --	628.2230	851.2418	986.0150
Frequencies --	1003.1751	1062.4406	1106.3782
Frequencies --	1107.1214	1193.6135	1251.4712
Frequencies --	1271.8824	1393.3682	1447.1545
Frequencies --	1513.5017	1520.6458	1526.4965
Frequencies --	1543.4936	1551.2362	1557.6166
Frequencies --	1700.4454	3121.6916	3125.4823
Frequencies --	3206.7451	3229.4255	3232.9383
Frequencies --	3252.4197	3276.6789	3405.5851
Frequencies --	3665.3730	3719.3765	3793.9124

$(CH_3OH)(CH_3CH_2CH_2OH)H^+$ proton-bound pair

1,1\C,2.1304778396,-2.5797813006,-0.9976170023\H,1.8396723744,-2.7297078564,0.0396763149\H,3.1909796366,-2.338879942,-1.0703506106\O,1.3256464503,-1.4526873053,-1.4771442914\H,

1.8809402219,-3.4595055437,-1.5888501149\H,1.4998373445,-1.2809522738,-2.4223484479\H,1.01495848,-0.404493035,-0.6313609391\O,0.697049952,0.3263907188,0.1099289026\H,1.2049868049,1.1629743967,0.0278875146\C,-0.7862790082,0.5879011265,0.1237631826\H,-1.0602397864,0.9551408639,-0.867872166\H,-1.206922669,-0.4030101315,0.2934237967\C,-1.1027003637,1.5613097245,1.2316166959\H,-0.7366937057,1.1573336105,2.1806527346\H,-0.5870706343,2.512356237,1.0480727456\C,-2.6136561286,1.8025606265,1.3006130585\H,-2.8398367817,2.5096493101,2.1013828501\H,-2.9957997331,2.2224800251,0.3657209636\H,-3.1534368046,0.8750459698,1.511432861\\Version=x86-Linux-G98RevA.7\HF=-308.5037433\MP2=-309.4067114\

Zero-point correction = 0.176746 (Hartree/Particle)

Frequencies --	36.7826	42.4054	73.4752
Frequencies --	97.0229	122.5985	142.2470
Frequencies --	237.9392	252.9552	335.8247
Frequencies --	390.9512	476.1252	552.8108
Frequencies --	790.0758	880.0712	917.0506
Frequencies --	950.3356	985.5788	1041.0901
Frequencies --	1077.6595	1096.8507	1176.5964
Frequencies --	1196.9743	1247.3986	1313.8462
Frequencies --	1328.5044	1354.3996	1376.5662
Frequencies --	1427.4621	1460.4043	1479.6928
Frequencies --	1516.8159	1542.5426	1542.9200
Frequencies --	1548.9941	1552.3499	1553.6203
Frequencies --	1560.3013	1709.5019	1913.3425
Frequencies --	3101.0699	3111.6552	3144.0052
Frequencies --	3155.4977	3167.1897	3200.1149
Frequencies --	3213.8414	3243.3359	3256.8431
Frequencies --	3273.2384	3671.9521	3741.8410

TS_a for the $(CH_3OH)(CH_3CH_2CH_2OH)H^+$ system

1,1\C\H,1,B2\H,1,B3,2,A3\O,1,B4,2,A4,3,D4,0\H,4,B5,1,A5,2,D5,0\H,4,B6,1,A6,2,D6,0\H,1,B7,2,A7,4,D7,0\O,1,B8,2,A8,4,D8,0\C,8,B9,1,A9,2,D9,0\H,9,B10,8,A10,1,D10,0\H,9,B11,8,A11,1,D11,0\H,9,B12,8,A12,1,D12,0\C,1,B13,2,A13,8,D13,0\H,13,B14,1,A14,2,D14,0\H,13,B15,1,A15,2,D15,0\C,13,B16,1,A16,2,D16,0\H,16,B17,13,A17,1,D17,0\H,16,1.09238853,13,A18,1,D18,0\H,16,B19,13,A19,1,D19,0\\B2=1.08953088\B3=1.08889308\B4=1.56404433\B5=0.98604194\B6=0.98662372\B7=3.58117662\B8=3.000582\B9=1.44609138\B10=1.08944197\B11=1.09291267\B12=1.09281068\B13=1.50122438\B14=1.09488701\B15=1.09690862\B16=1.52956059\B17=1.09786714\B19=1.09469567\D7=159.25290287\D8=182.62222395\D9=96.56129721\A3=112.3818761\A4=106.48559292\A5=112.72963811\A6=110.75714469\A7=36.52238441\A8=33.01199505\D10=-10.73953053\D11=107.9499677\D12=-129.38998799\D13=60.00915753\D14=181.18035723\D15=-64.46198029\A9=132.06772449\A10=106.2271263\A11=110.9163381\A12=110.95892412\A13=114.01174101\A14=110.19896024\A15=104.11511031\A16=113.73298928\A17=112.96225624\A18=110.04142595\A19=111.45146892\D4=-10.10759543\D5=52.23002937\D6=-69.14476212\D16=55.10949999\D17=71.90655024\D18=189.43433074\D19=-51.13015649\\Version=x86-Linux-G98RevA.7\HF=-308.4780587\MP2=-309.3760265\

Zero-point correction = 0.176989 (Hartree/Particle)

Frequencies --	-44.3969	23.2769	41.6566
Frequencies --	85.8966	93.1121	134.1126

Frequencies --	152.0943	188.2775	251.2343
Frequencies --	319.5208	395.7502	459.7819
Frequencies --	686.9598	795.7371	800.4362
Frequencies --	891.6697	957.3641	1008.6532
Frequencies --	1037.9287	1072.8283	1099.9613
Frequencies --	1173.4398	1192.8383	1195.4892
Frequencies --	1288.5270	1334.0322	1398.6997
Frequencies --	1411.4156	1450.5756	1477.2232
Frequencies --	1513.8573	1522.5666	1539.1196
Frequencies --	1547.4636	1558.7717	1562.8980
Frequencies --	1565.2607	1708.1629	3084.2689
Frequencies --	3112.2434	3117.2868	3160.8794
Frequencies --	3177.6136	3182.5965	3203.1185
Frequencies --	3208.2586	3234.3950	3275.8804
Frequencies --	3571.5897	3674.1772	3750.4511

IC for the $(CH_3OH)(CH_3CH_2CH_2OH)H^+$ system

1,1\C,-0.0586414371,0.6659796794,-0.3977207004\H,-0.0216550934,0.6649219063,0.688693527\
H,0.9442188669,0.6329844493,-0.8168645193\O,-0.4682813383,2.1519564835,-0.7000991967\C,
-1.0516148568,-0.2798350992,-1.0087874846\H,-1.3126932111,2.3988428426,-0.2555730083\H,-0
.5794006108,2.3169653448,-1.6660384153\H,-1.0421999003,-0.1859066616,-2.1021430756\H,-0.6
431236823,-1.2723482204,-0.7872583628\H,1.0346788764,-2.231894617,1.2367980455\O,1.3049
023166,-1.3301318691,0.9865815346\C,2.6562234445,-1.1298226342,1.4618768229\H,2.9290421
336,-0.1112347067,1.1863600576\H,2.7080451742,-1.2342495617,2.5484010869\H,3.3459526913,
-1.8298192009,0.9839715096\C,-2.4673809987,-0.14742464,-0.4502431433\H,-3.1075265655,-0.9
322311664,-0.8592231374\H,-2.47561918,-0.2470752358,0.6398849835\H,-2.9442042364,0.80306
40764,-0.7196203621\\Version=x86-Linux-G98RevA.7\HF=-308.4783077\MP2=-309.3758255\

Zero-point correction = 0.177062 (Hartree/Particle)

Frequencies --	14.8316	44.1810	76.1805
Frequencies --	87.2117	96.9164	142.3442
Frequencies --	161.2460	177.8594	247.0757
Frequencies --	324.8882	392.9910	459.9009
Frequencies --	666.2654	766.3624	832.7902
Frequencies --	877.8270	926.9038	983.0539
Frequencies --	1035.9176	1065.8588	1101.0085
Frequencies --	1146.6639	1193.6317	1233.1514
Frequencies --	1311.3949	1315.3668	1390.7264
Frequencies --	1400.2771	1431.6976	1478.7124
Frequencies --	1519.4818	1524.8964	1532.2288
Frequencies --	1544.7389	1546.4367	1561.0060
Frequencies --	1564.0195	1729.3139	3090.9924
Frequencies --	3105.6762	3111.9615	3160.0831
Frequencies --	3177.4588	3204.4161	3209.0805
Frequencies --	3211.9876	3229.6229	3300.9762
Frequencies --	3578.4870	3683.0540	3752.1282

TS_b for the $(CH_3OH)(CH_3CH_2CH_2OH)H^+$ system

1,1\C\H,1,B2\H,1,B3,2,A3\O,1,B4,2,A4,3,D4,0\H,4,B5,1,A5,2,D5,0\H,4,B6,1,A6,2,D6,0\H,1,B7,2,
A7,4,D7,0\O,1,B8,2,A8,4,D8,0\C,8,B9,1,A9,2,D9,0\H,9,1.08979486,8,A10,1,D10,0\H,9,B11,8,A11,
1,D11,0\H,9,B12,8,A12,1,D12,0\C,1,B13,2,A13,8,D13,0\H,13,B14,1,A14,2,D14,0\H, 13,B15,1,
A15,2,D15,0\C,13,B16,1,A16,2,D16,0\H,16,B17,13,A17,1,D17,0\H,16,B18,13,A18,1,D18,0\H,16,B
19,13,A19,1,D19,0\\B7=2.72399069\B8=2.13961923\B9=1.45567999\B11=1.09079137\B12=1.092
10189\A7=98.78279989\A8=81.16885001\A9=121.1903726\A10=106.09467192\A11=109.4240444
6\A12=110.86624792\D7=-195.22632775\D8=-188.98237577\D9=-23.52507137\D10=47.04182024
\D11=164.80263759\D12=-72.85237624\D4=-87.77265706\D5=-72.31301866\D6=56.10736205\
A3=117.446944804\A4=90.39367182\A5=116.98313816\A6=117.54915528\B2=1.08072948\B3=1.
08195644\B4=1.98472233\B5=0.97881545\B6=0.97925622\B13=1.48974906\B14=1.09668937\B1
5=1.09525566\B16=1.5249099\B17=1.09497656\B18=1.09226761\B19=1.09304333\A13=121.414
26954\A14=107.54258249\A15=107.15885194\A16=113.81394047\A17=111.91372533\A18=110.2
4984126\A19=110.61760867\D13=89.79290689\D14=128.29255755\D15=-119.56778284\D16=3.0
04894497\D17=60.24575944\D18=179.82986925\D19=-60.81178254\\Version=x86-Linux-G98Rev
A.7\HF=-308.4659009\MP2=-309.3617689\

Zero-point correction = 0.174705 (Hartree/Particle)

Frequencies --	-416.4265	33.2296	69.1399
Frequencies --	98.6876	129.3674	138.3275
Frequencies --	175.4514	209.5493	227.0571
Frequencies --	291.8675	372.2057	401.9127
Frequencies --	458.0584	502.3775	642.7851
Frequencies --	776.6846	907.6009	962.8888
Frequencies --	1012.1869	1058.6087	1095.8896
Frequencies --	1101.7150	1112.6422	1193.9296
Frequencies --	1199.1504	1266.6043	1321.3833
Frequencies --	1391.0913	1420.7209	1475.5434
Frequencies --	1506.5875	1518.5522	1521.0375
Frequencies --	1544.5096	1545.5374	1551.5839
Frequencies --	1556.3749	1700.3004	3107.2350
Frequencies --	3115.7900	3122.6169	3155.7855
Frequencies --	3194.3155	3214.3698	3227.5593
Frequencies --	3244.0436	3261.3506	3388.7780
Frequencies --	3660.5097	3714.9386	3788.3018

$(CH_3OH)((CH_3)_2CHOH)H^+$ proton-bound pair

1,1\H,0.4940298399,0.5201866862,-0.5580040929\O,0.5378932856,0.5643893463,0.5106355402\
H,1.4682223587,0.4782564786,0.8154428759\C,-0.3741042951,-0.4415741187,1.2132542635\H,-0
.0965819893,-1.4156985849,0.8005386183\C,-0.0572420484,-0.3385464805,2.6838931245\C,-1.77
4697869,-0.0408586188,0.8262193686\H,-0.6922475205,-1.0440469199,3.2274912077\H,0.982600
3536,-0.6035369006,2.9016566394\H,-0.2655326002,0.6683758305,3.0547675032\H,-2.474803706
5,-0.7441854321,1.2865337638\H,-2.0025713822,0.9633502323,1.1927585403\H,-1.9243862477,-
0.0810978115,-0.2557339547\O,0.3263721315,0.481719235,-1.9781087718\C,1.1338480124,-0.32
22328415,-2.8943620607\H,0.0796963078,1.3281686409,-2.3980695391\H,1.2999975739,-1.27265
01421,-2.391335979\H,0.5689572581,-0.4834794194,-3.8117295978\H,2.0816736183,0.176761049
3,-3.098558308\\Version=x86-Linux-G98RevA.7\HF=-308.5108584\MP2=-309.415996\

Zero-point correction = 0.176508 (Hartree/Particle)

Frequencies --	32.6104	48.5678	88.4260
Frequencies --	96.3637	145.6908	236.0423
Frequencies --	268.6798	288.1062	374.4089
Frequencies --	407.4192	428.7469	485.4753
Frequencies --	564.4498	753.2173	928.6958
Frequencies --	972.6974	975.2040	998.3205
Frequencies --	1028.3484	1089.8963	1129.7877
Frequencies --	1194.1837	1229.8575	1248.4043
Frequencies --	1330.1466	1382.7899	1429.5816
Frequencies --	1439.9806	1477.7493	1478.6150
Frequencies --	1519.8603	1526.3699	1533.2902
Frequencies --	1542.5353	1544.3393	1552.9311
Frequencies --	1557.1512	1733.4168	2152.0521
Frequencies --	3105.5482	3113.5557	3139.4028
Frequencies --	3155.9805	3195.5801	3207.1620
Frequencies --	3212.8488	3217.4411	3249.8185
Frequencies --	3265.4319	3662.9954	3737.8100

TS_a for the $(CH_3OH)((CH_3)_2CHOH)H^+$ system

1,1\C\H,1,B1\O,1,B2,2,A1\H,3,B3,1,A2,2,D1,0\H,3,B4,1,A3,2,D2,0\H,1,B5,2,A4,3,D3,0\O,1,B6,2,A5,3,D4,0\C,7,B7,1,A6,2,D5,0\H,8,B8,7,A7,1,D6,0\H,8,B9,7,A8,1,D7,0\H,8,B10,7,A9,1,D8,0\C,1,B11,2,A10,7,D9,0\H,12,B12,1,A11,2,D10,0\H,12,1.09330292,1,A12,2,D11,0\H,12,B14,1,A13,2,D12,0\C,1,B15,2,A14,7,D13,0\H,16,B16,1,A15,2,D14,0\H,16,B17,1,A16,2,D15,0\H,16,B18,1,A17,2,D16,0\\B11=1.50057257\B12=1.09278113\B14=1.094434\B15=1.5004966\B16=1.09436868\B17=1.09446826\B18=1.09272412\A10=113.12040657\A11=111.55323021\A12=106.91112208\A13=112.43046523\A14=113.16249958\A15=112.41936935\A16=106.92678584\A17=111.56331064\D9=65.67330685\D10=175.12341668\D11=-66.30061282\D12=51.06753792\D13=-69.50525796\D14=-51.047934\D15=66.22983573\D16=-175.16732225\B1=1.0899123\B2=1.5990387\B3=0.98619164\B4=0.98615246\B5=3.65070515\B6=3.00411755\B7=1.44625294\B8=1.08965404\B9=1.09286596\B10=1.09282724\A1=104.32650494\A2=112.01996365\A3=112.06216361\A4=34.05672176\A5=31.59469397\A6=126.88581206\A7=106.18895218\A8=110.91802643\A9=110.98864721\D1=60.89806885\D2=-60.50010026\D3=158.93442019\D4=181.91324093\D5=96.05419176\D6=-6.81358654\D7=111.8577869\D8=-125.47040697\\Version=x86-Linux-G98RevA.7\HF=-308.488209\MP2=-309.3871946\

Zero-point correction = 0.175990 (Hartree/Particle)

Frequencies --	-39.7842	34.5619	41.2363
Frequencies --	81.7466	96.6234	150.2048
Frequencies --	177.6941	237.6771	276.0184
Frequencies --	363.8084	366.0375	398.8214
Frequencies --	452.9771	593.3542	781.1170
Frequencies --	910.8844	928.1170	981.6354
Frequencies --	990.4056	1037.1383	1099.0175
Frequencies --	1106.7976	1193.9839	1243.5353
Frequencies --	1263.1830	1351.0391	1399.5092
Frequencies --	1440.5745	1471.1498	1484.0045
Frequencies --	1517.4502	1522.4225	1534.1432
Frequencies --	1537.0383	1547.0576	1547.6803
Frequencies --	1563.6209	1711.1661	3107.5527

Frequencies --	3110.3021	3111.8258	3196.4155
Frequencies --	3199.2718	3203.2414	3208.7388
Frequencies --	3215.2489	3227.4183	3231.9422
Frequencies --	3571.0877	3683.1793	3751.1909

IC for the $(CH_3OH)((CH_3)_2CHOH)H^+$ system

1,1\C,0.7106049728,0.3745183973,-0.4379747509\H,0.548668897,0.2115091333,0.6255507634\O,2.2962778265,0.5717406615,-0.4515551005\C,0.0808331884,1.6393594431,-0.9467454311\H,2.5785871204,1.3723199771,0.0504124252\H,2.6475608229,0.6542213896,-1.3696629444\H,0.3309756665,1.828025603,-1.9952639375\H,-1.0023227025,1.5009015093,-0.8770395983\H,-2.2910592335,0.4067205994,1.5426990652\O,-1.6167028813,-0.219389363,1.2229622967\C,-1.9261237968,-1.518948193,1.7778896431\H,-1.1479250111,-2.1946022527,1.4235313192\H,-1.9091923173,-1.4923872129,2.8702540816\H,-2.8990319113,-1.8718061801,1.4266723301\H,0.3407771366,2.5108039136,-0.3388328344\C,0.4924990853,-0.8652087598,-1.2546645808\H,1.0700238121,-1.7096337603,-0.8721461855\H,-0.5707072526,-1.1100439474,-1.1748934901\H,0.7201647133,-0.7031644857,-2.313567846\\Version=x86-Linux-G98RevA.7\HF=-308.4875704\MP2=-309.3868721\

Zero-point correction = 0.176094 (Hartree/Particle)

Frequencies --	39.0345	51.7424	63.7553
Frequencies --	86.5478	98.2933	149.7440
Frequencies --	171.5628	246.0705	282.2569
Frequencies --	362.5385	368.7810	403.8879
Frequencies --	446.0247	592.5596	778.8976
Frequencies --	904.8155	933.4599	962.4068
Frequencies --	981.3247	1035.6973	1099.4747
Frequencies --	1134.5218	1193.8724	1228.8232
Frequencies --	1264.1360	1345.9104	1398.9637
Frequencies --	1429.7016	1469.2099	1470.2198
Frequencies --	1515.9296	1522.1864	1532.3462
Frequencies --	1542.1822	1545.9519	1548.3598
Frequencies --	1563.6167	1714.0206	3104.1081
Frequencies --	3106.4849	3111.5298	3196.7956
Frequencies --	3198.6589	3203.2329	3203.9338
Frequencies --	3218.5184	3230.7581	3244.2766
Frequencies --	3568.4213	3680.3752	3750.5476

TS_b for the $(CH_3OH)((CH_3)_2CHOH)H^+$ system

1,1\C\H,1,B2\O,1,B3,2,A3\H,3,B4,1,A4,2,D4,0\H,3,B5,1,A5,2,D5,0\H,1,B6,2,A6,3,D6,0\O,1,B7,2,A7,3,D7,0\C,7,B8,1,A8,2,D8,0\H,8,B9,7,A9,1,D9,0\H,8,1.090791,7,A10,1,D10,0\H,8,B11,7,A11,1,D11,0\C,1,B12,2,A12,7,D12,0\H,12,B13,1,A13,2,D13,0\H,12,B14,1,A14,2,D14,0\H,12,B15,1,A15,2,D15,0\C,1,B16,2,A16,7,D16,0\H,16,B17,1,A17,2,D17,0\H,16,B18,1,A18,2,D18,0\H,16,B19,1,A19,2,D19,0\\D4=-75.21186452\D5=64.95773204\D6=162.11372973\D7=179.39989277\D8=55.48451554\D9=34.44944364\D10=152.62581702\D11=-84.90945654\B2=1.08035404\B3=2.18587608\B4=0.97697591\B5=0.9771256\B6=2.9286501\B7=2.3231766\B8=1.4533906\B9=1.08929189\B11=1.09212444\B12=1.47503425\B13=1.09323985\B14=1.09726847\B15=1.09010921\B16=1.47667269\B17=1.0898843\B18=1.09603696\B19=1.0944661\A3=84.32959813\A4=122.09017153\A5=121.87476903\A6=77.81524875\A7=77.28916862\A8=124.34063333\A9=106.20181534\A10=109.97226633\A11=110.82472403\A12=119.61183713\A13=110.18231483\A14=106.72849431\A15=112.

94220421\A16=119.84778482\A17=113.1231814\A18=107.98400301\A19=108.98081334\D12=88.68028023\D13=140.99287362\D14=-103.22230629\D15=16.51295202\D16=-86.65250322\D17=-3.27347659\D18=118.62846271\D19=-126.3341395\\Version=x86-Linux-G98RevA.7\HF=-308.4820199\MP2=-309.3732738\

Zero-point correction = 0.171904 (Hartree/Particle)

Frequencies --	-265.1650	43.6245	72.4765
Frequencies --	103.4339	121.5131	133.1402
Frequencies --	145.5130	157.0088	189.7373
Frequencies --	228.1076	256.3941	345.3816
Frequencies --	370.5244	405.6334	426.3173
Frequencies --	492.9421	872.4851	910.8263
Frequencies --	947.8455	972.6136	1019.0440
Frequencies --	1101.2330	1180.4377	1191.4273
Frequencies --	1194.2742	1222.6374	1388.3718
Frequencies --	1406.8740	1434.6554	1486.8481
Frequencies --	1502.2119	1514.0740	1520.4907
Frequencies --	1532.1333	1544.5788	1549.5151
Frequencies --	1559.5530	1702.2448	3102.2122
Frequencies --	3106.6189	3123.5112	3181.2183
Frequencies --	3188.9331	3224.3387	3237.0158
Frequencies --	3238.5655	3245.0836	3338.4150
Frequencies --	3683.9028	3728.5469	3812.7628

$(CH_3CHO)(CH_3OH)H^+$ proton-bound pair

1,1\C,1.0101930916,2.5495375975,0.9324316429\H,0.7362287979,2.9489490826,1.9168870727\H,2.0497207164,2.2220710175,0.9269025696\H,0.8580748275,3.3668422789,0.2165738601\C,0.0975618861,1.4406201157,0.5952125938\O,0.5088962312,0.2884921515,0.3461456156\H,-0.9839263932,1.6379385418,0.5630416769\H,-0.319526274,-0.7124137913,0.0476446585\O,-0.961213218,-1.585113815,-0.2422494822\H,-1.0400775526,-2.2188212981,0.5028307046\C,-0.5092571004,-2.267203416,-1.482614142\H,0.4795288678,-2.6928710214,-1.3208981806\H,-1.2551568157,-3.0243109367,-1.7105504431\H,-0.4973175432,-1.4921363483,-2.2437815542\\Version=x86-Linux-G98RevA.7\HF=-268.3039319\MP2=-269.0604696\

Zero-point correction = 0.122150 (Hartree/Particle)

Frequencies --	47.3906	71.6645	88.8063
Frequencies --	140.2314	144.0371	177.5142
Frequencies --	301.9076	562.7388	590.7572
Frequencies --	821.1659	946.3620	961.1995
Frequencies --	1051.3895	1161.3617	1175.3628
Frequencies --	1200.4416	1243.4583	1313.4255
Frequencies --	1435.3928	1460.9718	1484.7826
Frequencies --	1495.4582	1497.2637	1537.8757
Frequencies --	1538.7775	1588.6829	1748.4286
Frequencies --	1778.8487	3092.7654	3120.4033
Frequencies --	3159.9081	3166.3591	3242.3220
Frequencies --	3285.8354	3299.8570	3684.3495

TS_a for the $(CH_3CHO)(CH_3OH)H^+$ system

1,1\O\C,1,B2\H,1,B3,2,A3\H,1,B4,2,A4,3,D4,0\H,2,B5,1,A5,3,D5,0\H,2,B6,1,A6,3,D6,0\H,2,B7,1,
A7,3,D7,0\O,2,B8,1,A8,3,D8,0\C,8,B9,2,A9,1,D9,0\C,9,B10,8,A10,2,D10,0\H,9,B11,8,A11,2,D11,0
\H,10,B12,9,A12,8,D12,0\H,10,B13,9,A13,8,D13,0\H,9,B14,8,A14,2,D14,0\\B2=1.53312133\B3=0.
98627014\B4=0.98627041\B5=1.08566026\B6=1.0856589\B7=1.08549117\B8=2.99178306\B9=1.2
3452562\B10=1.49200752\B11=1.10394537\B12=1.09613073\B13=1.09613076\B14=2.1407786\A
3=112.65109116\A4=112.65014179\A5=103.72059974\A6=103.72076478\A7=108.82801775\A8=
137.79541431\A9=166.6657436\A10=124.45865329\A11=118.90344155\A12=109.38587207\A13=
109.38584041\A14=96.05540972\D4=122.7892681\D5=59.9921633\D6=177.21870716\D7=-61.39
695292\D8=-61.46157589\D9=-179.9532398\D10=-179.99500555\D11=0.00501305\D12=-121.746
16245\D13=121.74624155\D14=180.00503785\\Version=x86-Linux-G98RevA.7\HF=-268.2778933
\MP2=-269.0285557\

Zero-point correction = 0.122977 (Hartree/Particle)

Frequencies --	-84.6180	20.2965	37.2853
Frequencies --	48.6343	71.3921	132.4316
Frequencies --	152.6240	257.6685	519.7573
Frequencies --	789.3454	797.0687	815.7388
Frequencies --	934.7109	953.6299	1165.9846
Frequencies --	1176.1879	1184.9821	1311.9406
Frequencies --	1439.2969	1462.4013	1499.9956
Frequencies --	1507.1165	1508.0800	1523.3877
Frequencies --	1534.5295	1736.0168	1756.1754
Frequencies --	3058.4531	3097.2020	3174.8957
Frequencies --	3176.7805	3228.7209	3324.0751
Frequencies --	3330.7689	3578.0992	3675.0494

IC for the $(CH_3CHO)(CH_3OH)H^+$ system

1,1\C\H,1,R2\H,1,R3,2,A3\H,1,R4,2,A4,3,D4,0\O,1,R5,2,A5,3,D5,0\H,5,R6,1,A6,2,D6,0\H,5,R7,1,
A7,6,D7,0\H,1,R8,2,A8,3,D8,0\C,8,R9,1,A9,2,D9,0\C,9,R10,8,A10,1,D10,0\O,9,R11,8,A11,10,D11,
0\H,10,R12,9,A12,8,D12,0\H,10,R13,9,A13,12,D13,0\H,10,R14,9,A14,12,D14,0\\R2=1.08376636\R
3=1.08377024\R4=1.0843995\R5=1.54211573\R6=0.98577539\R7=0.98577575\R8=4.49232066\R9
=1.10397908\R10=1.49167225\R11=1.23451444\R12=1.09084317\R13=1.09616856\R14=1.09616
737\A3=112.2698087\A4=113.96224292\A5=103.78405271\A6=113.15455674\A7=113.15463354\
A8=82.99522576\A9=48.88954879\A10=116.65463734\A11=118.91243236\A12=111.04391808\A
13=109.37582421\A14=109.37646204\D4=131.46761935\D5=-111.44093343\D6=-59.33845542\
D7=-123.80215934\D8=79.2530019\D9=-56.35158117\D10=-179.97774294\D11=180.00039513\
D12=-180.00446166\D13=121.76879992\D14=-121.76879036\\Version=x86-Linux-G98RevA.7\
HF=-268.2797366\MP2=-269.0302881\

Zero-point correction = 0.123152 (Hartree/Particle)

Frequencies --	1.5167	36.0769	65.6686
Frequencies --	96.6076	111.1016	141.9466
Frequencies --	153.5145	266.7365	518.1068
Frequencies --	763.0042	786.4231	796.1277
Frequencies --	935.0828	947.3276	1166.4660
Frequencies --	1176.1636	1184.2618	1299.2988

Frequencies -- 1439.6430 1462.0109 1467.5009
Frequencies -- 1506.5859 1507.8146 1508.5692
Frequencies -- 1512.5694 1732.8011 1758.4226
Frequencies -- 3058.5007 3096.9911 3174.5584
Frequencies -- 3193.4942 3228.6465 3346.9347
Frequencies -- 3350.5108 3583.4179 3683.1683

TS_b for the $(CH_3CHO)(CH_3OH)H^+$ system

1,1\C\H,1,B2\H,1,B3,2,A3\H,1,B4,2,A4,3,D4,0\O,1,B5,2,A5,4,D5,0\H,5,B6,1,A6,2,D6,0\H,5,B7,1,
A7,2,D7,0\O,1,B8,2,A8,5,D8,0\C,8,B9,1,A9,2,D9,0\C,9,B10,8,A10,1,D10,0\H,10,B11,9,A11,8,D11,
0\H,10,B12,9,A12,8,D12,0\H,9,B13,8,A13,1,D13,0\H,9,B14,8,A14,1,D14,0\\B2=1.07937136\B3=1.
0783463\B4=1.07834644\B5=1.87210586\B6=0.97960437\B7=0.9796044\B8=2.03301877\B9=1.24
187521\B10=1.48247066\B11=1.09657094\B12=1.09012576\B13=1.10389797\B14=2.11285195\A
3=120.40547943\A4=120.40548761\A5=95.41296851\A6=116.84560184\A7=116.84570769\A8=9
0.46467569\A9=126.09670238\A10=123.07265069\A11=109.10159491\A12=111.00427916\A13=1
19.22713295\A14=133.87282663\D4=170.11915373\D5=94.94040734\D6=-64.36077236\D7=64.3
6062699\D8=-179.99999535\D9=0.00245681\D10=179.99661796\D11=-121.9528431\D12=-0.0001
2516\D13=-0.00348584\D14=-144.74691917\\Version=x86-Linux-G98RevA.7\HF=-268.264233\
MP2=-269.0173451\

Zero-point correction = 0.121580 (Hartree/Particle)

Frequencies -- -487.1136 45.8257 92.9175
Frequencies -- 92.9933 143.5303 170.9329
Frequencies -- 258.0411 300.0698 319.2106
Frequencies -- 535.4665 565.9786 731.7641
Frequencies -- 822.4940 945.9311 1149.1673
Frequencies -- 1165.0037 1188.1767 1192.0478
Frequencies -- 1332.2042 1435.6259 1444.8414
Frequencies -- 1454.7308 1463.4105 1498.5489
Frequencies -- 1500.2954 1704.6551 1737.8091
Frequencies -- 3062.3931 3095.9187 3171.9403
Frequencies -- 3214.9091 3239.5047 3423.1372
Frequencies -- 3431.1431 3655.1996 3781.7155

Part 2: Archives for NO-aromatic cluster ions (Chapters five and six)

NO Geometry Optimizations

1\1\GINC-MS6\Freq\UHF\6-31G(d)\N1O1(2)\JULIE\13-Nov-2002\0\\#N UHF/6-31G(D)FREQ\
HF/6-31G(d) NO Opt and Freq\\0,2\N,0.,0.,-0.601048859\O,0.,0.,0.5259177517\\Version=x86-
Linux-G98RevA.7\HF=-129.247883\S2=0.768006\S2-1=0.\S2A=0.750233\RMSD=3.347e-10\
RMSF=2.221e-05\\PG=C*V [C*(N1O1)]\

Zero-point correction = 0.005061 (Hartree/Particle)
Frequencies -- 2221.6076

1\1\GINC-MS6\Freq\UHF\6-31+G(d)\N1O1(2)\JULIE\13-Nov-2002\0\\#N UHF/6-31+G(D)
FREQ**HF/6-31+G(d)** NO Opt and Freq\\0,2\N,0.,0.,-0.60093032\O,0.,0.,0.52581403\\

Version=x86-Linux-G98RevA.7\HF=-129.251647\S2=0.76921\S2-1=0.\S2A=0.750269\
RMSD=9.486e-10\RMSF=3.490e-05\ PG=C*V [C*(N1O1)]\

Zero-point correction = 0.005032 (Hartree/Particle)
Frequencies -- 2208.8729

1\1\GINC-MS6\Freq\UHF\6-31G(d,p)\N1O1(2)\JULIE\13-Nov-2002\0\\#N UHF/6-31G(D,P)
FREQ**HF/6-31G(d,p)** NO Opt and freq\\0,2\N,0.,0.,-0.6010461245\O,0.,0.,0.525915359\\
Version=x86-Linux-G98RevA.7\HF=-129.247883\S2=0.768004\S2-1=0.\S2A=0.750233\
RMSD=8.814e-10\RMSF=3.001e-05\ PG=C*V [C*(N1O1)]\

Zero-point correction = 0.005061 (Hartree/Particle)
Frequencies -- 2221.6647

1\1\GINC-MS6\Freq\UHF\6-31+G(d,p)\N1O1(2)\JULIE\13-Nov-2002\0\\#N UHF/6-31+G(D,P)
FREQ**HF/6-31+G(d,p)** NO Opt and Freq\\0,2\N,0.,0.,-0.6009300619\O,0.,0.,0.5258138041\\
Version=x86-Linux-G98RevA.7\HF=-129.251647\S2=0.76921\S2-1=0.\S2A=0.750269\
RMSD=9.289e-10\RMSF=3.417e-05\PG=C*V [C*(N1O1)]\

Zero-point correction = 0.005032 (Hartree/Particle)
Frequencies -- 2208.8782

1\1\GINC-MS6\Freq\UHF\6-311G(d,p)\N1O1(2)\JULIE\13-Nov-2002\0\\#N UHF/6-311G(D,P)
FREQ**HF/6-311G(d,p)** NO Opt and Freq\\0,2\N,0.,0.,-0.5958408647\O,0.,0.,0.5213607567\\
Version=x86-Linux-G98RevA.7\HF=-129.2830534\S2=0.766455\S2-1=0.\S2A=0.750199\
RMSD=1.129e-09\RMSF=2.918e-06\PG=C*V [C*(N1O1)]\

Zero-point correction = 0.005088 (Hartree/Particle)
Frequencies -- 2233.5124

1\1\GINC-MS6\Freq\UHF\6-311+G(d,p)\N1O1(2)\JULIE\13-Nov-2002\0\\#N UHF/6-311+G(D,P)
FREQ**HF/6-311+G(d,p)** NO Opt and Freq\\0,2\N,0.,0.,-0.5961132134\O,0.,0.,0.5215990617\\
Version=x86-Linux-G98RevA.7\HF=-129.2860866\S2=0.767873\S2-1=0.\S2A=0.750234\
RMSD=4.146e-10\RMSF=1.184e-04\ PG=C*V [C*(N1O1)]\

Zero-point correction = 0.005051 (Hartree/Particle)
Frequencies -- 2217.0069

1\1\GINC-MS6\Freq\UHF\6-311+G(2df,p)\N1O1(2)\JULIE\13-Nov-2002\0\\#N UHF/6-311+G
(2DF,P) FREQ**HF/6-311+G(2df,p)** NO Opt and Freq\\0,2\N,0.,0.,-0.5948447335\O,0.,0.,0.5204
891418\\Version=x86-Linux-G98RevA.7\HF=-129.2956266\S2=0.76636\S2-1=0.\S2A=0.750201\
RMSD=2.692e-10\RMSF=1.593e-08\PG=C*V [C*(N1O1)]\

Zero-point correction = 0.005050 (Hartree/Particle)
Frequencies -- 2216.8702

1\1\GINC-MS6\Freq\UMP2-FC\6-31+G(d)\N1O1(2)\JULIE\13-Nov-2002\0\\#N UMP2(FC)/6-31+
G(D) FREQ**MP2/6-31+G(d)** NO Opt and Freq\\0,2\N,0.,0.,-0.6096134672\O,0.,0.,0.5334117838\\
Version=x86-Linux-G98RevA.7\HF=-129.2510307\MP2=-129.5668966\PUHF=-129.256668\PMP2
-0=-129.5712421\S2=0.781349\S2-1=0.766825\S2A=0.750574\RMSD=3.184e-10\RMSF=1.435e
-06\ PG=C*V [C*(N1O1)]\

Zero-point correction = 0.008780 (Hartree/Particle)
Frequencies -- 3854.0850

1\1\GINC-MS6\Freq\UQCISD-FC\6-31+G(d)\N1O1(2)\JULIE\13-Nov-2002\0\\#N UQCISD(FC)/
6-31+G(D) FREQ**QCISD/6-31+G(d)**NO Opt and Freq\\0,2\N,0.,0.,-0.6262334506\O,0.,0.,0.54795
42692\\Version=x86-Linux-G98RevA.7\HF=-129.247314\MP2=-129.5573218\MP3=-129.5571864\
MP4D=-129.5670349\MP4DQ=-129.5622382\PUHF=-129.2589863\PMP2-0=-129.5675342\PMP3-
0=-129.564604\MP4SDQ=-129.5711217\QCISD=-129.5792505\S2=0.885029\S2-1=0.850723\S2A
=0.753531\RMSD=2.994e-10\RMSF=5.408e-05\ PG=C*V[C*(N1O1)]\

Zero-point correction = 0.004398 (Hartree/Particle)
Frequencies -- 1930.2890

1\1\GINC-MS6\Freq\UCCSD-FC\6-31+G(d)\N1O1(2)\JULIE\13-Nov-2002\1\\#N CCSD(FC)/6-31
+G(D) FREQ**CCSD/6-31+G(d)** NO Opt and Freq\\0,2\N\O,1,NO\\NO=1.16627034\\Version=x86
-Linux-G98RevA.7\HF=-129.2484618\MP2=-129.5614508\MP3=-129.5601332\MP4D=-129.57015
34\MP4DQ=-129.5652354\PUHF=-129.2580292\PMP2-0=-129.5696778\PMP3-0=-129.5659891\
MP4SDQ=-129.5735017\CCSD=-129.5763734\S2=0.847301\S2-1=0.819641\S2A=0.752381\
RMSD=8.850e-09\RMSF=4.839e-05\PG=C*V [C*(N1O1)]\

Zero-point correction = 0.004416 (Hartree/Particle)
Frequencies -- 1938.3037

1\1\GINC-MS6\FOpt\UBLYP\6-31+G(d)\N1O1(2)\JULIE\13-Nov-2002\0\\# BLYP/6-31+G(D)
OPT FREQ **BLYP/6-31+G(d)** NO opt and f req\\0,2\N,0.,0.,-0.6265341131\O,0.,0.,0.54821734
9\\Version=x86-Linux-G98RevA.7\HF=-129.8881828\S2=0.751906\S2-1=0.\S2A=0.750003\
RMSD=8.943e-09\RMSF=1.709e-05\Dipole=0.,0.,0.0568264\PG=C*V [C*(N1O1)]\\@

Zero-point correction = 0.004214 (Hartree/Particle)
Frequencies -- 1849.7177

1\1\GINC-MS6\Freq\UB3LYP\6-31+G(d)\N1O1(2)\JULIE\13-Nov-2002\0\\#N UB3LYP/6-31+
G(D) FREQ**B3LYP/6-31+G(d)** NO Opt and Freq\\0,2\N,0.,0.,-0.6174239081\O,0.,0.,0.54024591
96\\Version=x86- Linux-G98RevA.7\HF=-129.8954773\S2=0.753016\S2-1=0.\S2A=0.750006\
RMSD=2.522e-09\RMSF=1.301e-06\ PG=C*V [C*(N1O1)]\

Zero-point correction = 0.004511 (Hartree/Particle)
Frequencies -- 1980.3100

1\1\GINC-MS6\Freq\UB3LYP\6-311++G(3df,2p)\N1O1(2)\JULIE\13-Nov-2002\0\\#N UB3LYP/6-
311++G(3DF,2P) FREQ**B3LYP/6-311++G(3df,2p)** NO Opt and Freq\\0,2\N,0.,0.,-0.6104728533\
O,0.,0.,0.5341637466\\Version=x86-Linux-G98RevA.7\HF=-129.9399026\S2=0.753333\S2-1=0.\
S2A=0.750007\RMSD=1.200e-09\RMSF=8.739e-07\PG=C*V[C*(N1O1)]\

Zero-point correction = 0.004509 (Hartree/Particle)
Frequencies -- 1979.2583

1\1\GINC-MS6\Freq\UB3PW91\6-31+G(d)\N1O1(2)\JULIE\13-Nov-2002\0\\#N UB3PW91/6-31+
G(D) FREQ**B3PW91/6-31+G(d)** NO Opt and Freq\\0,2\N,0.,0.,-0.6156413593\O,0.,0.,0.53868618
94\\Version=x86-Linux-G98RevA.7\HF=-129.8416715\S2=0.752911\S2-1=0.\S2A=0.750006\
RMSD=8.201e-10\RMSF=4.638e-09\PG=C*V [C*(N1O1)]\

Zero-point correction = 0.004578 (Hartree/Particle)
Frequencies -- 2009.2935

Singlet NO^+ Optimizations

1\1\GINC-MS6\Freq\RHF\6-31G(d)\N1O1(1+)\JULIE\12-Nov-2002\0\\#N RHF/6-31G(D) FREQ\\ **HF/6-31G(d)** NO+ Optimization and Frequency\\1,1\N,0.,0.,-0.5549107208\O,0.,0.,0.4855468807\\ Version=x86-Linux-G98RevA.7\State=1-SG\HF=-128.9096528\RMSD=2.598e-10\RMSF=1.716e-06\PG=C*V [C*(N1O1)]\

Zero-point correction = 0.006503 (Hartree/Particle)
Frequencies -- 2854.5484

1\1\GINC-MS6\Freq\RHF\6-31+G(d)\N1O1(1+)\JULIE\12-Nov-2002\0\\#N RHF/6-31+G(D) FREQ\\NO+ **HF/6-31+G(d)** \\1,1\N,0.,0 .,-0.5548359023\O,0.,0.,0.4854814145\\Version=x86-Linux-G98RevA.7\State=1-SG\HF=-128.912488\RMSD=9.382e-10\RMSF=3.531e-05\ PG=C*VC*(N1O1)]\

Zero-point correction = 0.006506 (Hartree/Particle)
Frequencies -- 2856.0189

1\1\GINC-MS6\Freq\RHF\6-31G(d,p)\N1O1(1+)\JULIE\12-Nov-2002\0\\#N RHF/6-31G(D,P) FREQ**HF/6-31G(d,p)** NO+ Opt and Freq\\1,1\N,0.,0.,-0.5549041781\O,0.,0.,0.4855411558\\ Version=x86-Linux-G98RevA.7\State=1-SG\HF=-128.9096528\RMSD=6.338e-10\RMSF=3.253e-05\PG=C*V [C*(N1O1)]\

Zero-point correction = 0.006503 (Hartree/Particle)
Frequencies -- 2854.6763

1\1\GINC-MS6\Freq\RHF\6-31+G(d,p)\N1O1(1+)\JULIE\12-Nov-2002\0\\#N RHF/6-31+G(D,P) FREQ**HF/6-31+G(d,p)** NO+ Opt and Freq\\1,1\N,0.,0.,-0.5548353094\O,0.,0.,0.4854808957\\ Version=x86-Linux-G98RevA.7\State=1-SG\HF=-128.912488\ RMSD=8.636e-10\RMSF=3.251e-05\PG=C*V [C*(N1O1)]\

Zero-point correction = 0.006507 (Hartree/Particle)
Frequencies -- 2856.0305

1\1\GINC-MS6\Freq\RHF\6-311G(d,p)\N1O1(1+)\JULIE\12-Nov-2002\0\\#N RHF/6-311G(D,P) FREQ**HF/6-311G(d,p)** NO+ Opt and Freq\\1,1\N,0.,0.,-0.5486415886\O,0.,0.,0.48006139\\ Version=x86-Linux-G98RevA.7\State=1-SG\HF=-128.9505501\RMSD=7.279e-11\RMSF=7.731 e-07\PG=C*V [C*(N1O1)]\

Zero-point correction = 0.006530 (Hartree/Particle)
Frequencies -- 2866.2256

1\1\GINC-MS6\Freq\RHF\6-311+G(d,p)\N1O1(1+)\JULIE\12-Nov-2002\0\\#N RHF/6-311+G(D,P) FREQ**HF/6-311+G(d,p)** NO+ opt and freq\\1,1\N,0.,0.,-0.5487059996\O,0.,0.,0.4801177497\\ Version=x86-Linux-G98RevA.7\State=1-SG\HF=-128.9524727\RMSD=1.117e-09\RMSF=5.512 e-05\PG=C*V [C*(N1O1)]\

Zero-point correction = 0.006523 (Hartree/Particle)
Frequencies -- 2863.3726

1\1\GINC-MS6\Freq\RHF\6-311+G(2df,p)\N1O1(1+)\JULIE\12-Nov-2002\0\\#N RHF/6-311+G(2D F,P) FREQ**HF/6-311+G(2df,p)** NO+ Opt and Freq\\1,1\N,0.,0.,-0.5473097461\O,0.,0.,0.4788960279\\Version=x86-Linux-G98RevA.7\State=1-SG\HF=-128.9648892\RMSD=1.754e-10\RMSF=1.440e-08\ PG=C*V [C*(N1O1)]\

Zero-point correction = 0.006472 (Hartree/Particle)
Frequencies -- 2840.9575

1\1\GINC-MS6\Freq\RMP2-FC\6-31+G(d)\N1O1(1+)\JULIE\12-Nov-2002\0\\#N RMP2(FC)/6-31+G(D) FREQ**MP2/6-31+G(d)** NO+ Opt and Freq\\1,1\N,0.,0.,-0.5884693376\O,0.,0.,0.5149106704\\Version=x86-Linux-G98RevA.7\State=1-SG\HF=-128.8984042\MP2=-129.2469778\RMSD=2.254e-10\RMSF=6.886e-07\ PG=C*V [C*(N1O1)]\

Zero-point correction = 0.004814 (Hartree/Particle)
Frequencies -- 2113.2245

1\1\GINC-MS6\Freq\RBLYP\6-31+G(d)\N1O1(1+)\JULIE\12-Nov-2002\0\\#N RBLYP/6-31+G(D) FREQ**BLYP/6-31+G(d)** NO+ opt and freq\\1,1\N,0.,0.,-0.5800506822\O,0.,0.,0.507544347\\Version=x86-Linux-G98RevA.7\State=1-SG\HF=-129.5322278\RMSD=1.581e-10\RMSF=1.885e-06\PG=C*V [C*(N1O1)]\

Zero-point correction = 0.005304 (Hartree/Particle)
Frequencies -- 2328.3556

1\1\GINC-MS6\Freq\RB3LYP\6-31+G(d)\N1O1(1+)\JULIE\12-Nov-2002\0\\#N RB3LYP/6-31+G(D) FREQ**B3LYP/6-31+G(d)** NO+ Opt and Freq\\1,1\N,0.,0.,-0.5720933593\O,0.,0.,0.5005816894\\Version=x86-Linux-G98RevA.7\State=1-SG\HF=-129.532154\RMSD=3.242e-10\RMSF=1.460e-06\PG=C*V [C*(N1O1)]\

Zero-point correction = 0.005650 (Hartree/Particle)
Frequencies -- 2480.2367

1\1\GINC-MS6\Freq\RB3PW91\6-31+G(d)\N1O1(1+)\JULIE\12-Nov-2002\0\\#N RB3PW91/6-31+G(D) FREQ**B3PW91/6-31+G(d)** NO+ Opt and Freq\\1,1\N,0.,0.,-0.5710831816\O,0.,0.,0.4996977839\\Version=x86-Linux-G98RevA.7\State=1-SG\HF=-129.4811022\RMSD=8.700e-10\RMSF=2.117e-09\PG=C*V [C*(N1O1)]\

Zero-point correction = 0.005702 (Hartree/Particle)
Frequencies -- 2502.9463

1\1\GINC-MS6\Freq\RQCISD-FC\6-31+G(d)\N1O1(1+)\JULIE\12-Nov-2002\0\\#NRQCISD(FC)/6-31+G(D) FREQ**QCISD/6-31+G(d)** NO+ Opt and Freq\\1,1\N,0.,0.,-0.5778735617\O,0.,0.,0.5056393665\\Version=x86-Linux-G98RevA.7\State=1-SG\HF=-128.9055621\MP2=-129.246033\MP3=-129.2270314\MP4D=-129.2428537\MP4DQ=-129.2375174\MP4SDQ=-129.245944 1\QCISD=-129.2435503\RMSD=2.154e-10\RMSF=1.273e-06\ PG=C*V [C*(N1O1)]\

Zero-point correction = 0.005431 (Hartree/Particle)
Frequencies -- 2383.8292

1\1\GINC-MS6\Freq\RCCSD-FC\6-31+G(d)\N1O1(1+)\JULIE\12-Nov-2002\1\\#NRCCSD(FC)/
6-31+G(D) FREQ**CCSD/6-31+G(d)** NO+ Opt and Freq\\1,1\N,0,0.,0.,B1\O,0,0.,0.,B2\\B1=-
0.60639393\B2=0.47388767\\Version=x86-Linux-G98RevA.7\State=1-SG\HF=-128.9065136\
MP2=-129.245688\MP3=-129.2273093\MP4D=-129.2428642\MP4DQ=-129.2375568\MP4SDQ=
-129.2458138\CCSD=-129.2409088\RMSD=3.874e-09\RMSF=3.741e-04\PG=C*V[C*(N1O1)]\

Zero-point correction = 0.005556 (Hartree/Particle)
Frequencies -- 2438.7903

1\1\GINC-MS6\Freq\RB3LYP\6-311++G(3df,2p)\N1O1(1+)\JULIE\13-Nov-2002\0\\#N RB3LYP
/6-311++G(3DF,2P) FREQ**B3LYP/6- 311++G(3df,2p)** NO+ Opt and Freq\\1,1\N,0.,0.,-0.5633914
555\O,0.,0.,0.4929675235\\Version=x86-Linux-G98RevA.7\State=1-SG\HF=-129.5838367\RMSD
=6.886e-10\RMSF=4.948e-05\ PG=C*V[C*(N1O1)] \

Zero-point correction = 0.005666 (Hartree/Particle)
Frequencies -- 2487.1947

Triplet NO^+ Geometry Optimizations

1\1\GINC-MS6\FOpt\UHF\6-31G(d)\N1O1(1+,3)\JULIE\11-Jul-2003\0\\# HF/6-31G(D) OPT
FREQ=NORAMAN\\NO+ Triplet **HF/6-31G(d)** Opt and Freq\\1 ,3\N,0.,0.,-0.6673717804\O,0.,0.,
0.5839503079\\Version=x86-Linux-G98RevA.7\HF=-128.6849111\S2=2.016124\S2-1=0.\S2A=
2.000117\RMSD=4.128e-09\RMSF=1.685e-04\ PG=C*V [C*(N1O1)]\\

Zero-point correction = 0.003586 (Hartree/Particle)
Frequencies -- 1574.1943

1\1\GINC-MS6\FOpt\UHF\6-31+G(d)\N1O1(1+,3)\JULIE\11-Jul-2003\0\\# HF/6-31+G(D) OPT
FREQ=NORAMAN\\NO+ Triplet Optimization and Frequency **HF/6-31+G(d)**\\1,3\N,0.,0.,-0.667
7089265\O,0.,0.,0.5842453107\\Version=x86-Linux-G98RevA.7\HF=-128.6878838\S2=2.01675\
S2-1=0.\S2A=2.000126\RMSD=4.565e-09\RMSF=1.647e-07\ PG=C*V [C*(N1O1)]\\

Zero-point correction = 0.003573 (Hartree/Particle)
Frequencies -- 1568.5397

1\1\GINC-MS6\FOpt\UHF\6-31G(d,p)\N1O1(1+,3)\JULIE\11-Jul-2003\0\\# HF/ 6-31G(D,P) OPT
FREQ=NORAMAN**HF/6-31G(d,p)** Triplet NO+ Opt and Freq\\1,3\N,0., 0.,-0.6369269884\O,0.,
0.,0.5573111148\\Version=x86-Linux-G98RevA.7\HF= -128.6882158\S2=2.565384\S2-1=0.\S2A=
2.010254\RMSD=2.749e-09\RMSF=7.63 9e-05\PG=C*V [C*(N1O1)]\\

Zero-point correction = 0.002940 (Hartree/Particle)
Frequencies -- 1290.7147

1\1\GINC-MS6\FOpt\UHF\6-31+G(d,p)\N1O1(1+,3)\JULIE\11-Jul-2003\0\\# HF/6-31+G(D,P) OPT
FREQ=NORAMAN**HF/6-31+G(d,p)** NO+ Triplet Opt and Freq\\1,3\N,0.,0.,-0.6369269884\O,0.,
0.,0.5573111148\\Version=x86-Linux-G98RevA.7\HF=-128.6912112\S2=2.567195\S2-1=0.\
S2A=2.010407\RMSD=2.390e-09\RMSF=1.023e-04\ PG=C*V [C*(N1O1)]\\

Zero-point correction = 0.002937 (Hartree/Particle)
Frequencies -- 1289.3204

1\1\GINC-MS6\FOpt\UHF\6-311G(d,p)\N1O1(1+,3)\JULIE\11-Jul-2003\0\\# HF /6-311G(D,P) OPT FREQ=NORAMAN**HF/6-311G(d,p)** NO+ Opt and Freq\\1,3\N,0.,0.,-0.6300321755\O,0.,0.,0.5512781535\\Version=x86-Linux-G98RevA.7\HF=-128.7233831\S2=2.54868\S2-1=0.\S2A=2.009489\RMSD=2.549e-09\RMSF=1.811e-06\\PG=C*V [C*(N1O1)]\\

Zero-point correction= 0.002987 (Hartree/Particle)
Frequencies -- 1311.1557
1\1\GINC-MS6\FOpt\UHF\6-311+G(d,p)\N1O1(1+,3)\JULIE\11-Jul-2003\0\\# HF/6-311+G(D,P) OPT FREQ=NORAMAN**HF/6-311+G(d,p)** NO+ Opt and Freq\\1,3\N ,0.,0.,-0.6308849834\O,0.,0.,0.5520243605\\Version=x86-Linux-G98RevA.7\HF=-128.7259312\S2=2.553755\S2-1=0.\S2A=2.009542\RMSD=2.525e-09\RMSF= 1.412e-04\PG=C*V [C*(N1O1)]\\

Zero-point correction = 0.002960 (Hartree/Particle)
Frequencies -- 1299.4385

1\1\GINC-MS6\FOpt\UHF\6-311+G(2df,p)\N1O1(1+,3)\JULIE\11-Jul-2003\0\\# **HF/6-311+G(2DF,P)** OPT FREQ=NORAMAN\\HF/6-311+G(2df,p) NO+ Opt and Freq\\1,3\N,0.,0.,-0.6281104682\O,0.,0.,0.5495966597\\Version=x86-Linux-G98RevA.7\HF=-128.7354808\S2=2.536051\S2-1=0.\S2A=2.010625\RMSD=4.902e-09\RMSF=2.317e-06\\PG=C*V [C*(N1O1)]\\

Frequencies -- 1317.5893
Zero-point correction = 0.003002 (Hartree/Particle)

1\1\GINC-MS6\FOpt\UMP2-FC\6-31+G(d)\N1O1(1+,3)\JULIE\27-Mar-2003\0\\#MP2/6-31+G(D) OPT FREQ=NORAMAN \\NO+ **MP2**/6-31+G(d)\\1,3\N,0.,0.,-0.6028172178\O,0.,0.,0.5274650655\\Version=x86-Linux- G98RevA.7\HF=-128.6868068\MP2=-128.9243584\PUHF=-128.705617\PMP2-0=-128.9416997\S2=2.411373\S2-1=2.346421\S2A=2.006769\RMSD=2.628e-09\RMSF=1.162e-05\ PG=C*V [C*(N1O1)]\\

Zero-point correction = 0.004069 (Hartree/Particle)
Frequencies -- 1786.0394

1\1\GINC-MS6\FOpt\UQCISD-FC\6-31+G(d)\N1O1(1+,3)\JULIE\11-Jul-2003\0\\ # **QCISD/6-31+G(D)** OPT FREQ\\QCISD/6-31+G(d) NO+ Opt and Freq\\1,3\N,0.,0.,-0.6304359857\O,0.,0.,0.5516314875\\Version=x86-Linux-G98RevA.7\HF=-128.691077\MP2=-128.9209872\MP3=-128.9326138\MP4D=-128.9391517\MP4DQ=-128.936128\PUHF=-128.7106332\PMP2-0=-128.9393755\PMP3-0=-128.9484894\MP4SDQ=-128.9470499\QCISD=-128.9837773\S2=2.54039\S2-1=2.475071\S2A=2.009735\RMSD=5.660e-09\RMSF=1.163e-04\PG=C*V [C*(N1O1)]\\

Zero-point correction= 0.003999 (Hartree/Particle)
Frequencies -- 1755.2851

1\1\GINC-MS6\POpt\UCCSD-FC\6-31+G(d)\N1O1(1+,3)\JULIE\11-Jul-2003\1\\# CCSD/6-31+G(D) OPT FREQ**CCSD/6-31+G(d)** NO+ Opt and Freq\\1,3\N,0,0.,0.,B1\O,0,0.,0.,B2\\B1=-0.65717587\B2=0.52451425\\Version=x86-Linux-G98RevA.7\HF=-128.6910684\MP2=-128.9210306\MP3=-128.9326433\MP4D=-128.939182\MP4DQ=-128.9361588\PUHF=-128.7106265\PMP2-0=-128.9394183\PMP3-0=-128.9485137\MP4SDQ=-128.9470814\CCSD=-128.9794625\S2=2.539537\S2-1=2.474195\S2A=2.009714\RMSD=4.452e-09\RMSF=7.977e-05\PG=C*V[C*(N1O1)]\\

Zero-point correction = 0.004037 (Hartree/Particle)

Frequencies -- 1771.9932

1\1\GINC-MS6\FOpt\UBLYP\6-31+G(d)\N1O1(1+,3)\JULIE\11-Jul-2003\0\\# BLYP/6-31+G(D) OPT FREQ **BLYP/6-31+G(d)** NO+ opt and freq\\1,3\N,0.,0.,-0.6335216684\O,0.,0.,0.5543314599 \\Version=x86-Linux-G98RevA.7\HF=-129.2850496\S2=2.007169\S2-1=0.\S2A=2.000022\RMSD= 1.456e-09\RMSF=2.530e-06\ \PG=C*V [C*(N1O1)]\\

Zero-point correction= 0.003966 (Hartree/Particle)
Frequencies -- 1740.7114

1\1\GINC-MS6\FOpt\UB3LYP\6-31+G(d)\N1O1(1+,3)\JULIE\11-Jul-2003\0\\# B3LYP/6-31+G(D) OPT FREQ**B3LYP/6-31+G(d)** NO+ Opt and Freq\\1,3\N,0.,0.,-0.6240928511\O,0.,0.,0.54608124 47\\Version=x86-Linux-G98RevA.7\HF=-129.2784662\S2=2.013854\S2-1=0.\S2A=2.000073\ RMSD=8.150e-09\RMSF=3.236e-07\\PG=C*V [C*(N1O1)]\\

Zero-point correction= 0.004183 (Hartree/Particle)
Frequencies -- 1836.2472

1\1\GINC-MS6\FOpt\UB3LYP\6-311++G(3df,2p)\N1O1(1+,3)\JULIE\11-Jul-2003 \0\\# B3LYP/6-311++G(3DF,2P) OPT FREQ**B3LYP/6-311++G(3df,2p)** NO+ Opt and Freq\\1,3\N,0.,0.,-0.6173 744112\O,0.,0.,0.5402026098\\Version=x86- Linux-G98RevA.7\HF=-129.3233474\S2=2.013979\ S2-1=0.\S2A=2.000076\RMSD= 4.674e-10\RMSF=8.810e-07\ PG=C*V [C*(N1O1)]\\

Zero-point correction= 0.004189 (Hartree/Particle)
Frequencies -- 1838.9314

C_6H_6 Geometry Optimizations

1\1\GINC-MS6\FOpt\RHF\6-31G(d)\C6H6\JULIE\12-Nov-2002\0\\# **HF/6-31G(D)** OPT FREQ= NORAMAN\\HF/6-31G(d) C6H6 Opt and Freq\\0,1\C,-1.2005710335, 0.0005460621,-0.693273806 8\C,-1.2006428669,0.0010494266,0.6931594667\C,-0.0001126766,0.0004330617,1.3863630982\C, 1.200611284,-0.0005358975,0.6932040286\C,1.200682759,-0.0009793864,-0.6930899212\C,0.000 0320163,-0.0004871057,-1.3863633889\H,-2.1319426295,0.0009614232,-1.231001637\H,-2.13207 00048,0.0017405111,1.2307937331\H,-0.0001063687,0.0007220803,2.4618200799\H,2.131924828 ,-0.001011175,1.2310335164\H,2.132053551,-0.0017256457,-1.230823064\H,0.0001437306,-0.000 8441586,-2.4618194876\\Version=x86-Linux-98RevA.7\HF=-230.7031367\RMSD=4.661e-09\ RMSF=1.381e-04\ PG=C01 [X(C6H6)]\\

Zero-point correction= 0.107667 (Hartree/Particle)

Frequencies --	453.6081	453.6130	665.4120
Frequencies --	665.4147	763.7874	777.1646
Frequencies --	960.9217	960.9262	1083.4223
Frequencies --	1096.5274	1099.8426	1099.8466
Frequencies --	1136.0101	1141.6266	1141.6359
Frequencies --	1196.2470	1293.7765	1293.7800
Frequencies --	1350.6629	1507.6191	1651.6050
Frequencies --	1651.6096	1796.5985	1796.6110
Frequencies --	3350.0623	3361.0136	3361.0222
Frequencies --	3379.4272	3379.4351	3391.2775

1\1\GINC-MS6\FOpt\RHF\6-31+G(d)\C6H6\JULIE\12-Nov-2002\0\\# **HF/6-31+G(D)** OPT FREQ =NORAMAN \\HF/6-31+G(d) Benzene Opt and Freq\\0,1\C,-1.2024199886,0.0005494135,-0.6943223326\C,-1.2024882674,0.0009652093,0.6942004052\C,-0.0000896066,0.0004530641,1.38848629 1\C,1.2024409853,-0.0005535301,0.694286049\C,1.2025091703,-0.0010011658,-0.6941641192\ C,0.0000476925,-0.0004232141,-1.3884863064\H,-2.1340296997,0.0009861312,-1.2322166919\H, -2.1341523564,0.001753092,1.2319996993\H,-0.0001113007,0.0008175119,2.4642310009\H,2.13 40202891,-0.000966273,1.2322329298\H,2.1341430046,-0.0017646041,-1.23201578\H,0.00013014 87,-0.0007645188,-2.4642310805\\Version=x86-Linux-G98RevA.7\HF=-230.7110917\RMSD=6.05 0e-09\RMSF=1.358e-04\=-0.0000003,0.0000217,0.0000002\PG=C01 [X(C6H6)]\\

Zero-point correction= 0.107542 (Hartree/Particle)

Frequencies --	451.8608	451.8616	663.5520
Frequencies --	663.5524	761.3933	775.6352
Frequencies --	961.0943	961.0946	1075.4003
Frequencies --	1096.4415	1109.0170	1109.0175
Frequencies --	1136.4174	1136.4195	1142.0688
Frequencies --	1200.3276	1291.3712	1291.3719
Frequencies --	1352.7951	1506.4336	1644.0966
Frequencies --	1644.0973	1784.6840	1784.6854
Frequencies --	3348.6201	3359.3836	3359.3847
Frequencies --	3377.4057	3377.4067	3388.3772

1\1\GINC-MS6\FOpt\RHF\6-31G(d,p)\C6H6\JULIE\13-Nov-2002\0\\# **HF/6-31G(D,P)** OPT FREQ =NORAMAN \\HF/6-31G(d,p) C6H6 Opt and Freq\\0,1\C,-1.2001842896,0.0005477338,-0.6930147473\C,-1.2002534968,0.0009874109,0.6928943385\C,-0.0000759208,0.000443161,1.3858974439\ C,1.2001910079,-0.0005478972,0.6930031291\C,1.200260211,-0.000990514,-0.6928827199\C,0.00 00624831,-0.0004401677,-1.3858974452\H,-2.1319692287,0.0009732808,-1.2310326288\H,-2.132 0922171,0.0017552661,1.2308186675\H,-0.0001201264,0.0007859867,2.4618558361\H,2.1319665 258,-0.0009727995,1.2310373515\H,2.132089515,-0.0017578712,-1.2308233848\H,0.000125563, -0.000782224,-2.4618558356\\Version=x86-Linux-G98RevA.7\HF=-230.71386\RMSD=4.200e-09 \RMSF=4.979e-06\\PG=C01 [X(C6H6)]\\

Zero-point correction= 0.107320 (Hartree/Particle)

Frequencies --	452.9321	452.9321	665.0981
Frequencies --	665.0981	763.6220	777.7824
Frequencies --	960.5799	960.5800	1083.2471
Frequencies --	1095.8122	1101.7992	1101.7992
Frequencies --	1135.5062	1139.1269	1139.1270
Frequencies --	1192.2030	1288.0355	1288.0356
Frequencies --	1349.6795	1500.6283	1646.0107
Frequencies --	1646.0108	1795.2471	1795.2471
Frequencies --	3331.4529	3342.6488	3342.6489
Frequencies --	3361.1110	3361.1110	3373.0773

1\1\GINC-MS6\FOpt\RHF\6-31+G(d,p)\C6H6\JULIE\13-Nov-2002\0\\# **HF/6-31+ G(D,P)** OPT FREQ=NORAMAN SYMM=LOOSE\\HF/6-31+G(d,p) C6H6 Opt and Freq \\0,1\C,1.3822666775, 0.1297328796,0.\C,0.5787813693,1.2619444973,0.\C,-0.8034853081,1.1322116177,0.\C,-1.382266 6775,-0.1297328796,0.\C,-0.5787813693,-1.2619444973,0.\C,0.8034853081,-1.1322116177,0.\H,2.

4533580186,0.2302603438,0.\H,1.0272677021,2.2398005406,0.\H,-1.4260903165,2.0095401968,0.\H,-2.4533580186,-0.2302603438,0.\H,-1 .0272677021,-2.2398005406,0.\H,1.4260903165,-2.0095401968,0.\\Version= x86-Linux-G98RevA.7\HF=-230.7218314\RMSD=6.282e-09\RMSF=1.624e-04\ PG=D06H [3C2'(H1C1.C1H1)]\\

Zero-point correction = 0.107178 (Hartree/Particle)

Frequencies --	451.2287	451.2771	662.9327
Frequencies --	662.9385	758.9722	776.9693
Frequencies --	958.2890	958.2892	1074.3477
Frequencies --	1095.5651	1105.8631	1105.8797
Frequencies --	1132.9968	1132.9991	1136.2045
Frequencies --	1194.5558	1284.4938	1284.4996
Frequencies --	1350.4515	1498.1421	1637.3621
Frequencies --	1637.3624	1781.8747	1781.8775
Frequencies --	3335.1945	3346.1093	3346.1114
Frequencies --	3363.9510	3363.9534	3374.8383

1\1\GINC-MS6\FOpt\RHF\6-311G(d,p)\C6H6\JULIE\13-Nov-2002\0\\# **HF/6-311G(D,P)** OPT FREQ=NORAMAN \\HF/6-311G(d,p) C6H6 Opt and Freq\\0,1\C,1.3796715949,0.1294893176,0.\C,0.5776947589,1.2595753089,0.\C,-0.8019768361,1.1300859913,0.\C,-1.3796715949,-0.1294893176,0.\C,-0.5776947589,-1.2595753089,0.\C,0.8019768361,-1.1300859913,0.\H,2.4506227539,0.230003625,0.\H,1.0261223947,2.2373033725,0.\H,-1.4245003592,2.0072997474,0.\H,-2.4506227539,-0.230003625,0.\H,-1.0261223947,- 2.2373033725,0.\H,1.4245003592,-2.0072997474,0.\\Version=x86-Linux-G98 RevA.7\State=1-A1G\HF=-230.7540968\RMSD=6.212e-09\RMSF=1.501e-04\ PG=D06H [3C2'(H1C1.C1H1)]\\

Zero-point correction = 0.106565 (Hartree/Particle)

Frequencies --	451.2348	451.2348	663.3869
Frequencies --	663.3869	757.4661	774.0313
Frequencies --	954.5858	954.5858	1071.8503
Frequencies --	1091.2460	1098.5614	1098.5614
Frequencies --	1125.3794	1129.1768	1129.1768
Frequencies --	1174.4635	1279.6812	1279.6812
Frequencies --	1335.5844	1491.3903	1631.2044
Frequencies --	1631.2044	1777.5668	1777.5668
Frequencies --	3310.0445	3321.4424	3321.4424
Frequencies --	3339.9809	3339.9809	3351.7272

1\1\GINC-MS6\FOpt\RHF\6-311+G(d,p)\C6H6\JULIE\13-Nov-2002\0\\# **HF/6-311+G(D,P)** OPT FREQ=NORAMAN \\HF/6-311+G(d,p) C6H6 Opt and Freq\\0,1\C,1.380216469,0.1295404569,0.\C,0.577922908,1.2600727534,0.\C,-0.802293561,1.1305322965,0.\C,-1.380216469,-0.1295404569,0.\C,-0.577922908,-1.2600727534,0.\C,0.802293561,-1.1305322965,0.\H,2.4511273715,0.230050986,0.\H,1.0263336877,2.2377640646,0.\H,-1.4247936838,2.0077130786,0.\H,-2.4511273715,-0.230050986,0.\H,-1.0263336877,-2.2377640646,0.\H,1.4247936838,-2.0077130786,0.\\Version=x86-Linux-G98RevA.7\HF=-230.7567737\RMSD=9.670e-09\RMSF=3.371e-05\=0.,0.,0.\PG=D06H [3C2'(H1C1.C1H1)]\\

Zero-point correction = 0.106509 (Hartree/Particle)

Frequencies --	448.5271	448.5368	661.9934
Frequencies --	661.9942	754.9665	768.0567
Frequencies --	953.3416	953.3476	1069.3779
Frequencies --	1090.6013	1099.9744	1099.9774
Frequencies --	1122.9384	1127.7517	1127.7527
Frequencies --	1179.5638	1279.5082	1279.5183
Frequencies --	1337.6901	1491.1425	1628.6757
Frequencies --	1628.6788	1773.2367	1773.2393
Frequencies --	3311.5514	3322.9152	3322.9154
Frequencies --	3341.1081	3341.1088	3352.2626

1\1\GINC-MS6\FOpt\RHF\6-311+G(2df,p)\C6H6\JULIE\13-Nov-2002\0\\# **HF/6-311+G(2DF,P)** OPT FREQ=NORAMAN \\HF/6-311+G(2df,p) C6H6 Opt and Freq\\0,1\C,1.3764374697,0.1291857783,0.\C,0.5763405691,1.2566227046,0.\C,-0.8000969006,1.1274369263,0.\C,-1.3764374697,-0.1291857783,0.\C,-0.5763405691,-1.2566227046,0.\C,0.8000969006,-1.1274369263,0.\H,2.446371778,0.229604649,0.\H,1.0243424302,2.2334224313,0.\H,-1.4220293478,2.0038177824,0.\H,-2.446371778,-0.229604649,0.\H,-1.0243424302,-2.2334224313,0.\H,1.4220293478,-2.0038177824,0.\\Version=x86-Linux-G98RevA.7\HF=-230.7721263\RMSD=8.113e-09\RMSF=7.332e-06\PG=D06H [3C2'(H1C1.C1H1)]\\

Zero-point correction = 0.106449 (Hartree/Particle)

Frequencies --	449.7364	449.7481	662.5815
Frequencies --	662.6139	757.2465	764.7777
Frequencies --	954.7299	954.7380	1071.2314
Frequencies --	1094.1883	1099.0357	1099.0976
Frequencies --	1118.9215	1128.2146	1128.2305
Frequencies --	1172.9061	1281.5541	1281.5562
Frequencies --	1337.0544	1496.9010	1633.2976
Frequencies --	1633.3150	1771.1819	1771.1849
Frequencies --	3304.9638	3316.1669	3316.1729
Frequencies --	3334.3584	3334.3734	3345.6477

1\1\GINC-MS6\FOpt\RMP2-FC\6-31+G(d)\C6H6\JULIE\13-Nov-2002\0\\# **MP2/6-31+G(D)** OPT FREQ \\MP2/6-31+G(d) C6H6 Opt and Freq\\0,1\C,1.3930728436,0.1307470942,0.\C,0.5833061168,1.2718100189,0.\C,-0.8097667268,1.1410629248,0.\C,-1.3930728436,-0.1307470942,0.\C,-0.5833061168,-1.2718100189,0.\C,0.8097667268,-1.1410629248,0.\H,2.4764091888,0.2324238154,0.\H,1.0369196658,2.2608451754,0.\H,-1.439489523,2.02842136,0.\H,-2.4764091888,-0.2324238154,0.\H,-1.0369196658,-2.2608451754,0.\H,1.439489523,-2.02842136,0.\\Version=x86-Linux-G98RevA.7\HF=-230.7096698\MP2=-231.4720037\RMSD=3.304e-09\RMSF=5.218e-06\PG=D06H [3C2'(H1C1.C1H1)]\\

Zero-point correction = 0.099424 (Hartree/Particle)

Frequencies --	274.1393	379.2164	379.2660
Frequencies --	617.9440	617.9594	672.1144
Frequencies --	828.6587	828.6657	858.9304
Frequencies --	877.3254	877.3355	1018.9613
Frequencies --	1019.8655	1076.9226	1076.9229
Frequencies --	1205.4093	1224.9849	1224.9951
Frequencies --	1388.7623	1464.1589	1529.7477

Frequencies -- 1529.7571 1660.1589 1660.1701
Frequencies -- 3207.7560 3217.5511 3217.5512
Frequencies -- 3232.6456 3232.6501 3241.7324

1\1\GINC-MS6\FOpt\RQCISD-FC\6-31+G(d)\C6H6\JULIE\16-Dec-2002\0\\# **QCISD/6-31+G(D)** OPT FREQ SYMM=LOOSE\\QCISD/6-31+g(d) C6H6 Opt and Freq\\0,1\C,1.3937811257,0.13081 35701,0.\C,0.583602688,1.2724566472,0.\C,-0.8101784377,1.1416430771,0.\C,-1.3937811257,-0.1 308135701,0.\C,-0.583602688,-1.2724566472,0.\C,0.8101784377,-1.1416430771,0.\H,2.478724754 6,0.2326411432,0.\H,1.0378892374,2.2629591781,0.\H,-1.4408355173,2.0303180349,0.\H,-2.4787 247546,-0.2326411432,0.\H,-1.0378892374,-2.2629591781,0.\H,1.4408355173,-2.0303180349,0.\\ Version=x86-Linux-G98RevA.7\HF=-230.7093885\MP2=-231.4719905\MP3=-231.499378\MP4D= -231.5191734\MP4DQ=-231.4984492\MP4SDQ=-231.5062577\QCISD=-231.5092682\RMSD=4.6 68e-10\RMSF=3. 283e-05\PG=D06H [3C2'(H1C1.C1H1)]\\

1\1\GINC-MS7\POpt\RCCSD-FC\6-31+G(d)\C6H6\JULIE\16-Jan-2003\1\\# **CCSD/6-31+G(D)** OPT NOSYMM\\CCSD/6-31+g(d) C6H6 Opt\\0,1\C,0,1.3930728446,0.1307470942,A\C,0,0.58330 61168,1.2718100189,0.\C,0,-0.8097667268,1.1410629248,0.\C,0,-1.3930728436,-0.1307470942,0. \C,0,-0.5833061168,-1.2718100189,0.\C,0,0.8097667268,-1.1410629248,0.\H,0,2.4764091888,0.23 24238154,0.\H,0,1.0369196658,2.2608451754,0.\H,0,-1.439489523, 2.02842136,0.\H,0,-2.4764091 788,-0.2324238154,0.\H,0,-1.0369196658,-2.2608451754,0.\H,0,1.439489523,-2.02842136,0.\\A=0. \\Version=x86-Linux-G98RevA.7\HF= -230.7096702\MP2=-231.4720274\MP3=-231.4994435\MP4 D=-231.5191965\MP4DQ=-231.4984987\MP4SDQ=-231.5062852\CCSD=-231.5076662\RMSD= 1.648e-09\RMSF=1.967e-07\PG=D06H [3C2'(H1C1.C1H1)]\\

1\1\GINC-MS6\FOpt\RBLYP\6-31+G(d)\C6H6\JULIE\13-Nov-2002\0\\# **BLYP/6-31+G(D)**OPT FREQ \\BLYP/6-31+G(d) C6H6 Opt and Freq\\0,1\C,1.4027602208,0.1316563046,0.\C,0.58736240 6,1.2806541389,0.\C,-0.8153978148,1.1489978343,0.\C,-1.4027602208,-0.1316563046,0.\C,-0.587 362406,-1.2806541389,0.\C,0.8153978148,-1.1489978343,0.\H,2.4926385437,0.2339470243,0.\H, 1.0437152057,2.2756618134,0.\H,-1.448923338,2.0417147891,0.\H,-2.4926385437,-0.2339470243 ,0.\H,-1.0437152057,-2.2756618134,0.\H,1.448923338,-2.0417147891,0.\\Version=x86-Linux-G98 RevA.7\HF=-232.1446008\RMSD=5.184e-09\RMSF=4.503e-05\PG=D06H[3C2'(H1C1.C1H1)]\\

Zero-point correction = 0.097558 (Hartree/Particle)

Frequencies -- 398.4261 399.2040 604.5358
Frequencies -- 604.5458 665.8038 688.6689
Frequencies -- 830.0015 832.7310 937.9245
Frequencies -- 939.6106 972.5524 979.7416
Frequencies -- 993.5578 1030.9352 1031.4029
Frequencies -- 1156.4358 1172.7033 1172.9287
Frequencies -- 1324.0735 1346.3751 1476.5232
Frequencies -- 1476.9373 1581.8304 1581.8797
Frequencies -- 3086.3840 3095.9455 3095.9887
Frequencies -- 3111.6299 3111.6627 3121.9815

1\1\GINC-MS6\FOpt\RB3LYP\6-31+G(d)\C6H6\JULIE\13-Nov-2002\0\\# **B3LYP/6-31+G(D)**OPT FREQ \\B3LYP/6-31+G(d) C6H6 Opt and req\\0,1\C,1.3924621776,0.13068978,0.\C,0.583050419 3,1.2712525096,0. \C,-0.8094117583,1.1405627296,0.\C,-1.3924621776,-0.13068978,0.\C,-0.58305 04193,-1.2712525096,0.\C,0.8094117583,-1.1405627296,0.\H,2.4749866218,0.2322903001,0.\H,1. 03632401,2.2595464386,0.\H,-1.4386626119,2.0272561385,0.\H,-2.4749866218,-0.2322903001,0.\ H,-1.03632401,-2.2595464386,0.\H,1.4386626119,-2.0272561385,0.\\Version=x86-Linux-G98Rev

A.7\HF=-232.2589297\RMSD=4.556e-09\RMSF=2.143e-5\PG=D06H[3C2'(H1C1.C1H1)]\\

Zero-point correction = 0.100580 (Hartree/Particle)

Frequencies --	411.9213	412.5845	620.4382
Frequencies --	620.4412	688.9211	712.0485
Frequencies --	862.0629	864.2315	980.1892
Frequencies --	981.5250	1013.9124	1014.0396
Frequencies --	1020.5120	1064.0624	1064.4095
Frequencies --	1183.6804	1204.6728	1204.8606
Frequencies --	1354.5212	1385.5957	1522.6682
Frequencies --	1522.9794	1645.5087	1645.5274
Frequencies --	3173.8503	3183.4376	3183.4499
Frequencies --	3199.1038	3199.1406	3209.1543

1\1\GINC-MS6\FOpt\RB3LYP\6-311++G(3df,2p)\C6H6\JULIE\14-Nov-2002\0\\#B3LYP/6-311++G(3DF,2P) OPT FREQ **B3LYP/6-311++G(3df,2p)** C6H6 Opt and Freq\\0,1\C,1.3849559354,0.1299852803,0.\C,0.5799074128,1.2643996634,0.\C,-0.8050485226,1.134414383,0.\C,-1.3849559354,-0.1299852803,0.\C,-0.5799074128,-1.2643996634,0.\C,0.8050485226,-1.134414383,0.\H,2.4623999382,0.2311089747,0.\H,1.031053726,2.2480553882, 0.\H,-1.4313462123,2.0169464134,0.\H,-2.4623999382,-0.2311089747,0.\H,-1.031053726,-2.2480553882,0.\H,1.4313462123,-2.0169464134,0.\\Version =x86-Linux-G98RevA.7\HF=-232.3277783\RMSD=8.611e-09\RMSF=2.088e-05\PG=D06H [3C2'(H1C1.C1H1)]\\

Zero-point correction = 0.099858 (Hartree/Particle)

Frequencies --	410.7063	411.4467	619.6993
Frequencies --	619.7002	690.6179	691.6652
Frequencies --	865.1958	867.6768	945.6387
Frequencies --	987.2218	988.2538	997.2125
Frequencies --	1012.8507	1059.7830	1060.1000
Frequencies --	1175.3441	1198.6562	1198.8467
Frequencies --	1332.4750	1383.9973	1513.3484
Frequencies --	1513.6151	1631.3049	1631.3634
Frequencies --	3150.1199	3163.5581	3163.5645
Frequencies --	3179.4237	3179.4747	3189.5217

1\1\GINC-MS6\FOpt\RB3PW91\6-31+G(d)\C6H6\JULIE\14-Nov-2002\0\\# **B3PW91 /6-31+G(D)** OPT FREQ \\B3PW91/6-31+G(d) C6H6 Opt and Freq\\0,1\C,1.3896999553,0.1304305312,0.\C,0.5818938243,1.2687307305,0.\C,-0.8078061311,1.1383001994,0.\C,-1.3896999553,-0.1304305312,0.\C,-0.5818938243,-1.2687307305,0.\C,0.8078061311,-1.1383001994,0.\H,2.472481618,0.2320551925,0.\H,1.0352751172,2.2572594879,0.\H,-1.43720650 08,2.0252042953,0.\H,-2.472481618,-0.2320551925,0.\H,-1.0352751172,-2. 2572594879,0.\H,1.4372065008,-2.0252042953,0.\\Version=x86-Linux-G98RevA.7\HF=-232.1666129\RMSD=1.745e-09\RMSF=8.261e-05\PG=D06H[3C2'(H1C1.C1H1)]\\

Zero-point correction = 0.100875 (Hartree/Particle)

Frequencies --	408.5398	409.2872	616.6687
Frequencies --	616.6791	687.4282	714.3823
Frequencies --	862.6003	864.2551	981.9297

Frequencies --	982.9048	1015.1451	1015.5496
Frequencies --	1023.0159	1069.9121	1070.1317
Frequencies --	1183.0832	1205.7293	1205.9703
Frequencies --	1378.2006	1380.4153	1523.7208
Frequencies --	1523.9390	1659.6502	1659.7813
Frequencies --	3185.6548	3195.3384	3195.3822
Frequencies --	3211.2424	3211.2654	3221.3338

$C_6H_6^+$ Geometry Optimizations

1\1\GINC-MS6\FOpt\UHF\6-31G(d)\C6H6(1+,2)\JULIE\14-Nov-2002\0\\# HF/6-31G(D) OPT FREQ=NORAMAN**HF/6-31G(d)** C6H6+ Opt and Freq\\1,2\C,-1.218761279,0.0005631331,-0.6664403591\C,-1.2403117176,0.0010199072,0.7160391815\C,-0.0324051677,0.0004692233,1.3887265202\C,1.2187797782,-0.0005758875,0.6664268967\C,1.2403153991,-0.0010262648,-0.7160328826\C,0.0323841957,-0.0004506378,-1.3887170407\H,-2.1350045636,0.0009624343,-1.2275507317\H,-2.1693334326,0.001781417,1.2522996863\H,-0.0046481564,0.0008042736,2.4627724504\H,2.1350064036,-0.0009831592,1.2275638286\H,2.1693138054,-0.0017916545,-1.2523350018\H,0.0046586925,-0.0007701527,-2.4627641282\\Version=x86-Linux-G98RevA.7\HF=-230.4229627\S2=0.867046\S2-1=0.\S2A=0.75754\RMSD=8.503e-09\RMSF=9.820e-05\PG=C01 [X(C6H6)]\\

Zero-point correction = 0.105014 (Hartree/Particle)

Frequencies --	344.5870	365.9012	453.2325
Frequencies --	532.9327	642.1385	750.1760
Frequencies --	927.4033	982.6978	990.3096
Frequencies --	1032.6390	1050.2054	1062.2905
Frequencies --	1106.1699	1117.0236	1117.2072
Frequencies --	1137.7346	1284.6187	1293.9216
Frequencies --	1461.4318	1501.9314	1513.1443
Frequencies --	1569.7235	1653.2031	1730.6441
Frequencies --	3398.2138	3404.7197	3408.7036
Frequencies --	3413.2243	3423.0506	3426.4816

1\1\GINC-MS6\FOpt\UHF\6-31+G(d)\C6H6(1+,2)\JULIE\15-Nov-2002\0\\# HF/6-31+G(D) OPT FREQ=NORAMAN **HF/6-31+G(d)** C6H6 opt and freq\\1,2\C,-1.2196482286,0.0005693504,-0.6672251832\C,-1.2410381654,0.0010222138,0.7164513267\C,-0.0321505925,0.0004616122,1.3898745189\C,1.2196537619,-0.0005646855,0.6672198933\C,1.2410402148,-0.0010222991,-0.7164477749\C,0.0321432567,-0.0004670984,-1.3898723901\H,-2.1361254399,0.0009748444,-1.2284554813\H,-2.1702404895,0.0017870759,1.252839066\H,-0.0044281142,0.0007896057,2.4641835314\H,2.1361230423,-0.000976234,1.2284623415\H,2.1702342179,-0.0017876092,-1.2528497499\H,0.0044355302,-0.0007822431,-2.4641822073\\Version=x86-Linux-G98RevA.7\HF=-230.4253056\S2=0.866539\S2-1=0.\S2A=0.757472\RMSD=8.308e-09\RMSF=5.933e-05\\PG=C01 [X(C6H6)]\\

Zero-point correction = 0.104833 (Hartree/Particle)

Frequencies --	341.9704	365.5311	452.5872
Frequencies --	526.3006	641.2242	749.2203
Frequencies --	924.5642	982.6992	987.7469
Frequencies --	1028.8799	1046.5245	1062.0012
Frequencies --	1102.1032	1109.2744	1113.7455
Frequencies --	1135.1041	1282.9921	1291.9513

Frequencies -- 1458.2203 1499.7567 1511.5076
Frequencies -- 1567.9476 1649.2804 1725.4600
Frequencies -- 3395.9278 3402.1906 3406.2681
Frequencies -- 3410.7559 3420.6967 3424.0638

1\1\GINC-MS6\FOpt\UHF\6-31G(d,p)\C6H6(1+,2)\JULIE\18-Nov-2002\0\\# **HF/6-31G(D,P)** OPT FREQ=NORAMAN \\HF/6-31+G(d) C6H6 opt and freq\\1,2\C,-1.2183021895,0.0005649092,-0.6660585966\C,-1.2401595737,0.0010209452,0.7159386126\C,-0.0324794521,0.0004652278,1.3881201257\C,1.2183041381,-0.0005704885,0.6660565885\C,1.2401604632,-0.0010215955,-0.7159370755\C,0.0324767378,-0.0004584554,-1.3881194393\H,-2.1351196123,0.0009723884,-1.2274989828\H,-2.1692517063,0.0017854172,1.252272287\H,-0.0047574733,0.0007888698,2.4628294131\H,2.1351185871,-0.0009770109,1.2275016466\H,2.1692491743,-0.0017876697,-1.2522766926\H,0.0047602877,-0.0007852515,-2.4628289628\\Version=x86-Linux-G98RevA.7\HF=-230.4336069\S2=0.866648\S2-1=0.\S2A=0.757481\RMSD=5.160e-09\RMSF=1.050e-04\PG=C01 [X(C6H6)]\\

Zero-point correction = 0.104577 (Hartree/Particle)

Frequencies -- 342.8186 364.8506 454.5806
Frequencies -- 530.1866 641.7560 748.1341
Frequencies -- 925.2678 981.4817 987.9015
Frequencies -- 1032.3416 1047.2932 1061.7289
Frequencies -- 1103.9953 1111.9741 1114.0646
Frequencies -- 1135.3910 1278.1400 1288.5069
Frequencies -- 1461.7305 1498.1651 1505.8673
Frequencies -- 1564.0444 1647.5622 1728.6504
Frequencies -- 3375.2147 3381.6427 3387.2873
Frequencies -- 3390.0214 3405.5435 3408.0018

1\1\GINC-MS6\FOpt\UHF\6-31+G(d,p)\C6H6(1+,2)\JULIE\19-Nov-2002\0\\# **HF/6-31+G(D,P)** OPT FREQ=NORAMAN \\HF/6-31+G(d,p) C6H6 opt and freq\\1,2\C,-1.2194647375,0.0005695826,-0.6671397594\C,-1.2408546842,0.0010219517,0.7163361067\C,-0.0321201402,0.0004609891,1.3896639656\C,1.2194654517,-0.0005656931,0.6671389825\C,1.2408550535,-0.0010217918,-0.7163354665\C,0.03211911,-0.0004654597,-1.389663736\H,-2.1364424739,0.0009766799,-1.228548157\H,-2.1701562123,0.0017874439,1.2527960926\H,-0.0045119559,0.0007869443,2.4644964067\H,2.136442047,-0.0009747766,1.2285491705\H,2.1701552263,-0.0017865687,-1.252797799\H,0.00451130492,-0.0007871946,-2.4644962711\\Version=x86-Linux-G98RevA.7\HF=-230.4360181\S2=0.866207\S2-1=0.\S2A=0.75742\RMSD=2.751e-09\RMSF=7.822e-05\PG=C01 [X(C6H6)]\\

Zero-point correction = 0.104369 (Hartree/Particle)

Frequencies -- 340.5856 364.9559 452.9492
Frequencies -- 524.4106 640.6866 746.6657
Frequencies -- 921.2809 981.0813 983.6989
Frequencies -- 1027.9661 1042.4183 1061.0463
Frequencies -- 1096.2111 1098.9472 1107.3794
Frequencies -- 1132.1349 1276.1600 1286.0406
Frequencies -- 1457.4902 1495.8244 1503.8470
Frequencies -- 1562.1228 1643.1269 1722.5982
Frequencies -- 3375.0694 3381.4264 3386.6550
Frequencies -- 3389.7578 3403.7184 3406.3205

1\1\GINC-MS6\FOpt\UHF\6-311G(d,p)\C6H6(1+,2)\JULIE\19-Nov-2002\0\\# **HF/6-311G(D,P)** OPT FREQ=NORAMAN \\HF/6-311G(d,p) C6H6 opt and freq\\1,2\C,-1.2174852438,0.0005656304,-0.6652038728\C,-1.2395950461,0.0010206648,0.7156064921\C,-0.032804143,0.0004640024,1.3869795057\C,1.2174855202,-0.0005686936,0.6652035619\C,1.2395952006,-0.0010208234,-0.7156062244\C,0.032803736,-0.0004605151,-1.3869794217\H,-2.1340589278,0.0009737411,-1.2267301701\H,-2.1684630538,0.0017853231,1.2518193179\H,-0.0048948803,0.0007871328,2.4615211391\H,2.1340587592,-0.0009755643,1.2267305569\H,2.1684626608,-0.0017860784,-1.2518199979\H,0.0048952991,-0.0007861476,-2.4615210912\\Version=x86-Linux-G98RevA.7\HF=-230.469278\S2=0.865198\S2-1=0.\S2A=0.75731\RMSD=6.064e-09\RMSF=1.265e-04\PG=C01 [X(C6H6)]\\

Frequencies --	340.5681	361.1459	439.3490
Frequencies --	520.6988	640.2731	743.9466
Frequencies --	916.3263	976.3880	981.4174
Frequencies --	1024.8598	1034.6160	1056.9461
Frequencies --	1081.1275	1090.9178	1100.6796
Frequencies --	1128.8359	1270.1427	1282.7715
Frequencies --	1444.5582	1486.6050	1496.5858
Frequencies --	1555.1308	1636.8553	1718.0068
Frequencies --	3351.6921	3358.7763	3363.9391
Frequencies --	3367.4108	3381.0038	3383.9396

Zero-point correction = 0.103738 (Hartree/Particle)

1\1\GINC-MS6\FOpt\UHF\6-311+G(d,p)\C6H6(1+,2)\JULIE\20-Nov-2002\0\\# HF/6-311+G(D,P) OPT FREQ=NORAMAN **HF/6-311+G(d,p)** C6H6 opt and freq\\1,2\C,-1.2180519889,0.000568364,-0.6657523219\C,-1.2398969846,0.0010210638,0.7157790047\C,-0.0326109318,0.0004614448,1.3877428643\C,1.218052102,-0.000566215,0.6657521944\C,1.2398970478,-0.0010209873,-0.7157788952\C,0.0326107647,-0.0004638408,-1.3877428303\H,-2.134742562,0.0009754311,-1.2276819098\H,-2.168997308,0.0017862695,1.252127922\H,-.0044126988,0.0007863369,2.4625874979\H,2.1347424997,-0.0009743335,1.2276820626\H,2.1689971515,-0.001785847,-1.2521281937\H,0.0044128627,-0.0007868338,-2.4625874757\\Version=x86-Linux-G98RevA.7\HF=-230.4703716\S2=0.865932\S2-1=0.\S2A=0.757406\RMSD=2.835e-09\RMSF=3.537e-05\PG=C01X(C6H6)]\\

Frequencies --	338.8218	360.1623	438.4748
Frequencies --	509.2129	639.5379	742.8241
Frequencies --	912.1658	975.2176	979.0891
Frequencies --	1022.8294	1031.9376	1054.9747
Frequencies --	1065.4045	1084.1050	1096.0551
Frequencies --	1127.2240	1269.2212	1281.9792
Frequencies --	1441.3052	1485.2579	1496.4313
Frequencies --	1554.0401	1634.9520	1715.0638
Frequencies --	3348.6429	3355.7912	3361.0665
Frequencies --	3364.5058	3378.3416	3381.2395

Zero-point correction = 0.103533 (Hartree/Particle)

1\1\GINC-MS6\FOpt\UHF\6-311+G(2df,p)\C6H6(1+,2)\JULIE\20-Nov-2002\0\\# **HF/6-311+G(2DF,P)** OPT FREQ=NORAMAN \\HF/6-311+G(2df,p) C6H6+ opt and freq\\1,2\C,-1.2144825406,0.0005653066,-0.663146468\C,-1.237248377,0.0010188026,0.7142490257\C,-0.0330815822,0.0004620271,1.3833477768\C,1.2144825699,-0.0005663844,0.6631464129\C,1.237248425,-0.0010188384,-0.7142489425\C,0.0330815199,-0.0004608549,-1.3833477789\H,-2.1297368077,0.000972125,

-1.2253723576\H,-2.1655135197,0.0017831359,1.250116839\H,-0.0039094106,0.0007847386,2.45
70967865\H,2.1297367094,-0.0009726694,1.2253723977\H,2.1655134437,-0.0017832972,-1.25011
69705\H,0.0039094944,-0.0007843842,-2.4570968514\\Version=x86-Linux-G98RevA.7\HF=-230.4
864431\S2=0.862865\S2-1=0.\S2A=0.757\RMSD=6.692e-09\RMSF=8.321e-06\PG=C01X(C6H6)]\

Zero-point correction = 0.103727 (Hartree/Particle)

Frequencies --	343.3167	364.9563	414.1543
Frequencies --	533.7699	640.7614	746.4584
Frequencies --	924.6265	975.5195	985.6658
Frequencies --	1023.2788	1024.9975	1059.5170
Frequencies --	1100.2033	1111.8228	1115.6401
Frequencies --	1130.7450	1269.8636	1284.4130
Frequencies --	1432.2862	1484.8759	1502.3019
Frequencies --	1559.5707	1640.4157	1713.5555
Frequencies --	3341.6220	3348.4503	3354.1528
Frequencies --	3357.4148	3371.9088	3374.7966

1\1\GINC-MS8\FOpt\UMP2-FC\6-31+G(d)\C6H6(1+,2)\JULIE\10-Sep-2003\0\\# **MP2/6-31+G(D)** OPT FREQ\\Test\\1,2\C,0.,-1.3836996376,0.\C,1.2487546749,-0.688195212,0.\C,-1.2487546749,-0.
688195212,0.\C,0.,1.3836996376,0.\C,-1.2487546749,0.688195212,0.\C,1.2487546749,0.68819521
2,0.\H,0.,-2.4716160588,0.\H,2.176970583,-1.2525562542,0.\H,-2.176970583,-1.2525562541,0.\H,
0.,2.4716160588,0.\H,-2.176970583,1.2525562542,0.\H,2.176970583,1.2525562541,0.\\Version=
x86-Linux-G98RevA.7\State=2-B2G\HF=-230.4227119\MP2=-231.1349195\PUHF=-230.430145\
PMP2-0=-231.1405153\S2=0.825319\S2-1=0.787826\S2A=0.750874\RMSD=9.906e-09\RMSF=
4.652e-05\\PG=D02H [C2"(H1C1.C1H1),SG(C4H4)]\\

Zero-point correction = 0.155706 (Hartree/Particle)

Frequencies --	224.1669	271.8851	308.0540
Frequencies --	602.5997	681.2751	732.0635
Frequencies --	775.8577	783.3588	942.1647
Frequencies --	942.4746	960.1596	983.2478
Frequencies --	994.8508	1091.2292	1148.3447
Frequencies --	1234.0666	1242.0406	1320.1318
Frequencies --	1403.0691	1521.7029	1625.8276
Frequencies --	1687.0875	2081.7903	3254.4574
Frequencies --	3257.2735	3260.5064	3270.5009
Frequencies --	3272.8539	3274.3565	25199.7086

1\1\GINC-MS\FOpt\UQCISD-FC\6-31+G(d)\C6H6(1+,2)\JULIE\11-Sep-2003\0\\# **QCISD/6-31+G
(D)** OPT FREQ\\Test\\1,2\C,0.,-1.3858464138,0.\C,1.2514329795,-0.6867936287,0.\C,-1.251432
9795,-0.6867936287,0.\C,0.,1.3858464138,0.\C,-1.2514329795,0.6867936287,0.\C,1.2514329795,
0.6867936287,0.\H,0.,-2.4758669787,0.\H,2.18046012,-1.2530516119,0.\H,-2.18046012,-1.253051
6119,0.\H,0.,2.4758669787,0.\H,-2.18046012,1.2530516119,0.\H,2.18046012,1.2530516119,0.\\
Version=x86-Linux-G98RevA.7\State=2-B2G\HF=-230.4225811\MP2=-231.1348386\MP3=-231.
1741261\MP4D=-231.191565\MP4DQ=-231.1728571\PUHF=-230.4300648\PMP2-0=-231.140482
8\PMP3-0=-231.1776566\MP4SDQ=-231.181647\QCISD=-231.1849586\S2=0.826377\S2-1=0.78
8567\S2A=0.7509\RMSD=6.284e-09\RMSF=1.800e-04\PG=D02H[C2"(H1C1.C1H1),SG(C4H4)]\\

1\1\GINC-MS8\POpt\UCCSD-FC\6-31+G(d)\C6H6(1+,2)\JULIE\11-Sep-2003\1\\# **CCSD/6-31+G (D)** OPT NOSYMM FREQ\\Test\\1,2\C,0,0.,-1.3880575008,0.\C,0,1.2525185995,-0.6888967497,0.\ C,0,-1.2525185995,-0.6888967497,0.\C,0,0.,1.3880575008,0.\C,0,-1.2525185995,0.6888967497,0.\ C,0,1.2525185995,0.6888967497,0.\H,0,0.,-2.4727216457,0.\H,0,2.1765317946,-1.252884515,0.\H, 0,-2.1765317946,-1.252884515,0.\H,0,0.,2.4727216457,0.\H,0,-2.1765317946,1.252884515,0.\H,0, 2.1765317946,1.252884515,A\\A=0.\\Version=x86-Linux-G98RevA.7\HF=-230.42274\MP2=-231. 1348034\MP3=-231.1740671\MP4D=-231.1914751\MP4DQ=-231.1727287\PUHF=-230.4302289\ PMP2-0=-231.1404551\PMP3-0=-231.1776037\MP4SDQ=-231.1815459\CCSD=-231.1828191\S2 =0.826685\S2-1=0.788796\S2A=0.750899\RMSD=1.288e-09\RMSF=7.241e-08\PG=D02H [C2 "(H1C1.C1H1),SG(C4H4)]\\

1\1\GINC-MS9\FOpt\UBLYP\6-31+G(d)\C6H6(1+,2)\JULIE\10-Sep-2003\0\\# **BLYP/6-31+G(D)** OPT FREQ\\Test\\1,2\C,0.,-1.3971600215,0.\C,1.2589732236,-0.6925342672,0.\C,-1.2589732236,-0.6925342672,0.\C,0.,1.3971600215,0.\C,-1.2589732236,0.6925342672,0.\C,1.2589732236,0.692 5342672,0.\H,0.,-2.4917396609,0.\H,2.1922579544,-1.260902826,0.\H,-2.1922579544,-1.2609028 26,0.\H,0.,2.4917396609,0.\H,-2.1922579544,1.260902826,0.\H,2.1922579544,1.260902826,0.\\ Version=x86-Linux-G98RevA.7\State=2-B2G\HF=-231.8194647\S2=0.756509\S2-1=0.\S2A=0.75 0014\RMSD=1.280e-09\RMSF=2.080e-05\PG=D02H [C2"(H1C1.C1H1),SG(C4H4)]\\

Zero-point correction =0.094672 (Hartree/Particle)

Frequencies --	142.3213	283.3174	330.1880
Frequencies --	361.4248	586.5163	659.4609
Frequencies --	756.2951	864.1084	901.0166
Frequencies --	937.6372	945.2427	966.7368
Frequencies --	974.2453	983.2547	987.0300
Frequencies --	1039.9656	1180.0542	1190.8698
Frequencies --	1331.2942	1354.8040	1369.5864
Frequencies --	1420.1020	1501.8906	1611.9205
Frequencies --	3133.0174	3136.3605	3145.2325
Frequencies --	3148.6306	3155.6033	3158.1341

1\1\GINC-MS9\FOpt\UB3LYP\6-31+G(d)\C6H6(1+,2)\JULIE\10-Sep-2003\0\\# **B3LYP/6-31+G (d)**OPT FREQ\\Test\\1,2\C,0.,-1.3851525117,0.\C,1.2506206969,-0.686508085,0.\C,-1.2506206969 ,-0.6865080849,0.\C,0.,1.3851525117,0.\C,-1.2506206969,0.686508085,0.\C,1.2506206969,0.68650 80849,0.\H,0.,-2.4726366034,0.\H,2.1776581539,-1.2514338523,0.\H,-2.177658154,-1.2514338522 ,0.\H,0.,2.4726366034,0.\H,-2.1776581539,1.2514338523,0.\H,2.177658154,1.2514338522,0.\\ Version=x86-Linux-G98RevA.7\State=2-B2G\HF=-231.92627\S2=0.763396\S2-1=0.\S2A=0.75003 7\RMSD=7.681e-09\RMSF=1.394e-04\PG=D02H[C2"(H1C1.C1H1),SG(C4H4)]\\

Zero-point correction = 0.097968 (Hartree/Particle)

Frequencies --	250.1674	292.7103	341.9303
Frequencies --	414.0909	601.6376	682.1661
Frequencies --	794.5642	897.8143	958.6818
Frequencies --	966.2410	978.5726	1001.7661
Frequencies --	1010.6386	1015.6401	1024.9629
Frequencies --	1073.7232	1209.8250	1223.3551
Frequencies --	1378.7943	1394.0953	1417.7349
Frequencies --	1461.3681	1553.2043	1679.5907
Frequencies --	3216.5121	3219.9757	3228.9809

Frequencies -- 3232.3931 3239.6813 3242.2384

1\1\GINC-MS9\FOpt**UB3LYP\6-311++G(3df,2p)**\C6H6(1+,2)\JULIE\10-Sep-2003\0\\# B3LYP/6-311++G(3DF,2P) OPT FREQ\\Test\\1,2\C,0.,-1.3776744656,0.\C,1.2446038968,-0.6824288388,0.\C,-1.2446038968,-0.6824288388,0.\C,0.,1.3776744656,0.\C,-1.2446038968,0.6824288388,0.\C,1.2446038968,0.6824288388,0.\H,0.,-2.4607435909,0.\H,2.1672075938,-1.2455340116,0.\H,-2.1672075938,-1.2455340116,0.\H,0.,2.4607435909,0.\H,-2.1672075938,1.2455340116,0.\H,2.1672075938,1.2455340116,0.\\Version=x86-Linux-G98RevA.7\ State=2-B2G\HF=-231.992191\S2=0.763183\S2-1=0.\S2A=0.750041\RMSD=9.494e-09\RMSF=5.207e-05\PG=D02H [C2"(H1C1.C1H1),SG(C4H4)]\

Zero-point correction = 0.097070(Hartree/Particle)

Frequencies --	231.2456	288.2177	340.7456
Frequencies --	393.4441	599.8234	684.6351
Frequencies --	795.0617	893.0514	938.2777
Frequencies --	949.7285	967.8794	977.3833
Frequencies --	1001.1654	1015.2042	1018.8940
Frequencies --	1068.9964	1204.3146	1219.2261
Frequencies --	1368.6754	1391.4526	1398.7166
Frequencies --	1455.4921	1544.5046	1667.5856
Frequencies --	3181.7546	3187.9096	3199.1499
Frequencies --	3201.9311	3210.7954	3213.6542

1\1\GINC-MS9\FOpt**UB3PW91\6-31+G(d)**\C6H6(1+,2)\JULIE\10-Sep-2003\0\\# B3PW91/6-31+G(D) OPT FREQ\\Test\\1,2\C,0.,-1.3828935418,0.\C,1.2485964051,-0.6855378897,0.\C,-1.2485964051,-0.6855378897,0.\C,0.,1.3828935418,0.\C,-1.2485964051,0.6855378897,0.\C,1.2485964051,0.6855378897,0.\H,0.,-2.4707050688,0.\H,2.1758294887,-1.2508754778,0.\H,-2.1758294887,-1.2508754778,0.\H,0.,2.4707050688,0.\H,-2.1758294887,1.2508754778,0.\H,2.1758294887,1.2508754778,0.\\Version=x86-Linux-G98RevA.7\State=2-B2G\HF=-231.8323478\S2=0.765889\S2-1=0.\S2A=0.750054\RMSD=5.343e-09\RMSF=2.695e-05\PG=D02H[C2"(H1C1.C1H1),SG(C4H4)]\\

Zero-point correction = 0.098298 (Hartree/Particle)

Frequencies --	286.3148	299.5283	337.8661
Frequencies --	402.6771	598.4217	680.2726
Frequencies --	792.9088	897.3501	970.0943
Frequencies --	980.1952	985.8866	1000.8483
Frequencies --	1007.1301	1017.0923	1025.4768
Frequencies --	1079.2447	1208.6603	1223.5884
Frequencies --	1383.7399	1390.0777	1434.6851
Frequencies --	1458.8297	1556.8161	1690.8794
Frequencies --	3226.0602	3229.6218	3238.8399
Frequencies --	3242.3400	3249.9083	3252.4715

(C_6H_6)(NO) Geometry Optimizations

1\1\GINC-MS6\FOpt\UHF\6-31G(d)\C6H6N1O1(2)\JULIE\01-Feb-2003\0\\# HF/6 -31G(D) OPT=TIGHT FREQ=NORAMAN SCF=QC **HF/6-31G(d)** opt and freq\\0,2\C,-1.4539178442,-0.6011308034,-0.6639058155\C,-1.4320121306,-0.5900732313,0.7318029015\C,-0.2600826978,-0.921397191,1.4140126828\C,0.8897832547,-1.2631905845,0.7005607821\C,0.8679280861,-1.2737234519,-0.6949614217\C,-0.3039378977,-0.942954516,-1.3771589077\H,-2.3568658197,-0.3460091052,-1.

18942354\H,-2.3180142172,-0.3265896358,1.2814516228\H,-0.2433192079,-0.9130029383,2.4892891633\H,1.754307643,-1.5357440676,-1.2446016715\H,-0.3205027801,-0.9506147605,-2.4524184878\N,0.2796338844,2.6952458712, 0.2548143287\O,1.2359348382,2.5347043359,-0.319520992\H,1.7929138617,-1.5175766086,1.2260692199\\Version=x86-Linux-G98RevA.7\HF=-359.9551683\S2=1.249437\S2-1=0.\S2A=0.971947\RMSD=0.000e+00\RMSF=5.841e-08\PG=C01 [X(C6H6N1O1)]\\

Zero-point correction = 0.111088 (Hartree/Particle)

Frequencies --	9.6723	25.4190	27.1651
Frequencies --	37.8130	65.0302	426.0700
Frequencies --	426.0940	651.2816	651.3199
Frequencies --	723.9768	731.2118	904.3278
Frequencies --	904.6582	981.4388	1033.9382
Frequencies --	1033.9486	1068.5049	1097.2743
Frequencies --	1107.9266	1107.9963	1240.9568
Frequencies --	1264.1187	1264.1471	1387.1936
Frequencies --	1500.3177	1625.4837	1625.5552
Frequencies --	1704.0945	1704.1945	2221.8999
Frequencies --	3349.3830	3358.9920	3359.2772
Frequencies --	3376.8105	3377.0823	3387.2440

1\1\GINC-MS6\FOpt\UHF\6-31+G(d)\C6H6N1O1(2)\JULIE\03-Feb-2003\0\\# HF/ 6-31+G(D) OPT FREQ=NORAMAN SCF=QC **HF/6-31+G(d)** opt and freq\\0,2\C,-1.4856242324,-0.6893127107,-0.6633175735\C,-1.4613153667,-0.6769974812,0.7329094392\C,-0.286597037,-1.0037275276,1.4136361143\C,0.8637587037,-1.3427027353,0.698202172\C,0.8394333053,-1.3550352194,-0.6979381045\C,-0.3352177457,-1.028195445,-1.3786698651\H,-2.390454674,-0.4376886596,-1.1876414884\H,-2.347344366,-0.4157662054,1.2839517331\H,-0.2678885696,-0.9942979774,2.4890517782\H,1.725703108,-1.6152257116,-1.24900414\H,-0.3537857518,-1.0372834653,-2.4540712773\N,0.3285964127,2.9177199071,0.2001672644\O,1.3447813326,2.7807233002,-0.2668656107\H,1.7687189398,-1.593737017,1.2225343356\\Version=x86-Linux- G98RevA.7\HF=-359.9659245\S2=1.20207\S2-1=0.\S2A=0.929686\RMSD=0.000e+00\RMSF=1.032e-05\PG=C01[X(C6H6N1O1)]\\

Zero-point correction = 0.110998 (Hartree/Particle)

Frequencies --	3.5140	16.6805	18.0719
Frequencies --	23.8982	46.5431	426.6475
Frequencies --	427.1359	651.2008	651.2421
Frequencies --	725.5438	731.1582	909.5550
Frequencies --	909.7320	979.7772	1047.3582
Frequencies --	1047.8432	1077.8501	1096.8855
Frequencies --	1107.2926	1107.3225	1238.6430
Frequencies --	1264.6681	1264.7098	1384.5690
Frequencies --	1499.5142	1622.2042	1622.2144
Frequencies --	1704.7526	1704.7543	2209.1931
Frequencies --	3348.3494	3358.0678	3358.2535
Frequencies --	3375.7505	3375.9454	3385.6399

1\1\GINC-MS6\FOpt\UHF\6-31G(d,p)\C6H6N1O1(2)\JULIE\06-Feb-2003\0\\# HF/6-31G(D,P) OPT FREQ=NORAMAN SCF=QC**HF/6-31+G(d,p)** opt and freq\\0,2\C,-1.4535121761,-0.6019992423,-0.6645540428\C,-1.4320920744,-0.5908038517,0.730864288\C,-0.2605324833,-0.92155474

78,1.413366\C,0.88947316,-1.2629079696,0.7004866624\C,0.8681222402,-1.2734698068,-0.69473
19582\C,-0.3033951298,-0.943308273,-1.377230492\H,-2.3566827517,-0.3472239597,-1.19055729
67\H,-2.3186700204,-0.3275204197,1.2803516485\H,-0.2441286714,-0.9130379479,2.4889873979
\H,1.7551231668,-1.5350899422,-1.244231887\H,-0.319551193,-0.9509979508,-2.4528342999\N,
0.28 71425911,2.6935880954,0.2688422353\O,1.2290956094,2.5375189755,-0.3299134277\H,1.79
27652371,-1.5171349041,1.2264934676\\Version=x86-Linux-G98RevA.7\HF=-359.9658531\S2=1.
247749\S2-1=0.\S2A=0.970227\RMSD=0.000e+00\RMSF=5.215e-06\PG=C01[X(C6H6N1O1)]\\

Zero-point correction = 0.110743 (Hartree/Particle)

Frequencies --	8.7654	25.2832	27.0026
Frequencies --	37.5544	64.5006	425.6583
Frequencies --	425.6883	650.9573	650.9967
Frequencies --	724.6885	730.4571	903.8718
Frequencies --	904.1996	980.7228	1035.6609
Frequencies --	1035.6690	1067.8158	1096.5414
Frequencies --	1105.3535	1105.4235	1234.4683
Frequencies --	1258.4315	1258.4748	1386.5325
Frequencies --	1493.0402	1619.3377	1619.4137
Frequencies --	1701.9220	1702.0140	2221.9278
Frequencies --	3332.5335	3342.2377	3342.4961
Frequencies --	3360.0608	3360.3061	3370.4539

1\1\GINC-MS6\FOpt\UHF\6-31+G(d,p)\C6H6N1O1(2)\JULIE\03-Feb-2003\0\\# HF/6-31+G(D,P)
OPT FREQ=NORAMAN SCF=QC //**HF/6-31+ G(d,p)** opt and freq\\0,2\C,-0.4087633943,1.684207
1618,-0.344354904\C,0.1584923027,1.5037920153,0.9189201278\C,-0.206919746,0.403747308,1.6
976884888\C,-1.1394838454,-0.5158584234,1.2132117126\C,-1.7067143329,-0.3354321626,-0.049
9776736\C,-1.341230262,0.7645177253,-0.8287951731\H,-0.1273355956,2.5315307852,-0.944179
4035\H,0.8768984589,2.2120509378,1.2920135077\H,0.2299537693,0.2648164033,2.670723693\H
,-2.4243061333,-1.0442148744,-0.4235229939\H,-1.7778464043,0.9032158279,-1.8019574109\N,
2.4964953334,-1.1679084485,-1.0318104955\O,1.8794154525,-2.0448008473,-1.3779198854\H,-1.
4204393816,-1.3634749071,1.8127996883\\Version=x86-Linux-G98RevA.7\HF=-359.9766472\S2=
1.200947\S2-1=0.\S2A=0.928638\RMSD=0.000e+00\RMSF=1.084e-04\PG=C01[X(C6H6N1O1)]

Zero-point correction = 0.110650 (Hartree/Particle)

Frequencies --	3.5071	18.9648	20.0940
Frequencies --	24.1007	46.3637	426.2093
Frequencies --	426.7607	650.6044	650.6499
Frequencies --	726.2476	728.8171	907.0811
Frequencies --	907.2567	978.2964	1044.6965
Frequencies --	1045.1203	1072.4023	1095.8965
Frequencies --	1103.8749	1103.9023	1231.0126
Frequencies --	1257.9513	1257.9957	1382.7044
Frequencies --	1491.1547	1615.1304	1615.1395
Frequencies --	1701.3737	1701.3751	2209.1901
Frequencies --	3335.8161	3345.5421	3345.7495
Frequencies --	3363.0082	3363.2237	3372.6884

1\1\GINC-MS6\FOpt\UHF\6-311G(d,p)\C6H6N1O1(2)\JULIE\14-Feb-2003\0\\# HF/6-311G(D,P)
OPT=TIGHT FREQ=NORAMAN SCF=QC **HF/6-311G(d,p)** opt and freq\\0,2\C,-1.392918725,

-1.0388331087,-0.0437002871\C,-1.0113994597,-0.5878151897,-1.3065666012\C,-0.5694800134,
0.7238377642,-1.4741350065\C,-0.5086348301,1.5841559252,-0.3788581098\C,-0.8897368464,1.1
329955175,0.883959522\C,-1.332027778,-0.1784169711,1.0514970874\H,-1.7338589115,-2.05061
81844,0.0854906513\H,-1.0580217951,-1.2516383014,-2.1514092752\H,-0.2752503451,1.0717114
293,-2.4483282031\H,- 0.8413658734,1.7962357758,1.7290905959\H,-1.6255085944,-0.52648660
83,2.0258162892\N,2.5882773266,-1.1149135087,0.1161280931\O,2.7260276935,-0.4557553998,
1.0076427573\H,-0.1669713994,2.5956900246,-0.5078783975\\Version=x86-Linux-G98RevA.7\
HF=-360.0405888\S2=1.209225\S2-1=0.\S2A=0.934247\RMSD=0.000e+00\RMSF=1.704e-08\\
PG=C01 [X(C6H6N1O1)]\\

Zero-point correction = 0.110139 (Hartree/Particle)

Frequencies --	7.2966	21.0266	21.0550
Frequencies --	32.2965	57.0467	425.7868
Frequencies --	425.9300	650.3353	650.3909
Frequencies --	725.0930	727.3400	902.7455
Frequencies --	903.1011	973.4360	1037.7271
Frequencies --	1037.7881	1063.0923	1091.9443
Frequencies --	1099.2674	1099.2911	1221.1268
Frequencies --	1252.3927	1252.4844	1367.7175
Frequencies --	1484.3674	1608.1136	1608.1546
Frequencies --	1692.8384	1692.8597	2233.0101
Frequencies --	3310.9232	3320.8821	3321.2303
Frequencies --	3338.9128	3339.2573	3349.1824

1\1\GINC-MS6\FOpt\UHF\6-311+G(d,p)\C6H6N1O1(2)\JULIE\24-Feb-2003\0\\# HF/6-311+G(D,P
) OPT=TIGHT FREQ=NORAMAN SCF=QC \\ **HF/6-311+G(d,p)** opt and freq\\0,2\C,-0.40313823
67,1.6683685381,-0.3494900096\C,0.1648416873,1.4893752061,0.9113581456\C,-0.2051211272,
0.3961127895,1.6938432898\C,-1.1425697723,-0.5184213943,1.2152230055\C,-1.710329555,-0.33
95637273,-0.0456868152\C,-1.3405808452,0.7537948665,-0.8280469779\H,-0.1177346579,2.5116
300596,-0.9529967723\H,0.888431009,2.1944077368,1.2802156393\H,0.2330116367,0.258093727
7,2.666343174\H,-2.4326423723,-1.0455056985,-0.4152341348\H,-1.7781599168,0.8914148372,-
1.8008355926\N,2.4927232116,-1.1740176722,-0.9724863194\O,1.8758550902,-1.9909805779,-
1.4214642076\H,-1.427421807,-1.3620700064,1.8184217544\\Version=x86-Linux-98RevA7\HF=-
360.0459321\S2=1.189971\S2-1=0.\S2A=0.918854\RMSD=0.000e+00\RMSF=2.194e-08\\PG=C01
[X(C6H6N1O1)]\\

Zero-point correction =0.110027 (Hartree/Particle)

Frequencies --	5.2998	16.4479	19.0889
Frequencies --	23.7338	49.9749	424.6158
Frequencies --	425.2325	649.7673	649.7956
Frequencies --	718.7642	726.1490	903.6514
Frequencies --	903.8949	972.9102	1039.9180
Frequencies --	1040.3359	1060.6753	1090.5778
Frequencies --	1099.2895	1099.2948	1220.9047
Frequencies --	1253.2952	1253.3875	1367.0636
Frequencies --	1484.3088	1607.0537	1607.0672
Frequencies --	1693.0787	1693.0929	2216.0032
Frequencies --	3311.3058	3321.3189	3321.6025
Frequencies --	3339.1205	3339.3817	3348.9508

1\1\GINC-MS7\FOpt**UHF\6-311+G(2df,p)**\C6H6N1O1(2)\JULIE\27-Jul-2003\0\\# HF/6-311+G (2DF,P) OPT=TIGHT FREQ SCF=QC\\TEST\\0,2\C,1.0623249011,-0.6847707891,-1.2035996595 \C,1.0743423117,-1.3795963493,-0.0000565714\C,1.0623209412,-0.6848770095,1.2035478125\C, 1.0375143474,0.7046208407,1.2035684251\C,1.0250265403,1.3994021719,0.000065996\C,1.0375 182282,0.7047270589,-1.2034977021\H,1.0717294874,-1.2219754663,-2.1341638388\H,1.0929004 875,-2.4539555193,-0.0001039435\H,1.0717224119,-1.2221638351,2.1340646016\H,1.005017852, 2.4737153573,0.0001133802\H,1.0276257243,1.2419930191,-2.1340100512\N,-2.8412474678,-0.6 14447824,-0.000017169\O,-3.0252707749,0.4855851256,-0.000009742\H,1.0276188909,1.241804 6669,2.134128167\\Version=x86-Linux-G98RevA.7\HF=-360.0702625\S2=1.14446\S2-1=0.\S2A =0.882922\RMSD=0.000e+00\RMSF=9.582e-08\PG=C01 [X(C6H6N1O1)]\\

Zero-point correction = 0.110187 (Hartree/Particle)

Frequencies --	8.7225	20.2759	21.4546
Frequencies --	22.7004	47.0579	429.5288
Frequencies --	429.9347	651.9118	651.9429
Frequencies --	724.9083	731.9630	910.9269
Frequencies --	911.0925	976.1726	1047.2097
Frequencies --	1047.5516	1068.1823	1094.7619
Frequencies --	1102.7007	1102.7028	1215.4363
Frequencies --	1257.2284	1257.3124	1359.8762
Frequencies --	1490.8798	1613.8952	1613.9318
Frequencies --	1697.8315	1697.8548	2216.4961
Frequencies --	3305.0242	3315.0645	3315.2666
Frequencies --	3332.9074	3333.0992	3342.7921

1\1\GINC-MS6\FOpt\UMP2-FC\6-31+G(d)\C6H6N1O1(2)\JULIE\27-Sep-2003\0\\# MP2/6-31+G (D) OPT FREQ **MP2/6-31+g(d)** opt and freq\\0,2\C,-0.2180327451,1.4940277024,-0.4787629065 \C,0.3840864016,1.2867706025,0.7679828816\C,-0.0251936166,0.2185308679,1.574854339\C,-1.0 25126516,-0.6513005734,1.128273985\C,-1.6191797106,-0.4502567447,-0.12304345\C,-1.219119 4081,0.6249118035,-0.9245530602\H,0.0995309512,2.3261099527,-1.1037675356\H,1.166256321, 1.9599816349,1.1126046083\H,0.4421322289,0.0599789806,2.5445549408\H,-2.3954242051,-1.12 86309468,-0.4713862858\H,-1.6839300247,0.7819923561,-1.895781665\N,2.1530178826,-0.76653 61246,-0.7318583247\O,1.3719089436,-1.5355045343,-1.0604456643\H,-1.3395684304,-1.485744 7798,1.7518387906\\Version=x86-Linux-G98RevA.7\HF =-359.9582278\MP2=-361.044502\PUHF =-359.9638326\PMP2-0=-361.0488163\S2=0.781075\S2-1=0.766609\S2A=0.750568\RMSD=8.574 e-09\RMSF=1.470e-04\ PG=C01 [X(C6H6N1O1)]\\

Zero-point correction = 0.109886 (Hartree/Particle)

Frequencies --	20.2868	70.9990	76.9628
Frequencies --	81.6889	128.4808	387.9341
Frequencies --	388.3552	480.8145	616.7860
Frequencies --	617.1340	676.6698	838.5953
Frequencies --	839.6019	902.4256	905.6612
Frequencies --	915.3825	1019.6343	1019.7278
Frequencies --	1075.6625	1077.1498	1205.5036
Frequencies --	1224.2116	1224.5312	1387.2558
Frequencies --	1470.4575	1528.0787	1529.3860
Frequencies --	1657.7563	1658.5521	3208.8096
Frequencies --	3218.6242	3218.8065	3233.6130

Frequencies -- 3233.6723 3242.5716 3852.4218

1\1\GINC-MS6\FOpt**UBLYP\6-31+G(d)**\C6H6N1O1(2)\JULIE\07-Sep-2003\0\\# BLYP/6-31+G (D) OPT FREQ \\BLYP/6-31+G(d) opt and freq\\0,2\C,0.7493395244,0.7398859746,1.2409351808 \C,0.5548107725,1.4415864232,0.0339265667\C,0.7854593862,0.7997635783,-1.1997356017\C, 1.2065534583,-0.5440165445,-1.2263939919\C,1.3979774533,-1.2462818726,-0.0195477515\C,1.1 70790806,-0.6038407045,1.2139902115\H,0.5709562296,1.2391083867,2.1986113245\H,0.226838 0469,2.4855888629,0.0546742979\H,0.6353557328,1.3456332954,-2.1366052749\H,1.7247058914 ,-2.2908863567,-0.0403516452\H,1.3206925663,-1.1495580525,2.1510311698\N,-2.7235312439, 0.3523834481,0.0067054681\O,-2.7484729181,-0.8219811298,-0.043641743\H,1.3843651805,-1.0 433023606,-2.1842118875\\Version=x86-Linux-G98RevA.7\HF=-362.0332173\S2=0.752071\S2-1=0.\S2A=0.750003\RMSD=2.437e-09\RMSF=2.447e-05\PG=C01 [X(C6H6N1O1)]\\

Zero-point correction = 0.102141 (Hartree/Particle)

Frequencies --	10.9080	16.8383	29.3897
Frequencies --	30.5913	81.3086	397.5020
Frequencies --	398.6772	603.8981	603.9994
Frequencies --	669.0497	683.8151	831.5878
Frequencies --	835.7419	940.9602	943.2270
Frequencies --	973.6839	979.2138	991.4745
Frequencies --	1029.7195	1031.8051	1157.1535
Frequencies --	1172.7363	1172.8732	1324.6452
Frequencies --	1346.6309	1475.3240	1477.3068
Frequencies --	1579.1161	1580.7799	1834.0444
Frequencies --	3087.4618	3096.9036	3097.7787
Frequencies --	3112.6402	3113.3425	3122.7980

1\1\GINC-MS6\FOpt**UB3LYP\6-31+G(d)**\C6H6N1O1(2)\JULIE\05-Sep-2003\0\\# B3LYP/6-31+G(D) OPT FREQ \\B3LYP/6-31+G(d) opt and freq\\0,2\C,-0.3536954079,1.5270665499,-0.4416569 069\C,0.2617897737,1.3086389033,0.7956439847\C,-0.162512523,0.2547206915,1.6117775741\C, -1.2003519369,-0.5822188849,1.1894396222\C,-1.8141085752,-0.365078312,-0.0485337745\C,-1. 3915594275,0.6903010024,-0.8637079852\H,-0.0237538042,2.3468472535,-1.0751329327\H,1.069 9435947,1.9582667416,1.1225441286\H,0.3157479188,0.0856465528,2.5734762819\H,-2.6205889 919,-1.0163466258,-0.3768779238\H,-1.8699646175,0.8593177828,-1.8254005525\N,2.488737418 ,-0.8461799804,-0.8096253416\O,1.8999921007,-1.7386199617,-1.2540131614\H,-1.5298542503, -1.4020918493,1.8230985941\\Version=x86-Linux-G98RevA.7\HF=-362.1551011\S2=0.753046\ S2-1=0.\S2A=0.750006\RMSD=8.602e-09\RMSF=8.219e-05\PG=C01 [X(C6H6N1O1)]\\

Zero-point correction = 0.105430 (Hartree/Particle)

Frequencies --	5.3371	15.5340	26.9293
Frequencies --	32.9420	69.1468	411.6288
Frequencies --	412.1243	620.0099	620.1261
Frequencies --	691.2737	707.9141	864.2344
Frequencies --	865.7951	982.2454	983.6894
Frequencies --	1013.6068	1014.2700	1019.1053
Frequencies --	1063.3647	1064.5439	1184.0128
Frequencies --	1204.6618	1204.8906	1354.4217
Frequencies --	1385.6578	1521.8802	1523.1461
Frequencies --	1644.0962	1644.6223	1975.4929

Frequencies -- 3174.3304 3183.9107 3183.9956
Frequencies -- 3199.8277 3200.2722 3209.4141

1\1\GINC-MS6\FOpt**UB3PW91\6-31+G(d)**\C6H6N1O1(2)\JULIE\07-Sep-2003\0\\# B3PW91/6-31+G(D) OPT FREQ \\B3PW91/6-31+G(d) opt and freq\\0,2\C,0.8634656267,0.5828240598,1.301320909\C,0.7285149731,1.4177659444,0.1902253058\C,0.9124995757,0.9047547243,-1.0952077211\C,1.2311899374,-0.4433352233,-1.2695705248\C,1.3656811152,-1.2780972079,-0.1586687014\C,1.1822142975,-0.7650148501,1.1268899876\H,0.7192630872,0.9829267733,2.3022886177\H,0.479077494,2.4675243184,0.3264380904\H,0.8068271582,1.5551920755,-1.9603954708\H,1.6136374631,-2.3282895704,-0.2945783638\H,1.2872271593,-1.4157638349,1.9919331742\N,-2.9265483422,0.4178039818,0.0092472317\O,-2.9370085057,-0.732050003,-0.0911967615\ H,1.3744809265,-0.8432022941,-2.2707781088\\Version=x86-Linux-G98RevA.7\HF=-362.0085953\S2=0.752926\S2-1=0.\S2A=0.750006\RMSD=7.897e-09\RMSF=4.289e-05\PG=C01 [X(C6H6N1O1)]\

Zero-point correction = 0.105654 (Hartree/Particle)

Frequencies -- - 13.8982 8.3026 15.1586
Frequencies -- 21.3996 50.2438 408.5964
Frequencies -- 409.2062 616.7861 616.9265
Frequencies -- 688.7076 710.1818 863.8568
Frequencies -- 864.7734 983.2283 983.5794
Frequencies -- 1014.1596 1014.6873 1022.0798
Frequencies -- 1069.6778 1070.1322 1183.1374
Frequencies -- 1205.6074 1205.8513 1377.2674
Frequencies -- 1380.4478 1523.2480 1523.7124
Frequencies -- 1658.3352 1658.6326 2008.0543
Frequencies -- 3185.7773 3195.6355 3195.7337
Frequencies -- 3210.7282 3211.4510 3221.3522

1\1\GINC-MS6\FOpt**UB3LYP\6-311++G(3df,2p)**\C6H6N1O1(2)\JULIE\11-Sep-2003\\# B3LYP/6-311++G(3DF,2P) OPT FREQ \\B3LYP/6-311++G(3df,2p) opt and freq\\0,2\C,-0.3567935648,1.5208492951,-0.4371250619\C,0.2558377235,1.3031846524,0.7929428236\C,-0.1669297688,0.2556307816,1.6051130068\C,-1.1994557173,-0.5763577507,1.185376269\C,-1.8101900624,-0.3603107513,-0.0457990541\C,-1.38942716,0.6889002578,-0.8567131874\H,-0.0285258705,2.3365420581,-1.0678678041\H,1.0604943078,1.9493183382,1.1182055524\H,0.309014738,0.0873038346,2.5622367695\H,-2.6133765192,-1.0079285554,-0.3721504319\H,-1.8655016694,0.8575298416,-1.8137559241\N,2.4892110014,-0.8514302622,-0.8127548169\O,1.9053670901,-1.7327851258,-1.252070909\H,-1.5277674186,-1.391851585,1.8164140521\\Version=x86-Linux-G98RevA.7\HF=-362.2681798\S2=0.753341\S2-1=0.\S2A=0.750008\RMSD=8.206e-09\RMSF=3.797e-05\PG=C01[X(C6H6)N1O1]

Zero-point correction = 0.104839 (Hartree/Particle)

Frequencies -- 11.2968 21.1603 30.2014
Frequencies -- 31.1573 68.9220 410.9103
Frequencies -- 411.5903 619.8149 620.0029
Frequencies -- 691.6754 697.2326 867.3084
Frequencies -- 868.7549 961.5148 991.4606
Frequencies -- 991.5893 1007.6286 1012.6695
Frequencies -- 1059.1256 1060.1210 1175.8241
Frequencies -- 1198.7479 1198.9983 1332.8547

Frequencies --	1384.2313	1513.0086	1513.8905
Frequencies --	1630.5652	1631.1096	1974.1564
Frequencies --	3151.8073	3164.3148	3164.7406
Frequencies --	3179.8565	3180.4043	3190.2503

Singlet $(C_6H_6)(NO)^+$ Geometry Optimizations

1\1\GINC-MS6\FOpt\RHF\6-31G(d)\C6H6N1O1(1+)\JULIE\17-Mar-2003\0\\# **HF/6-31G(D)** OPT FREQ\\C6H6NO+ opt and Freq HF/6-31G(d)\\1,1\C,-1.3205224578,-0.308812931,-0.7027665061\C,-1.2699351247,-0.22611652,0.6947711429\C,-0.1205114519,-0.6307162966,1.3858849003\C,0.9882698912,-1.0567567769,0.679561066\C,0.951853668,-1.0871663124,-0.7144337505\C,-0.2086620768,-0.7356737636,-1.4037333077\H,-2.2253321948,-0.0476836181,-1.2207463049\H,-2.1407709509,0.0857150074,1.243159968\H,-0.1103094244,-0.6150402447,2.4605116628\H,1.8148347173,-1.4198985968,-1.2615309988\H,-0.2363405073,-0.8034308055,-2.4755200456\N,-0.0191976048,1.9684380811,0.3144493602\O,0.8793057404,1.8328137028,-0.2227352758\H,1.8749009823,-1.3697823297,1.1991611339\\Version=x86-Linux-G98RevA.7\HF=-359.6508545\RMSD=4.429e-09\RMSF=3.629e-05\PG=C01[X(C6H6N1O1)]\\

Zero-point correction = 0.116144 (Hartree/Particle)

Frequencies --	47.9770	136.7397	155.7823
Frequencies --	200.7498	367.3674	437.3974
Frequencies --	450.2339	653.3316	653.9543
Frequencies --	738.8921	809.5356	983.6453
Frequencies --	1013.0362	1068.3633	1096.9454
Frequencies --	1121.4858	1131.4295	1133.3461
Frequencies --	1142.0173	1152.0689	1239.1933
Frequencies --	1289.6617	1293.7383	1381.3751
Frequencies --	1510.3417	1633.6520	1651.8861
Frequencies --	1749.4110	1770.9572	2601.1033
Frequencies --	3377.7730	3387.9062	3388.1437
Frequencies --	3399.3701	3402.8965	3409.8236

1\1\GINC-MS6\FOpt\RHF\6-31+G(d)\C6H6N1O1(1+)\JULIE\21-Mar-2003\0\\# HF/6-31+G(D) OPT FREQ **HF/6-31+G(d)** Opt and Freq C6H6NO+\\1,1\C,0.453907869,0.8208620827,1.2139866586\C,0.1847795917,1.4641510348,0.0000960037\C,0.4538746286,0.8210199806,-1.2138865497\C,0.9433689139,-0.4745255356,-1.211618326\C,1.1702574409,-1.1285017541,-0.0000875974\C,0.9433999405,-0.4746836694,1.2115352382\H,0.2952059873,1.3408301778,2.1415873398\H,-0.1698567453,2.4796552972,0.00016673\H,0.2951475515,1.3411096729,-2.141414808\H,1.5589333874,-2.1307138108,-0.0001578973\H,1.1613048412,-0.9728500818,2.1385311848\N,-2.0419709731,0.0694165571,0.0000093035\O,-1.8632148043,-0.9676637603,-0.0000305979\H,1.1612499165,-0.9725699065,-2.1386854556\\Version=x86-Linux-G98RevA.7\HF=-359.6585821\RMSD=6.063e-09\RMSF=1.310e-05\PG=C01 [X(C6H6N1O1)]\\

Zero-point correction = 0.115803 (Hartree/Particle)

Frequencies --	28.7748	126.5259	144.5847
Frequencies --	176.9338	330.8923	438.8527
Frequencies --	449.0095	653.4173	653.9231
Frequencies --	739.2031	804.8143	983.3894
Frequencies --	1005.7584	1064.6835	1095.6594

Frequencies -- 1120.6005 1128.4388 1130.1546
Frequencies -- 1137.6784 1145.7687 1233.8749
Frequencies -- 1288.7733 1291.7018 1377.4677
Frequencies -- 1508.8981 1631.5828 1646.2945
Frequencies -- 1747.8399 1764.5402 2643.3876
Frequencies -- 3373.0600 3383.3308 3383.3523
Frequencies -- 3395.0477 3398.1729 3405.2847

1\1\GINC-MS6\FOpt\RHF\6-31G(d,p)\C6H6N1O1(1+)\JULIE\22-Mar-2003\0\\# **HF/6-31G(D,P)** OPT FREQ \\HF/6-31G(d,p) Opt and Freq C6H6NO+\\1,1\C,0.4377420331,0.8144761826,1.2148787362\C,0.1625008915,1.4549890181,0.0000946631\C,0.4377102348,0.8146344682,-1.2147805839\C,0.9268726077,-0.4776687715,-1.2118238839\C,1.1493388776,-1.1311783255,-0.0000876932\C,0.9269029012,-0.4778269992,1.2117400263\H,0.273907354,1.3339734293,2.1418404387\H,-0.1989015234,2.4681862627,0.0001652545\H,0.2738512213,1.3342530402,-2.1416700115\H,1.5308743279,-2.1363550869,-0.0001580322\H,1.1417507089,-0.9788048629,2.1379317549\N,-1.9915211132,0.0859312839,0.0000192316\O,-1.8086170845,-0.9536000242,-0.0000356041\H,1.1416971042,-0.9785250126,-2.1380867795\\Version=x86-Linux-G98RevA.7\HF=-359.6614693\RMSD=3.380e-09\RMSF=9.047e-05\PG=C01 [X(C6H6N1O1)]\\

Zero-point correction = 0.115732 (Hartree/Particle)

Frequencies -- 38.3948 136.3843 155.3569
Frequencies -- 201.1781 366.6772 437.0501
Frequencies -- 449.8764 653.0029 653.6316
Frequencies -- 739.5395 807.9944 982.0690
Frequencies -- 1011.3847 1067.5416 1096.0754
Frequencies -- 1119.0026 1130.4071 1132.2205
Frequencies -- 1139.0167 1149.2301 1233.5179
Frequencies -- 1283.8918 1287.9365 1380.0648
Frequencies -- 1503.2482 1627.9406 1646.0683
Frequencies -- 1747.0893 1768.7298 2601.8353
Frequencies -- 3359.1980 3368.7220 3369.8748
Frequencies -- 3380.6971 3384.4786 3391.0469

1\1\GINC-MS6\FOpt\RHF\6-31+G(d,p)\C6H6N1O1(1+)\JULIE\23-Mar-2003\0\\#**HF/6-31+G(D,P)** OPT FREQ \\HF/6-31+G(d,p) Opt and Freq C6H6NO+\\1,1\C,0.4542424771,0.8201579868,1.2138809078\C,0.1848633476,1.4632667225,0.0000943842\C,0.4542116957,0.8203164858,-1.2137832276\C,0.9435112586,-0.4750544758,-1.2115095749\C,1.1700167731,-1.1290132382,-0.0000878685\C,0.9435412372,-0.4752128529,1.2114252556\H,0.2956245016,1.3402811503,2.1416521742\H,-0.1699282627,2.4789815702,0.0001651319\H,0.2955702349,1.340561115,-2.1414823935\H,1.5584257157,-2.1316142645,-0.0001581794\H,1.1615837625,-0.9735034094,2.1385454074\N,-2.0422559051,0.0712868031,0.0000225047\O,-1.863667017,-0.9659067613,-0.0000373093\H,1.1615307836,-0.9732234613,-2.1387004596\\Version=x86-Linux-G98RevA.7\HF=-359.6691966\RMSD=5.915e-09\RMSF=3.714e-05\PG=C01 [X(C6H6N1O1)]\\

Zero-point correction = 0.115420 (Hartree/Particle)

Frequencies -- 31.8223 126.5549 144.6449
Frequencies -- 177.0125 331.6047 438.2405
Frequencies -- 448.3019 652.8839 653.4415
Frequencies -- 739.0233 802.9307 981.2085

Frequencies -- 1003.4095 1063.7165 1094.2166
Frequencies -- 1117.6173 1125.1177 1126.2674
Frequencies -- 1134.5146 1140.6516 1228.0539
Frequencies -- 1282.5584 1285.4590 1375.8932
Frequencies -- 1501.0530 1625.3485 1640.1795
Frequencies -- 1745.0387 1762.1420 2642.1963
Frequencies -- 3357.0988 3367.2864 3367.6459
Frequencies -- 3378.9681 3382.3770 3389.2519

1\1\GINC-MS6\FOpt\RHF\6-311G(d,p)\C6H6N1O1(1+)\JULIE\24-Mar-2003\0\\# HF/6-311G(D,P) OPT FREQ **HF/6-311G(d,p)** Opt and Freq C6H6NO+\\1,1\C,0.4534156117,0.8255891089,1.2116909107\C,0.1885345644,1.4694749272,0.0000946906\C,0.4533848823,0.8257473568,-1.2115926508\C,0.9369381822,-0.4698874256,-1.2091690431\C,1.1611190552,-1.1236995263,-0.0000875022\C,0.9369680496,-0.4700455609,1.209085385\H,0.2974444578,1.3460011849,2.1392981061\H,-0.1614231458,2.4864089813,0.0001654777\H,0.2973902632,1.3462809132,-2.1391277565\H,1.5468242148,-2.1269826198,-0.0001578447\H,1.1533695959,-0.9687874124,2.1359842677\N,-2.0379942675,0.0484342758,0.0000208892\O,-1.8503905446,-0.9745658191,-0.0000375666\H,1.153316771,-0.968507706,-2.1361386832\\Version=x86-Linux-G98RevA.7\HF=-359.7389967\RMSD=6.870e-09\RMSF=2.106e-05\PG=C01 [X(C6H6N1O1)]\\

Zero-point correction = 0.114802 (Hartree/Particle)

Frequencies -- 21.3518 130.6185 144.4748
Frequencies -- 181.8066 328.1236 438.2483
Frequencies -- 447.9911 652.7610 652.8942
Frequencies -- 734.6389 800.2566 977.1322
Frequencies -- 998.3421 1059.8112 1086.0641
Frequencies -- 1113.9151 1117.5792 1119.0201
Frequencies -- 1126.2292 1129.6720 1213.8666
Frequencies -- 1278.4878 1281.0267 1359.8347
Frequencies -- 1493.0038 1618.3679 1632.0487
Frequencies -- 1740.0402 1755.7326 2661.0314
Frequencies -- 3332.4631 3342.9744 3343.1680
Frequencies -- 3355.2928 3358.2341 3365.6553

1\1\GINC-MS7\FOpt\RHF\6-311+G(d,p)\C6H6N1O1(1+)\JULIE\25-Jul-2003\0\\# HF/6-311+G(D,P)OPT FREQ=NORAMAN**HF/6-311+G(d,p)**\\1,1\C,-0.54224658,-1.3226194722,0.5853266827\C,-0.1354554981,-0.2826338025,1.4194854445\C,-1.1431128965,-1.0380613781,-0.6372812868\C,-0.3269688321,1.0411964201,1.0248527032\C,-1.3357727659,0.2814479092,-1.0280670173\C,-0.9270443728,1.3209415222,-0.2002112065\H,-0.4182341238,-2.3432128994,0.8998550191\H,0.298120053,-0.5005869039,2.3793111832\H,-1.4779505424,-1.8402551707,-1.2694218209\H,-0.039054284,1.8442550118,1.6794624064\H,-1.8186655694,0.4990703138,-1.9632340787\H,-1.0962073032,2.3410132846,-0.4939216194\N,1.5114218024,-0.0000926991,-0.5734926601\O,2.5544556032,-0.0001577418,-0.5252792986\\Version=x86-Linux-G98RevA.7\HF=-359.7458044\RMSD=7.291e-09\RMSF=7.024e-05\=1.8021891,-0.0002032,-0.5415291\PG=C01 [X(C6H6N1O1)]\\

Zero-point correction = 0.115095 (Hartree/Particle)

Frequencies -- 32.3774 92.1880 185.5920
Frequencies -- 348.2062 362.5005 435.4807
Frequencies -- 435.6141 648.2328 648.3980

Frequencies -- 734.7304 795.6967 984.9568
Frequencies -- 986.5047 1057.2041 1085.3502
Frequencies -- 1113.4048 1114.0943 1120.6772
Frequencies -- 1121.0321 1130.1877 1229.0001
Frequencies -- 1276.4503 1276.6070 1374.0086
Frequencies -- 1493.7443 1622.9393 1623.4354
Frequencies -- 1734.1254 1734.9567 2625.7267
Frequencies -- 3332.3268 3342.9744 3343.3250
Frequencies -- 3355.5292 3357.4991 3365.5782

1\1\GINC-MS6\FOpt\RHF\6-311+G(2df,p)\C6H6N1O1(1+)\JULIE\12-Jul-2003\0\ \# HF/6-311+G(2DF,P) OPT FREQ=NORAMAN **HF/6-311+G(2df,p)** Opt and Freq C6H6NO+\\1,1\C,0.5064658067,0.8025021856,1.207608607\C,0.2886720426,1.4616165815,0.0000947432\C,0.5064449492,0.8026615255,-1.2075100372\C,0.9072238053,-0.5186873546,-1.2054548347\C,1.092873029,-1.1834703611,-0.0000870239\C,0.9072442017,-0.518846507,1.2053718603\H,0.3808145675,1.3295579911,2.1352739731\H,0.001457091,2.4972648468,0.000165517\H,0.3807777197,1.3298399359,-2.1351035805\H,1.4156806414,-2.2079767985,-0.0001573724\H,1.0887319707,-1.0296653641,2.1324323942\N,-2.0435093487,0.1502057318,0.0000220101\O,-1.9131419288,-0.8769666927,-0.0000398637\H,1.0886958747,-1.0293836118,-2.1325859807\\Version=x86-Linux-G98RevA.7\HF=-359.7710967\RMSD=6.564e-09\RMSF=8.165e-05\ PG=C01[X(C6H6N1O1)]\\

Zero-point correction = 0.114889 (Hartree/Particle)

Frequencies -- 22.2238 131.1732 141.2793
Frequencies -- 170.8197 307.5076 444.6407
Frequencies -- 452.5886 654.3605 654.4283
Frequencies -- 757.2597 804.7280 984.3444
Frequencies -- 1002.8994 1060.1223 1093.8229
Frequencies -- 1115.3861 1128.5973 1132.0509
Frequencies -- 1133.4915 1153.3247 1207.4032
Frequencies -- 1281.2115 1283.2492 1355.1326
Frequencies -- 1500.1969 1623.7498 1635.1283
Frequencies -- 1739.0237 1751.7474 2669.3561
Frequencies -- 3322.6693 3332.9804 3333.3736
Frequencies -- 3345.7898 3348.4346 3356.0353

1\1\GINC-MS6\Freq\RMP2-FC\6-31+G(d)\C6H6N1O1(1+)\JULIE\17-Apr-2003\0\\ # FREQ **MP2/6-31+G(D)** \\Singlet Benzene-NO structure\\1,1\C,0.6916656488,-1.0471205372,0.9478764977\C,0.7167916032,-1.3370947565,-0.428618614\C,0.7335513189,-0.2899063848,-1.3679108535\C,0.7251643798,1.0472811945,-0.9309303897\C,0.7000570895,1.3374672632,0.4454816094\C,0.6833120951,0.2902508551,1.3849926287\H,0.6860231916,-1.8570865211,1.6746123871\H,0.730657546,-2.3714112643,-0.7665297612\H,0.7604301589,-0.5142494684,-2.4323872472\H,0.7455240082,1.8572366251,-1.6573825047\H,0.7009172682,2.3718078155,0.7836363309\H,0.6711856755,0.5146133794,2.4497693197\N,-1.3748540558,-0.0003468474,-0.0206918931\O,-2.5217515336,-0.000468555,-0.0265275681\\Version=x86-Linux-G98RevA.7\HF=-359.6373116\MP2=-360.7878723\RMSD=2.315e-09\RMSF=2.738e-06\.

Zero-point correction = 0.108090 (Hartree/Particle)

Frequencies -- 18.0644 18.2879 271.0024
Frequencies -- 361.4164 361.4218 476.9805

Frequencies --	476.9955	589.6666	600.5527
Frequencies --	600.5564	718.1239	880.7849
Frequencies --	880.7858	979.2504	979.3092
Frequencies --	979.6002	1006.0016	1014.4582
Frequencies --	1067.4720	1067.4784	1221.8783
Frequencies --	1223.7452	1223.7523	1393.3777
Frequencies --	1508.9254	1520.3992	1520.4037
Frequencies --	1629.3129	1629.3205	1776.0268
Frequencies --	3229.5711	3236.8338	3236.8343
Frequencies --	3247.4485	3247.4525	3252.4476

1\1\GINC-MS7\FOpt**RQCISD-FC\6-31+G(d)**\C6H6N1O1(1+)\JULIE\02-Aug-2003\0\\# QCISD /6-31+G(D) OPT SCF=QC\\QCISD/6-31+G(D)\\1,1\O,-0.2038265956,2.5427034368,-0.0000000042\N,-0.2143610631,1.4337935817,-0.0000000021\C,1.4561124099,-0.4581221163,-0.0000000032\C,-1.3064183816,-0.9831962325,0.0000000055\H,2.5299898272,-0.2752996812,-0.0000000066\H,-2.3729820486,-1.2029407562,0.0000000089\C,0.7642997123,-0.5893848772,-1.2184878913\C,0.7642997191,-0.5893848726,1.2184878892\C,-0.6170212613,-0.8519708922,1.2170924347\C,-0.6170212681,-0.8519708967,-1.217092428\H,1.302987461,-0.5070003501,-2.1615654783\H,1.3029874731,-0.5070003421,2.1615654729\H,-1.1486740375,-0.970881052,2.1600616591\H,-1.1486740496,-0.9708810601,-2.1600616491\\Version=x86-Linux-G98RevA.7\State=1-A'\HF=-359.6518063\MP2=-360.7848363\MP3=-360.7825309\MP4D=-360.8206873\MP4DQ=-360.7865907\MP4SDQ=-360.8048401\QCISD=-360.8050002\RMSD=0.000e+00\RMSF=4.376e-05\PG=CS [SG(C2H2N1O1),X(C4H4)]\\

1\1\GINC-MS8\POpt**RCCSD-FC\6-31+G(d)**\C6H6N1O1(1+)\JULIE\04-Aug-2003\1\\# CCSD/6-31+G(D) OPT FREQ SCF=QC NOSYMM\\CCSD/6-31+G(D)\\1,1\O,0,-0.2043891329,2.4741891601,0.\N,0,-0.2010653759,1.3512034058,0.\C,0,1.4634152792,-0.487387013,0.\C,0,-1.3058599369,-1.0100604229,0.\H,0,2.5308374056,-0.2978794135,0.\H,0,-2.3686986633,-1.2220863616,0.\C,0,0.7696369911,-0.617807061,-1.2212306237\C,0,0.7696369911,-0.6178070699,1.2212306237\C,0,-0.6150433481,-0.8793569529,1.2195974663\C,0,-0.6150433481,-0.8793569529,-1.2195974663\H,0,1.3044398157,-0.5285258881,-2.1598946468 \H,0,1.3044398157,-0.5285258881,2.1598946468\H,0,-1.145484027,-0.9907178776,2.1581868278\H,0,-1.145484027,-0.9907178776,A\\A=-2.16361815\\Version=x86-Linux-G98RevA.7\HF=-359.6468265\MP2=-360.7867296\MP3=-360.7812183\MP4D=-360.8205387\MP4DQ=-360.7853241\MP4SDQ=-360.8043667\CCSD=-360.7996838\RMSD=0.000e+00\RMSF=1.401e-05\PG=C01 X(C6H6N1O1)]\\

1\1\GINC-MS5\FOpt\RBLYP\6-31+G(d)\C6H6N1O1(1+)\JULIE\24-Jul-2003\0\\#BLYP/6-31+G(D) OPT FREQ**BLYP/6-31+G(d)**\\1,1\C,-0.5197817471,-1.3470800992,0.5913083999\C,-0.1009686947,-0.2877917575,1.439369849\C,-1.1353731619,-1.0563658941,-0.6509364034\C,-0.2985051676,1.0610791411,1.0381012797\C,-1.3318641959,0.2863843719,-1.0478369347\C,-0.9142975483,1.3448240573,-0.207222632\H,-0.3712677483,-2.3853542211,0.9006985331\H,0.3691110738,-0.5092771348,2.4017711067\H,-1.4618662663,-1.8724221083,-1.3013162292\H,0.0200805181,1.8779411124,1.6917373503\H,-1.8105799912,0.5076516766,-2.0056501906\H,-1.0695144331,2.3826017403,-0.5146810765\N,1.4040270302,-0.0004472626,-0.5086207024\O,2.5375738411,-0.000538643,-0.573614491\\Version=x86-Linux-G98RevA.7\HF=-361.7696085\RMSD=8.399e-09\RMSF=3.034e-05\PG=C01 [X(C6H6N1O1)]\\

Zero-point correction = 0.104819 (Hartree/Particle)

Frequencies --	23.6352	63.8759	210.8305
Frequencies --	353.7920	356.5981	400.9829

Frequencies -- 426.6215 583.1062 585.0051
Frequencies -- 612.9377 705.8682 862.1504
Frequencies -- 864.6631 964.2173 976.1087
Frequencies -- 983.8680 988.2040 998.6757
Frequencies -- 1019.6448 1020.3087 1169.4108
Frequencies -- 1169.7546 1176.0097 1354.3499
Frequencies -- 1356.4411 1466.3769 1467.1878
Frequencies -- 1536.1778 1537.1109 1952.0831
Frequencies -- 3125.0619 3132.2536 3132.6625
Frequencies -- 3142.3552 3143.2810 3148.6633

1\1\GINC-MS8\FOpt\RB3LYP\6-31+G(d)\C6H6N1O1(1+)\JULIE\23-Jul-2003\0\\# B3LYP/6-31+G(D) OPT=TIGHT FREQ**B3LYP/6-31+G(d)** geometry optimization of C6H6NO+\\1,1\C,-0.5112924814,-1.3370654611,0.5838285552\C,-0.102197665,-0.285804535,1.4286451516\C,-1.1124531871,-1.0485079558,-0.6537504759\C,-0.2952028049,1.0529232627,1.0290849667\C,-1.3043495518,0.2842370174,-1.0491096102\C,-0.8966238631,1.3346833938,-0.2114604655\H,-0.3682403582,-2.3685286612,0.893442581\H,0.3551022218,-0.5058797452,2.3894926667\H,-1.4328854492,-1.8591656653,-1.3018654985\H,0.0139309235,1.8642988222,1.6822310709\H,-1.7733003418,0.5041145228,-2.0038901184\H,-1.0500562272,2.3657000792,-0.5171572296\N,1.3791656982,-0.0002892597,-0.4974167722\O,2.491750833,-0.0001636084,-0.5529705996\\Version=x86-Linux-G98RevA.7\HF=-361.8717003\RMSD=7.025e-09\RMSF=1.633e-05\PG=C01[X(C6H6N1O1)]\\

Zero-point correction = 0.108320 (Hartree/Particle)

Frequencies -- 18.0152 69.1957 228.2518
Frequencies -- 369.7902 372.9809 424.1050
Frequencies -- 449.8999 598.0908 599.7085
Frequencies -- 644.8332 731.3374 897.2738
Frequencies -- 899.7620 998.5774 1011.9271
Frequencies -- 1021.9024 1022.5988 1037.6733
Frequencies -- 1053.7784 1054.2510 1199.5302
Frequencies -- 1200.4851 1204.2033 1392.5423
Frequencies -- 1399.1083 1512.4071 1513.0000
Frequencies -- 1594.1370 1595.0039 2104.9249
Frequencies -- 3209.0240 3216.0346 3216.6692
Frequencies -- 3226.1060 3227.2521 3232.7709

1\1\GINC-MS8\FOpt**RB3PW91\6-31+G(d)**\C6H6N1O1(1+)\JULIE\08-Sep-2003\0\\# B3PW91/6-31+G(D) OPT FREQ\\B3PW91 C6H6NO+ Optimization\\1,1\C,-0.5038851007,-1.3360432711,0.5785500056\C,-0.0934406748,-0.2867386217,1.4211722321\C,-1.1055774605,-1.0476420504,-0.6560620067\C,-0.2849896858,1.0498982474,1.0218526225\C,-1.2963046655,0.2826482488,-1.0509344891\C,-0.8867243502,1.3311967839,-0.2160552633\H,-0.3602009876,-2.3679883123,0.8879249676\H,0.3662081786,-0.5069868036,2.381438135\H,-1.4267914055,-1.8585587929,-1.3041873152\H,0.027417723,1.8615024866,1.6739924253\H,-1.7653616422,0.502748546,-2.0060814639\H,-1.038059789,2.3627291741,-0.5226616763\N,1.3558931124,0.0002092418,-0.4897333248\O,2.4663834701,0.0056466235,-0.5341788007\\Version=x86-Linux-G98RevA.7\HF=-361.7276371\RMSD=5.926e-09\RMSF=7.262e-06\PG=C01 [X(C6H6N1O1)]\\

Zero-point correction = 0.108703 (Hartree/Particle)

Frequencies -- 8.9496 73.0600 234.9868

Frequencies --	365.0582	368.5927	436.6306
Frequencies --	463.0531	594.7210	596.4105
Frequencies --	644.6546	731.4962	898.8078
Frequencies --	901.5318	1006.8824	1009.6056
Frequencies --	1021.0004	1023.8095	1037.8274
Frequencies --	1059.8527	1060.6955	1200.0378
Frequencies --	1203.1211	1205.1380	1387.4218
Frequencies --	1420.3697	1512.8261	1513.8020
Frequencies --	1608.5218	1609.4816	2130.7125
Frequencies --	3218.2779	3225.5793	3226.3509
Frequencies --	3235.9369	3237.2119	3242.7035

1\1\GINC-MS7\Freq\RB3LYP\6-311++G(3df,2p)\C6H6N1O1(1+)\JULIE\22-Aug-2003\0\\# **B3LYP/6-311++G(3DF,2P)** FREQ \\Geometry optimization of C6H6NO+\\1,1\C,-0.517031449,-1.3295078327,0.577702207\C,-0.1160379892,-0.2843804829,1.4206812572\C,-1.1069899963,-1.0424835206,-0.6566176765\C,-0.3052962353,1.0467656432,1.0222213913\C,-1.2955483583,0.2827394937,-1.0506815719\C,-0.8954637496,1.3270911326,-0.2150260835\H,-0.3767008167,-2.3565061952,0.8868655769\H,0.3323715849,-0.5036405645,2.380606153\H,-1.4215514901,-1.8495684517,-1.3041396121\H,-0.0018920216,1.8545348791,1.6747012555\H,-1.7560793626,0.5018012133,-2.0043612642\H,-1.0463193026,2.3536650456,-0.5201608644\N,1.3948550715,-0.0001098931,-0.4932537199\O,2.4905490719,-0.0001079094,-0.5313015433\\Version=x86-Linux-G98RevA.7\HF=-361.9859402\RMSD=5.979e-9\RMSF=5.760e-06\

Zero-point correction = 0.107791 (Hartree/Particle)

Frequencies --	9.8724	72.9634	223.9693
Frequencies --	372.1976	374.9048	417.2958
Frequencies --	444.4489	599.1307	600.8346
Frequencies --	647.6509	734.3967	901.7799
Frequencies --	904.7401	982.7122	998.7140
Frequencies --	1028.8829	1031.3444	1047.4881
Frequencies --	1051.0535	1051.6621	1194.3849
Frequencies --	1196.3449	1199.0453	1377.8854
Frequencies --	1392.1092	1506.7148	1507.5464
Frequencies --	1584.1610	1584.9345	2117.4968
Frequencies --	3178.6208	3187.7146	3188.3684
Frequencies --	3198.2021	3199.5270	3205.6804

Triplet $(C_6H_6)(NO)^+$ Geometry Optimizations

1\1\GINC-MS6\Freq\UHF\6-31G(d)\C6H6N1O1(1+,3)\JULIE\21-Nov-2003\1\\# **HF/6-31G(D)** OPT=(EF,CALCALL) SCF=QC\\Optimization 3C6H6NO+\\1,3\C\C,1,R2\C,1,R3,2,A3\H,1,R4,2,A4,3,D4,0\C,2,R5,1,A5,3,D5,0\C,3,R6,1,A6,2,D6,0\H,2,R7,1,A7,5,D7,0\H,3,R8,1,A8,6,D8,0\C,5,R9,2,A9,1,D9,0\H,5,R10,2,A10,9,D10,0\H,6,R11,3,A11,1,D11,0\H,9,R12,5,A12,2,D12,0\N,1,R13,2,A13,3,D13,0\O,13,R14,1,A14,2,D14,0\\R2=1.38226632\R3=1.44478333\R4=1.07433805\R5=1.38319833\R6=1.38226642\R7=1.07249995\R8=1.07433806\R9=1.44462501\R10=1.07407995\R11=1.07249995\R12=1.07407995\A3=120.90415167\A4=120.60389965\A5=118.2109792\A6=120.90415217\A7=120.8977796\A8=118.49194821\A9=120.88486938\A10=120.79771119\A11=120.89777817\A12=118.31741967\D4=179.9999473\D5=0.00018602\D6=-0.00010979\D7=-180.00012282\D8=180.00002681\D9=-0.00011425\D10=-180.00018335\D11=180.00002755\D12=-180.00020848\D13=-0.01550848\D14=-0.19369712\R13=6.03442748\R14=1.12305949\A13=37.77962395\A14=

173.12464459\\Version=x86-Linux-G98RevA.7\HF=-359.6726506\S2=2.135626\S2-1=0.\S2A=
2.00877\RMSD=0.000e+00\RMSF=1.223e-07\

Zero-point correction = 0.110720 (Hartree/Particle)

Frequencies --	20.4484	23.9845	47.9443
Frequencies --	49.4130	83.2430	345.0448
Frequencies --	367.3948	459.0069	533.7413
Frequencies --	642.4591	752.5591	928.1734
Frequencies --	983.8271	994.7244	1032.6714
Frequencies --	1053.0022	1062.1256	1107.2018
Frequencies --	1117.1257	1121.7335	1138.3630
Frequencies --	1283.7569	1293.9749	1461.3846
Frequencies --	1502.6754	1513.3988	1569.3172
Frequencies --	1652.8900	1730.2362	2239.4791
Frequencies --	3400.2491	3408.8608	3410.3887
Frequencies --	3416.4321	3424.8598	3428.5837

1\1\GINC-MS6\Freq\UHF\6-31+G(d)\C6H6N1O1(1+,3)\JULIE\25-Nov-2003\1\\# **HF/6-31+G(D)**
OPT=(EF,CALCALL) Optimization C6H6NO+\1,3\C\C,1,R2\C,1,R3,2,A3\H,1,R4,2,A4,3,D4,0\
C,2,R5,1,A5,3,D5,0\ C,3,R6,1,A6,2,D6,0\H,2,R7,1,A7,5,D7,0\H,3,R8,1,A8,6,D8,0\C,5,R9,2,A9,
1,D9,0\H,5,R10,2,A10,9,D10,0\H,6,R11,3,A11,1,D11,0\H,9,R12,5,A12,2,D12,0\N,1,R13,2,A13,3,D
13,0\O,13,R14,1,A14,2,D14,0\\R2=1.3832039\R3=1.44530063\R4=1.07462788\R5=1.38414365\R6
=1.38320465\R7=1.07288747\R8=1.07462788\R9=1.4451823\R10=1.07439325\R11=1.07288748\R
12=1.07439313\A3=120.88665158\A4=120.59617255\A5=118.2471144\A6=120.88663332\A7=12
0.87981217\A8=118.51718975\A9=120.86623406\A10=120.73789695\A11=120.87979922\A12=11
8.39588786\D4=179.99998678\D5=0.00005979\D6=-0.00001989\D7=-180.00004304\D8=179.9999
9925\D9=-0.00005147\D10=-180.00001105\D11=179.99999454\D12=-180.00000174\D13=-0.0038
2269\D14=-0.05299935\R13=6.12304431\R14=1.12310532\A13=37.66011358\A14=173.21890715
\\Version=x86-Linux-G98RevA.7\HF=-359.6784795\S2=2.136201\S2-1=0.\S2A=2.008954\
RMSD=4.224e-09\RMSF=3.923e-07

Zero-point correction = 0.110468 (Hartree/Particle)

Frequencies --	22.0032	22.3311	41.0406
Frequencies --	43.6428	82.3988	342.4211
Frequencies --	367.6738	457.7089	528.5405
Frequencies --	641.4668	750.3441	924.6250
Frequencies --	984.1426	990.2213	1029.4528
Frequencies --	1049.6132	1062.1494	1103.0143
Frequencies --	1110.6974	1115.1782	1135.7123
Frequencies --	1282.5253	1291.9177	1459.1924
Frequencies --	1500.9681	1511.5088	1568.1317
Frequencies --	1649.2260	1725.6705	2226.4788
Frequencies --	3397.3846	3405.7544	3407.1365
Frequencies --	3413.4099	3420.9915	3425.0012

1\1\GINC-MS6\Freq\UHF\6-31G(d,p)\C6H6N1O1(1+,3)\JULIE\30-Nov-2003\1\\#**HF/6-31G(D,P)**
OPT=(EF,CALCALL)\\Optimization 3C6H6NO+\1,3\C\C,1,R2\C,1,R3,2,A3\H,1,R4,2,A4,3,D4,0\
C,2,R5,1,A5,3,D5,0\C,3,R6,1,A6,2,D6,0\H,2,R7,1,A7,5,D7,0\H,3,R8,1,A8,6,D8,0\C,5,R9,2,A9,1,
D9,0\H,5,R10,2,A10,9,D10,0\H,6,R11,3,A11,1,D11,0\H,9,R12,5,A12,2,D1 2,0\N,1,R13,2,A13,3,D

13,0\O,13,R14,1,A14,2,D14,0\\R2=1.38195509\R3=1.44447217\R4=1.07504275\R5=1.38291137\R6=1.38195508\R7=1.07281222\R8=1.07504274\R9=1.44430213\R10=1.0747694\R11=1.07281221\R12=1.0747694\A3=120.90409017\A4=120.5935613\A5=118.2114307\A6=120.90408782\A7=120.89735839\A8=118.50234887\A9=120.88447969\A10=120.8007197\A11=120.89735875\A12=118.31480128\D4=179.99999925\D5=0.00000943\D6=-0.00000154\D7=-180.00000896\D8=179.9999994\D9=-0.0000106\D10=-180.00001426\D11=179.99999832\D12=-180.00000618\D13=-0.00103995\D14=-0.01307601\R13=6.024776\R14=1.12303114\A13=37.78900192\A14=173.1146923\\Version x86-Linux-G98RevA.7\HF=-359.6833079\S2=2.13532\S2-1=0.\S2A=2.008726\RMSD=9.759e-09\RMSF=7.052e-07\

Zero-point correction = 0.110275 (Hartree/Particle)

Frequencies --	20.4660	24.3391	48.6817
Frequencies --	49.6994	83.6318	343.6899
Frequencies --	366.8622	459.7352	531.5442
Frequencies --	642.0886	751.2259	926.6302
Frequencies --	982.4082	992.4575	1032.0015
Frequencies --	1049.3197	1061.3670	1105.5256
Frequencies --	1112.7702	1118.3804	1135.6020
Frequencies --	1277.1780	1288.2201	1461.0411
Frequencies --	1498.9276	1506.1702	1563.6821
Frequencies --	1646.9031	1727.6981	2239.7420
Frequencies --	3376.7813	3385.5189	3388.0460
Frequencies --	3393.2358	3405.3808	3408.2746

1\1\GINC-MS6\Freq**UHF\6-31+G(d,p)**\C6H6N1O1(1+,3)\JULIE\25-Nov-2003\1\\# HF/6-31+G(D,P) OPT=(EF,CALCALL)\\Optimization 3C6H6NO+\\1,3\C\C,1,R2\C,1,R3,2,A3\H,1,R4,2,A4,3,D4,0\C,2,R5,1,A5,3,D5,0\C,3,R6,1,A6,2,D6,0\H,2,R7,1,A7,5,D7,0\H,3,R8,1,A8,6,D8,0\C,5,R9,2,A9,1,D9,0\H,5,R10,2,A10,9,D10,0\H,6,R11,3,A11,1,D11,0\H,9,R12,5,A12,2,D12,0\N,1,R13,2,A13,3,D13,0\O,13,R14,1,A14,2,D14,0\\R2=1.3829584\R3=1.44504973\R4=1.07515034\R5=1.38391907\R6=1.38295838\R7=1.07301419\R8=1.07515034\R9=1.4449289\R10=1.07491272\R11=1.07301419\R12=1.07491269\A3=120.88645636\A4=120.58524791\A5=118.24795066\A6=120.88646937\A7=120.87880505\A8=118.52828961\A9=120.86559273\A10=120.73913069\A11=120.87880619\A12=118.3952763\D4=179.99999159\D5=0.00003771\D6=-0.00001267\D7=-180.00002736\D8=179.99999957\D9=-0.00003211\D10=-180.00000829\D11=179.99999703\D12=-180.00000279\D13=-0.00249284\D14=-0.03265648\R13=6.10720273\R14=1.12307747\A13=37.6815368\A14=173.2062596\\Version=x86-Linux-G98RevA.7\HF=-359.6891975\S2=2.135824\S2-1=0.\S2A=2.008901\RMSD=2.939e-09\RMSF=3.395e-07

Zero-point correction = 0.110001 (Hartree/Particle)

Frequencies --	21.4917	22.1377	41.3825
Frequencies --	44.2363	82.4652	340.8151
Frequencies --	366.8591	458.2455	525.9029
Frequencies --	640.9254	747.7644	921.0943
Frequencies --	982.5733	986.1251	1028.6136
Frequencies --	1045.5962	1061.1275	1097.1912
Frequencies --	1100.3018	1108.6030	1132.7364
Frequencies --	1275.6698	1285.9618	1458.6594
Frequencies --	1497.0746	1503.9723	1562.3351

Frequencies --	1643.1541	1722.8756	2226.7334
Frequencies --	3376.5836	3384.8194	3387.5300
Frequencies --	3392.5165	3403.9059	3406.9070

1\1\GINC-MS6\Freq**UHF\6-311G(d,p)**\C6H6N1O1(1+,3)\JULIE\30-Nov-2003\1\\# HF/6-311 G(D,P) OPT=(EF,CALCALL)\\Optimization 3C6H6NO+\\1,3\C\C,1,R2\C,1,R3,2,A3\H,1,R4, 2,A4,3,D4,0\C,2,R5,1,A5,3,D5,0\C,3,R6,1,A6,2,D6,0\H,2,R7,1,A7,5,D7,0\H,3,R8,1,A8,6,D8,0\C,5, R9,2,A9,1,D9,0\H,5,R10,2,A10,9,D10,0\H,6,R11,3,A11,1,D11,0\H,9,R12,5,A12,2,D12,0\N,1,R13,2 ,A13,3,D13,0\O,13,R14,1,A14,2,D14,0\\R2=1.38082478\R3=1.44401337\R4=1.07494264\R5=1.38 191029\R6=1.38082304\R7=1.07258955\R8=1.07494262\R9=1.44379188\R10=1.07464643\R11=1. 07258954\R12=1.07464653\A3=120.91457839\A4=120.60659378\A5=118.19250596\A6=120.9145 5231\A7=120.9099501\A8=118.47882022\A9=120.89291405\A10=120.83678459\A11=120.909995 47\A12=118.27029047\D4=179.99999232\D5=0.00002381\D6=-0.00001614\D7=-180.00001402\ D8=180.00000461\D9=-0.00001192\D10=-180.00002211\D11=180.00000452\D12=-180.00003089 \D13=-0.00181426\D14=-0.0223656\R13=6.01648706\R14=1.11297478\A13=37.8088103\A14= 173.10927236\\Version=x86-Linux-G98RevA.7\HF=-359.7545351\S2=2.131796\S2-1=0.\S2A= 2.008134\RMSD=6.304e- 09\RMSF=1.785e-07

Zero-point correction = 0.109511 (Hartree/Particle)

Frequencies --	21.2463	28.3962	50.1455
Frequencies --	53.2984	88.2776	341.6726
Frequencies --	363.6388	445.4982	522.4609
Frequencies --	640.5789	747.3666	917.9872
Frequencies --	977.2702	986.3545	1024.2935
Frequencies --	1036.6393	1056.4876	1082.8129
Frequencies --	1092.7285	1104.3349	1128.7574
Frequencies --	1268.9719	1282.4643	1443.4595
Frequencies --	1487.4852	1496.5274	1554.5990
Frequencies --	1636.0647	1716.7414	2259.3088
Frequencies --	3352.7954	3362.2797	3364.2548
Frequencies --	3370.0795	3380.5710	3384.0450

1\1\GINC-MS6\Freq**UHF\6-311+G(d,p)**\C6H6N1O1(1+,3)\JULIE\24-Nov-2003\1\\# HF/6-311+ G(D,P) OPT=(EF,CALCALL)\\Optimization 3C6H6NO+\\1,3\C\C,1,R2\C,1,R3,2,A3\H,1,R4,2,A4, 3,D4,0\C,2,R5,1,A5,3,D5,0\C,3,R6,1,A6,2,D6,0\H,2,R7,1,A7,5,D7,0\H,3,R8,1,A8,6,D8,0\C,5,R9,2, A9,1,D9,0\H,5,R10,2,A10,9,D10,0\H,6,R11,3,A11,1,D11,0\H,9,R12,5,A12,2,D12,0\N,1,R13,2,A13, 3,D13,0\O,13,R14,1,A14,2,D14,0\\R2=1.38109881\R3=1.44411538\R4=1.07517546\R5=1.3821617 4\R6=1.38109908\R7=1.07278271\R8=1.07517545\R9=1.44397422\R10=1.0749259\R11=1.072782 72\R12=1.07492584\A3=120.91039863\A4=120.60366119\A5=118.20218683\A6=120.91038214\A 7=120.90586456\A8=118.48595024\A9=120.88740818\A10=120.78425768\A11=120.90586452\A1 2=118.32836163\D4=179.99996756\D5=0.00013512\D6=-0.00004389\D7=-180.00009657\D8= 179.99999687\D9=-0.00011647\D10=-180.00000734\D11=179.99998568\D12=-179.99999081\ D13=-0.00561248\D14=-0.09546669\R13=6.07741982\R14=1.11392698\A13=37.73011394\ A14=173.17268939\\Version=x86-Linux-G98RevA.7\HF=-359.7582821\S2=2.133872\S2-1=0.\ S2A=2.008523\RMSD=8.780e-09\RMSF=8.395e-07

Zero-point correction = 0.109251 (Hartree/Particle)

Frequencies --	23.8532	25.8204	43.6752
Frequencies --	50.9705	82.0737	340.1904

Frequencies --	363.5823	445.2639	514.3325
Frequencies --	639.9164	744.2011	912.9107
Frequencies --	976.6493	981.7523	1023.2429
Frequencies --	1035.4438	1055.6312	1067.2133
Frequencies --	1085.1032	1097.5171	1127.7801
Frequencies --	1268.4721	1281.7468	1441.9295
Frequencies --	1486.7136	1496.4578	1554.0784
Frequencies --	1634.7959	1714.9421	2240.0410
Frequencies --	3350.2875	3359.2576	3361.9768
Frequencies --	3367.2845	3378.5510	3381.8706

1\1\GINC-MS6\Freq**UHF\6-311+G(2df,p)**\C6H6N1O1(1+,3)\JULIE\30-Nov-2003\1\\# HF/6-311+G(2DF,P) OPT=(EF,CALCALL)\\Optimization 3C6H6NO+\\1,3\C\C,1,R2\C,1,R3,2,A3\H,1,R4,2,A4,3,D4,0\C,2,R5,1,A5,3,D5,0\C,3,R6,1,A6,2,D6,0\H,2,R7,1,A7,5,D7,0\H,3,R8,1,A8,6,D8,0\C,5,R9,2,A9,1,D9,0\H,5,R10,2,A10,9,D10,0\H,6,R11,3,A11,1,D11,0\H,9,R12,5,A12,2,D12,0\N,1,R13,2,A13,3,D13,0\O,13,R14,1,A14,2,D14,0\\R2=1.37708246\R3=1.44058929\R4=1.07413699\R5=1.37815627\R6=1.37708319\R7=1.07184138\R8=1.07413699\R9=1.44047563\R10=1.07390324\R11=1.07184135\R12=1.07390321\A3=120.94772401\A4=120.62444736\A5=118.12852999\A6=120.94773674\A7=120.94233886\A8=118.42782941\A9=120.92374847\A10=120.79656686\A11=120.94231595\A12=118.27968389\D4=179.99998273\D5=0.00005957\D6=-0.00002061\D7=-180.00003859\D8=179.99999592\D9=-0.00004919\D10=-180.00000463\D11=179.99999227\D12=-179.99999916\D13=-0.00287899\D14=-0.04423201\R13=6.08534376\R14=1.11142048\A13=37.74543541\A14=173.20215479\\Version=x86-Linux-G98RevA.7\HF=-359.7839049\S2=2.129029\S2-1=0.\S2A=2.007793\RMSD=9.774e-09\RMSF=2.053e-07

Zero-point correction = 0.109423 (Hartree/Particle)

Frequencies --	23.6033	24.5618	40.5102
Frequencies --	42.9076	82.7951	344.4918
Frequencies --	367.8014	421.2987	537.6634
Frequencies --	641.0748	748.1915	925.7858
Frequencies --	976.7392	988.5933	1025.1009
Frequencies --	1026.2541	1059.4371	1101.1936
Frequencies --	1113.3625	1118.5186	1131.0599
Frequencies --	1269.1798	1284.2409	1432.5764
Frequencies --	1486.2628	1502.2891	1559.5633
Frequencies --	1640.1884	1713.2218	2246.4719
Frequencies --	3342.9661	3351.6157	3354.7801
Frequencies --	3359.8764	3371.8970	3375.1555

1\1\GINC-MS9\Freq**UBLYP\6-31+G(d)**\C6H6N1O1(1+,3)\JULIE\05-Jan-2004\1\\ # BLYP/6-31+G(D) OPT=(EF,CALCALL) \\BLYP/6-31+G(d) 3C6H6NO+ NO optimization\\1,3\C\C,1,R2\C,1,R3,2,A3\H,1,R4,2,A4,3,D4,0\C,2,R5,1,A5,3,D5,0\C,3,R6,1,A6,2,D6,0\H,2,R7,1,A7,5,D7,0\H,3,R8,1,A8,6,D8,0\C,5,R9,2,A9,1,D9,0\H,5,R10,2,A10,9,D10,0\H,6,R11,3,A11,1,D11,0\H,9,R12,5,A12,2,D12,0\N,1,R13,2,A13,3,D13,0\O,13,R14,1,A14,2,D14,0\\R2=1.42742126\R3=1.45511143\R4=1.09445008\R5=1.38767138\R6=1.38727496\R7=1.09247923\R8=1.09310345\R9=1.45565082\R10=1.09303847\R11=1.09248902\R12=1.09465788\R13=6.01128534\R14=1.17021761\A3=121.42721022\A4=119.74020716\A5=118.81865247\A6=119.76962093\A7=119.91419998\A8=118.98718234\A9=119.7818087\A10=121.53434087\A11=121.24472361\A12=118.48735847\A13=39.88649236\A14=176.55705663\D4=180.05169736\D5=0.13029324\D6=-0.09183307\D7=-180.07720213\D8=180.03971771\D9=-0.10269292\D10=-179.92147457\D11=180.01292657\D12=-179.70066145\D13=4.26

003742\D14=61.45158827\\Version=x86-Linux-G98RevA.7\HF=-361.7104836\S2=2.00872\S2-1=
0.\S2A=2.000037\RMSD=5.816e-09\RMSF=1.539e-05\

Zero-point correction = 0.099323 (Hartree/Particle)

Frequencies --	2.3703	17.6963	47.7262
Frequencies --	59.7720	83.5313	151.8861
Frequencies --	285.1842	327.4146	354.9047
Frequencies --	586.9411	662.2351	771.6125
Frequencies --	861.0097	907.9031	933.6152
Frequencies --	943.7559	969.1629	975.2659
Frequencies --	980.9650	986.1279	1043.5403
Frequencies --	1178.5887	1185.2484	1331.6940
Frequencies --	1354.2974	1366.0358	1425.2633
Frequencies --	1498.8166	1583.6676	1851.5419
Frequencies --	3131.0228	3135.1058	3144.3956
Frequencies --	3147.0426	3155.0656	3157.1918

1\1\GINC-MS9\Freq**UB3LYP\6-31+G(d)**\C6H6N1O1(1+,3)\JULIE\08-Dec-2003\1\ \# B3LYP/6-
31+G(D) FREQ \\B3LYP/6-31+G(d) 3C6H6NO+ NO optimization\\1,3\C\C,1,R2\C,1,R3,2,A3\H,
1,R4,2,A4,3,D4,0\C,2,R5,1,A5,3,D5,0\C,3,R6,1,A6,2,D6,0\H,2,R7,1,A7,5,D7,0\H,3,R8,1,A8,6,D8,0
\C,5,R9,2,A9,1,D9,0\H,5,R10,2,A10,9,D10,0\H,6,R11,3,A11,1,D11,0\H,9,R12,5,A12,2,D12,0\N,1,R
13,2,A13,3,D13,0\O,13,R14,1,A14,2,D14,0\\R2=1.42636641\R3=1.43799712\R4=1.08735824\R5=
1.37391758\R6=1.3735821\R7=1.08542263\R8=1.08571395\R9=1.43846481\R10=1.08567795\R11
=1.08543057\R12=1.08746165\R13=5.92741652\R14=1.15369396\A3=121.59014624\A4=119.403
15861\A5=118.99225736\A6=119.43389164\A7=119.62948579\A8=119.22176305\A9=119.447291
88\A10=121.66010079\A11=121.35529333\A12=118.66155875\A13=39.40418488\A14=176.79573
594\D4=180.00154232\D5=-0.00719771\D6=0.00406229\D7=-179.99670726\D8=179.99886245\
D9=0.00369299\D10=-179.99889203\D11=179.99947778\D12=-179.99294373\D13=0.21862014
\D14=8.27020664\\Version=x86-Linux-G98RevA.7\HF=-361.824721\S2=2.0164\S2-1=0.\S2A
=2.000093\

Zero-point correction = 0.103218 (Hartree/Particle)

Frequencies --	25.7424	28.8908	54.9818
Frequencies --	61.3341	87.0455	271.9786
Frequencies --	295.5908	344.3044	415.2074
Frequencies --	602.1730	685.5043	799.5628
Frequencies --	900.3860	963.9351	966.6798
Frequencies --	978.2457	1004.8371	1009.5535
Frequencies --	1017.5367	1027.3964	1073.4691
Frequencies --	1208.5735	1221.5217	1378.5874
Frequencies --	1393.2391	1416.1875	1461.3635
Frequencies --	1551.5847	1673.5171	2006.2001
Frequencies --	3217.1432	3220.7127	3229.1594
Frequencies --	3232.4610	3240.1219	3242.5864

1\1\GINC-MS9\Freq**UB3PW91\6-31+G(d)**\C6H6N1O1(1+,3)\JULIE\15-Nov-2003\0\\# B3PW91
/6-31+G(D) FREQ\\B3PW91/6-31+G(d) 3C6H6NO+ NO optimization\\1,3\C,-2.0345074561,0.067
5252281,-1.8649535263\C,-2.0359764561,0.0586022281,-0.4108655263\C,-0.8122004561,0.06456
52281,-2.6089905263\H,-2.9915144561,0.0761662281,-2.3957095263\C,-0.8323514561,0.0466012

281,0.2760114737\C,0.3915985439,0.0520642281,-1.9214905263\H,-2.9919194561,0.0617482281,
0.1189494737\H,-0.8414094561,0.0710632281,-3.7011235263\C,0.3906035439,0.0446252281,-0.4
673705263\H,-0.8000464561,0.0406942281,1.3677734737\H,1.3472075439,0.0479122281,-2.4519
215263\H,1.3453425439,0.0406922281,0.0666464737\N,1.9723945439,-0.1708917719,2.73597947
37\O,2.5903225439,-0.1432417719,3.7286854737\\Version=x86-Linux-G98RevA.7\HF=-361.6737
836\S2=2.020068\S2-1=0.\S2A=2.000142\RMSD=2.188e-09\

Zero-point correction = 0.103221 (Hartree/Particle)

Frequencies --	44.4685	90.9988	98.4444
Frequencies --	209.9976	246.8975	254.7341
Frequencies --	324.1480	371.9049	448.3958
Frequencies --	597.8620	717.1627	831.0774
Frequencies --	912.4985	941.9946	947.8220
Frequencies --	953.5953	1000.8649	1016.5042
Frequencies --	1030.5973	1037.4628	1063.1276
Frequencies --	1209.1942	1216.3476	1373.7024
Frequencies --	1381.0760	1391.0649	1453.1978
Frequencies --	1528.1556	1627.7972	1896.4471
Frequencies --	3165.9744	3175.2876	3179.6024
Frequencies --	3185.0087	3190.4388	3195.0303

1\1\GINC-MS9\Freq\UB3LYP\6-311++G(3df,2p)\C6H6N1O1(1+,3)\JULIE\24-Dec-2003\1\\#
B3LYP/6-311++G(3DF,2P) FREQ \\B3LYP/6-311++G(3df,2p) 3C6H6NO+ NO optimization\\1,3\
C\C,1,R2\C,1,R3,2,A3\H,1,R4,2,A4,3,D4,0\C,2,R5,1,A5,3,D5,0\C,3,R6,1,A6,2,D6,0\H,2,R7,1,A7,5,
D7,0\H,3,R8,1,A8,6,D8,0\C,5,R9,2,A9,1,D9,0\H,5,R10,2,A10,9,D10,0\H,6,R11,3,A11,1,D11,0\H,9,
R12,5,A12,2,D12,0\N,1,R13,2,A13,3,D13,0\O,13,R14,1,A14,2,D14,0\\R2=1.41869913\R3=1.43131
955\R4=1.08300983\R5=1.36555778\R6=1.36514476\R7=1.08069181\R8=1.08105836\R9=1.43186
164\R10=1.08107368\R11=1.08071672\R12=1.08320456\R13=5.899715\R14=1.14042077\A3=121
.64218672\A4=119.3943522\A5=118.94717809\A6=119.42290256\A7=119.63828272\A8=119.190
50966\A9=119.45053101\A10=121.71704569\A11=121.39147453\A12=118.59579543\A13=39.758
81203\A14=176.48996021\D4=180.00140559\D5=-0.00302153\D6=0.00146993\D7=-179.999028
24\D8=179.99969456\D9=0.00082657\D10=-179.99833861\D11=179.99994379\D12=-179.9925
033\D13=0.1783386\D14=4.75560279\\Version=x86-Linux-G98RevA.7\HF=-361.9353249\S2=2.0
16477\S2-1=0.\S2A=2.000102\RMSD=9.381e-09\RMSF=2.564e-05

Zero-point correction = 0.102351 (Hartree/Particle)

Frequencies --	23.7244	26.3059	54.7870
Frequencies --	59.4849	90.3016	245.2032
Frequencies --	290.5880	342.1190	403.7502
Frequencies --	600.7049	688.1484	801.9318
Frequencies --	897.7512	942.5710	953.1486
Frequencies --	968.2124	977.4374	1008.8821
Frequencies --	1018.8983	1024.8704	1069.3518
Frequencies --	1203.1450	1217.4761	1368.7148
Frequencies --	1390.4276	1398.4255	1455.8109
Frequencies --	1543.5185	1661.9161	2006.6985
Frequencies --	3181.1827	3187.2287	3198.8398
Frequencies --	3201.3304	3210.6682	3213.4411